The Convection Rolls System of Earth‘s Mantle

Heat transfer within the Earth and how it is revealed on its surface

©Steingrímur Þorbjarnarson
2026

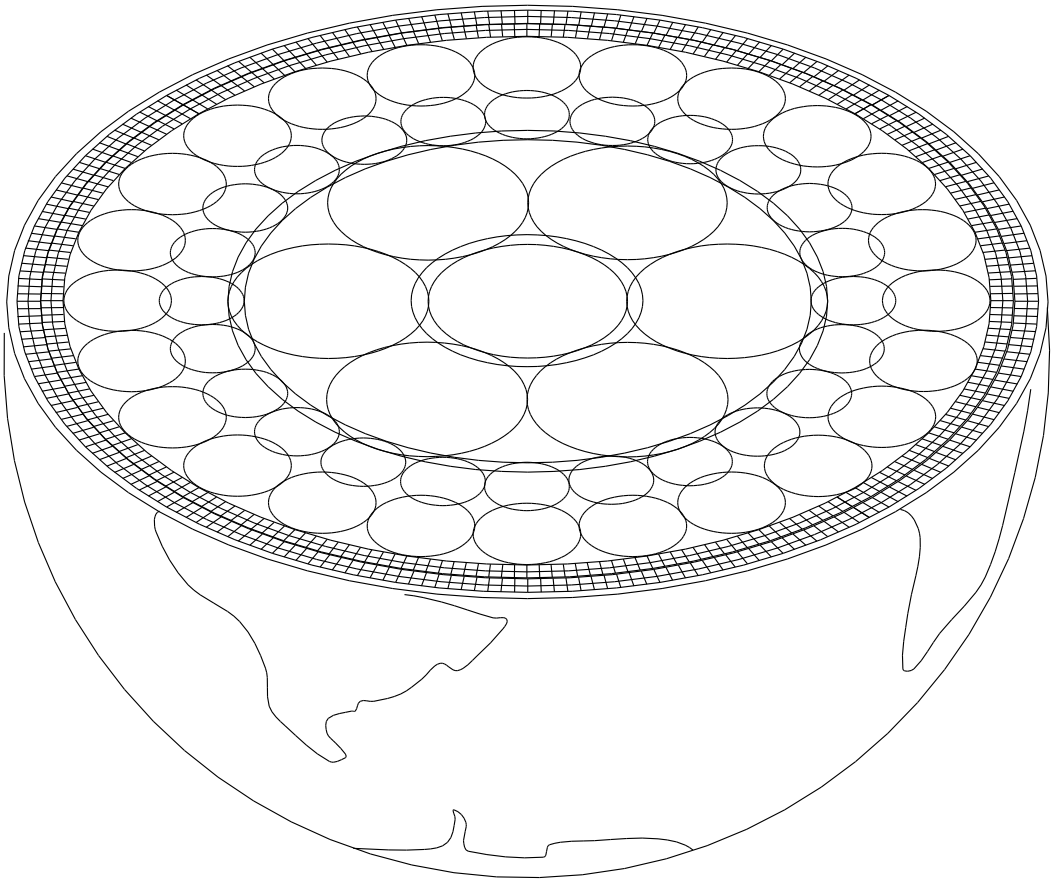

Table of Contents

Figures: 5

Preface 7

Part I - From the core of the Earth to the crust 10

Chapter 1 - Background of the theory 11

1.1. The model based on Earth's layers 11

1.2. Referring to physics: Rayleigh-Bénard convection and Coriolis effect 13

1.3. Francis Bacon, Alfred Wegener, Harry Hess and many others 16

1.4. The current cell system proposed by Harry Hess 17

1.5. Description of a system 19

Chapter 2 - Dimensions of a cross section of the convection cells 21

2.1. The 'core' of this analysis 21

2.2. The similarities and dissimilarities between atmosphere, ocean and mantle 23

2.3. The current system 26

2.4. Height and breadth of convection cells 27

2.5. Different levels of geometrical constraint within the model 31

Chapter 3 - The 410 km and 670 km Discontinuities 34

3.1. Uppermost Convection Cells of the Asthenosphere 34

3.2. The Structure of the Upper Layers 40

3.3. Convection Cells Compared with the Upper Layers 42

Chapter 4 - The Shape of the Convection Cell System 45

4.1. The Coriolis Effect on the Convection Cells 46

4.2. The Diameter of Circular Horizontal Flow on a Perfect Sphere 47

4.3. The Average Diameter of Horizontal Circulation 51

4.4. The Basic Horizontal Model 53

4.5. Equations for the World Map of Convection Cells 54

4.6. Differentiation of the Flow Equation to Determine Cell Direction 55

4.7. Degree of Accuracy 57

Chapter 5 – MORB and OIB 60

5.1. MORB and OIB layers 61

5.2. Individual sections of essentially circular horizontal flow 63

5.3. Flow in convection cells: east-west component due to convection and north-south component due to secondary horizontal flow 65

5.4. Horizontal circulation 66
Chapter 6 - Radiation and the Munroe effect 67
6.1. The Role of Radiation 67
6.2. The Munroe Effect 70
6.3. The Function of the Munroe Lines 72
6.4. Horizontal Transfer of Heat Within the Mantle 77
Chapter 7 - Intersection Zones of Horizontal Flow 78
7.1. Intersection Zones 78
7.2. Connection Between the MORB and OIB Layers Within the Intersection Zones 80
7.3. Layers Within the Horizontal Intersection Zones 81
7.4. The Intersection Zones Between 60.7° and 67.3° 82
7.5. Is There Something Special About the Polar Areas? 85
7.6. The Equatorial Intersection Parallel 86
7.7. Vertical View Versus a View Along the Plane of Rotation 87
7.8. Conclusion 89
Part II - How Is the System Revealed at the Surface? 90
Chapter 8 - The Distribution of Land and Ocean Along the Equator 90
8.1. A "Fit" 91
8.2. Measurements Along the Equator 92
8.3. Ocean Ridges Along the Equator 97
8.4. Why Might the Equatorial Pattern Have Been Overlooked? 99
Chapter 9 - The World Map 103
9.1. Preconditions for Tracing the System North and South 103
9.2. Global View 105
9.3. Connection Between Iceland and Hawaii 107
9.4. The North Atlantic 111
9.5. Kamchatka and Iceland Compared 113
9.6. Trenches 117
9.7. The Arctic 118
Chapter 10 - Iceland 120
10.1. The hemispheric and polar lines over Iceland 121
10.2. A pattern in the distribution of the most active sites 123
10.3. High-temperature geothermal areas 126
10.4. Low-temperature geothermal areas 128
10.5. The South Iceland Seismic Zone (SISZ) 129

10.6. Explanation of fracture orientations within the SISZ 132
10.7. Seismic areas in general 134
10.9. The volcanic zones 135
10.10. The 64th latitude 137
10.11. The longitude axis of Öræfajökull – Kverkfjöll – Theistareykir 139
10.12. The mirrored location and morphology of the two Snæfell volcanoes 140
10.13. An example of a fault in Iceland 144
10.14. Bedrock boundaries 145
10.15. The Holuhraun eruption 146
Chapter 11 - Tectonic drift 149
11.1. Tectonic drift of Iceland 149
11.2. The division line between the American and European plates through Iceland 151
11.3. Why does the drift direction follow the lines? 156
11.4. Tectonic drift of the whole world 157
11.5. Grid of reference 158
11.6. The tectonic drift of Iceland reversed 159
11.7. The continental microplate extending from Jan Mayen to Öræfajökull 161
Chapter 12 - Back to the beginning with the 'Ocean Basins' 162
12.1. Pinpointing the regional and local systems 162
12.2. Zooming in on Iceland and then zooming out 164
12.3. Ocean ridges around Iceland 165
12.5. Taking more examples 166
Chapter 13 – The Ring of Fire and the two other Tectonic Rings 170
13.1. Antarctica as a Geometrical Reference 170
13.2. Extending the Geometry Beyond the Pacific 171
13.3. Correspondence with Major Tectonic Structures 172
13.4. Overlapping Tectonic Rings 173
13.5. The Red Sea as a Particularly Strong Correspondence 173
13.6. Repeated Ridge Orientations at 90° Intervals 174
13.6. A Working Global Hypothesis 175
Chapter 14 Examples of Tectonic Plates ..... **Error! Bookmark not defined.**
1. The Mediterranean and the Gibraltar sector ..... **Error! Bookmark not defined.**
2. Transition to the next N–S axis ..... **Error! Bookmark not defined.**
3. Southeastward segment ..... **Error! Bookmark not defined.**
4. Equatorial E–W segment ..... **Error! Bookmark not defined.**

5. Long N–S oceanic boundary ..... **Error! Bookmark not defined.**

6. Southeastward turn toward the Antarctic triple-junction regionError! Bookmark not defined.

7. E–W boundary toward the Atlantic ellipse ..... **Error! Bookmark not defined.**

8. Along the inner Atlantic ellipse ..... **Error! Bookmark not defined.**

9. Excursion into the African continent ..... **Error! Bookmark not defined.**

10. African–Somali Plate boundary ..... **Error! Bookmark not defined.**

11. From the inner to the outer Atlantic ellipse ..... **Error! Bookmark not defined.**

12. The Red Sea ..... **Error! Bookmark not defined.**

The African Plate as a large-scale geometrical structure ..... **Error! Bookmark not defined.**

Proof? 180

Appendix 1: Basic Model Compared with the World Map 183

The Convection System of Earth's Mantle and the Transfer of Heat to the Surface 189

Works Cited 190

Additional Sources Consulted During Preparation 191

Figures:

Figure 1: Earth's layers drawn to scale with circles representing convection cells 13
Figure 2: A schematic drawing of the current system along the equatorial plane. 15
Figure 3: A drawing by Antonio Snider Pelligrini (1858) 16
Figure 4: Hess' drawing of convection cells. 18
Figure 5: Layering and convection cells ..... **Error! Bookmark not defined.**
Figure 6: A 3D sketch of the current cells as if cut along the equator line. 22
Figure 7: Surface Ocean Currents. 23
Figure 8: The Global Conveyor Belt. 24
Figure 9: The 12 main division lines of the system. 27
Figure 10: The point corresponding to the conditions within the mantle if the conditions were balanced, as explained by Manneville (Manneville 2010). 28
Figure 11: A convection cell with equal height and breadth. 29
Figure 122: A convection cell with equal height and breadth. 31
Figure 13: The inner structure of the Earth as interpreted with convection rollls model. 35
Figure 14: Trigonometric construction used to calculate the dimensions of the uppermost convection cells 37
Figure 15: The 410 km and 670 km discontinuities and the convection-cell system. 38
Figure 16: The discontinuities of 120, 410 and 670 km, as calculated. 39
Figure 17: The convection-cell model with the four uppermost layers of smaller cells included. 40
Figure 18: The upper layers of the Earth. 41
Figure 19: Convection cells of the asthenosphere and upper mantle 42
Figure 20: According to Smet et al. (1999), the mantle is less depleted below 250 km. 43
Figure 21: Relationship between a horizontal circle on a rotating sphere and the Earth's radius. 48
Figure 22: Calculated dimensions of the horizontal circulation path of the convection rolls. 49
Figure 23: Schematic horizontal geometry of the proposed convection-cell system. 53
Figure 24: The big mantle cells shown underneath in red and the OIB-layer (blue) and the uppermost MORB layer (also red). Drawing by Jón Leósson. 61
Figure 25: A convection cell map with the central line of the North Atlantic marked red. 61
Figure 26: A drawing representing the alignment of MORB layer convection cells. 63
Figure 27: The MORB and OIB layers. 66
Figure 28: The rise in conductivity around 1,300°C is attributed here mainly to increasing mantle transparency to radiation at high temperature. 68
Figure 29: Radiation from the Earth's outer layers proposed to heat the core. 68
Figure 30: The Munroe effect. 70
Figure 31: Proposed development of a narrow jet of molten material from convection cells through the Munroe effect. 71
Figure 32: Proposed flow associated with the Munroe effect cutting through the ductile part of the lithosphere. 72
Figure 33: Schematic cross-section showing how a main lower-mantle Munroe line is proposed to influence smaller cells above and strengthen several Munroe lines in the asthenosphere. 73
Figure 34: A typical tectonic-plate polygon proposed to be formed by convection cells. 73
Figure 35: Example of how OIB-type magma is proposed to enter a tectonic-plate polygon. 74
Figure 36: Convection cells in the cross-section between points A and B, shown with thicker lines. Point B is located at Öræfajökull volcano. 75
Figure 37: Section of convection rolls beneath Iceland, with Munroe lines shown on the map. 76
Figure 38: Overview of heat flow through the Earth's crust, as presented on the website www.mantelplume.org. 77
Figure 39: The proposed northern intersection zone between hemispheric and polar lines. 79
Figure 40: Schematic structure of convection cells within the intersection zone. 81
Figure 41: World map highlighting the distinction between hemispheric and polar cells. 82
Figure 42: Proposed thinning of the convection rolls where MORB and OIB layers originating from the north and south intersect within these latitude bands. 83
Figure 43: Drawing to scale, tilted 26°, showing the proposed intersection zone between hemispheric and polar convection rolls. 84
Figure 44: Maintenance of approximately circular convection along the stress axis perpendicular to the Earth's rotation axis. 88
Figure 45: Comparison between the proposed lower-mantle convection cells and the distribution of land and ocean along the equator. 91
Figure 46: Equatorial span of South America, approximately 30° in the measurement shown. 92

Figure 47: Equatorial width of the Atlantic Ocean between South America and Africa, approximately 60°. 93
Figure 48: Equatorial span from western Africa to the Great Rift Valley, approximately 30°. 94
Figure 49: Equatorial span from the Great Rift Valley to Indonesia, approximately 60°. 94
Figure 50: Equatorial width of Indonesia, approximately 30° in the measurement shown. 95
Figure 51: Schematic summary of the 30°-60° land-ocean pattern along the equator. 96
Figure 52: Equatorial cross-section showing the distribution of the main Pacific, Atlantic and Indian Ocean ridge systems. 97
Figure 53: Comparison between the proposed convection-cell divisions and major tectonic features along the equator. 98
Figure 54: Proposed intersection point of large convection cells beneath Africa. 100
Figure 55: World-map summary of the proposed 30° divisions along the equator. 101
Figure 56: Transition from the internal geophysical model to comparisons with surface features. 104
Figure 57: Global map showing the twelve principal division lines of the proposed system. 105
Figure 58: Iceland shown in relation to the horizontal convection-cell model. 106
Figure 59: Global convection-cell framework with selected volcanic regions shown for comparison. 107
Figure 60: North Atlantic section of the more detailed convection-cell model. 107
Figure 61: Hawaii and Iceland shown in relation to convection-cell lines separated by 120° in the proposed framework. 109
Figure 62: Schematic North Atlantic pattern used for comparison with the equatorial framework. 111
Figure 63: Comparison between the calculated convection-cell direction and the dominant topographic trend of Kamchatka. 113
Figure 64: Comparison of the calculated trend from Equation 6 with the EVZ in Iceland and the Kamchatka example. 114
Figure 65: Simplified comparison between the calculated direction and the Tjörnes Fracture Zone. 116
Figure 66: Schematic example of the Pacific Plate underthrusting the Australian Plate in relation to the proposed convection-cell framework. 117
Figure 67: The hemispheric convection-cell pattern over Iceland. 121
Figure 68: The polar convection-cell pattern over Iceland. 121
Figure 69: The combined Icelandic grid of convection cells. 122
Figure 70: Upwelling lines marked with red lines and downwelling lines blue. 123
Figure 71: Prominent volcanic and geothermal sites compared with calculated intersection points. 124
Figure 72: Geothermal activity compared with the convection-cell grid. 126
Figure 73: Most low-temperature geothermal areas in Iceland occur within distinct grid polygons. 128
Figure 74: The South Iceland Seismic Zone in relation to the proposed grid polygon. 130
Figure 75: The 64th parallel as the central line of the proposed transition zone. 137
Figure 76: The north–south axis from Öræfajökull to Theistareykir in relation to the polygon arrangement. 139
Figure 77: Detailed maps of Snæfellsjökull and Snæfell shown side by side. 140
Figure 78: Calculated direction compared with an important geothermal fault. 144
Figure 79: Earthquake map from the Icelandic Meteorological Office, with calculated directions superimposed. 146
Figure 80: Locations of the Laki and Eldgjá fissure systems relative to the proposed grid. 149
Figure 81: The tectonic drift vectors with lines superimposed. 150
Figure 82: Theoretical boundary between N-American and Eurasian Tectonic Plates 151
Figure 83: Division lines 153
Figure 84: Comparing the convection cells of 64°N and the division line between the tectonic plates. 154
Figure 85: The drift of the tectonic plates (from the Internet). 157
Figure 86: How the Eurasian and North American plates rotate in opposite directions (http://www.geologyin.com/2015/03/driving-forces-of-plate-motion.html) 158
Figure 87: Resemblance between polar cells and continental microplate between Iceland and Jan Mayen. 161
Figure 88: Examining Iceland helps increasing accuracy of global model. 164
Figure 89: Comparison of tectonic orientations near Hekla and Trondheim, 30° apart. 167
Figure 90: Juan de Fuca with calculated direction 169
Figure 91: The Ring of Fire, along with Rings of both Indian Ocean and Atlantic Ocean. 170
Figure 92: Antarcit Tectonic Plate and its elliptical form. 171
Figure 93: The African Tectonic Plate. 176

Preface

This work presents a step towards a three-dimensional model of the convection system within the Earth's mantle. The positions and orientations of the proposed convection cells are derived from a combination of geometrical relationships, physical principles and geophysical measurements, opening up possibilities for quantitative analysis and comparison with geological structures throughout the world. Until recently, it would have seemed unlikely that the orientation of Iceland's volcanic zones could be derived from a relatively simple set of premises. The model presented here suggests that this may indeed be possible. A regular system of mantle convection cells, if correctly identified, could substantially increase our understanding of geological processes. In many respects, this work can be regarded as a continuation of the line of thought presented by Harry Hess in his 1962 essay "History of Ocean Basins." Hess referred to his speculative approach as "geopoetry," yet his arguments were sufficiently compelling to be taken seriously. His ideas about mantle convection are particularly relevant to the approach developed in this book. I argue that many of the structural details of the system described only in general terms by Hess can be investigated more explicitly. The model presented here is based on calculations derived from physical principles and geophysical measurements. To make each step in the derivation as clear as possible, I combine diagrams with explanations and refer to measurements and physical principles wherever possible. The study necessarily approaches the boundary between what is well established and what remains hypothetical, with the aim of extending the range of what can be understood. After approximately twenty five years of working on this problem, I believe that the resulting framework deserves to be presented and examined as a coherent whole.

Perhaps the most intriguing figure in the study is the one showing how the thicknesses of the outer core and mantle correspond to a regular pattern of circular convection cells, each with the same characteristic diameter as the inner core. In that sense, "seeing is believing," and I therefore suggest that the reader first examine this figure. It represents the simplest visual expression of the underlying idea, somewhat analogous to noticing that the coastlines of Africa and South America appear to fit together. Once the proposed convection-cell system has been derived from this basic

relationship, several geological features become easier to visualize and interpret. Some relationships that initially appear complicated may then seem surprisingly natural.

The approach developed here deliberately begins with a small number of basic premises. Two factors are particularly important: the transfer of heat through the Earth and the rotation of the Earth about its axis. These provide the physical framework within which a wealth of geophysical observations can be considered in order to identify the principal features of the Earth's internal structure.

The first set of geophysical constraints is provided by the depths and thicknesses of the Earth's internal layers. A central clue, pursued throughout this book, is the proposed relationship between the thickness of the mantle and a system of twelve convection cells whose vertical and horizontal dimensions are approximately equal. Owing to the geometry involved, their characteristic dimensions are also related to the diameter of the inner core. A corresponding relationship is proposed between six convection cells in the outer core and twelve in the lower mantle. Of particular importance is the transition region at the core–mantle boundary, associated here with the D" region and the Gutenberg discontinuity. In the proposed model, this region provides an intersection zone between the convection systems of the outer core and the lower mantle. Investigating this possibility proved to be one of the most productive steps in developing the model. This book therefore examines in detail the relationship between the thicknesses of the Earth's layers and a system of convective cells with comparable height and breadth.

The apparent consistency between the dimensions of the Earth's internal layers, the proposed convection cells and the relevant physical principles is striking, and its implications are explored systematically. Under balanced conditions, the convective system of the mantle may tend towards cells whose height and width are of the same general order, as discussed in relation to Rayleigh–Bénard convection in Chapter 2. In the model proposed here, these cells form rolls arranged side by side. The rotation of the Earth, through the Coriolis effect, is then considered as an influence on the geometry of these rolls. Particular attention is given to the horizontal components of particle motion and to the geometrical patterns derived from the relevant equations. This analysis subsequently leads to the identification of two layers within the upper mantle (see Chapter 4).

The work is divided into two main parts. The first develops a three-dimensional model of the proposed convection-cell system and examines the physical

and geophysical premises on which it is based. The second considers how this internal system may be expressed at the Earth's surface, with particular emphasis on Iceland. After the convection system has been derived progressively from the Earth's interior towards the surface, its predictions can be compared with tectonic, topographic and volcanic features. The strength of the model therefore depends on the degree of consistency between the physical framework, geophysical measurements and observable surface geology.

Recognizing a possible geometrical relationship between a system of convection cells and the internal layering of the Earth was only the beginning. Considerable additional work was required to investigate how mantle material could circulate within such a system. The resulting model reveals a three-dimensional geometry in which spherical mathematics and a comprehensive convection system are closely interconnected. Its combination of horizontal and vertical components may help explain why the pattern has remained difficult to recognize, even though several of its features appear relatively simple once the geometry has been reconstructed. An earlier version of the model included 12 convection rolls in the lower mantle, which was a simplification. It is clear, however, that internal boundaries exist within the lower mantle, and mathematically the geometry is consistent with an arrangement of 24 convection rolls distributed between two layers. This produces pronounced boundaries at 15° intervals. The earlier version is still used partly here, but that does not affect the outcome of the analysis in general.

When introducing a subject that one has studied intensively for many years, there is always a temptation to assume that the reader will approach every detail with the same degree of interest. I have deliberately tried to avoid that. My main objective is instead to explain as clearly as possible what I believe to be the fundamental structure of the model, the reasoning by which it was derived and the observations against which it can be tested. Choosing between presenting this work as an article or as a book was not straightforward. Ultimately, the book format was chosen because the scope of the subject has become too broad and interconnected to be adequately presented in a single article.

A poster presenting an earlier version of this system was exhibited at the GEORG Geothermal Workshop 2016, held at the Grand Hotel in Reykjavík, and is reproduced here.

Part I - From the core of the Earth to the crust

Chapter 1 - Background of the theory

It is generally accepted that convection occurs within the Earth's mantle, although the detailed geometry, dimensions and locations of individual convection units remain uncertain. The approach developed in this work is based on the proposition that these characteristics can, to a considerable extent, be derived from the known internal structure of the Earth. A large body of geophysical information is available concerning the depths and thicknesses of the Earth's principal layers, and the central observation explored here is that the proposed convection units correspond closely to those dimensions. Exploring the implications of this possibility is the main subject of the book. The study is divided into two broadly distinct but complementary parts: the first examines the physical premises and geophysical constraints involved, while the second presents examples of how the proposed convection-cell system may be expressed at the Earth's surface. Earlier stages of this work formed the basis of three conference presentations: one at the World Geothermal Congress in Iceland in 2020 and two at the Stanford Geothermal Workshop in 2023 and 2024. The associated papers provide concise overviews of material developed in greater detail here.

1.1. The model based on Earth's layers

Looking at a diagram of the Earth's internal layers, one can immediately recognize a certain degree of geometrical regularity. The more difficult question is whether this regularity is merely coincidental or reflects an underlying physical organization. The starting point of the present study is the observation that a regular system of convective cells can be constructed in such a way that its principal dimensions correspond closely to the layering of the Earth. Ever since I first drew a simple pattern of circles within a scaled cross-section of the Earth, I have worked on deriving the possible geometry of such a convection system. The investigation has proved highly productive, and I have become convinced that the model presented here can provide a useful framework for interpreting a wide range of geological and geophysical observations. A three-dimensional convection system is not always easy to describe in words alone, and diagrams are therefore essential to the argument. The underlying geometry is, in many respects, surprisingly simple, but because the ideas developed here differ in important ways from conventional descriptions of mantle convection, I have chosen to explain the reasoning in some detail. A few additional pages are

worthwhile if they make the derivation easier to follow and allow the reader to distinguish clearly between observations, physical premises, deductions and interpretations. There is an extensive scientific literature dealing with mantle convection, the structure of the Earth, plate tectonics and related subjects. References to that work are necessary, but the principal purpose here is not to reproduce existing descriptions. The main emphasis is on the logic of the proposed model. Observational constraints are first identified, physical principles are then applied, and the resulting geometrical relationships are compared with geological evidence. By considering the physical principles that influence the form and behaviour of mantle convection, it becomes possible to construct a more comprehensive picture of the Earth's interior. One of the most striking geometrical observations in the model is that the characteristic diameter assigned to each circular cell representing convection in the lower mantle corresponds to the diameter of the inner core. The correspondence is sufficiently close to justify investigating whether it forms part of a broader geometrical relationship within the Earth's interior (Þorbjarnarson 2000). If the convection cells are arranged vertically and laterally within an equatorial cross-section, the same geometry can be represented schematically as follows:

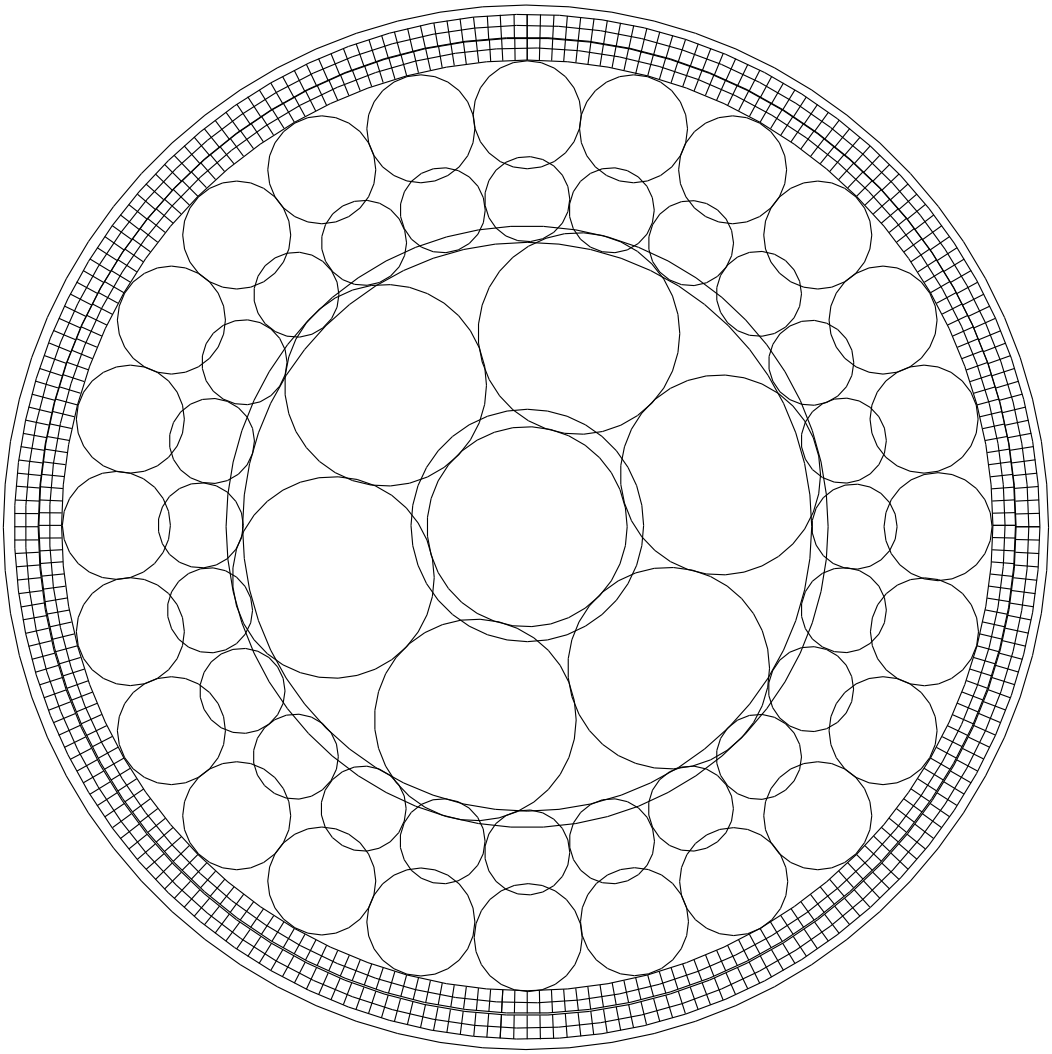

Figure 1: Earth's layers drawn to scale with circles representing convection cells

This provides a convenient way of illustrating convection cells with approximately comparable vertical and horizontal dimensions. The actual flow paths within such cells would, of course, not be perfect circles. The circular representation is therefore a geometrical approximation rather than a literal description of particle trajectories. It is useful to introduce this basic diagram at an early stage so that the reader can become familiar with the geometry before the physical reasoning behind it is discussed in detail. The following sections examine whether the proposed arrangement is compatible with the physical behaviour expected of convective systems and with the measured dimensions of the Earth's internal layers. A basic requirement of the model is that the proposed convection cells must fit consistently within these distinct layers.

1.2. Referring to physics: Rayleigh-Bénard convection and Coriolis effect.

The novelty of the present study does not lie primarily in introducing new physical laws or new measurements. Rather, it lies in organizing existing geophysical measurements within a particular geometrical framework and examining that framework in relation to well-established physical principles. Two concepts are especially important: Rayleigh–Bénard convection and the Coriolis effect. Geophysical measurements of the depths and thicknesses of the Earth's internal layers provide an additional set of observational constraints. The analysis can therefore be summarized in three principal components:

1. The dimensions of the Earth's internal layers are compared with a regular system of convection cells. Under appropriate conditions, thermal convection can organize itself into cellular or roll-like structures. Rayleigh–Bénard convection provides a useful physical analogue for considering such organization. In idealized convective systems, cells may develop with vertical and horizontal dimensions of the same general order, although their precise aspect ratios depend on boundary conditions and other physical parameters (Manneville 2010). In Manneville's discussion of convection between solid plates, this is referred to as RB convection, where 'R' stands for Rayleigh and 'B' for Bénard.
2. The effects of the Earth's rotation are considered through the Coriolis effect (Paldor and Killworth 1988). Motion within a rotating reference frame is subject to Coriolis deflection. In the model developed here, the Coriolis effect is used to investigate how the geometry and orientation of the proposed convection system may change with latitude.
3. Predictions derived from the proposed convection system are compared with geological observations. If the model represents a real component of the Earth's internal dynamics, its geometry should have observable consequences at the surface. These may include relationships with tectonic boundaries, volcanic zones, topography and plate motion. Iceland provides a particularly detailed example, but the model can also be compared with geological structures elsewhere in the world.

A combination of geological, geophysical and topographical observations therefore provides a means of evaluating the proposed system. Throughout this work, individual geological phenomena are examined in relation to the geometry predicted by the convection model. This includes aspects of plate motion and the development

of tectonic structures through geological time. Modern GPS measurements have greatly improved our ability to measure present-day crustal motion, making it possible to compare observed displacement vectors with directions predicted by the proposed convection-cell system.

The model can consequently be examined from both vertical and horizontal perspectives. The vertical component is represented primarily by the measured thicknesses and boundaries of the Earth's internal layers. The reasons for considering convection cells with comparable height and breadth are discussed in relation to Rayleigh–Bénard convection (Manneville 2010). In the second half of the book, greater emphasis is placed on the horizontal expression of the system at the Earth's surface. One example considered in this context is an apparent sequence of approximately 30°, 60°, 30°, 60° and 30° between major continental and oceanic sectors along the equatorial region, where the Coriolis effect is zero. Such a regular sequence deserves closer investigation and can be tested against the geometrical predictions of the model and the probability of comparable patterns occurring by chance.

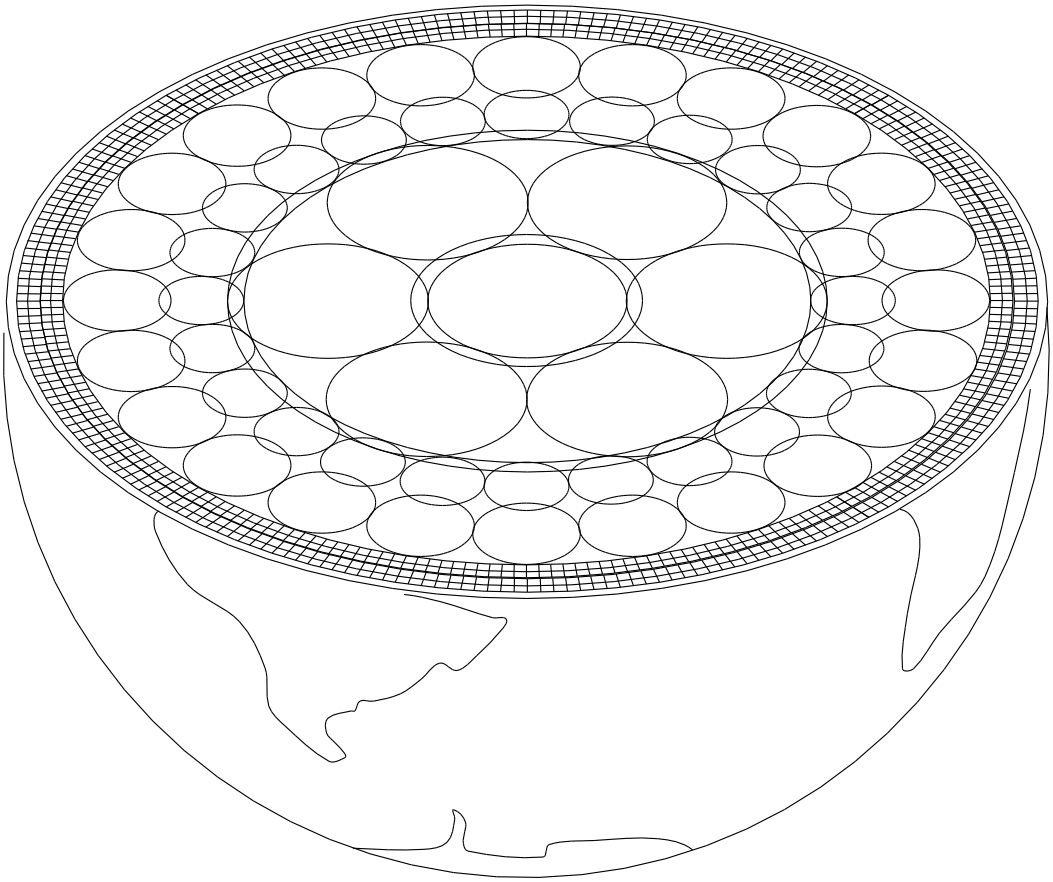

Figure 2: A schematic drawing of the current system along the equatorial plane.

The dynamics of tectonic drift are also considered. Displacement vectors derived from measurements by the National Land Survey of Iceland, including the ISN93 and ISN2004 reference systems (Valsson 2008), can be compared with the directions predicted by the convection-cell system described here.

When these geophysical, topographical and dynamic relationships are considered together, they provide several independent ways of evaluating the proposed framework. The possibility then arises that a range of geological phenomena that remain difficult to explain may be examined within a common model.

1.3. Francis Bacon, Alfred Wegener, Harry Hess and many others

The content of this work extends existing ideas concerning several aspects of geology and does not, in itself, conflict with the established framework of plate tectonics. Because of its relationship to the development of ideas about continental and plate motion, it is useful to recall briefly the history of that field. Once the coastlines of Africa and South America had been mapped, their apparent fit attracted attention and encouraged speculation about former connections between the continents. Francis Bacon drew attention to similarities between the opposing shores in 1620 and suggested that the resemblance was probably "no coincidence" (Grand 1988). Later, reconstructions showing the continents joined together were produced, including the well-known drawing by Antonio Snider-Pellegrini in 1858[1].

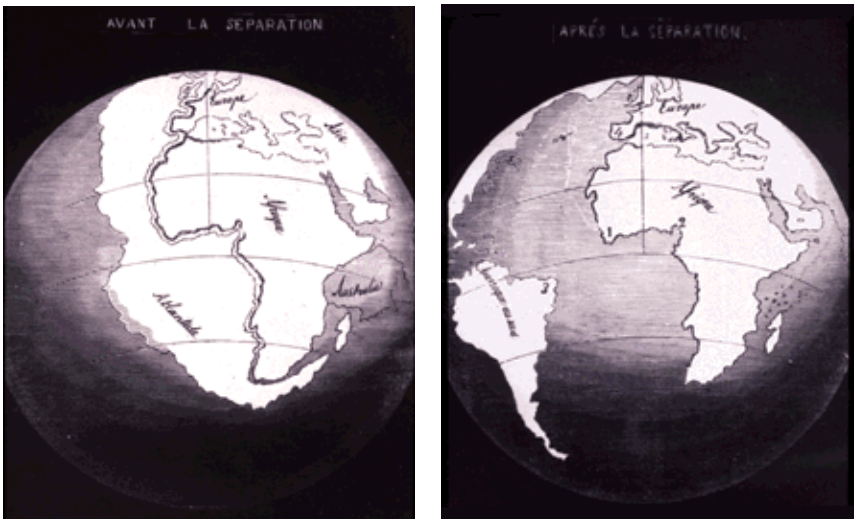

Figure 3: A drawing by Antonio Snider Pelligrini (1858)

[1] http://courses.science.fau.edu/~rjordan/phy1931/WEGENER/VG05.gif

A major step was taken in the early twentieth century by Alfred Wegener, a meteorologist who examined evidence including the former movement of glaciers. He argued that glacial paths and other geological and biological observations could be reconciled by reconstructing the continents as parts of a formerly unified landmass. In this way, he developed a coherent account of continental drift and its geological history (Stanley, 1999).

Harry Hess's description of seafloor spreading provides another essential background to this work, particularly through its emphasis on the role of mid-ocean ridges (Hess, 1962). These successive developments were all supported by advances in mapping and measurement. The history of this scientific development is fascinating, but because it has been described extensively elsewhere, it is only summarized briefly here. Readers interested in the history of geoscience are especially encouraged to explore the story of Alfred Wegener and the reception of his ideas.

1.4. The current cell system proposed by Harry Hess

In the essay *History of Ocean Basins* (Hess 1962), which played an important role in the development of modern ideas about the ocean basins, Hess placed particular emphasis on oceanic geology. His direct experience of seafloor observations gave him a perspective that differed from that of many geologists whose work had traditionally focused on the continents. The Mid-Atlantic Ridge provided one of his clearest examples of the relationship between mantle convection and seafloor spreading:

> The Mid-Atlantic Ridge is truly median because each side of the convecting cell is moving away from the crest at the same velocity, ca. 1 cm/yr. a more acceptable mechanism is derived for continental drift whereby continents ride passively on convecting mantle instead of having to plow through oceanic crust.

Hess then considered the possible shape and dimensions of these convecting cells:

> Vening Meinesz (1959) analyzed the spherical harmonics of the Earth's topography up to the thirty-first order. The peak shown in the values from the third to fifth harmonic would correlate very nicely with mantle-sized convection currents; cells would have the approximate diameter of 3000 to 6000 km in cross section (the other horizontal dimension might be 10,000 to 20,0000 km, giving them a banana-like shape).

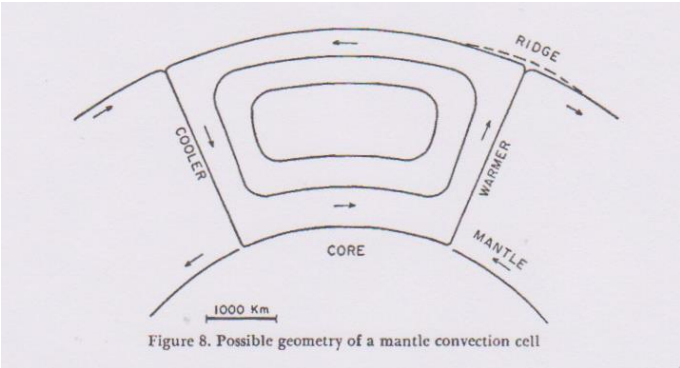

Figure 4: Hess' drawing of convection cells.

Hess's general description of mantle convection has several notable similarities to the system developed in greater detail in the following chapters. A simple comparison of dimensions illustrates the point. According to the principal proposition used in this work, a lower-mantle convection cell has a diameter of about 2,500 km and corresponds, at the equator, to an east–west surface interval of about 3,333 km. This lies within the order of magnitude of the 3,000–6,000 km cross-sectional dimensions discussed by Hess. Likewise, a semicircular convection path extending from the equator towards approximately 64°N is of the order of 10,000 km, while a corresponding mirrored structure in the opposite hemisphere gives a total horizontal scale of about 20,000 km. Thus, several of the basic dimensions and geometrical characteristics considered here are already foreshadowed in Hess's 1962 discussion. The purpose of the present work is to develop such relationships quantitatively and to derive a more explicit geometrical model. One possible reason why such a system was not developed directly from Hess's description is that later work increasingly focused on the more complex distribution of hotspots, ridges and subduction zones.

1.5. Description of a system

The main purpose of this work is to describe a proposed system of convection cells within the Earth's mantle and core and to examine whether regular parameters in the Earth's interior can help explain the more complex geological patterns observed at the surface. Regularity is treated here as an important working premise, grounded in physical reasoning and geometrical consistency. Conditions that have persisted for billions of years within a rotating, approximately spherical Earth may reasonably be expected to display some degree of organized structure.

The analysis begins with the observation that the proposed cells of the outer core and lower mantle have a characteristic diameter comparable to that of the inner core. Further relationships are then examined to determine whether they support the same general framework. The great thickness of the mantle and the long timescale over which convection has operated suggest the possibility of a dynamically balanced state (Walzer 1971). The fact that convection cells with the proposed dimensions can be fitted into the measured layering of the Earth can therefore be regarded, quite literally, as the "core" of this analysis. The depths of the major internal layers are known with considerable accuracy, making it possible to test geometrically how cells of comparable height and breadth fit within them. Physical arguments for considering such dimensions are discussed in relation to convection theory (Manneville 2010).

Harry Hess's 1962 work on mid-ocean ridges and seafloor spreading is fundamental to the background of this study. He argued that mantle convection could move the tectonic plates as new oceanic material was formed at spreading ridges (Hess, 1962). The present work attempts to develop this line of reasoning further by considering whether a more complete convection system within the mantle and core can be described geometrically.

Models in which convective circulation extends through large parts of the mantle have been proposed in several forms. McBirney discusses alternative interpretations of the relationship between mantle layering and convection (McBirney 1993):

> The mantle is thought to turn over slowly, transferring heat generated in the core and in the mantle itself to the asthenosphere and the lithosphere. The temperature within any convecting horizon is probably close to an adiabatic gradient. That is to say, the heat content of the rocks remains nearly constant while temperature varies with pressure, much as it does in the earth's atmosphere, where the temperature decreases as air rises and

> expands but increases as it descends and is compressed. And just as the temperature of air is buffered by the heat absorbed or released when minerals melt, crystallize, or change their crystalline structure in response to changes in pressure.
> [Two] conceptions of the mantle [are] consistent with these principles. In one, the entire mantle convects as a single unit, while in the other the upper and lower mantle convect as essentially separate systems.

In the present analysis, the second of these alternatives is adopted: separate convective systems are proposed for different depth intervals. This follows from the geometrical premise that the characteristic size of the lower-mantle convection cells is related to the diameter of the inner core. In many textbooks, the lower mantle is defined as the interval between approximately 670 and 2,700–2,900 km depth. In the model developed here, however, a different functional division is explored, in which the boundary between the principal lower- and upper-mantle convection systems is placed near 410 km depth. The reasons for adopting this arrangement are developed in the following chapters.

Chapter 2 - Dimensions of a cross section of the convection cells

Here we begin with a simple representation of the Earth as if it were cut into two halves along the equator. Each aspect of the model is examined in greater detail throughout the book, including the reasoning behind it and its possible implications for the Earth's surface.

2.1. The 'core' of this analysis

A scale drawing of the mantle and core shows that a system of circular convection cells can be made to fit exactly within the principal layers. It has been proposed that convection cells within the Earth's mantle can be approximated by circles (Walzer 1971). The radius of the inner core is measured to be 1,221 km. Using this value, the basic convection-cell system of the outer core and lower mantle can be drawn very simply.

The drawing is based on the following data (Allen 1983) (Cristopherson 1992) (Francis 2000):

Lithosphere and asthenosphere	0-250 km
Transition zone	250 km
Olivine gives way to spinel	410 km
Lower mantle	670 – 2,700 km
Gutenberg layer	2,700 – 2,890 km
Outer core	2,900 – 5,150 km
Inner core	5,150 – 6,371 km

Here the conventional presentation is reversed. Instead of measuring the depth of each layer downward from the surface, the center of the Earth is taken as the origin, and the radial distance to each boundary is measured outward.

The table can then be presented as follows:

Inner core	0 - 1,221 km
Outer core	1,221 - 3,481 km
Gutenberg layer	3,481 - 3,671 km
Mantle to the depth of 410 km	3,671 - 5,961 km
120 and 410 km discontinuities	5,961 - 6,251 km
Tectonic plates to surface	6,251 - 6,371 km

A convection-cell system, drawn in accordance with the physical premises considered by (Walzer 1971), fits within this layering and corresponds to the

transition zone between the mantle and outer core (the Gutenberg discontinuity).

Beneath North America these slab relics are massive, almost vertical walls extending from 800 to 2,000 km depth, and typically 400–600 km wide (Sigloch 2013) . An additional lower-mantle division is introduced accordingly. In the geometrical model, the overlap zone extends approximately from 1,858 to 1,980 km depth, with a central flow division near 1,919 km.

Figure 1 shows how the Earth's internal layers and the proposed convection-cell system fit together. The crust itself is barely visible at this scale. The upper boundary of the large convection-cell system is marked at a depth of about 410 km. Another boundary, at about 670 km, is not shown in the figure. In the interpretation followed here, this boundary most likely reflects changes in mineral structure under the relevant pressures, producing changes in seismic-wave velocity (Foulger 2010). At about 410 km depth, olivine adopts a denser, spinel-like structure, and at about 670 km an even denser structure described as perovskite (McBirney 1993). Unlike the transition near 670 km, the 410 km boundary may represent a change in chemical composition as well as a structural change (Foulger 2010). The mineral transformation and the geometry of the convection model coincide at approximately 410 km depth. At about 2,700-2,900 km depth lies the region referred to here as the Gutenberg layer. The drawing shows the outer-core and mantle convection cells intersecting within this zone. A comparable transition is found deeper down at the surface of the inner core.

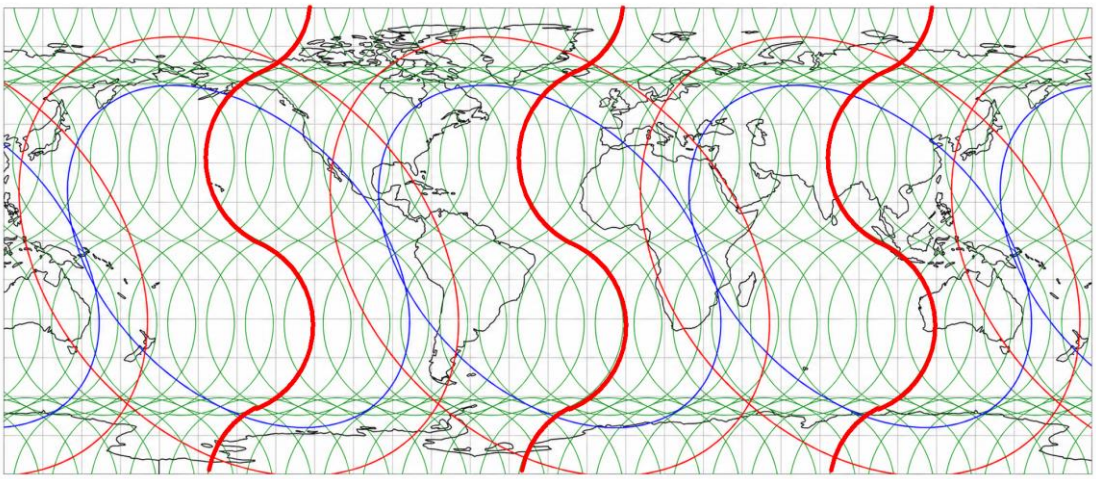

Figure 5: Convection rolls of lower mantle and tectonic rings.

Later, the concept of tectonic rings has to be introduced. It begins with the

Ring of Fire, and it can then be extrapolated to derive the outlines of its counterparts. In this representation, the cells also become narrower toward the poles while retaining approximately the same thickness, while their geometry is influenced by the Coriolis effect (Condon and Hugh 1967). This provides a striking correspondence between geophysical measurements and the physical principle that, under conditions of this kind, convective cells tend toward similar height and breadth (Manneville 2010). The apparent fit is therefore difficult to dismiss without further examination and deserves detailed analysis.

2.2. The similarities and dissimilarities between atmosphere, ocean and mantle

Before taking the next step from a 2D equatorial section to a 3D model of the entire Earth, it is useful to consider what is commonly known about comparable natural systems. Analogies with atmospheric and oceanic circulation can help in analyzing mantle convection, but a clear distinction must be made between the thermal and rotational factors governing particle motion. The thermal conditions differ greatly among the three systems, whereas the same rotational framework applies to all of them. Ocean currents may provide a somewhat closer analogy to mantle circulation in this respect because their heat capacity per unit volume is much greater than that of the atmosphere. The important point is that the thermal and rotational components can be considered separately in the atmosphere and oceans; the same distinction is applied here to flow within the Earth's mantle.

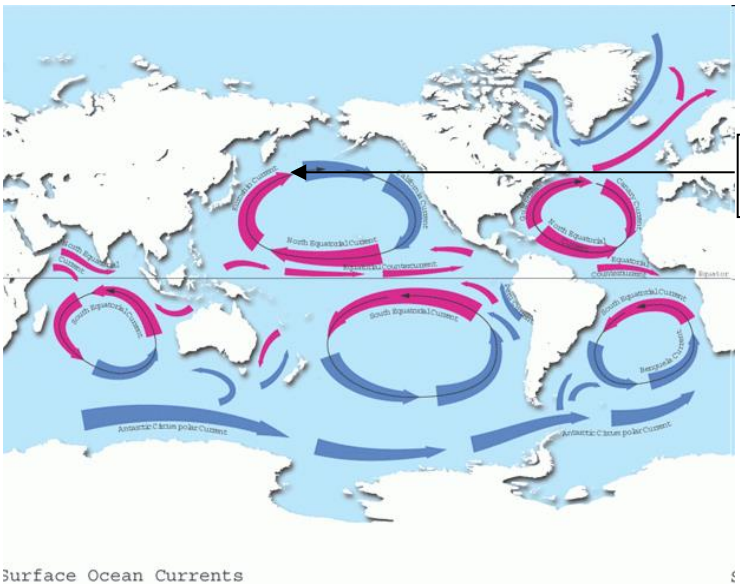

A large circular current, extending from equator.

Figure 6: Surface Ocean Currents.

The Conveyor Belt of the ocean currents is also systematically arranged:

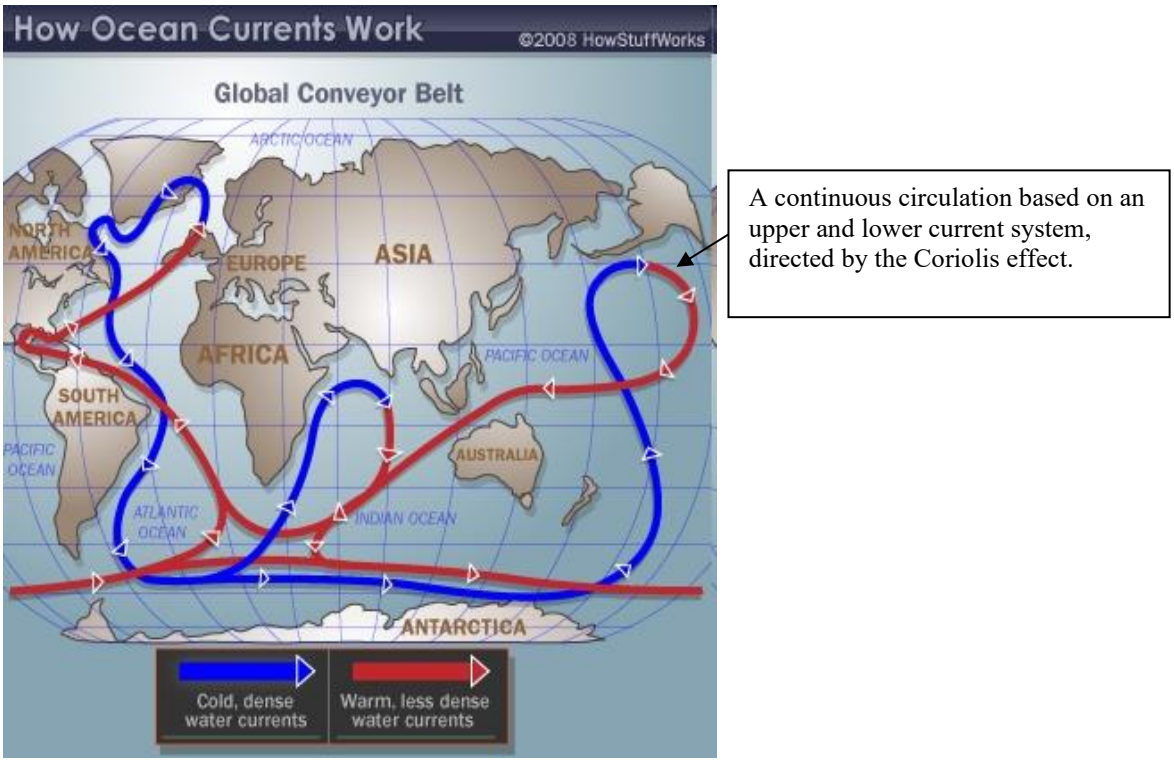

Figure 7: The Global Conveyor Belt.

Atmospheric and oceanic circulation are often viewed mainly in the horizontal plane, whereas the analysis here begins with a vertical section through the mantle convection cells. When the system is later considered in the horizontal plane, however, a pattern emerges that has similarities to both atmospheric and oceanic circulation.

Studying ocean currents provides a useful analogy when deriving the mantle-current model. The main difference, as treated in this model, is that heat within the Earth is assumed to be distributed much more evenly between latitudes. It is useful to keep the oceanic conveyor belt in mind, especially when reading Chapter 4 - The Shape of the Convection Cell System.

This book is intended as a contribution to geoscience. Scientific progress can take many forms, and the approach used here is less common: the accumulated work of many researchers is brought together in an attempt to derive a single, holistic framework. This raises the question of proof and, more importantly, falsifiability. The model makes both quantitative and qualitative claims, and it should therefore be possible for new data or calculations to contradict it. The 'fit' between a convection system in which the cells have equal height and breadth, on the one hand, and geophysical measurements of the Earth's internal layers, on the other, cannot by itself be regarded as proof that the proposed system exists. Coincidence remains possible, as does an alternative cause. The fit is therefore only the starting point for a broader

analysis that can be tested against accumulating data on the Earth's internal layers and improved understanding of convection physics. When a rule described in the physical literature[1] agrees with geophysical data[2], there is good reason to investigate whether it leads to further results. In the present case, it led to the convection-cell model developed in this book. The analysis that follows from the simple drawing is based on one central proposition[3], which is itself not entirely new[4]. If a wide range of independent phenomena can consistently be related to a simple proposition, the resulting framework may eventually become sufficiently reliable to be used as a scientific model.

1 Manneville (2010) explains conditions under which convection cells can develop with similar height and breadth and can therefore be approximated by circles in a simplified drawing.

2 Many textbooks provide information on the depths of the Earth's principal layers, including the outer core and mantle.

3 The proposition is that the convection cells should have the same diameter as the inner core.

4 A related proposition was put forward by Uwe Walzer (1971).

2.3. The current system

Any description of the proposed convection-cell system must begin with a cross-section of the Earth showing its principal layers drawn to scale and a pattern of circles superimposed on them. Each circle has the same diameter as the inner core. This is the geometrical approximation used for the dimensions of the convection cells (Walzer 1971), as explained in greater detail below.

Textbooks covering basic physics generally describe three principal mechanisms of heat transfer: radiation, conduction and convection (Condon and Hugh 1967). All three are relevant to understanding how heat is transferred within the Earth, although the main emphasis here is on convection. Starting with a two-dimensional representation of the mantle convection system, a three-dimensional model must then be developed. The initial picture can be summarized simply. In the proposed model, the lower mantle contains 24 convection cells, producing twelve ascending currents and twelve descending currents between adjacent cells. To visualize this arrangement in three dimensions, the geometry of the cells must be defined. The model should then make it possible to trace these 12 lines of ascending and 12 lines of descending flow at the Earth's surface.

An additional 240 convective cells are drawn in the upper mantle and asthenosphere. Surface mapping based on this system can then be carried out to a defined degree of accuracy. The first requirement is to visualize the three-dimensional shape of the cells. In a vertical cross-section at the equator, they can be represented as circular. In comparable cross-sections north or south of the equator, however, they must become elliptical in the east-west direction in order to remain within the Earth's layers while fitting the progressively smaller circumference at higher latitudes.

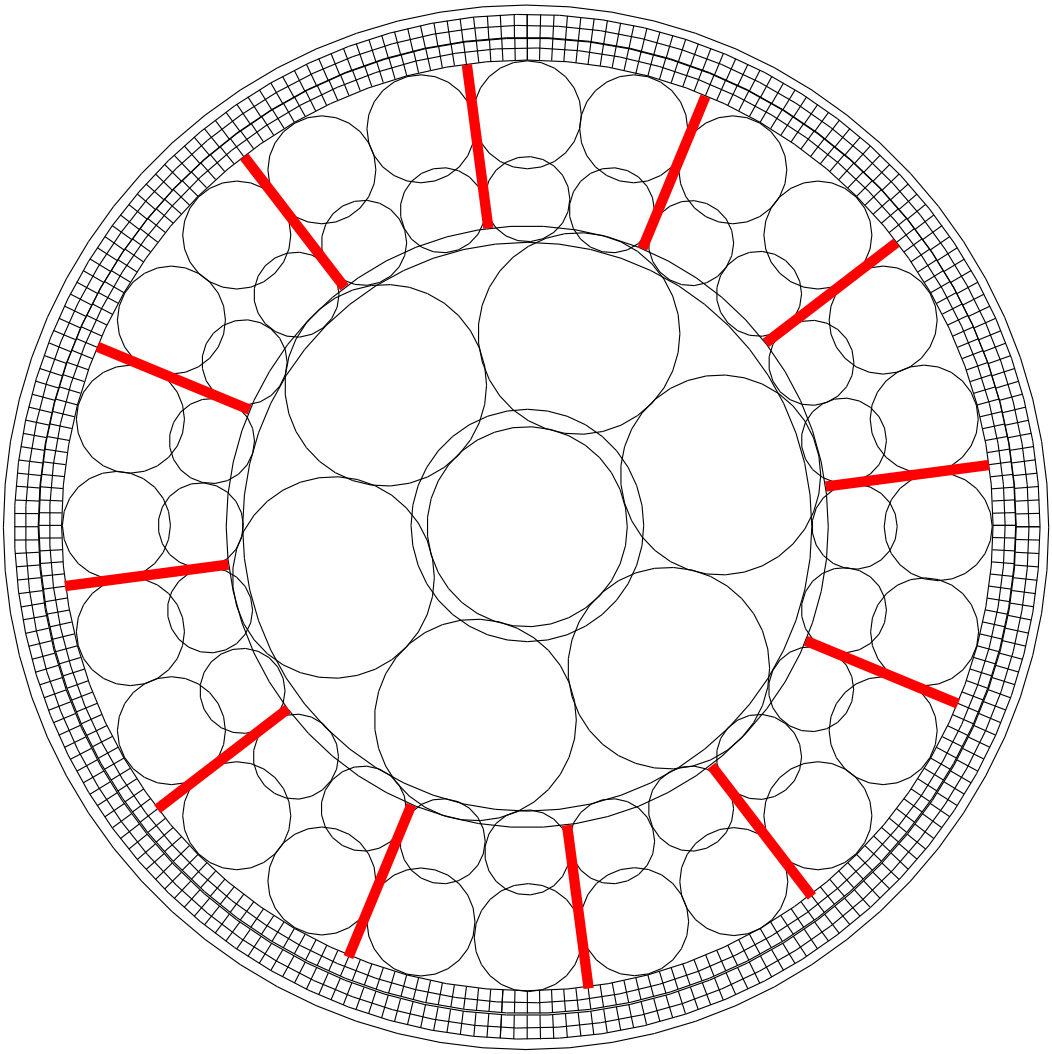

Figure 8: The 12 main division lines of the system.

2.4. Height and breadth of convection cells

The reasoning used here begins with the assumption that conditions within the Earth's mantle tend toward a balanced state. This is based on the immense timescale involved - more than four billion years - the size of the Earth, and the relative long-term stability observed at the surface. On this basis, a stable system must exist for transferring internally generated heat toward the surface. In the terminology used here, such a system would tend to minimize 'frictional factors'[1] that disturb an otherwise balanced pattern of flow.

The starting point is the pattern of circular convection cells whose diameter is the same as that of the inner core. As noted earlier, the clue leading to this line of

1 The term 'frictional factor' is used here to describe conditions that would disturb a perfectly balanced dynamic system.

analysis is that the inner-core diameter is equal to the thickness assigned here to the outer core together with the Gutenberg layer. Extending the same geometrical comparison, the inner-core diameter also corresponds to the thickness of the mantle interval from about 410 to 2,900 km.

Geophysical reasoning also encourages consideration of such a regular state. In relation to Bénard convection (Manneville 2010) (Walzer 1971) (Paldor and Killworth 1988), regular systems of material flow can occur under balanced conditions[1]. Given the long timescale and the relatively uniform conditions considered within an individual convection cell, the model assumes that upwelling forces and resistance can approach a balanced state. This provides the physical premise used here for convection cells whose height and breadth are approximately equal.

It is noteworthy that the geometrical model can be compared with a theoretical framework describing conditions under which such regular convection may develop. This provides an independent basis for examining the many observations that are compared with the convection-cell model.

The graph below illustrates the relevant relationship described by Manneville (2000).

boundary conditions (5) obtained by Pellew & Southwell (1940). The minimum of each curve defines the corresponding threshold above which convection sets in, $R_c = 27\pi^4/4 \simeq 657.5$ and $R_c \simeq 1708$ for stress-free and no-slip conditions

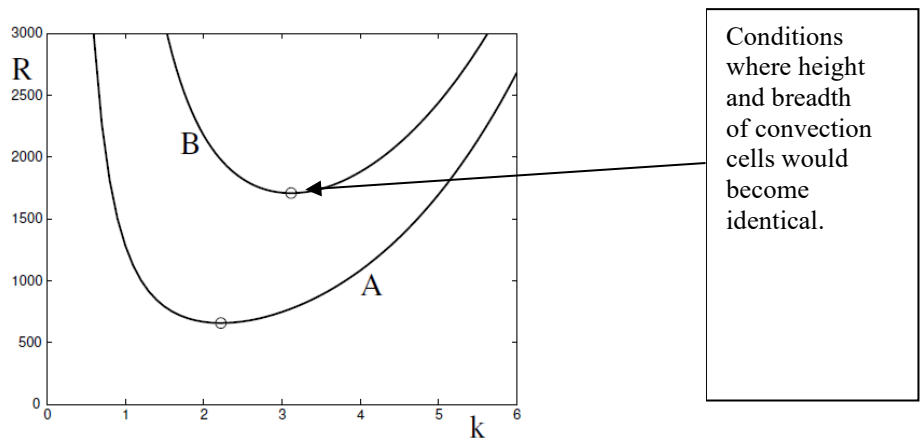

Fig. 3. Marginal stability curves for stress-free (A) and no-slip (B) velocity boundary conditions and isothermal plates (infinitely large conductivity).

Figure 9: The point corresponding to the conditions within the mantle if the conditions were balanced, as explained by Manneville (Manneville 2010).

1 Here, 'balanced conditions' within a system of material flow refers to a balance between factors such as buoyancy and viscosity, so that no net factor continuously accelerates or decelerates the prevailing flow.

At the lowest point on curve B, the convection cells approach a geometry in which height and breadth are almost identical. The resulting form of convection is illustrated below:

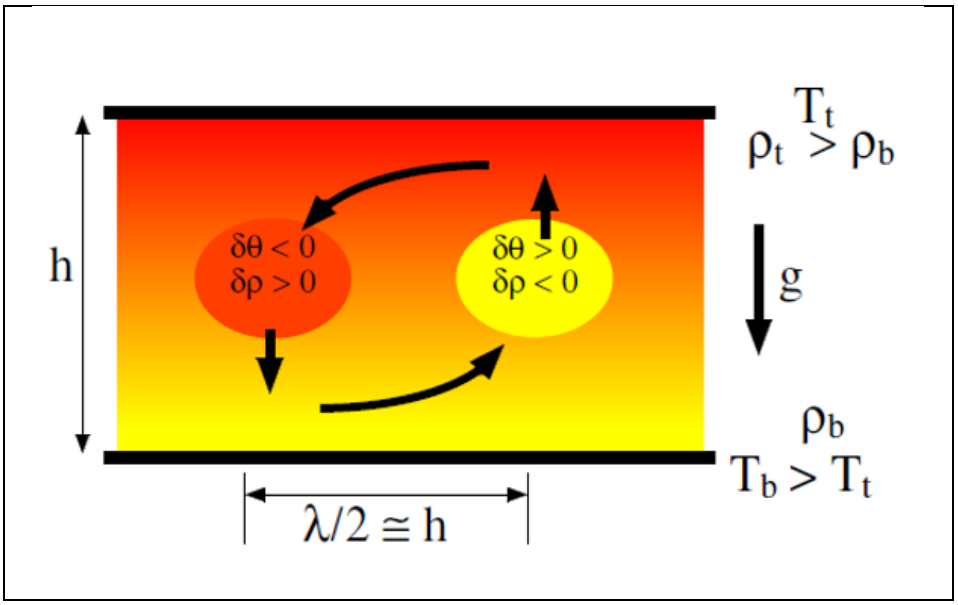

Figure 10: A convection cell with equal height and breadth[1].

The regularity of this system has a basis in the physics of the model. The expected diameter of the convection cells is half of the so-called critical wavelength, $\lambda c = 2\pi / kc$, where kc is very close to π (Manneville 2010).

The figures illustrate the conditions proposed for the Earth's interior, including the balanced conditions discussed by (Walzer 1971) and the geometrical fit between convection currents of approximately equal height and breadth and the layering of the Earth.

Conditions in such a system of material flow have been analyzed in detail in the context of Rayleigh-Bénard (RB) convection (Manneville 2010), where 'R' stands for Rayleigh and 'B' for Bénard. Manneville's discussion, particularly Chapter 2, 'RB convection at threshold,' is directly relevant here. In that chapter, he describes the conditions under which regular convection rolls appear. The boundary conditions considered include stress-free and no-slip cases. Manneville presents two marginal-stability curves for stress-free (A) and no-slip (B) velocity boundary conditions with

[1] From Manneville (2000).

isothermal plates (assumed to have infinitely large conductivity):

> A straightforward calculation from the Boussinesq equations (1-4) and boundary condition (6) yields the marginal stability condition:
>
> $$R_m(k) = \frac{(k^2 + \pi^2)^3}{k^2}$$
>
> Where k is the length of the horizontal wave-vector k_h. The curve is displayed in Fig. 3, together with that corresponding to the more realistic no-slip velocity boundary condition (5) obtained by Pellew & Southwell (1940). The minimum of each curve defines the corresponding threshold above which convection sets in, $R_c = 27\ \pi^4/4 \approx 657.5$ and $R_c \approx 1708$ for stress-free and no-slip conditions respectively. The expected diameter of the expected convection cells is half the critical wavelength $\lambda_c = 2\pi/kc$. In the no-slip case $kc \approx 3.12$ which makes the predicted diameter very close to the height of the cell.

To relate this theoretical value more directly to the proposed geometry, Manneville's discussion can be used to examine why the height and breadth of convective rolls may become comparable (Manneville 2010):

> As the Rayleigh number exceeds the threshold value, part of the heat is transported by convection which decreases the potential for instability, while thermal diffusion and viscous friction increases due to the horizontal gradients implied by the modulation. This explains that the amplitude of the motions saturates beyond threshold. For rolls, the bifurcation turns out to be supercritical, i.e. behaves continuously in the vicinity of the threshold and the system builds up a well-defined steady pattern.

To examine further the possibility that convection currents may have an approximately circular basic geometry, I also refer to Uwe Walzer (1971). Walzer presents several systematic ideas about the possible distribution of convection cells within the Earth. In the summary of his article, he emphasizes a high degree of regularity in the convection system (Walzer 1971):

> Here it is essential, for the reason of symmetry, that the current system has a degree of regularity as high as possible and is modified only in the upper part, mainly due to the distribution of continents and oceans.

The specific pattern used in this book does not appear in Walzer's work, possibly because his model does not allow the convection layers to intersect. Nevertheless, he regarded the correspondence between a regular convection system and the Earth's

structure as quantitatively significant, writing that 'the system yields the seismic discontinuities of the Earth's mantle as a secondary product.'

2.5. Different levels of geometrical constraint within the model

An important distinction should be made between the convection-roll system proposed for the depth interval from approximately 120 to 670 km and its extension into the lower mantle. The four upper roll sets are geometrically much more tightly constrained. Each set contains 240 rolls distributed around the Earth, corresponding to an angular spacing of approximately 1.5°. As the radius of the Earth decreases with depth, the dimensions of the rolls decrease progressively as well. The resulting sequence of roll dimensions is highly regular, and the calculated geometry corresponds closely to the principal mantle boundaries near 120, 410 and 670 km.

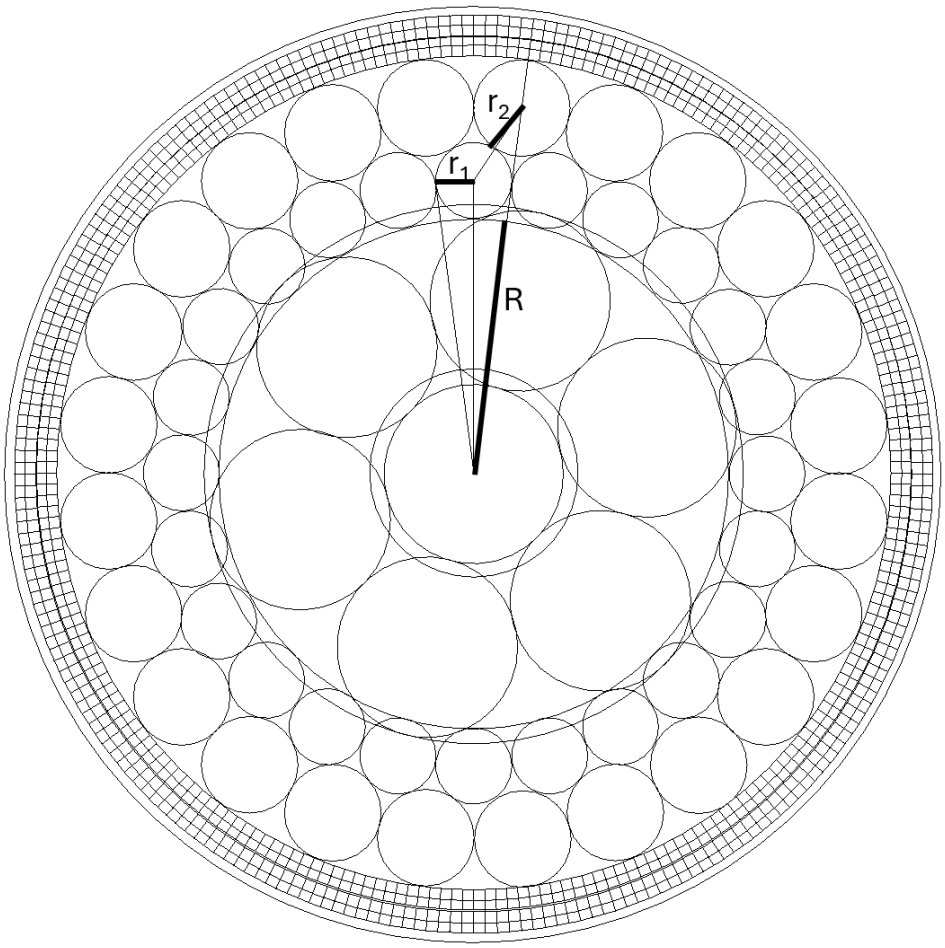

Figure 112: A convection cell with equal height and breadth.

As R is 6,371 km -2,900 km = 3,471 km, r1 = 519 km and r2 = 657 km. The transition zone of lower mantle is calculated from 1,858 to 1,980 km depth, with a central flow division near 1,919 km.

This part of the model is therefore not dependent on assigning a single constant roll size throughout the interval. Instead, the dimensions change systematically with depth while the same geometrical rule is maintained. The overlap between adjacent roll layers is also comparatively regular because neighbouring rolls are similar in size. In such a system, the geometrical midpoint of the overlap provides a reasonable approximation to the physical boundary between adjacent convection layers. The correspondence of this four-layer system with the 120, 410 and 670 km boundaries has been presented previously and constitutes one of the more tightly constrained geometrical elements of the model.

The situation in the lower mantle is less certain. The proposed arrangement there consists of 24 rolls in each of two layers, giving an angular spacing of approximately 15°. Unlike the shallower system, however, the rolls in the two lower-mantle layers differ substantially in size. Consequently, the geometrical interaction between the layers is inherently less symmetrical. A construction based on idealized circles or near-circular roll profiles can therefore only approximate the real overlap between the two convective systems.

In particular, the mathematical point of contact between two idealized roll profiles should not necessarily be identified directly with a physical boundary in the mantle. Real convection involves distributed deformation, viscous flow, thermal gradients, mineralogical changes and compositional effects. Where rolls of unequal size interact, the overlap may also be asymmetrical, so that the effective boundary may be displaced relative to the geometrical contact point. R1r_1

Preliminary geometrical examination suggests that such asymmetry could be sufficient to account for differences of several tens of kilometres between the idealized construction and the observed depth of the approximately 660–670 km discontinuity. This possibility is of interest, but it should at present be regarded as exploratory rather than as a demonstrated physical mechanism. Establishing the actual position and nature of internal boundaries within the lower mantle would require substantially more geophysical and fluid-dynamical investigation.

The principal point is therefore that the highly regular four-layer system between approximately 120 and 670 km can be considered separately from the more tentative extension into the lower mantle. The former provides a closely constrained geometrical framework, whereas the latter represents a possible continuation of the same underlying organization whose detailed internal structure remains less well determined.

Chapter 3 - The 410 km and 670 km Discontinuities

The convection-cell system above the 410 km discontinuity is particularly important to analyze because it lies relatively close to the Earth's surface. The larger convection cells below are more readily identified, as described in Chapter 2 and discussed again in Chapter 7. They can therefore provide a reference for tracing the upper cells. Without this regular system of large convection cells, it would be difficult to determine where the uppermost system should begin. Since the diameter of the core provides the principal dimensional reference for the model developed in this book, attention is naturally directed to the interval between depths of 410 and 120 km, where convection is not expected to occur in the crustal part of the mantle above 120 km (Francis 2000).

3.1. Uppermost Convection Cells of the Asthenosphere

This section examines the asthenosphere and seeks to identify the convection cells of the upper mantle. These upper-mantle cells can be approached in a manner similar to the larger cells proposed for the lower mantle and outer core. In the vertical construction, the uppermost 410 km lies beyond the reach of the lower-mantle convection cells[1]. The number of convection cells can then be calculated from the postulates used in this book and compared with geological and geographical observations. The first indications of the dimensions of the uppermost cells are found at the surface. Mapping in Iceland, using the directions already derived for the system, gives one line every 1.5° from east to west, corresponding to 240 cells around the Earth. The next question is whether sufficient space exists for such cells. According to measurements (Cristopherson 1992), a transition zone occurs at a depth of about 250 km. The upper boundary of this convecting region is placed at about 120 km. This is described as follows (Francis 2000):

> Plate tectonics concern lithospheric plates, rather than drifting continents. Within the rigid lithosphere, heat is transferred to the surface by conduction and temperature increases progressively with depth. At a depth of about 120 km, the temperature reaches about 1350°C, rocks are no longer rigid, heat is transferred by convection, so temperature increases much less rapidly with

[1] In this model, the conventional definition of the lower mantle as beginning below 670 km is not followed, in order to remain consistent with the proposition used here that the lower-mantle convection cells have the same diameter as the inner core.

depth. It is convenient to define the boundary between lithosphere and asthenosphere at the intersection between the two thermal gradients.

This provides the basis for placing the upper limit of the convection-cell system at a depth of about 120 km. Above this lies an essentially rigid plate, divided into brittle and ductile parts, with the well-known Moho representing one of the principal boundaries. This leaves an interval of about 550 km in which convection may occur within the upper mantle and asthenosphere. These dimensions are based on the measurements cited above.

When considering the arrangement of convection cells close to the crust, I retain the measured thicknesses of the relevant layers. One reason for examining whether this entire interval can be occupied by regular convection cells is the geometrical relationship shown in the following figure.

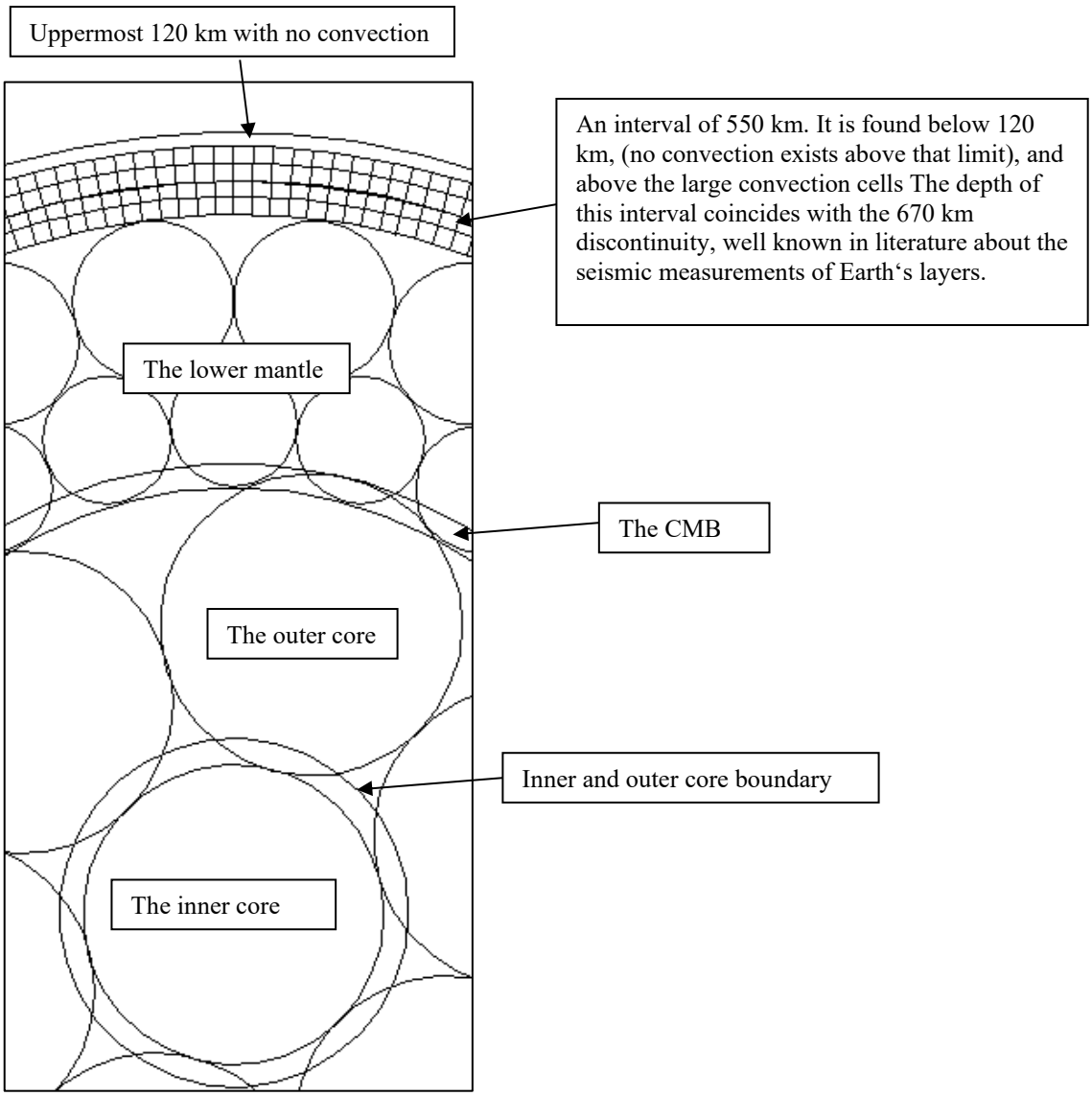

Figure 12: The inner structure of the Earth as interpreted with convection rollls model.

Given this correspondence—namely, that the Gutenberg layer coincides in the model with the mathematical intersection of convection cells of equal height and breadth—it is natural to examine whether similar regularity can be found in the remaining interval between 120 and 410 km, assuming that the balanced physical conditions described by (Walzer 1971) are retained.

Simple trigonometry is sufficient to estimate the basic dimensions of the cells within this 'gap' (see the figure below). Petrological considerations lead us to examine two layers, discussed elsewhere in the book, one associated with MORB and the other with OIB (McBirney 1993). Several aspects of the model suggest that two broadly similar layers may occupy the interval between the large mantle cells and the tectonic plates. One is the requirement for horizontal circulation, which can be represented if two separate layers occur within these boundaries.

A double-layer arrangement with an intersection zone can be calculated by constructing a right-angled triangle with sides a, b and c. The angle between a and b is 90°. Line c passes through the centres of two identical circular convection cells, and its length is twice that of b. At the surface, this gives the following relationship:

$$(2b)^2 = b^2 + a^2;\ (2b)^2 - b^2 = 290;\ 3b^2 = 290^2;\ b = \underline{167{,}4\ \text{km}}$$

With a=290, we get b=167,4, c=325. And: 40,000 km / 167.4 ≈ 240

Because the number of cells is required in this model to be divisible by 12, 240 convection cells are used in each layer, with the centre of each cell at a depth of approximately 194 km (see below).

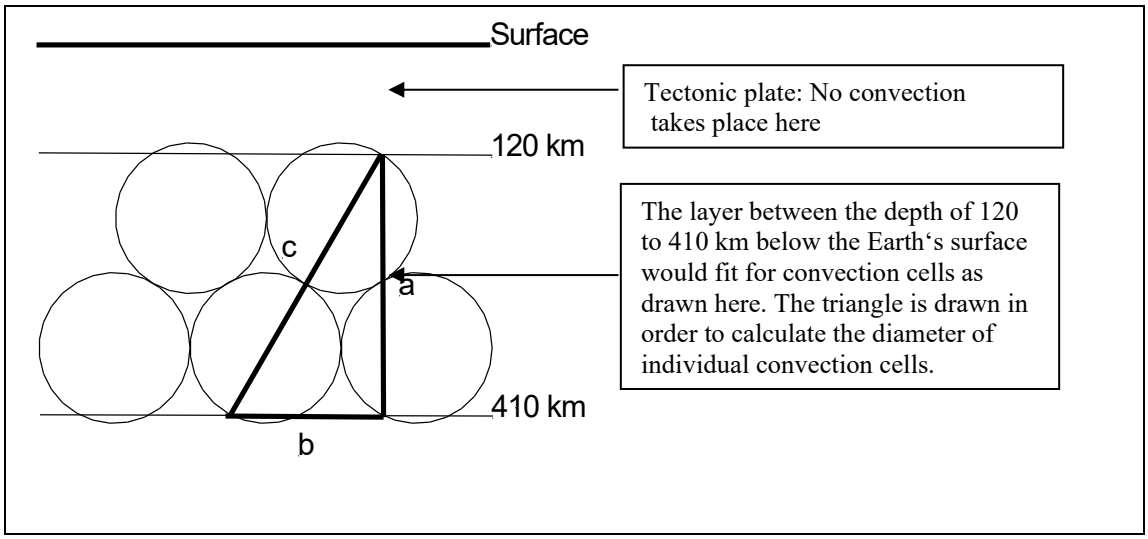

Figure 13: Trigonometric construction used to calculate the dimensions of the uppermost convection cells[1]

The basic calculations based on Figure 13 are as follows. The approximate circumference of the Earth at this depth is:

$$(120\ \text{km} + (\cos 30° * (167/2)) \approx 194\ \text{km}$$

$$2 * \pi * (6{,}371 - 194) \approx \underline{38{,}811\ \text{km}}.$$

[1] Note that the circles represent dimensions rather than literal flow lines. For geometrical clarity, the upper circles extend into the tectonic plate so that the triangle dimensions can be shown clearly (c = 2b). When the curvature of the Earth is taken into account in Figure 15, the uppermost cells no longer intersect the ductile layer of the tectonic plate.Figure 14

The approximate diameter of each cell is then obtained by dividing the calculated circumference at this depth by the number of cells:

$$38{,}811 \text{ km} / 240 \approx \underline{162 \text{ km}}.$$

The flat-layer model can then be set aside in order to examine how the curvature of the Earth and the 410 km and 670 km discontinuities fit the convection-cell model. The interval from 410 km to 670 km is taken here as 250 km, 30 km less than the 290 km interval between the ductile layer and the 410 km discontinuity. Another system of 240 convection cells in each layer would fit within this interval as well. The diameter of the cells becomes smaller as the circumference decreases:

Approximate radius of cells in upper layers:
Layer 1: 162 km
Layer 2: 158 km
Layer 3: 154 km
Layer 4: 150 km

The resulting cross-section, showing the curvature of the Earth's surface together with the 410 km and 670 km discontinuities, is shown below:

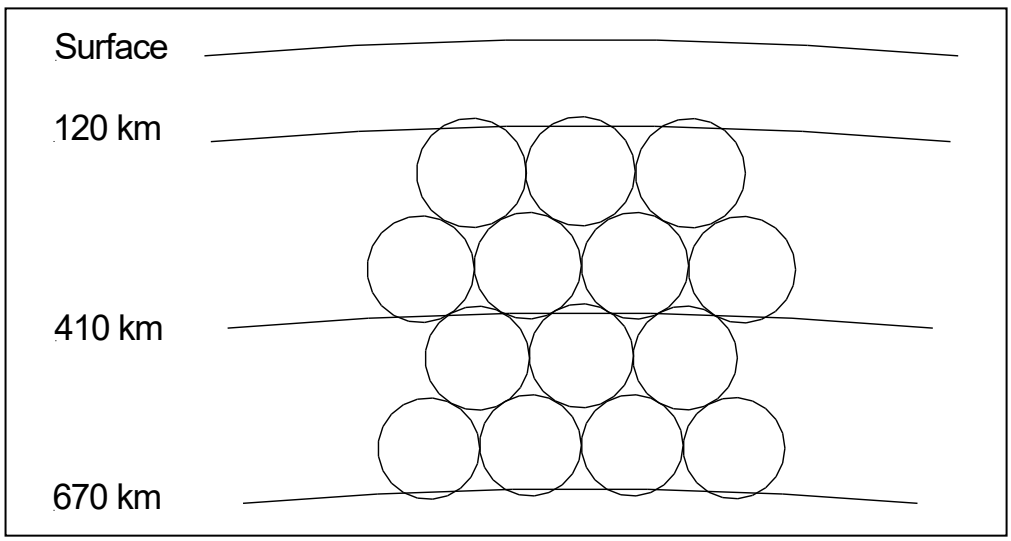

Figure 14: The 410 km and 670 km discontinuities and the convection-cell system.

This can be calculated in detail as shown here:

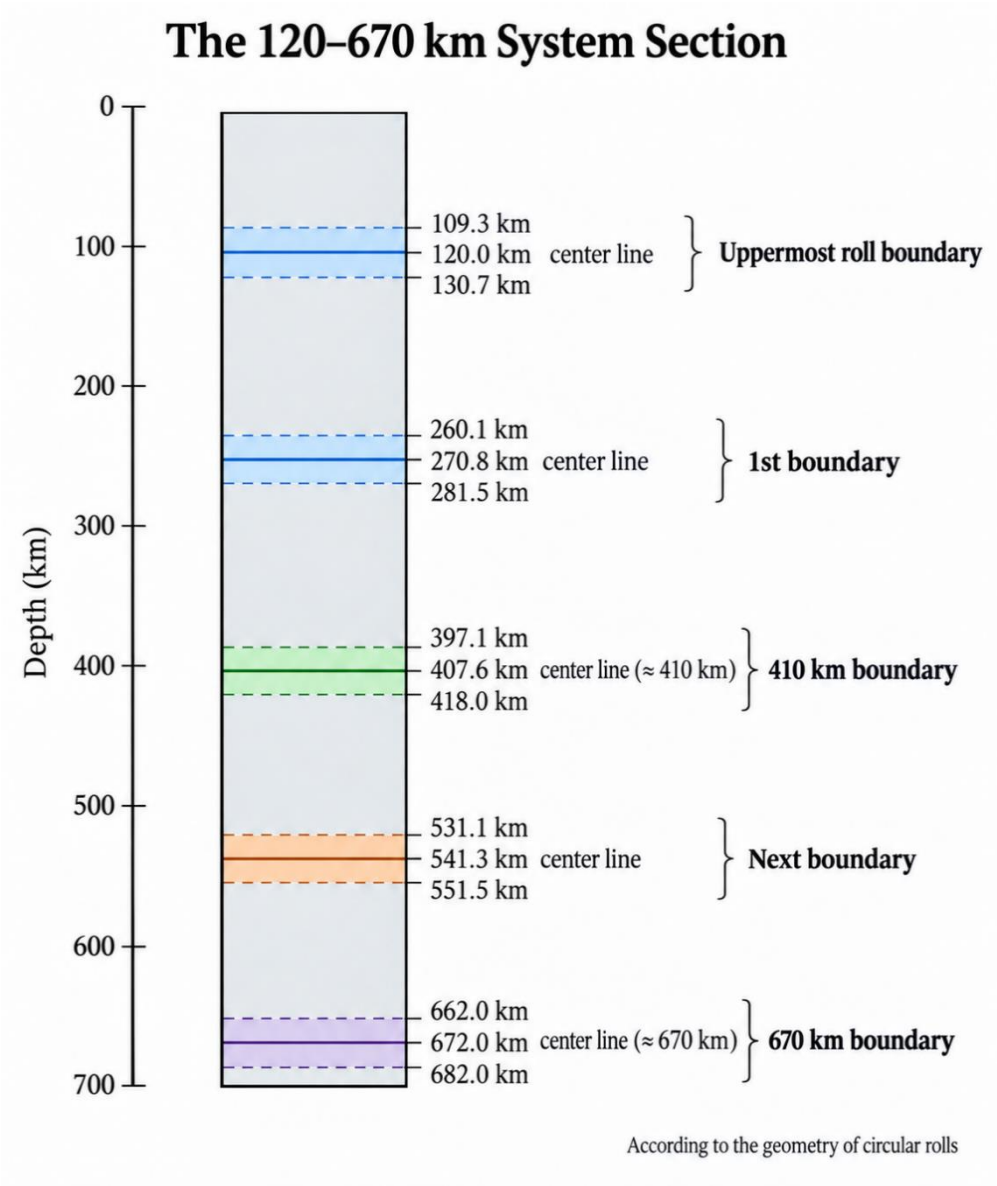

Figure 15: The discontinuities of 120, 410 and 670 km, as calculated.

Further mathematical refinement is not required at this stage, because the purpose of the calculation is to identify a simple whole-number proportion. The result gives 10 smaller cells in one layer above each of the 24 large lower-mantle cells. Figure 16 therefore combines the large cells with the smaller cells above them. Extrapolating according to the outer and inner core boundary further adds to the picture, as a speculative part.

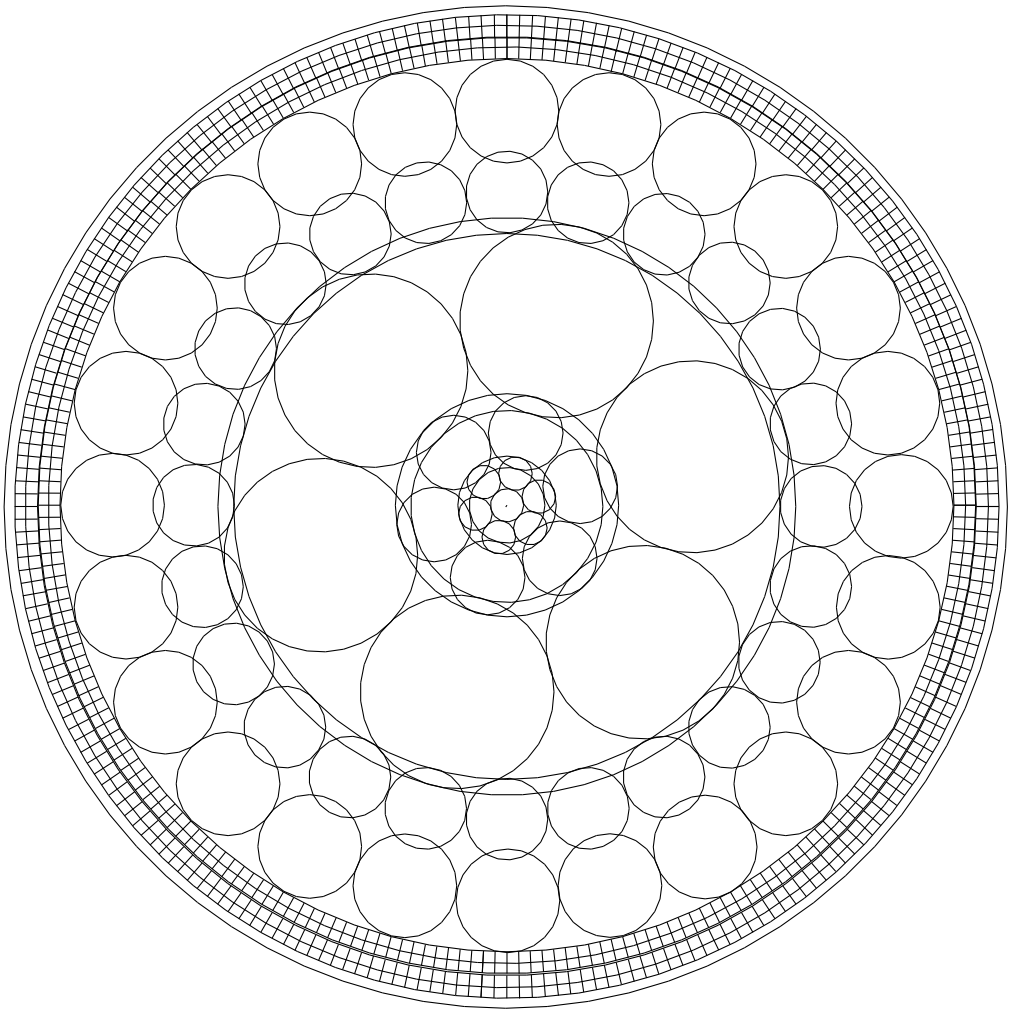

Figure 16: The convection-cell model with the four uppermost layers of smaller cells included.

This picture emerges when the convection cells between the 410 km and 670 km discontinuities are included. At that stage, a flow-line model is more appropriate than the dimensional model[1] described above.

3.2. The Structure of the Upper Layers

The layers beneath the crust and within the crustal part of the mantle can be represented in different ways. When considered in relation to the proposed convection-cell system, however, a clearer structural picture emerges.

[1] The dimensional model uses circles only to indicate the height and breadth of each cell. A flow-line model would instead include vectors showing the direction of material (magma) flow.

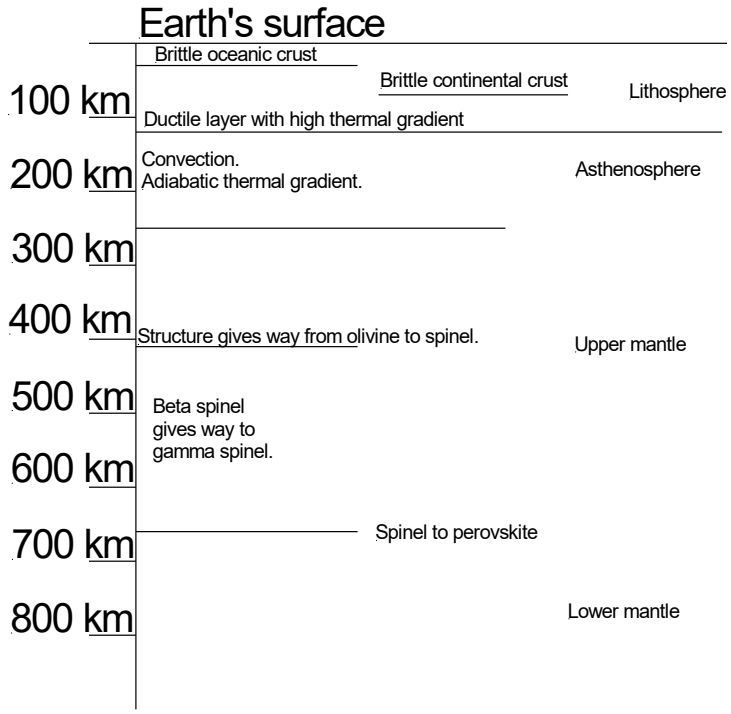

The uppermost layers of the mantle and crust

Drawn according to McBirney (1993) and Christopherson (1992).

Figure 17: The upper layers of the Earth.

The lithosphere consists of several layers, including a brittle crust and a ductile region in which convection does not occur to any significant extent. In the model developed here, this ductile layer plays an important role in determining the distance from the brittle crust to the uppermost convection layer. With these constraints in place, the vertical arrangement of the convection system through the Earth's upper layers can be outlined.

At the equator, the cells should be positioned directly above one another. The intersection zone is expected to change shape continuously while maintaining the same balance between the outer core and mantle.

3.3. Convection Cells Compared with the Upper Layers

The mathematical approach of the preceding section and the geophysical measurements considered here provide two complementary perspectives. The next step is to draw the convection cells below the crust and compare their geometry with the principal features of the layers identified by geophysical measurements.

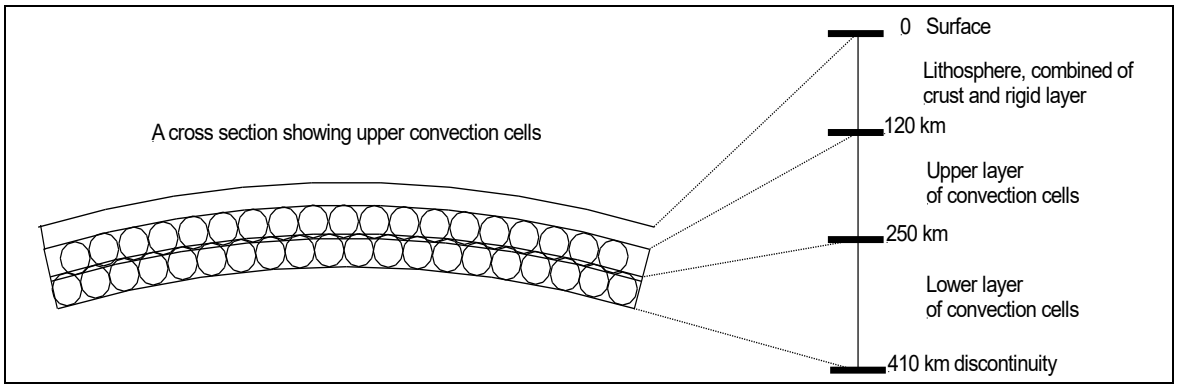

Figure 18: Convection cells of the asthenosphere and upper mantle

The layers close to the Earth's surface are shown here over a 30° section of the equator. The lithosphere can move over the asthenosphere. Discontinuities occur at depths of about 410 km, where olivine gives way to spinel, and 670 km, where spinel gives way to perovskite (Francis 2000). The 410 km discontinuity is emphasized because the convection-cell system proposed here fits this boundary, whereas no indication is found that the 670 km discontinuity represents a difference in chemical composition (Foulger 2010). In the model, the 670 km transition zone nevertheless fits as a continuation of the asthenospheric convection-cell system described in the previous section. The coexistence of two explanations for the layering—pressure-induced mineral transformations at particular depths and a geometrical correspondence with the convection-cell pattern—is treated here as compatible rather than contradictory.

A theoretical transition zone is introduced at a depth of about 265 km. In the simplest calculation, this lies approximately midway between 120 km and 410 km, and the relevant transition layer is expected to be about 20 km thick. A mathematically derived transition layer of approximately 15 km thickness is placed between about 255 and 270 km[1]. Smet et al. (1999) report that the mantle above 250

[1] The simple trigonometry used to calculate the dimensions of the uppermost cells cannot be applied here directly, because the lower cells lie on an inner, slightly smaller circle and are therefore smaller as well.

km is more depleted than the mantle below that depth. Their model divides the crust and upper mantle into four layers: Hc from 0–16 km, Hl from 16–50 km, depleted mantle from 50–250 km, and undepleted mantle from 250–670 km.

The heat-flow values for these layers are:

Hc = 4,13 μWm^{-3}, Hl = 0,9 μWm^{-3},

Hd = 0,04μWm-3, and Hu = 0,09 μWm-3.

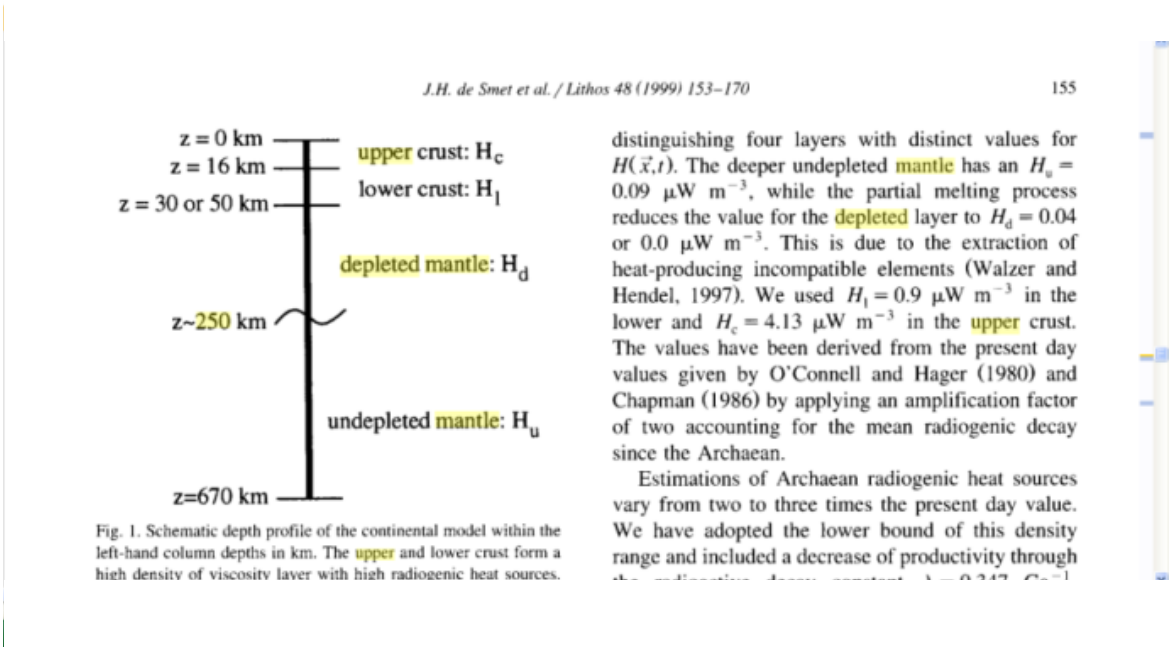

Figure 19: According to Smet et al. (1999), the mantle is less depleted below 250 km[1].

This is interpreted here as strong evidence that two sets of convection cells are separated at a depth of about 250 km. The result is consistent with the present analysis because this depth lies approximately midway between 120 km, where the adiabatic heat gradient replaces the higher gradient of the tectonic plates (Francis 2000), and 410 km, the upper boundary of the large lower-mantle convection cells.

In the model, the convection-cell system beneath the lithosphere maintains the same basic pattern around the globe. Continuous flow requires a complete circulation

[1] J.H. de Smet et al. / Lithos 48 (1999) 153-170

of mantle material; the system cannot simply terminate. The different layers must therefore include a mechanism that allows material to be redistributed while maintaining steady circulation in the required directions. Here this is represented as an "exchange system" of magma, allowing material to pass between adjacent parts of the system. An intersection zone must consequently be large enough for the convection units to overlap. This relationship is then used to derive the dimensions of the complete system, both vertically and horizontally, producing a three-dimensional model of convection within the Earth.

Internal consistency is an important requirement of the model, particularly in the transition zones between individual convection-cell layers. In this description, the Gutenberg layer is treated as a larger-scale analogue of the transition layer measured near 250 km depth. On this basis, a double set of convection cells, each with a diameter of about 160 km, can be fitted into the measured layering of the Earth.

Chapter 4 - The Shape of the Convection Cell System

To develop a three-dimensional model of the Earth's convection-cell system from the equator to the poles, the geometry must first be traced from the equatorial region, where the proposed relationships are most clearly expressed. The upper layers between approximately 120 and 410 km depth must also be considered in sufficient detail to connect the vertical model developed in the preceding chapters with its horizontal expression.

The analysis in the previous chapter proposes 240 convection cells within the asthenospheric system, corresponding to a spacing of 1.5° around each latitude (360°/240 = 1.5°). The uppermost convection-cell system can therefore be represented on a geographical map as a grid of parallel, curved lines whose east-west spacing remains 1.5° in angular terms. Once the positions of these cells have been defined, a basic horizontal model of the uppermost regular convection system can be constructed. In the second part of this work, Iceland is used as a regional example to examine whether this predicted pattern corresponds with the distribution of geothermal and tectonic features. Before the vertical model can be projected horizontally onto the Earth's surface, however, the relevant physical and geometrical relationships must be considered.

4.1. The Coriolis Effect on the Convection Cells

Within the model, the curvature of the convection cells is attributed primarily to the Coriolis effect (Condon and Hugh 1967). To establish the geometrical conditions governing the system, it is therefore necessary to consider how the Coriolis effect acts on moving material. Two components are particularly relevant here: its influence on vertical motion and its influence on horizontal motion. Atmospheric and oceanic circulation provide useful analogies because they also involve large-scale motion on a rotating Earth, although their physical properties differ greatly from those of the mantle. These analogies are especially useful for visualizing the distinction between lower- and higher-latitude circulation. Ocean circulation also provides a conceptual comparison for the uppermost mantle layers between approximately 120 and 410 km depth, where different circulation levels may interact.

In each of these systems - atmosphere, ocean and mantle - motion must be considered within the rotating frame of the Earth. In the mantle, however, the vertical scale is much greater than in atmospheric and oceanic circulation, and the velocities and physical properties are very different.

In the proposed model, ascending mantle material is displaced westward relative to the overlying crust, while descending material is displaced eastward. The horizontal and vertical components of circulation must therefore form a coherent three-dimensional system. For this reason, the horizontal component is as important as the vertical component when the overall geometry of the convection-cell system is considered.

As developed in the following section, the Coriolis-based geometry of moving material is used within this model to derive the dimensions of the horizontal convection paths.

4.2. The Diameter of Circular Horizontal Flow on a Perfect Sphere

The atmosphere and oceans provide useful points of comparison when considering the possible shape and scale of horizontal circulation within the mantle. The geometrical problem can be approached using the following description of inertial motion (Paldor and Killworth 1988):

> Inertia currents are characterized by the simplest possible dynamics; no forces whatsoever act on any element of fluid. Under the assumptions of zero pressure gradient, no friction or boundary effects, and that buoyancy forces suitably cancel, a two-dimensional inertial motion on a geopotential surface will occur. The length scale associated with such a flow is quite large, as no retarding forces obstruct the propagation of a fluid element and is usually of the order of the earth's radius.

This description provides the physical starting point used here to search for a mathematical relationship between the Earth's radius and the characteristic scale of horizontal circulation. In the model, horizontal flow is arranged symmetrically about the equator in a mirrored pattern of circular arcs. A defining condition is that the east-west diameter of each modeled circle, measured along its central latitude, corresponds to the radius of the Earth.

Additional reference points can be obtained by requiring the same circle to intersect the equator at two points 30° apart. The proposed north-south horizontal circulation originates from convection that is predominantly vertical, and it must therefore remain geometrically consistent with the underlying heat-transfer system[1]. In this construction, horizontal circulation beginning at an upwelling boundary between two large lower-mantle cells returns towards the corresponding downwelling side of the same convective system[2]. The pattern is repeated around the Earth and, when represented on a world map, the modeled flow is generally directed from west to east. With these conditions specified, the horizontal geometry can be calculated on a rectangular grid in which one degree of latitude and one degree of longitude are represented by equal units.

---

[1]Keep in mind that radioactive elements generate heat and that the movement of mantle material transports heat upward.

[2] See the *Teaching material*, added as appendix to this essay.

This condition is satisfied close to the 32nd parallel, as illustrated below:

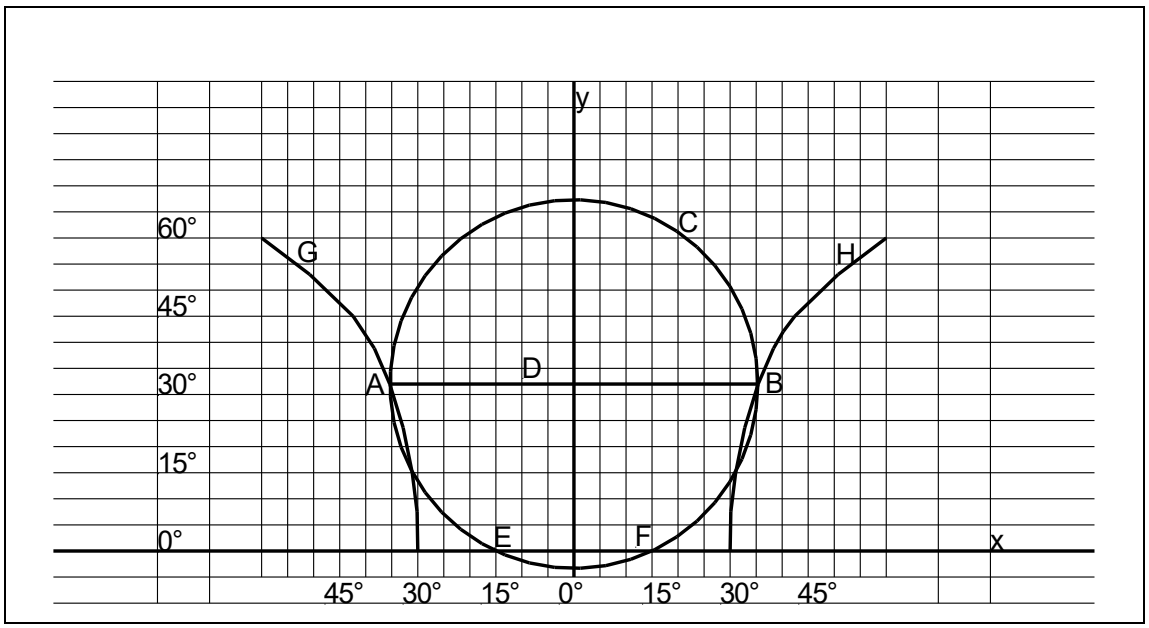

Figure 20: Relationship between a horizontal circle on a rotating sphere and the Earth's radius.

Explanation:

The graph represents longitude and latitude on a rectangular grid. Longitude is arbitrary here, so 0° need not correspond to Greenwich. Circle C has diameter D between points A and B and intersects the x-axis, representing the equator, at E, 15° east of the y-axis, and F, 15° west of it. The two equatorial intersections are therefore 30° apart. Lines G and H are defined by Equation I:

(I) $$x = \pm(1/\cos\varphi)*30$$

Here φ denotes latitude, represented by the y-coordinate of the grid. The two lines intersect the equator at ±30°. By definition in this construction, the distance between these two points corresponds to the radius of the sphere, i.e. the Earth.

The lines therefore show the longitudinal separation, expressed in degrees along each parallel, required for the physical distance between them to equal the Earth's radius. The objective is to identify the latitude at which these lines intersect the modeled circle in such a way that the same intersection points also define the diameter of that circle.

Because a circle is defined by x2 + y2 = r2, the circle equation can be combined with Equation I. The modeled circle must cross the x-axis at ±15. The resulting geometry can be represented as a right triangle whose horizontal side is 15 units,

whose vertical side is unknown, and whose hypotenuse is defined by Equation I for the corresponding value of y.

The Pythagorean relation (a2 + b2 = c2) can then be applied, using Equation I for side c:

(II) $$x^2 + y^2 = ((1/\cos(y))*30)^2$$

The latitude at which the center of the modeled circular path is located on a perfect sphere is obtained by solving:

(III) $$((30/\cos(y))^2 - y^2 - 15^2 = 0$$

The solution is y ≈ 32.066, corresponding to approximately 32°N and 32°S.

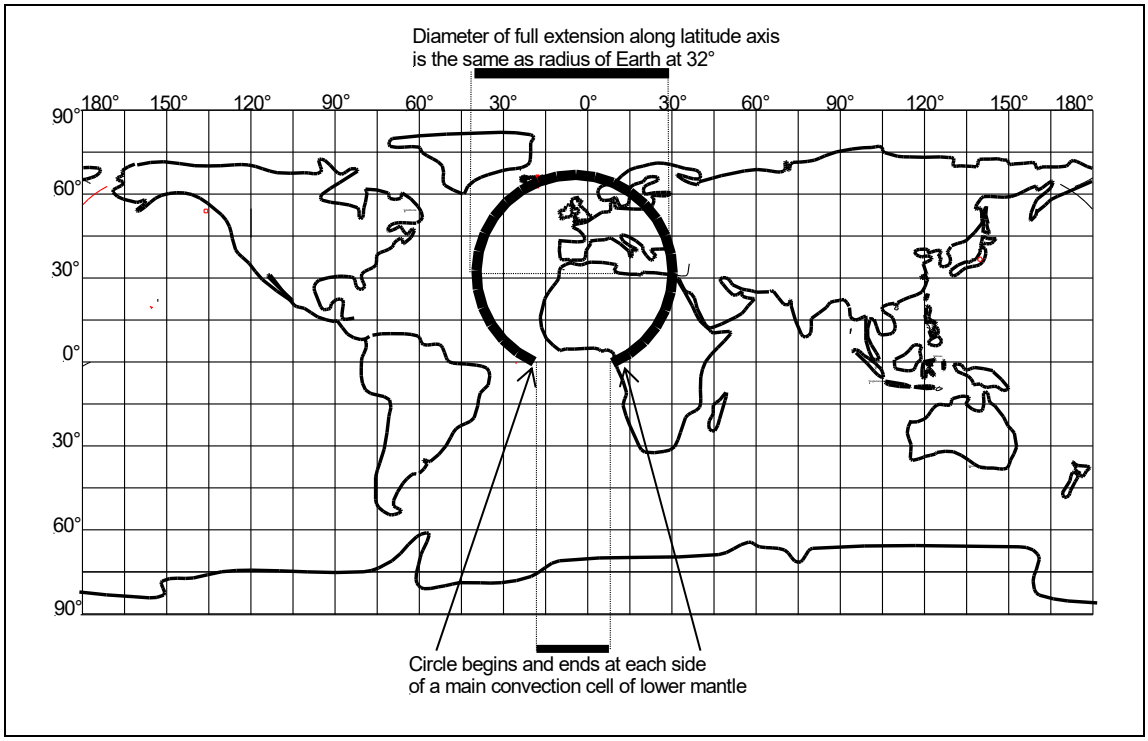

Figure 21: Calculated dimensions of the horizontal circulation path of the convection rolls.

Figure 22 illustrates the resulting arc. Two points on the path are fixed on the equator, providing the first geometrical constraint. The second is obtained by requiring the diameter of the modeled circle, measured along its central parallel, to correspond to the reference scale defined above. Together, these conditions determine the circular approximation used in the model.

For a mathematically perfect sphere, the construction therefore gives a unique

circle satisfying the stated conditions: it intersects the equator at points A and B and has the prescribed diameter D[1].

The real Earth is not a perfect sphere, so the precision implied by the mathematical solution must be treated cautiously. For the purposes of this model, the central latitude is therefore expressed as approximately 32.0° ± 0.1°. The effects of the Earth's geoid form and the associated uncertainty are considered further below.

A second geometrical solution, illustrated earlier in Figure 17, occurs at approximately 18.5°N and 18.5°S. From an equatorial starting point, this path extends 60° eastward, providing a second characteristic scale within the proposed circulation system. In the model, the 410-670 km transition interval is associated with this geometry as part of the larger convection-cell arrangement.

4.3. The Average Diameter of Horizontal Circulation

The calculated central latitude for the modeled horizontal circulation on a perfect sphere is 32.066°. The additional decimal places are not retained in the working model because the Earth is not a perfect sphere and the intended level of geographical accuracy is lower. The geoid form of the Earth[1] implies that the curvature differs slightly from the idealized spherical case. The earlier description of an inertial flow with a length scale 'of the order of the earth's radius' (Paldor and Killworth 1988) is therefore used here as a scale relationship rather than as an assertion of exact identity on the real Earth.

The span of the theoretical circle along the 32nd parallel is therefore:

$$1/\cos(32))*30 = 35.34 \text{ degree units}$$

Using this method, the circular approximation becomes:

$$(x)^2 + (y - 32)^2 = 35.34^2$$

This gives a modeled horizontal-flow diameter of $2 \times 35.34° \approx 70.7°$,
or 70.7 units on the rectangular degree grid used in the construction.

The modeled convection-cell circle therefore spans approximately 70.7° along the 32nd parallel. Converting this angular span back to a physical distance provides a further comparison with the characteristic length scale of the Earth used in the model:

(cos32*111.111km per degree) * 70.7 degrees * (3/π)
which gives:
$$0{,}848*111{,}111*70.7*(3/\pi) = 6{,}360 \text{ km}$$

The calculated value of approximately 6,360 km is close to the reference value of about 6,371 km used in this construction. Some uncertainty is expected when a geometrical result derived for a perfect sphere is compared with the real Earth. The important point for the present model is the correspondence with the statement that 'the length scale of such a flow is usually of the order of the earth's radius' (Paldor

[1] en.wikipedia.org/wiki/Geoid

and Killworth 1988). The model further assumes that, over the very long timescales involved, the relevant convective circulation approaches a stable relationship between buoyancy and viscous resistance under the conditions discussed above (Paldor and Killworth 1988). On that basis, the horizontal circulation is treated as having a characteristic diameter of the order of the Earth's radius.

The close numerical correspondence is only a first approximation, however. The non-spherical form of the Earth must also be considered.

For this purpose, the model refers to the standard expression for the radius of an oblate spheroid at a given geodetic latitude[1]:

The distance from the Earth's center to a point on the spheroid surface at geodetic latitude φ is:

$$R = R(\varphi) = \sqrt{\frac{(a^2 \cos\varphi)^2 + (b^2 \sin\varphi)^2}{(a \cos\varphi)^2 + (b \sin\varphi)^2}}$$

where a and b are the equatorial and polar radii, respectively.

$a =$ Equatorial radius (6,378 km)
$b =$ Polar radius (6,357 km)

Using the values given above, the calculated Earth radius at the 32nd parallel is approximately 6,371 km, close to the mean value used in the model. Thus, the latitude identified as the center of the modeled horizontal circulation also lies close to the latitude at which this radial value is obtained. Because the present construction uses circular approximations, the more detailed effects of changing curvature along the path are not incorporated at this stage. The working model therefore uses circles centered at approximately 32.0°N and 32.0°S. The resulting uncertainty is discussed in Section 4.7.

[1] Earth radius - Wikipedia, the free encyclopedia.htm

4.4. The Basic Horizontal Model

For clarity, the horizontal system is approximated by circles. It can be mapped on a rectangular geographical grid in which degrees of latitude and longitude are represented by equal units; this projection allows the modeled paths to retain a circular form despite the convergence of meridians on the globe. The first set of circular paths is centered on the 32nd parallels north and south and is referred to here as the hemispheric system. A second set is associated with the polar regions[1] and is referred to as the polar system[2]. In the rectangular construction, the centers of the polar circles are placed on the imaginary lines y = ±96°. The individual paths are arranged so that their east-west spacing remains 1.5° along each latitude.

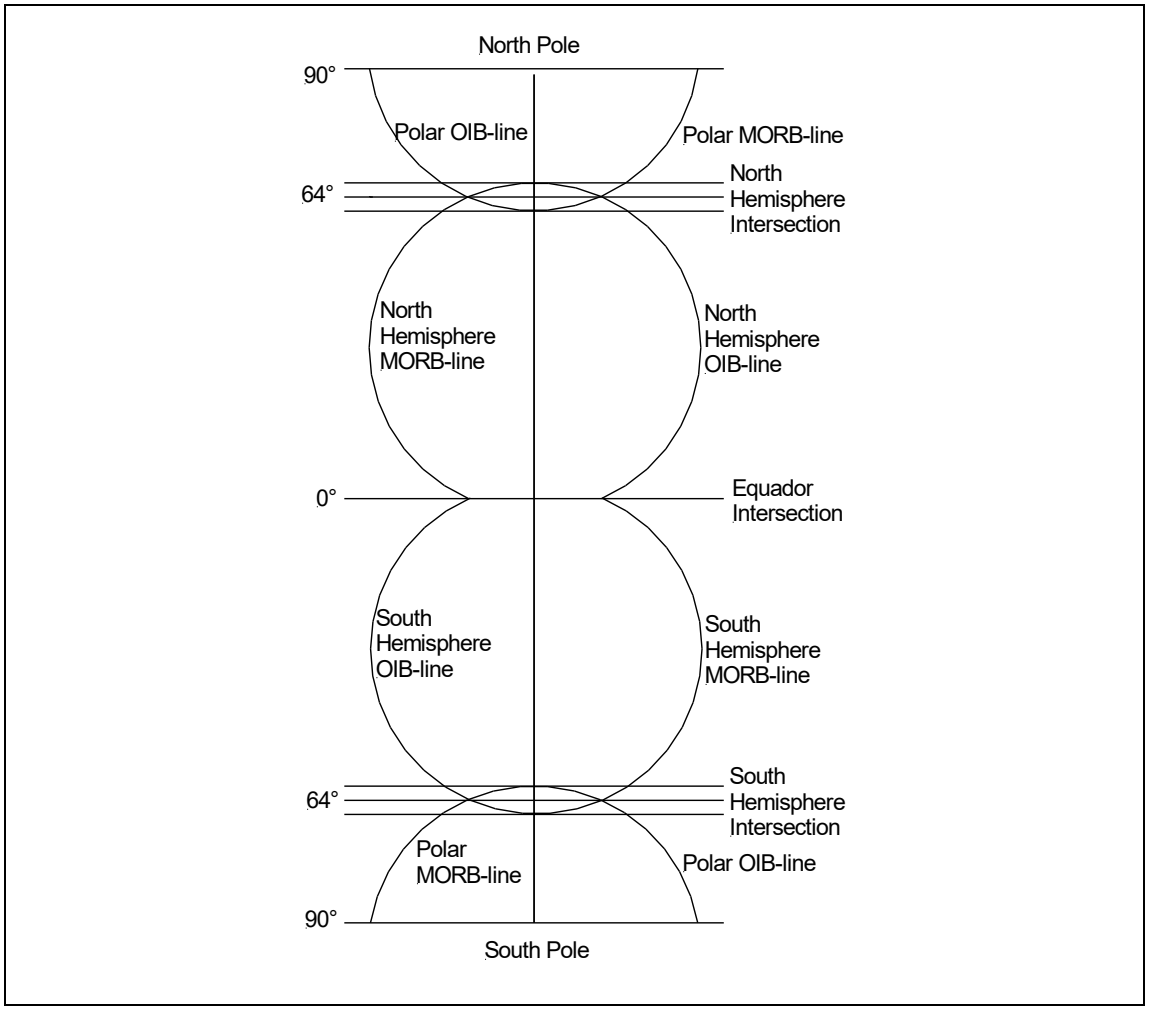

Figure 22: Schematic horizontal geometry of the proposed convection-cell system.

The resulting construction provides a continuous geometrical framework for the proposed circulation of mantle material. At global scale, 240 parallel convection-

[1]In the model, the same basic horizontal curvature is maintained globally in relation to the Earth's curvature.
[2]These components are discussed in greater detail in the next section.

roll paths are represented in each of four sectors - North Polar, Northern Hemispheric, Southern Hemispheric and South Polar - giving a total of 960 circular or semicircular elements in the complete schematic model. The circular approximation is defined mathematically in the following section.

4.5. Equations for the World Map of Convection Cells

The preceding sections introduced two proposed layers between approximately 120 and 410 km depth: an upper layer extending roughly from 120 to 265 km and a lower layer from about 265 to 410 km. In the horizontal model, each is further represented by hemispheric and polar components. These components are defined mathematically below.

In the rectangular grid used here, the equation of a circle with its center at the origin (0,0) is x2 + y2 = r2. The origin of the geographical grid is the intersection of the equator with the reference longitude 0°. Because the centers of the hemispheric circles are placed on y = 32, corresponding to the 32nd parallels, the two sets of circles between the equator and approximately 67.3°N and 67.3°S can be represented as follows.

The circular approximation for the boundaries of the hemispheric convection rolls is:

Equation 1 $$(x - C_n)^2 + (y - 32)^2 = 35.34^2$$

where Cn = {-178.7, -177.2, -175.7, …, -0.2, 1.3, 2.8, …, 179.8} for n from 1 to 240. In this notation, longitude is represented by the horizontal coordinate relative to Cn, while y represents latitude. The Cn values are spaced at intervals of 1.5° around the globe.

The corresponding expression for the polar division lines, extending approximately from the 61st parallels towards the North and South Poles, is:

Equation 2 $$(x - C_n)^2 + (y - 96)^2 = 35.34^2$$

where Cn = {-178.7, -177.2, -175.7, …, -0.2, 1.3, 2.8, …, 179.8} for the sequence used in the polar construction.

Equation 2 has the same form as Equation 1, except that the centers of the circles are placed on y = 96 in the rectangular grid.

With these equations, the proposed convection-cell geometry can be represented continuously from the Earth's interior towards the crust and horizontally from the South Pole to the North Pole.

4.6. Differentiation of the Flow Equation to Determine Cell Direction

The orientation of a modeled convection-roll boundary at any geographical position can be obtained from the slope of the tangent to the corresponding circle.

In a rectangular Cartesian grid with center at (x,y) = (0,0), the slope a of the tangent to a circle at a given coordinate is:

Equation 3

$$a = -(x/y)$$

The angle γ, measured in degrees from the x-axis (west-east direction), is then:

Equation 4

$$\gamma = \arctan(a)$$

On the spherical Earth, longitudinal distances decrease with latitude by a factor of cos(φ), where φ is latitude. The rectangular grid used for the model compensates for this convergence by applying the corresponding correction factor. The direction equation used in the geographical representation is therefore:

Equation 5

$$\arctan[-(x/y)(1/\cos\varphi)]$$

where φ is latitude, with the same expression used for northern and southern latitudes. The result gives the modeled angle between the convection-roll boundary and the west-east axis.

A corresponding direction angle α can then be defined for the hemispheric rolls and β for the polar rolls. Because geographical directions are normally expressed relative to north rather than west, the result from Equation 5 is subtracted from 90°.

Owing to the assumed symmetry of the convection-cell system about a north-south axis, a single calculation gives two mirrored directions, west and east of north.

For the hemispheric lines, from the equator to slightly above the 67th parallel, the directions Nα°W and Nα°E are given by Equation 6:

Equation 6 $$\alpha = 90° - \arctan \{[(35.34^2 - (\varphi - 32)^2)^{0.5} / (\varphi - 32)](1/\cos \varphi)\}$$

From approximately the 61st parallel to the North Pole, the directions ±β° from north are given by Equation 7:

Equation 7 $$\beta = 90° - \arctan \{[(35.34^2 - (\varphi - 96)^2)^{0.5} / (\varphi - 96)](1/\cos \varphi)\}$$

The same equations are applied symmetrically in the Southern Hemisphere.

For the lower convection cells associated with the transition interval, the following expression is used:

Equation 8: $$\gamma = 90° - \arctan \{[(35.34^2 - ((-\varphi) - 18.5)^2)^{0.5} / ((-\varphi) - 18.5)](1/\cos \varphi)\}$$

Because this equation refers to a deeper convection layer, its predicted geometry is less directly compared with surface structures. In the model, the lower layer adjacent to the 670 km discontinuity crosses the equator midway between the crossings of the convection cells immediately beneath the 410 km discontinuity, giving a separation of 30° from the neighbouring equatorial crossings.

This raises the next question: how far can the same construction be extended vertically and horizontally? The model allows for additional internal convection cells, but each extension must be examined against the physical premises, geophysical measurements and observable geological relationships used throughout this study.

4.7. Degree of Accuracy

The calculations in this chapter form an idealized mathematical model based on relationships drawn from the cited literature and from the geometrical premises developed in the preceding sections. It is therefore important to distinguish mathematical precision from physical accuracy. Once three or four reference points are fixed on a rectangular grid, the corresponding circle can be calculated to arbitrary numerical precision. That numerical precision does not, however, imply that the natural system itself is known to the same degree of accuracy.

The theoretical construction can be summarized as follows. Two reference points on the equator are placed 30° apart, while a second geometrical relationship uses a 60° separation to represent the reference length associated with the Earth's radius. Combining these constraints with a circle that intersects the equator at the prescribed points gives a central latitude close to 32° and a calculated radius of 35.34 grid units. Here, a 'unit' represents one degree on the rectangular longitude-latitude grid used in the model.

Within the model, the circular approximation represents the path of an idealized moving particle in a balanced rotating system. The convergence of meridians towards the poles is compensated on the rectangular map by the factor $1/\cos\phi$, where ϕ is latitude. This transformation allows the horizontal path to be represented approximately as a circle on the working grid.

Because the map treats one degree of latitude and one degree of longitude as equal graphical units, the model can also express directions in the same rectangular coordinate system. The value 35.34 is retained as the calculated reference radius, although this number implies greater precision than is justified for the real Earth. In practical terms, the center of the modeled circle is taken as approximately 32.0° ± 0.1°, and its mean radius as approximately 35.3 ± 0.1 grid units. Additional uncertainty arises from the non-spherical form of the Earth and from the way the idealized path is projected onto the geographical surface.

There is nevertheless a reason within the model to use 32° as the working latitude rather than retain the full spherical result of 32.066°. The polar radius of the Earth is about 1/300 shorter[1] than the equatorial radius. The implications considered here are:

[1] Wikipedia

1) The Earth's curvature differs slightly from that of a perfect sphere, and if the modeled paths follow that curvature accordingly (Paldor and Killworth 1988), the effective radius of the arc between the equator and approximately 67° will differ slightly from the idealized spherical value.
2) The term 'circle' is itself an approximation: the geographical path represented here is an arc, with part of the idealized circle absent along the equatorial side of the construction.
3) The resulting adjustment is expected, within the assumptions of the model, to be smaller than 1/300 and closer to the order of 1/500. For this reason the working model uses the 32nd parallels directly rather than retaining the additional digits of 32.066°.

A further source of uncertainty is the east-west position of the center of each circle along the 32nd parallel. Unlike the curvature and direction, this position is not derived from the same geometrical equation. Instead, geographically distinct reference locations - including Hawaii, Iceland and selected equatorial coastal points - are used to position the grid. The first center is therefore given in Equation 1 and Equation 2 as -178.7° ± 0.1° relative to Greenwich.

The locations of the circle centers and the adopted radius are therefore subject to a finite uncertainty, in addition to the approximation involved in representing the geoid by a rectangular-grid circle. The purpose of this work is primarily to describe and test the proposed geometry, rather than to imply unlimited positional precision. Comparisons with real geological structures should therefore take account of the difference between the idealized grid and the physical Earth.

A more exact treatment would have to follow the changing curvature of the Earth along the modeled path, because this is the surface geometry experienced by the idealized moving particle[1]. In the present construction, the path is expected to curve slightly more strongly between the equator and 32°N or S than between 32° and approximately 67.3°. The discrepancy is treated as being of the order of 1/500, and the circular approximation is therefore retained throughout this work.

The additional calculations required to trace such a path on the geoid are not carried out here. Instead, the value 35.34 is retained as the reference radius of the circular construction on a perfect-sphere grid. Within this approximation, the

[1]The term "moving particle" is used here for an idealized infinitesimal element of material within the modeled flow.

curvature radius would be slightly different on the equatorial and poleward sides of the 32nd parallels, potentially shifting the effective central latitude slightly. A more complete geodetic treatment would be required to quantify that adjustment.

The practical value of the model is that it provides a reproducible equation for comparing predicted convection-roll directions with geological structures at any latitude.

The basic horizontal form used here is circular. The same equation can therefore be used to calculate a predicted direction for the convection-cell boundaries at different locations and to compare those directions with major geological structures (see Section 4.6. *Differentiation of the Flow Equation to Determine Cell Direction*). Any such comparison remains subject to the uncertainty of the assumptions, measurements and geometrical approximations on which the equations are based.

The approach developed here is intended as an extension of the geometrical reasoning used in earlier developments of tectonic theory. If the large-scale organization of mantle circulation can be described in a reproducible way, it may provide a simpler framework for examining a range of geological relationships. The following chapters test that possibility against increasingly detailed observations.

The final simplification used in the rectangular map is based on the latitude dependence assigned here to the Coriolis effect (Condon and Hugh 1967). By compensating for the convergence of longitude with latitude, the square-grid representation allows the proposed horizontal trajectory to be approximated by a circle. This circular form is the mathematical basis for the global mapping developed in the following chapters.

Chapter 5 – MORB and OIB

With direct calculations based on geophysical measurements, the dimensions of the proposed convection-cell system within the asthenosphere and mantle can be derived. Petrology provides an additional source of information about the Earth's internal structure. This chapter considers the distinction between MORB and OIB in relation to the proposed convection system.

MORB and OIB are petrological concepts based on two distinct rock types observed at the Earth's surface. These two types are interpreted as originating from different magma sources distributed around the globe (Foulger 2010). Within the present analysis, the proposed source regions correspond to the upper and lower convection-cell layers between 120 and 410 km below the Earth's surface.

5.1. MORB and OIB layers

$$\alpha = \frac{\sqrt{(\varphi\text{-}32)2\text{-}35^2}}{(\varphi\text{-}32)}$$

To clarify further the two uppermost layers between 120 and 410 km below the Earth's surface, the following two figures are shown together. The same horizontal circle is highlighted in each: one figure presents the system in three dimensions and the other in two dimensions.

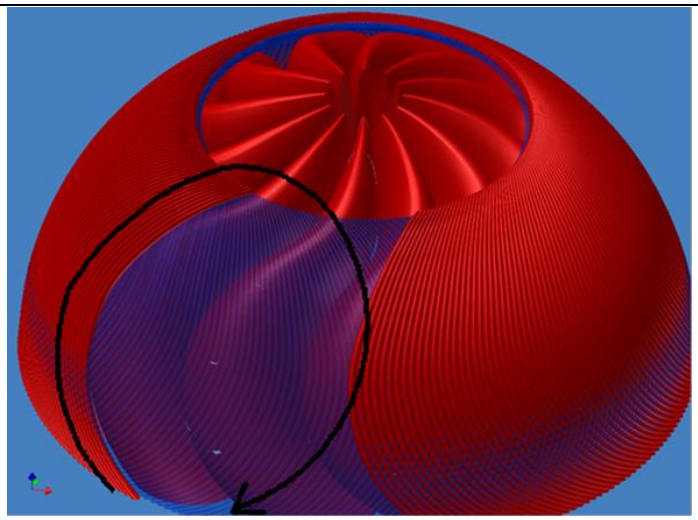

Figure 23: The big mantle cells shown underneath in red and the OIB-layer (blue) and the uppermost MORB layer (also red). Drawing by Jón Leósson.

For comparison:

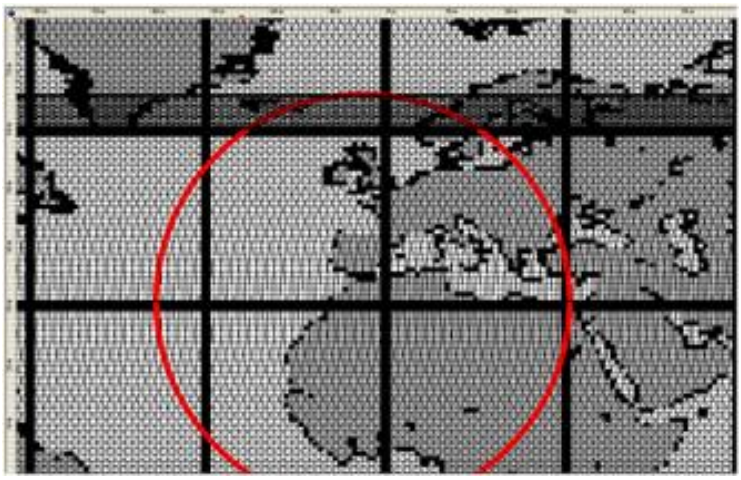

Figure 24: A convection cell map with the central line of the North Atlantic marked red.

Having defined the convection-cell model mathematically, the next step is to

examine its functioning in greater detail, particularly within the two uppermost layers, which are proposed here as the source regions of two different magma types commonly referred to as MORB and OIB. For this purpose, a three-dimensional figure was prepared to show how the convection rolls form a side-by-side pattern around the globe.

For clarity, the figure shows the small cells of the so-called hemispheric system while omitting the polar cells. In the three-dimensional representation, red semicircles of the upper layer and blue semicircles of the lower layer join end to end to form complete circles. Within the model, this connection between the MORB and OIB layers is essential for maintaining circulation. The volume of material transferred horizontally within the system must, however, be limited; otherwise, there would be little difference between the compositions of MORB and OIB.

A circle with an arrowhead indicates the direction followed by an imaginary particle along one convection-roll circuit: first northward along a red semicircle in the upper layer, and then southward along a blue semicircle in the lower layer. In this way, the rolls of the two layers are connected to form a continuous circulation system.

The pattern shown in the next figure results from placing these circles side by side, with each circle representing the boundary of one convection cell within the asthenosphere and uppermost mantle.

One circle is highlighted in red because it is defined by Equation 1:

$$(x - (-4.7))^2 + (y - 32)^2 = 35.34^2$$

This particular circle passes exactly through the middle of the Atlantic Ocean at the equator and also marks the western edge of the Eastern Volcanic Zone in Iceland (see Chapter 10 - Iceland).

The apparent accuracy of this geometrical relationship may at first seem surprising, but several factors can be identified that help explain it within the framework of the model.

5.2. Individual sections of essentially circular horizontal flow

The essentially circular geometry of the horizontal flow has now been described and the relevant calculations presented, allowing the convection-cell system to be represented mathematically. When the two layers between 120 and 410 km depth are considered in the horizontal plane, however, the system is seen to consist of connected semicircular sections. The sections referred to here as hemispheric and polar rolls meet their corresponding sections end to end at the equator and near 64°N and 64°S, allowing the convection cells to be represented as continuous structures.

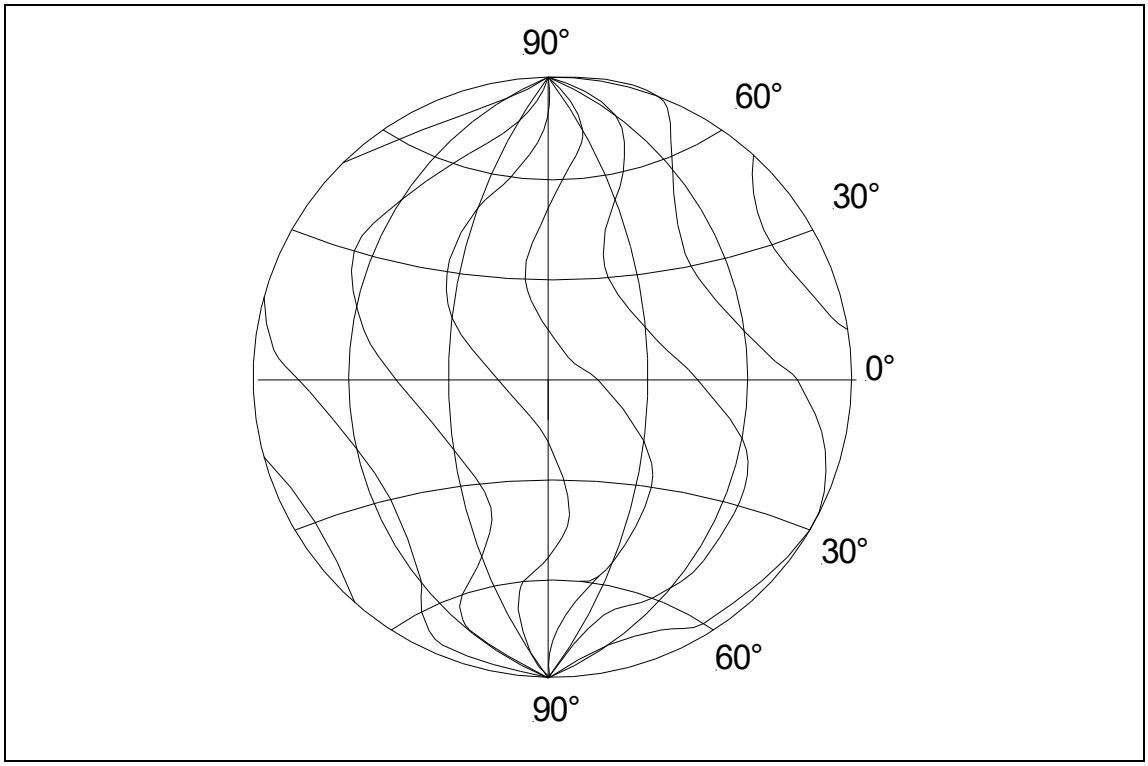

Figure 25: A drawing representing the alignment of MORB layer convection cells.

The figure shows the basic geometry of the uppermost convection cells when traced from pole to pole. This is the layer referred to here as the MORB layer, and the drawing illustrates how the hemispheric convection rolls connect with the polar rolls. Only a few representative lines are shown for clarity and they are not drawn to scale. A complete representation of the MORB layer would contain 240 such lines arranged side by side around the globe. Beneath this layer lies the proposed OIB layer, which can be constructed by mirroring each of the lines shown here.

This generalized sketch illustrates the geometry of the uppermost convection-cell layer. The principal curves are centered close to the 32nd parallel. The transition to the polar sections occurs near the 64th parallel, where the so-called intersection zones are located.

These intersection zones play an essential role in regulating the proposed circulation system. Material flowing horizontally along the rolls can be redistributed

within these zones. The geometry of the circle helps illustrate how this may occur: a semicircle belonging to a polar convection roll is tangent to its counterpart in the hemispheric system, providing a possible connection for material exchange. These tangent points emerge directly from the mathematical model. At the equator, they provide horizontal connections and also allow for possible exchange between layers; near 64°N and 64°S, the tangent points connect the different layers of the system.

5.3. Flow in convection cells: east-west component due to convection and north-south component due to secondary horizontal flow

The recognition of tectonic drift greatly advanced our understanding of geological processes. Within the present model, such drift is related to the movement of material within the mantle and asthenosphere. The separation of Africa and South America provides a useful example: in the proposed geometry, it corresponds to two adjacent rolls circulating in opposite directions, one toward the east and the other toward the west. The rolls are assumed to influence the plates through their cooler upper parts. A second component of motion is also inherent in the model: flow along the rolls between the polar regions and the equator.

According to the proposed convection-cell model, circulation within the Earth follows a highly regular pattern. Particular attention is given to the uppermost mantle immediately below the lithosphere, because this part of the system should have the most direct influence on surface geology. It is necessary to distinguish between the east-west circulation visible in vertical cross-sections of the convection cells and the horizontal flow that follows the rolls in the north-south direction. The model therefore requires consistency between these vertical and horizontal components of circulation.

In the present model, the MORB source lies above the OIB source of magma (Davies 1999). It is therefore necessary to identify which semicircular sections belong to the MORB layer and which correspond to the OIB layer. One of the principal surface features used for this purpose is the Mid-Atlantic Ridge. Within the model, its geometry—particularly that of the Reykjanes Ridge—is interpreted as following the MORB layer and indicating northward flow. The ridge has an overall S-shaped form centered on the equator, and according to the Coriolis effect a particle following this path would be moving northward (Condon and Hugh 1967).

The polar regions provide the complementary part of this pattern. In the proposed MORB layer, the polar convection rolls show the opposite orientation, with horizontal flow directed southward. This relationship is examined in greater detail later in the book.

This directional tendency appears to have persisted over a long period. Stanley (1998), for example, describes a general northward movement of the continents during the last 500 million years.

5.4. Horizontal circulation

As shown in the previous section, the asthenosphere cells in this model include a horizontal component of flow. Material is carried northward along a normally shaped convection cell to approximately 67°N. This is interpreted as the layer from which MORB material originates and as the source supplying basalt to the ocean ridges. The proposed MORB and OIB source regions are distinguished as follows (Davies 1999):

> Since MORBs are rather clearly derived from the shallowest mantle, as will be discussed in more detail later, the OIBs are by implication sampling deeper parts of the mantle.

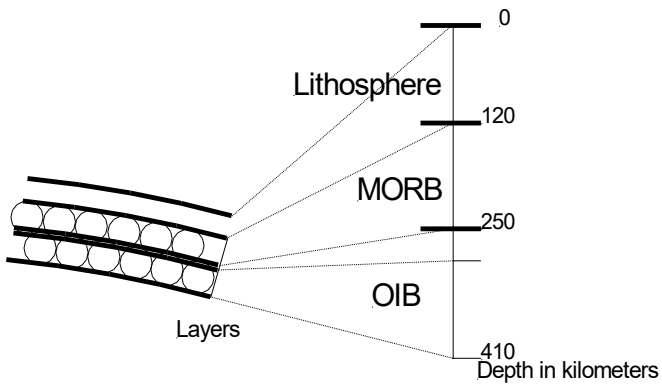

Figure 26: The MORB and OIB layers.

Under the "MORB layer", a reservoir for the OIB material is found. The reverse shaped system and the layer below 250 km depth is a candidate for the source of OIB.

The asthenosphere cells are drawn in the figure. It can be reasoned that the upper more

The upper cells represent the normally shaped curves, while the lower cells represent the reverse lines, as drawn on the world map.

The individual systems are ultimately connected at the intersection zones near the polar circles and the equator, allowing them to be traced as parts of an integrated circulation system. Some exchange of material is proposed to occur between the different components—for example, between the MORB and OIB layers or between hemispheric and polar sections of the convection rolls—within these intersection zones. The resulting model therefore describes a regular, interconnected system for the circulation of material within the Earth.

Chapter 6 - Radiation and the Munroe effect

Essentially, this essay concerns heat transfer within the Earth, which can occur through mass transport, conduction, and radiation. Identifying the underlying processes is both interesting and often useful. In geology teaching, at least in Iceland, students are taught that part of the Earth's internal heat is generated by radioactive elements. However, there may be another part of the picture that has received little attention. My father, Thorbjörn A. Fridriksson, pointed out what he regarded as a missing element in explanations of radiative heat transfer within the Earth: the possibility that radiation from the crust and the uppermost mantle contributes to heating the core, after which heat is transported upward again by convection.

6.1. The Role of Radiation

Although some readers may regard the ideas presented in this essay as unconventional, an additional topic must be considered in an attempt to understand more fully how heat is transported within the Earth. Most radioactive material is concentrated in the lithosphere or close to it, while the core is much hotter than the mantle. This contrast raises an important question: if a large proportion of the radiogenic heat is produced far above the core, how is the very high temperature of the core maintained?

One possible explanation is that much of the heat still present in the core is residual heat dating from the formation of the Earth about 4.6 billion years ago.

The graph below is presented here as an argument for a form of heat transfer that appears to have received little attention in geological literature. According to the graph, the mantle becomes increasingly transparent to radiation at high temperature. If so, radiation from the upper mantle could travel downward toward the core. In the interpretation proposed here, the inner core receives part of this radiation and is heated, after which heat is transferred upward again, mainly by convection through the outer core and mantle.

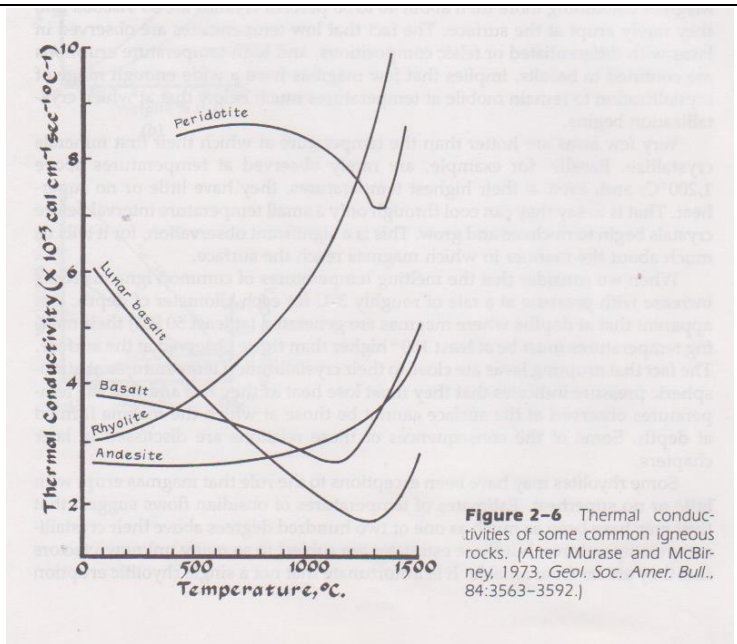

Figure 27: The rise in conductivity around 1,300°C is attributed here mainly to increasing mantle transparency to radiation at high temperature.

As is known from studies of the distribution of elements within the Earth, most radioactive elements are concentrated in the mantle and crust, with relatively little in the core itself. In the model proposed here, radiation can therefore be directed from the upper layers toward the core.

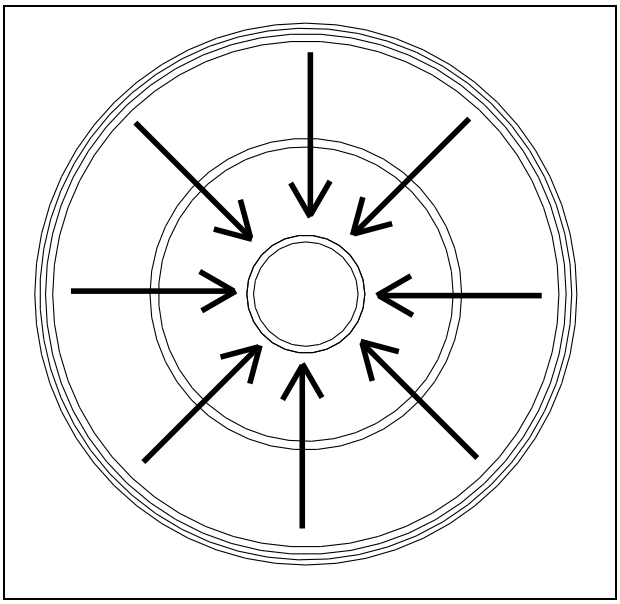

Figure 28: Radiation from the Earth's outer layers proposed to heat the core.

When considering how heat is transferred outward from the core, it is also relevant to ask how that heat reached the core in the first place. The process proposed here is analogous, in a general sense, to solar radiation heating the Earth's surface, after

which energy is transferred away by long-wave radiation and by heating the atmosphere. David A. Rothery provides a useful description on Encyclopedia.com (accessed 9 April 2011) of the three principal radioactive elements within the Earth:

> Only three radioactive elements occur within the Earth in sufficient abundance and release enough heat per decay event to be significant contributors to radioactive heat production. These are uranium, thorium, and potassium. Uranium has two radioactive isotopes (uranium-235 (^{235}U) and uranium-238 (^{238}U)); thorium and potassium have one each (thorium-232 (^{232}Th) and potassium-40 (^{40}K)). Each so-called heat- producing isotope decays at a different rate, so that the total rate of radioactive heat generation has declined and the relative importance of each isotope has varied over time (Fig. 1). Potassium-40 has remained the most important heat-producing isotope throughout the Earth's history, but uranium-235, which has the fastest decay rate (or shortest half-life), and now makes the smallest contribution of the four, was the second biggest contributor during the Earth's first half-billion years.

Radioactive elements are concentrated mainly in the Earth's outer layers, while heat is continually transported outward from the core by convection. The possibility that radiation from the upper layers of the mantle could travel inward toward the core appears to have received little attention in geological literature. My father, Thorbjörn A. Fridriksson, drew my attention to McBirney's graph of mantle transparency and suggested that it implies that the core is continually heated by radiation from the uppermost layers of the Earth.

6.2. The Munroe Effect

Within the model proposed here, it would be difficult to maintain a narrow flow of magma from the asthenosphere into the brittle part of the crust without a focusing mechanism. I propose that the Munroe effect, discovered in 1888 by Professor Charles E. Munroe, provides such a mechanism. A cone emitting energy symmetrically inward into another material can result in localized melting and the formation of a comparatively narrow, self-regulating jet of molten material directed outward from the cone (Munroe 1943).

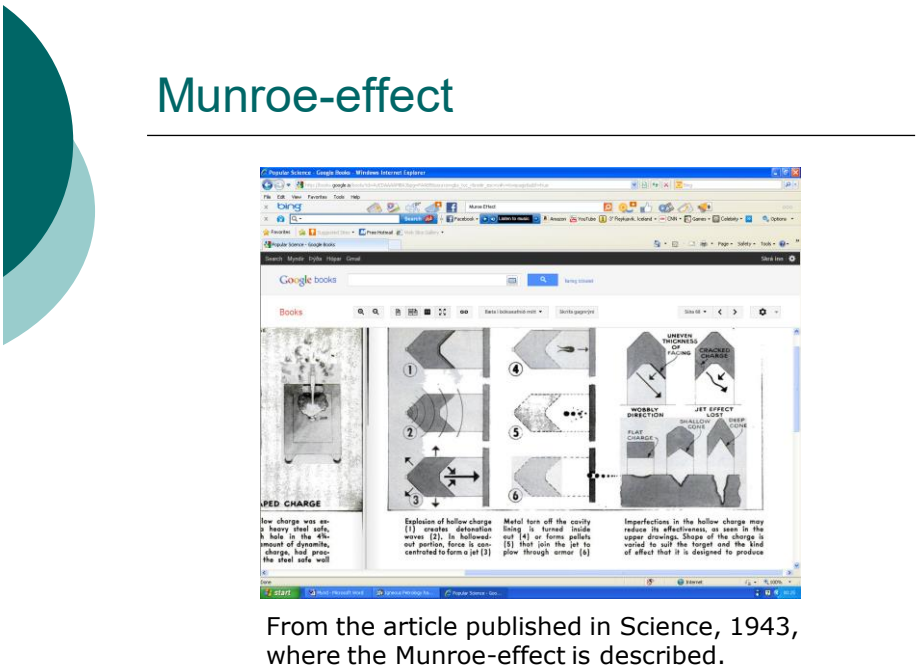

Figure 29: The Munroe effect.

The convection cells transport heat toward their upper parts and, in the model proposed here, release part of that energy as radiation. This is proposed to generate an upward flow of magma through a narrow pathway guided by radiation.

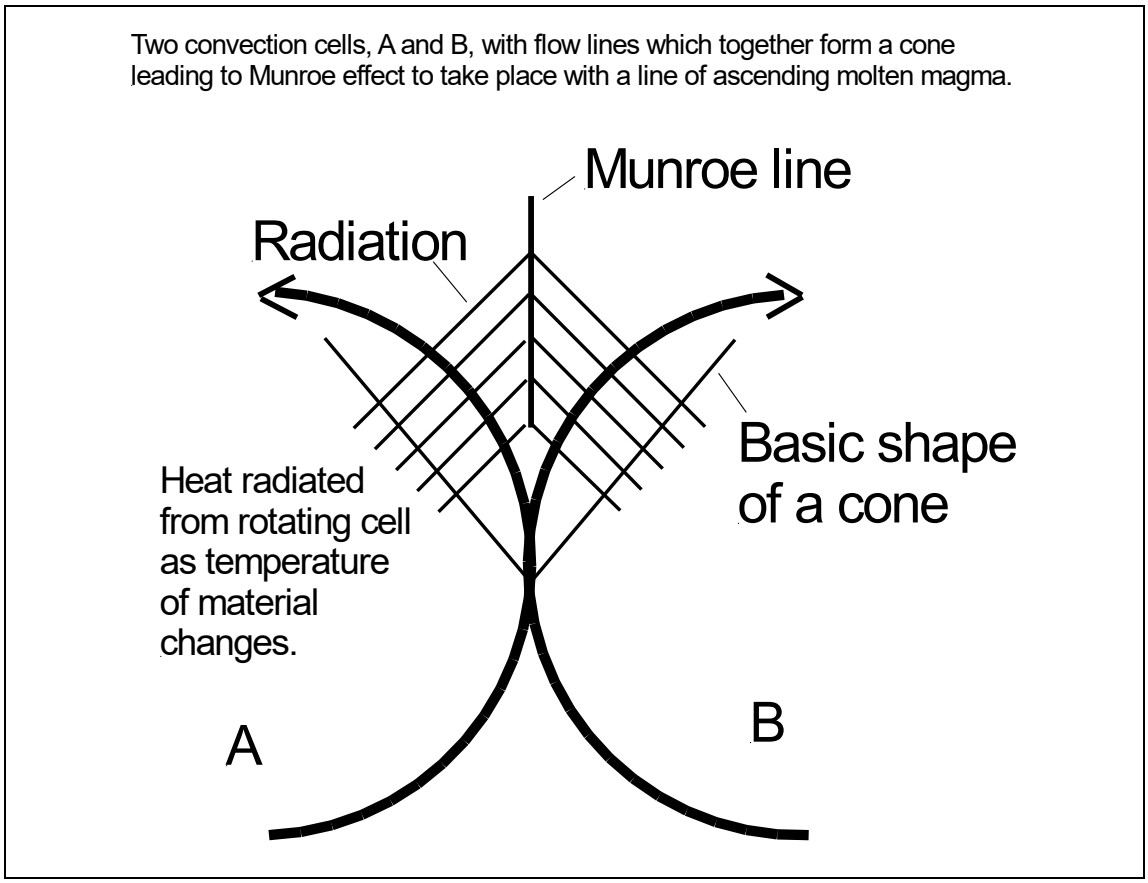

Figure 30: Proposed development of a narrow jet of molten material from convection cells through the Munroe effect.

Again, my father, Thorbjörn A. Fridriksson, pointed out that this natural phenomenon might arise where two regularly shaped convection cells rotate side by side, releasing radiation as the temperature of the material changes.

The two cells on either side of a Munroe line contribute to the continuous heating of the vertical magma flow, which is further enhanced by the Munroe effect within the walls of the line itself. The width of such a line may eventually be calculable; as an initial estimate, the inner ascending flow is here considered to be on the order of half a metre wide.

The flow within a Munroe line is proposed to have both vertical and horizontal components. The vertical component follows directly from the description above, while horizontal flow along the lines is also an important part of the model. As previously described, the system produces a continuous northward flow in the uppermost hemispheric cells, and the horizontal component of flow along the Munroe lines must also be consistent with the Coriolis effect.

In the model, magma-filled walls cut through and segment the ductile part of the lithosphere. The height to which these Munroe walls extend is likely to vary

considerably from place to place. Their extent may be easiest to estimate where they intersect magma chambers and continuously supply magma to them.

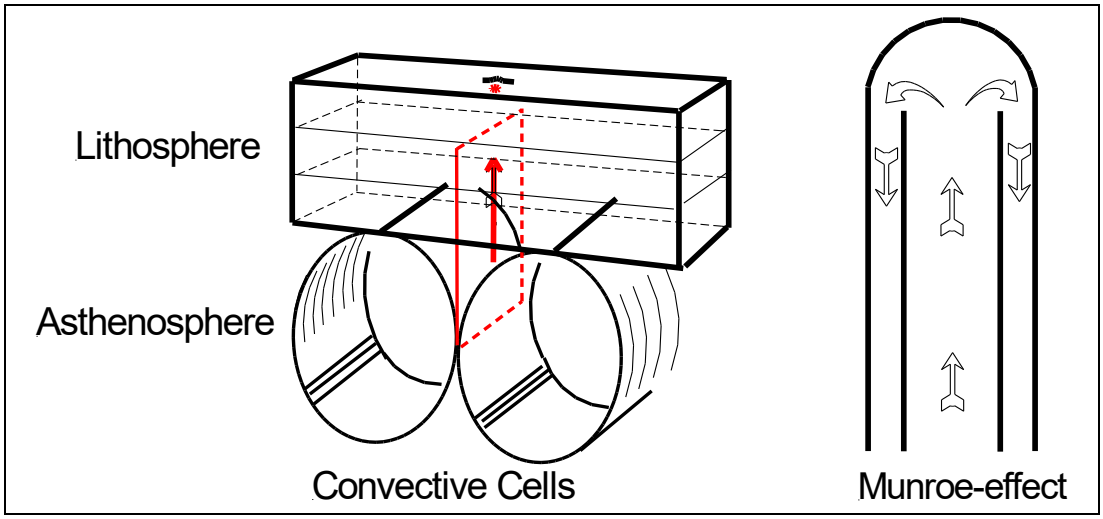

Figure 31: Proposed flow associated with the Munroe effect cutting through the ductile part of the lithosphere.

The drawing illustrates how the proposed magma flow cuts upward through the lithosphere.

One particularly distinctive geological setting provides an indication that the ductile part of the crust may be 'cut' with a high degree of regularity by Munroe lines of the type described here.

There is a strong indication, within this interpretation, that the South Iceland Seismic Zone (SISZ) is framed by a diamond-shaped area defined by the lines between convection cells. This is discussed further in Chapter 11.

6.3. The Function of the Munroe Lines

A Munroe line is probably one of the most surprising aspects of the system described in this book. It should, in principle, be possible to detect such a line using geophysical measurements, although the lines are proposed to be narrow and to occur mainly beneath the brittle part of the crust.

Munroe lines extending into the lithosphere

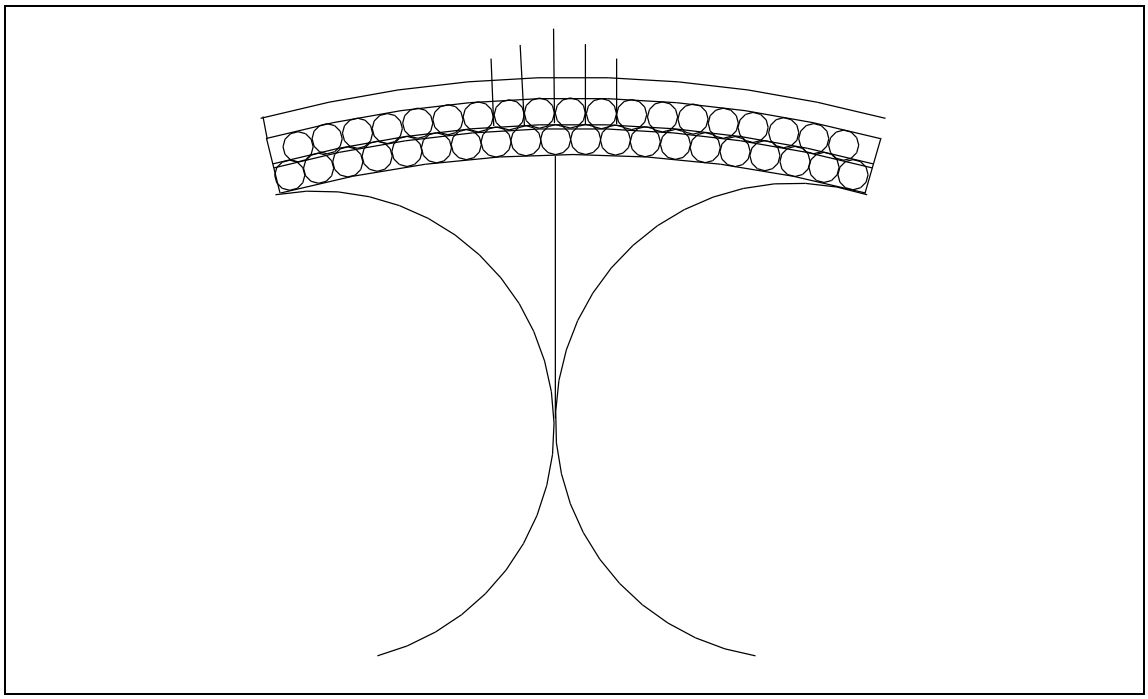

Figure 32: Schematic cross-section showing how a main lower-mantle Munroe line is proposed to influence smaller cells above and strengthen several Munroe lines in the asthenosphere.

The model distinguishes two types of Munroe lines, MORB and OIB, in reference to their petrological associations. This distinction is used here to explain why OIB is often associated with islands, whereas MORB occurs mainly along mid-ocean ridges:

Imagine a diamond-shaped polygon bounded by two parallel MORB lines and two parallel OIB lines. The OIB magma must travel a greater distance, but according to the stand-off relationships associated with the Munroe effect (Munroe 1943), this need not prevent the proposed process.

The following drawings illustrate examples of the proposed combined effect of MORB- and OIB-type Munroe lines cutting through the lithosphere.

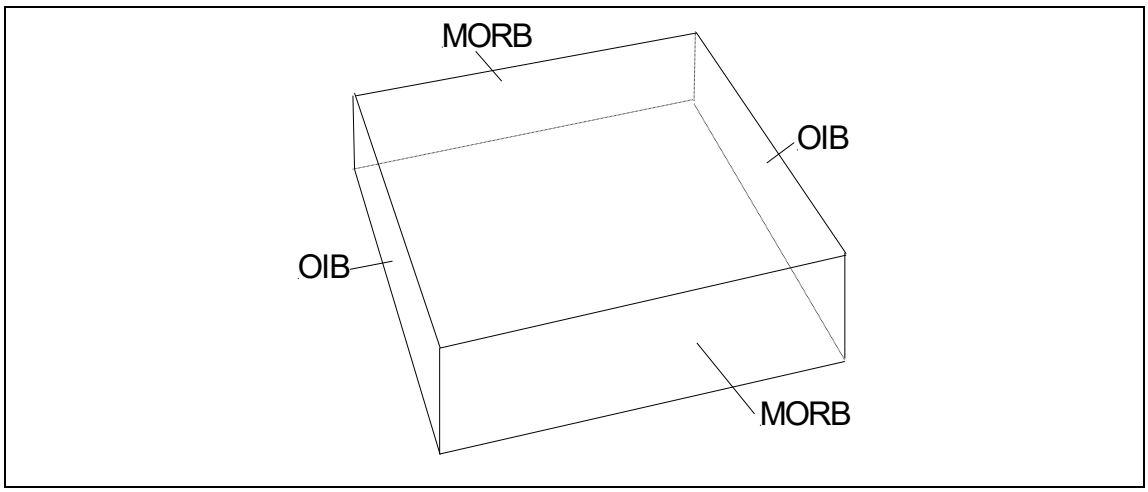

Figure 33: A typical tectonic-plate polygon proposed to be formed by convection cells.

This is the basic pattern proposed for a large part of the world. The following figure shows how these conditions may lead to the formation of a volcanic island composed of rock of the type referred to as OIB.

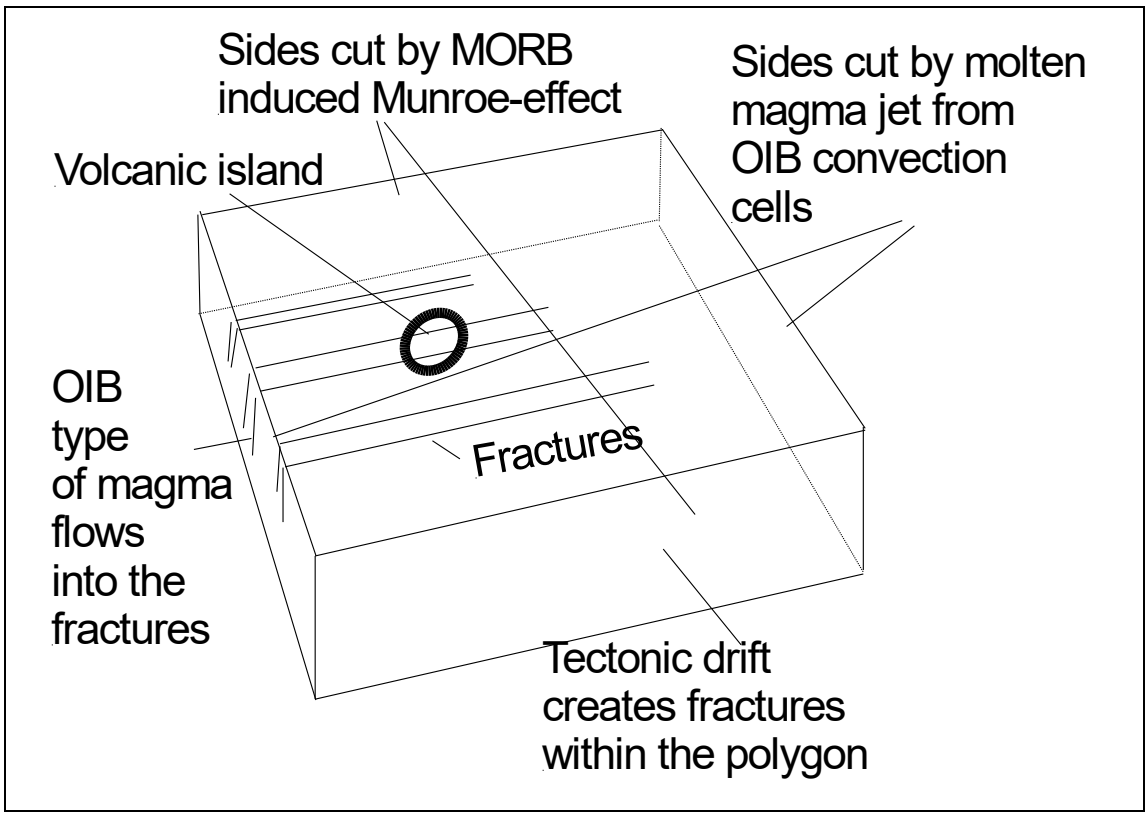

Figure 34: Example of how OIB-type magma is proposed to enter a tectonic-plate polygon.

Along mid-ocean ridges, by contrast, the MORB jets are proposed to form dykes parallel to the ridge. In this interpretation, the formation of volcanic islands with OIB-type magma and the generation of oceanic crust along ridges represent two expressions of the same underlying system.

In Iceland, examples of nearly all the functions proposed for the Munroe-line system can be examined. At Hekla volcano, for example, the MORB and OIB lines are interpreted here as merging into a single line. The following chapters compare the model with geological observations and provide the background needed to consider the different configurations that may result. For readers familiar with Icelandic geology, a useful first step is to examine the following cross-section:

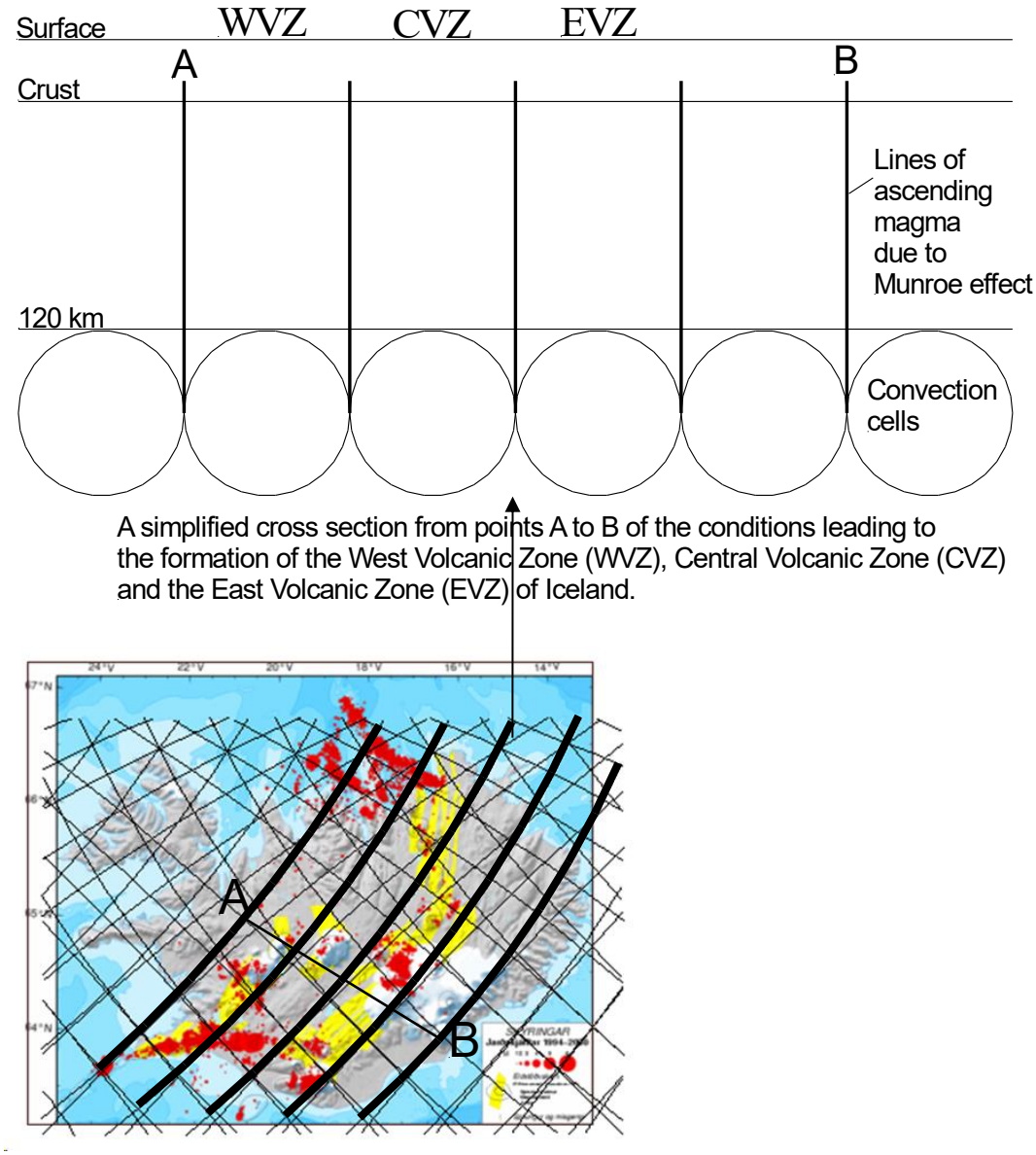

Figure 35: Convection cells in the cross-section between points A and B, shown with thicker lines. Point B is located at Öræfajökull volcano.

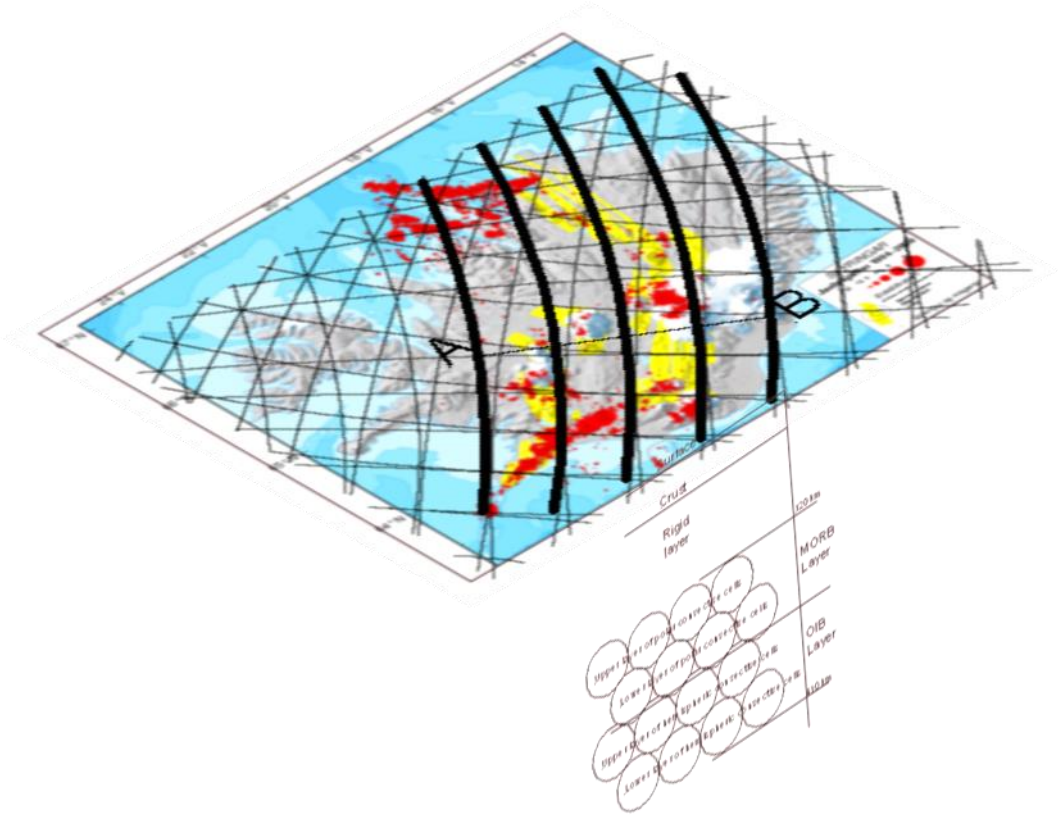

Figure 36: Section of convection rolls beneath Iceland, with Munroe lines shown on the map.

The same cross-section can also be represented in this way. Each layer of convection rolls produces one set of Munroe lines within the tectonic plate. In the model proposed here, magma at temperatures above 1,000°C can reach the surface because the Munroe effect maintains a focused flow into and through the brittle crust.

6.4. Horizontal Transfer of Heat Within the Mantle

At the Earth's surface, heat transmitted from below is very unevenly distributed. The variation in seismic shear-wave velocity relative to the relevant average value is only on the order of ±1.5% (Ritsema, van Heijst and Woodhouse 1999). How, then, can surface heat flow reach around 400 mW/m² in some areas while being virtually undetectable in others?

This is explained here by combining radiative heat transfer within the Earth with the Munroe effect. Munroe lines are proposed to transfer heat efficiently toward the crust. If heat is absorbed there, the return flow along the corresponding Munroe line would contain proportionally more crystallized material and would absorb thermal radiation from its surroundings. In this way, the Munroe line would receive an additional input of energy where it intersects an overlying mid-ocean ridge that is losing heat.

A comparison between maps of mid-ocean ridges and surface heat flow shows a pattern that is consistent with the convection-cell model. Along the equator, the East Pacific Rise and the Indian Ocean ridge are close to being equidistant from the central Atlantic region. Large amounts of heat are released along these two ridges. In the model, they are interpreted as representing two of the six principal ascending currents of the lower mantle. This gives the following basic picture:

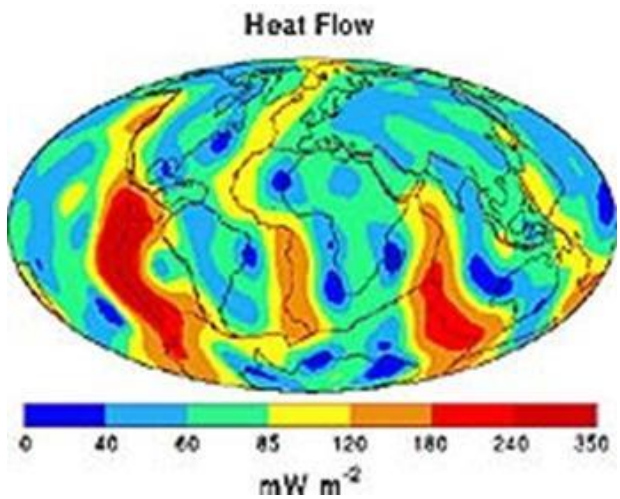

Figure 37: Overview of heat flow through the Earth's crust, as presented on the website www.mantelplume.org.

Such large-scale lateral transfer of heat, as required by this interpretation, would be difficult to explain without radiative heat transfer within the Earth.

Chapter 7 - Intersection Zones of Horizontal Flow

An essential element in understanding how the proposed convection-cell system operates is that circulation must remain continuous in both its vertical and horizontal components. Intersections between convection rolls are therefore treated here as an integral part of the system, providing both continuity and a mechanism for exchange between horizontally flowing branches. This framework can then be compared with geological phenomena and with the distribution of major volcanic and geothermal regions shown on the world map. In the model, the curvature of the convection rolls is related to the Coriolis effect, while the intersection zones allow the circulation to remain connected rather than consisting of isolated flow paths.

7.1. Intersection Zones

In the basic pattern described here, the largest component consists of the so-called hemispheric rolls, which extend approximately from the equatorial region toward the polar region. Focusing on the MORB layer, a hemispheric roll reaches its northern limit where its horizontal direction becomes east-west. Similarly, the polar rolls reach their corresponding limit near the 61st parallel. The region between these limits is defined here as an intersection zone.

In the mathematical model of the horizontal dimensions of the hemispheric and polar convection cells presented in this book (Equations 1 and 2), the corresponding circles intersect within the interval from approximately 60.7°N to 67.3°N. This is one of the more complex parts of the proposed system, but it may also be especially suitable for comparison with observations because Iceland lies within this latitude range. When the curves defined by Equations 1 and 2 are projected onto a world map, the volcanic zones of Iceland provide an opportunity to 'zoom in' on a grid formed by four sets of lines. In the interpretation developed here, this grid shows relationships with several elements of Icelandic tectonics. The pattern is more complex in Iceland than in many other regions because both hemispheric and polar lines are present.

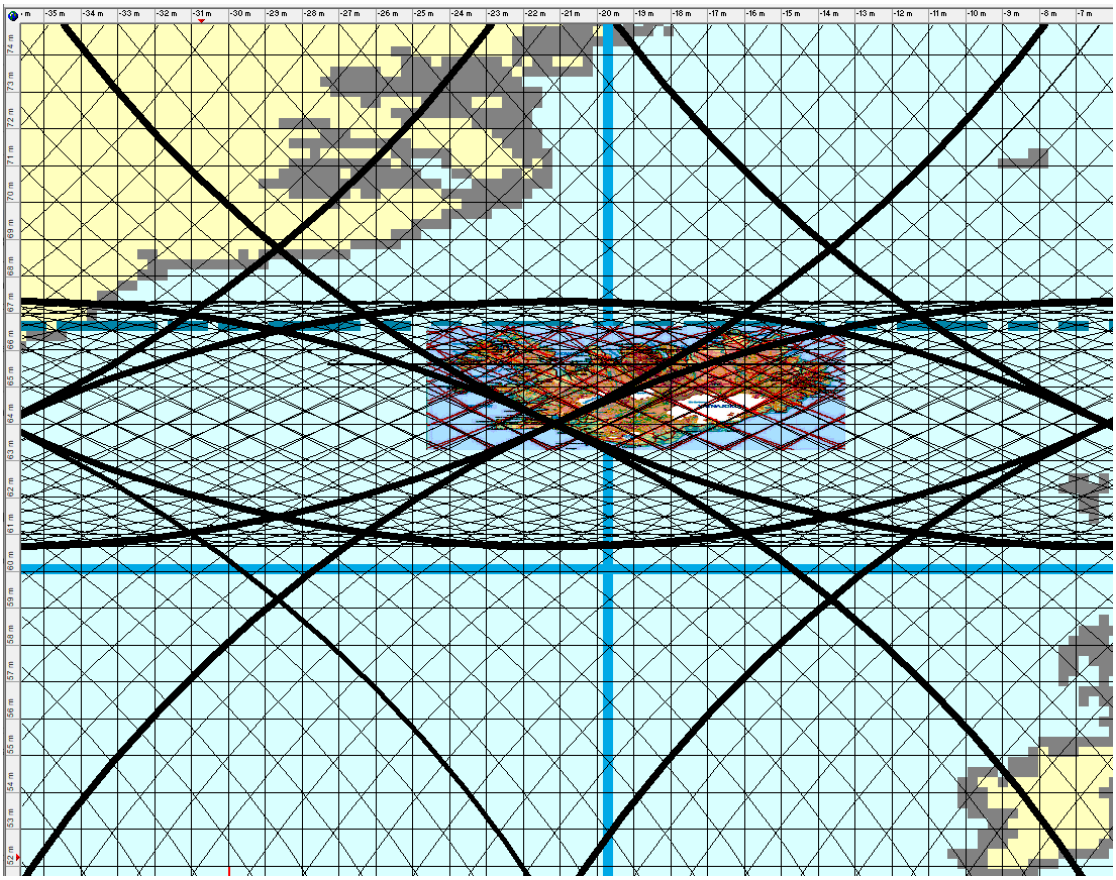

Figure 38: The proposed northern intersection zone between hemispheric and polar lines.

The figure illustrates the geometry proposed for the northern intersection zone. The red line represents N0 in the global identification system used in this model. This is one of the principal lines of the system, and its polar section passes through the Jan Mayen region.

7.2. Connection Between the MORB and OIB Layers Within the Intersection Zones

To examine the intersection between hemispheric and polar convection rolls, it is useful to consider the horizontal path of a particle moving within the system. In the model, a MORB roll reaches its northern boundary at approximately 67.3°N, where its direction is due east. At the same location, but in the layer below, an OIB roll reaches its boundary while pointing due west. The two semicircular paths therefore combine geometrically to form a complete circle, one half belonging to the MORB layer and the other to the OIB layer.

Within the horizontal intersection zone, the 64th parallel has a particularly important role in the proposed transfer of moving material between hemispheric and polar convection rolls. The corresponding curves are tangent at this latitude and therefore have the same local direction. In the model, this creates conditions under which material can pass from one system to the other without an abrupt change in its Coriolis-controlled trajectory. This relationship may also provide a framework for interpreting the change in the direction of tectonic motion observed in Iceland near this latitude.

The combined MORB and OIB semicircles form a complete circle on the latitude-longitude grid. In the geometry used here, the circle spans 30° from east to west at both the equator and 64°N, with a corresponding relationship at 64°S.

The centre of this circle lies near the 32nd parallel, and in the geometry used here its diameter is equal to the radius of the Earth. This dimension is considered in relation to the analysis of Paldor (1988).

7.3. Layers Within the Horizontal Intersection Zones

To maintain a particle trajectory consistent with Coriolis deflection under the balanced conditions discussed by (Paldor and Killworth 1988), the model requires the horizontal intersection zones to contain four layers. A division is therefore proposed near 60.7°N, where one roll layer separates into two. To visualize this geometry, consider a roll in the MORB layer with a vertical diameter of approximately 160 km. North of 60.7°N, the model divides this into two roll layers, each with a vertical diameter of about 80 km. The combined vertical dimension remains unchanged, but all four layers can contribute to the surface pattern, making the intersection-zone latitudes more complex than regions outside them.

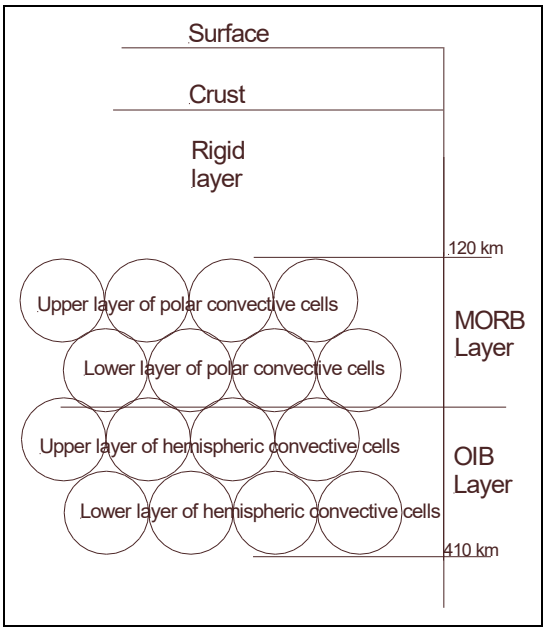

Figure 39: Schematic structure of convection cells within the intersection zone.

The proposed conversion from one layer to two near 60.7° and 67.3°, respectively, requires special consideration. How a thicker roll approaching from the south might pass above or below a thinner roll approaching from the north remains one of the more speculative aspects of the model. Present-day measurements of tectonic motion, including ISNET 2004, provide one possible source of observational information for examining how horizontal flow might behave within this transition zone.

7.4. The Intersection Zones Between 60.7° and 67.3°

The dimensions of the hemispheric rolls were derived directly in the preceding analysis. Here, a more straightforward geometrical approach is used to introduce another aspect of the overall convection-cell system. In the model, the hemispheric rolls span theoretically about 70.7° from east to west along the 32nd parallel and extend approximately from the equator to 67.3°N, with a mirror-image arrangement from the equator to 67.3°S. More precise calculations could, of course, incorporate the geoid form of the Earth.

The term 'polar cells' is introduced here to distinguish this part of the system from the hemispheric cells; the two groups are also referred to as polar and hemispheric rolls. First, it is useful to review several properties of the hemispheric rolls. Locating the centre of a horizontal circle near the 32nd parallel implies a northern limit, which the mathematical construction places at approximately 67.34°N, while the southern limit of the northern hemispheric system is the equator. The 64th parallel has a special role in this geometry, comparable in some respects with that of the equator. In the proposed model, it provides a zone of exchange both between vertical layers and between the hemispheric and polar sections of the system. North of the 64th parallel, the polar section is constructed according to the same basic geometrical premises as the hemispheric circle between the equator and 67.3°. A mirrored arrangement is proposed for the Southern Hemisphere.

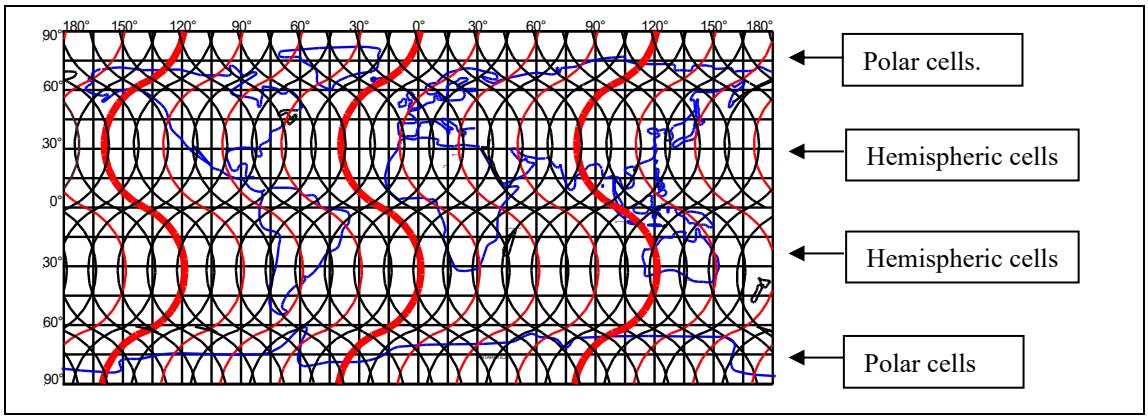

Figure 40: World map highlighting the distinction between hemispheric and polar cells.

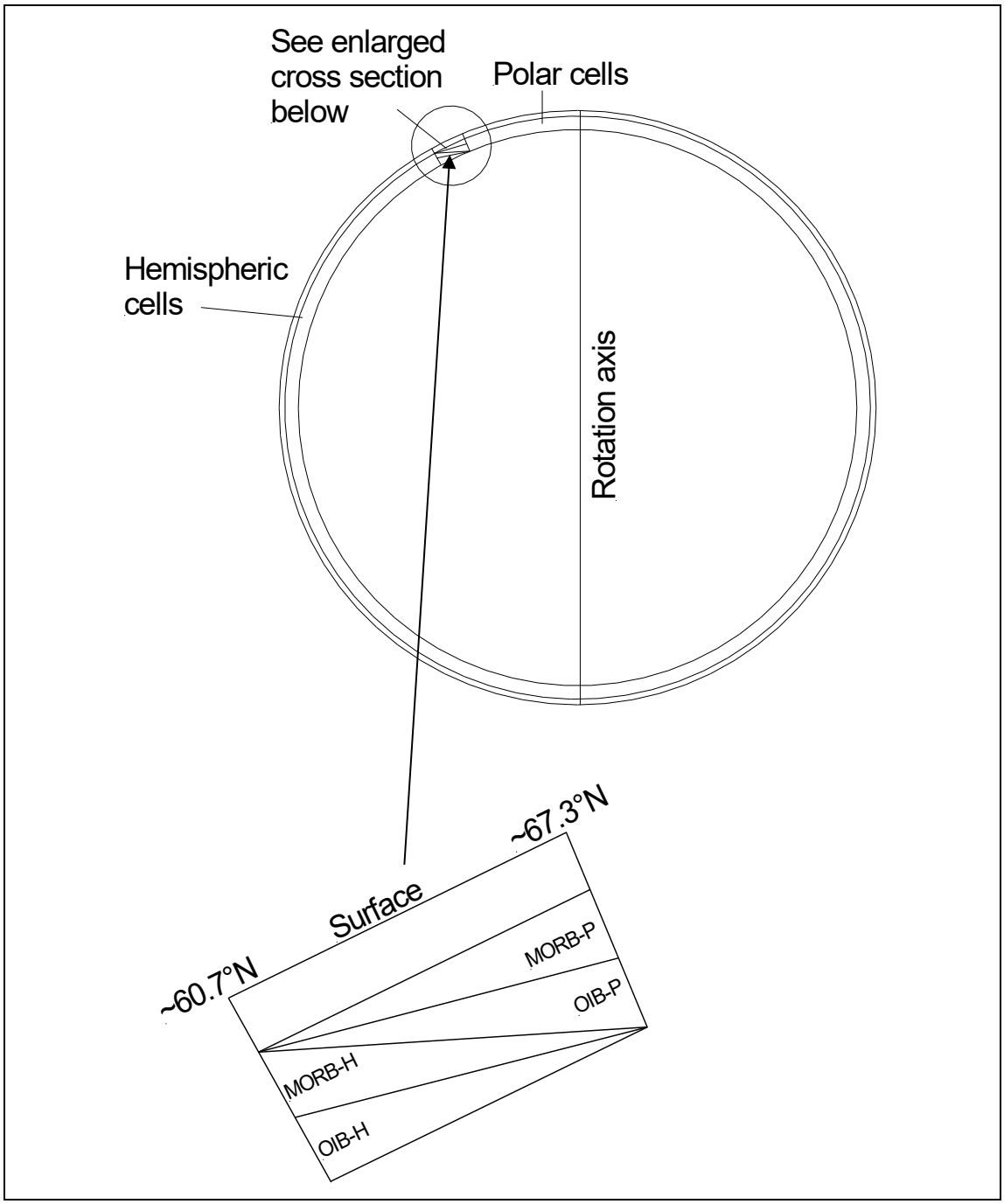

Figure 41: Proposed thinning of the convection rolls where MORB and OIB layers originating from the north and south intersect within these latitude bands.

To examine the intersection zone in greater detail, the model assumes that the horizontal-flow component within the convection rolls is, on average, effectively doubled within this region:

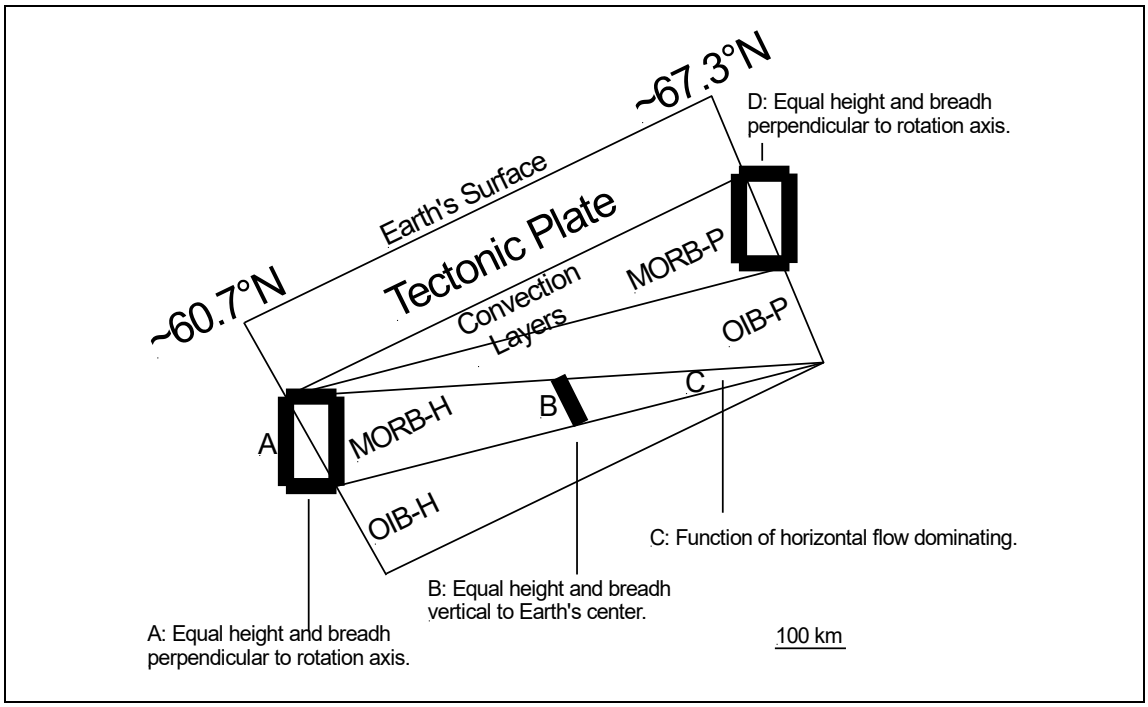

Figure 42: Drawing to scale, tilted 26°, showing the proposed intersection zone between hemispheric and polar convection rolls.

The original cell proportions - approximately 3.14 units along the axis perpendicular to the Earth's rotation axis and 3.12 units in width - are altered within the intersection zone. At 64°N, the model proposes a new geometrical balance in which the relevant cell orientation becomes vertical and the strain axis lies approximately along a line from the Earth's centre toward the surface. Where the rolls become thinnest, the horizontal component of flow is therefore interpreted as becoming increasingly important relative to the vertical convective component.

The special geometry of the horizontal transition zone can, in turn, be used to estimate the relative volumes of vertical convective flow and horizontal flow per unit time. As a first approximation, the model assumes that these two flow components are equal. Under that assumption, a convection cell viewed in a plane perpendicular to the Earth's rotation axis at 64°N would appear to have approximately half the height relative to its width. South of 60.7°N and north of 67.3°N, the cells return to the proportions proposed for the rest of the globe outside the intersection zone - approximately equal height and breadth when viewed in the plane of the Earth's rotation.

The transition is interpreted here in relation to the reported increase in heat flow north of approximately 61°N (Foulger 2010). On this basis, the model proposes that the polar convection rolls transport more heat than the hemispheric rolls in this

latitude range. The polar-roll material is consequently interpreted as relatively buoyant and as occupying the upper position where the two systems overlap.

These relationships imply that the region between approximately 61° and 67° latitude has distinctive conditions. The higher heat flow reported north of the 61st parallel (Foulger 2010) is considered here to be consistent with the proposed intersection-zone geometry, in which the orientation of the convection rolls differs from that of regions where the roll axis is simply perpendicular to the Earth's rotation axis.

It should also be noted that the proposed division plane between the polar and hemispheric cells is almost perpendicular to the Earth's rotation axis. In the framework developed here, the stress-alignment factor $\pi/3.12$ discussed in Chapter 2.4 is interpreted as contributing to a balance between convection and rotational effects.

7.5. Is There Something Special About the Polar Areas?

In the interpretation proposed here, the contrasting conditions of the northern and southern polar regions are related to the opposite ways in which material enters the polar-cell system. The model proposes a predominantly southward horizontal-flow component beneath both the Arctic Ocean and Antarctica and associates this difference in circulation geometry with the contrasting distribution of ocean around the North Pole and continental landmass around the South Pole.

The polar regions occupy a comparatively small part of the Earth's surface, and the east-west width available to the convection cells decreases strongly toward the poles. Nevertheless, the same latitude-longitude grid can be used to describe the proposed geometry there. Later in the book, the model is compared with the Arctic tectonic pattern; one example is the proposed relationship between the western volcanic zone of the Gakkel Ridge and volcanic zones in Iceland more than 2,000 km away.

7.6. The Equatorial Intersection Parallel

At the equator, the transition between the two hemispheres has an important effect on the proposed convection-cell system. Consider, for example, a northward-moving particle crossing the equator from the Southern into the Northern Hemisphere. The sign of the Coriolis deflection changes across the equator: an apparent deflection to the left in the Southern Hemisphere becomes a deflection to the right in the Northern Hemisphere. In the model developed here, this change imposes strong geometrical constraints along the equatorial line and is compared later with the distribution of ocean floor and continental landmass.

The equator can therefore be treated as a transition line. Within the proposed geometry, a particle crossing the equator cannot continue with the same sense of horizontal curvature; it must either change its horizontal direction or transfer to another layer and return. The model associates this transition with the regular pattern of land and ocean described later along the equator. In this sense, the equatorial transition is considered analogous to the intersection zones near 64°N and 64°S. The tangent points of the circles extending from the Northern and Southern Hemispheres along the equator occur at the same longitudes as their counterparts along the 64th parallels. In the model, this allows a particle following its local trajectory to pass continuously from one hemispheric system to the other. The principal difference is that the equatorial transition does not involve the doubling of layers proposed for the intersection zones near 64°N and 64°S.

7.7. Vertical View Versus a View Along the Plane of Rotation

Two different cross-sectional views must be distinguished. A vertical section is taken perpendicular to the Earth's surface, whereas a section along the plane of rotation is defined relative to the Earth's rotation axis. Both perspectives are required to visualize the three-dimensional geometry proposed here.

If the physical framework used in this model favours convection cells with approximately equal height and breadth, that relationship should not be restricted to the equator. The proposed solution is that approximately circular flow geometry is retained in sections taken perpendicular to the Earth's rotation axis.

The system is most easily visualized in an equatorial cross-section. Extending it into three dimensions requires additional geometrical considerations. At 60° north or south, for example, the east-west width available to a cell is only about half its corresponding value at the equator. A vertical section relative to the local surface would therefore make a cell appear about twice as deep as it is wide. In a section referenced instead to the plane of the Earth's rotation, however, the model retains an approximately circular flow pattern. Mathematically, the width observed perpendicular to the surface decreases by $\cos\varphi$, where φ is latitude. In the model, the principal elongation direction is also related to the axis perpendicular to the Earth's rotation axis. These geometrical factors are used here to reconcile the proposed convection-cell form with the geoid shape of the Earth.

The drawing also shows that additional factors must be considered when deriving the exact flow direction at a given latitude, because each convection roll has a finite north-south extent when viewed perpendicular to the rotation axis. The use of $\cos\varphi$ for both the latitudinal reduction in width and the corresponding axial geometry is therefore presented as a first-order approximation for understanding how the convection cells may conform to the geoid.

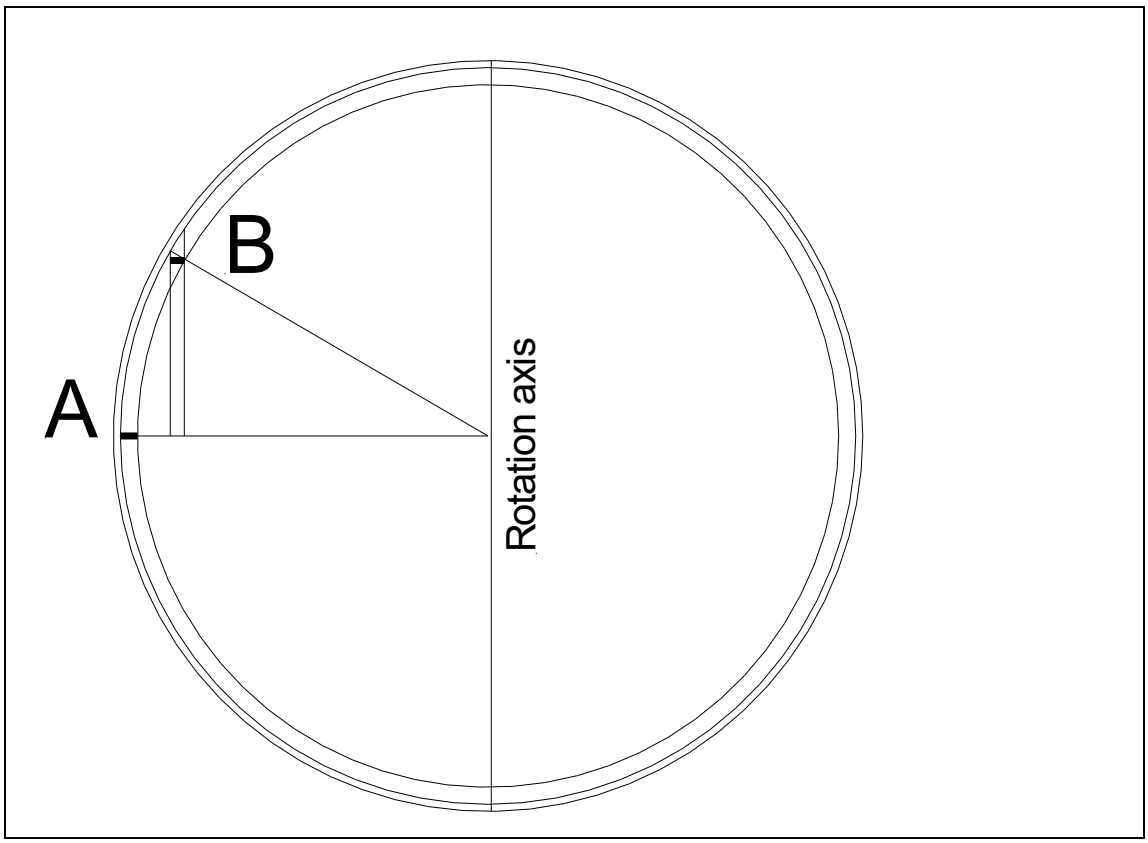

Figure 43: Maintenance of approximately circular convection along the stress axis perpendicular to the Earth's rotation axis.

Viewed from above, parallel to the Earth's rotation axis, the cross-section of the flow lines perpendicular to that axis appears circular at both positions A and B. The angle between the local plane of latitude and the vertical direction to the surface is φ in each case. Both relevant dimensions are therefore reduced by $\cos\varphi$, so that the two effects compensate geometrically. In the model, this allows the approximately circular form of the flow lines, when referenced to the Earth's rotation axis, to be retained at different latitudes. The same construction is also used to relate the proposed cell elongation - previously expressed by the factor $\pi/3.12$ - to the geoid form of the Earth.

7.8. Conclusion

At the end of this first part of the book, it is useful to return to the broader question of the Earth's internal structure. Modern geodetic measurements allow plate motion to be observed directly, while mantle convection is widely considered an important component of the dynamics associated with plate tectonics. The purpose of the preceding chapters has been to examine whether a more regular geometrical organization of that convection can be derived from the dimensions and rotation of the Earth.

Although many aspects of the proposed system have been discussed, its initial premises are relatively simple. The starting point is the geometrical observation that circular convection cells with a characteristic dimension related to the inner core can be fitted to the outer core and mantle in an equatorial cross-section. The remainder of Part I has explored how such a system might be extended into a three-dimensional arrangement.

Seismic observations provide the basic constraints on the Earth's internal layering. The inner core is interpreted as solid, the surrounding outer core as liquid, and the mantle above as predominantly solid but capable of slow ductile flow over geological timescales. Mantle convection is therefore physically possible (McBirney 1993). Within the simplified framework adopted in this model, the mantle is treated as sufficiently regular in its large-scale physical conditions for an organized system of convection rolls to be investigated.

Part II - How Is the System Revealed at the Surface?

Chapter 8 - The Distribution of Land and Ocean Along the Equator

Part I developed the proposed convection-cell system from the Earth's internal layering, physical constraints and geometrical relationships. Part II approaches the model from the opposite direction by asking whether its predicted geometry can be recognized in geological and geographical features at the surface. The method therefore changes from deriving an internal framework to comparing that framework with mapped observations.

The equator provides a particularly simple place to begin this comparison. In the model, the twelve large lower-mantle cells divide the equatorial circumference into intervals of 30°. If this geometry has a surface expression, major land, ocean and tectonic boundaries should show relationships with those intervals. The measurements presented in this chapter are therefore treated as an independent surface test of the dimensions derived in Part I, rather than as a substitute for that derivation.

Along the equator, the sequence examined here is approximately as follows: South America 30°, the Atlantic Ocean 60°, western Africa to the Great Rift Valley 30°, the Great Rift Valley to Indonesia 60°, Indonesia 30°, and the remaining Pacific sector about 150°. The following sections examine these relationships in greater detail.

8.1. A "Fit"

The correspondence between the proposed convection cells and the measured thicknesses of the Earth's internal layers is most easily seen in cross-section. At the surface, however, the world map provides a more familiar frame of reference. The equatorial distribution of land and ocean therefore offers a simple visual comparison with the dimensions of the large lower-mantle cells. Like the historical observation that the coastlines of South America and Africa appear to fit together, such a geometrical correspondence is a clue to be investigated rather than, by itself, a proof.

The equator also has a specific physical significance. The Coriolis parameter associated with horizontal deflection is zero there and changes sign between the Northern and Southern Hemispheres. In addition, the equatorial plane provides the simplest geometrical cross-section of the proposed convection-cell system. For these reasons, the equator is a natural reference line when moving from the internal model to comparisons with surface features.

When the principal equatorial distances are plotted, a strikingly regular sequence appears. In the interpretation proposed here, that sequence corresponds to the twelve large lower-mantle cells, each spanning 30° along the equator.

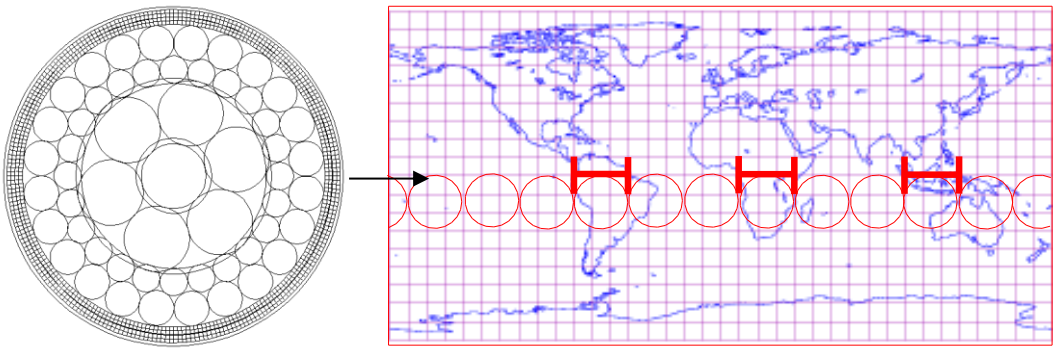

Figure 44: Comparison between the proposed lower-mantle convection cells and the distribution of land and ocean along the equator.

The circles shown on the map represent the characteristic dimensions assigned to the large convection cells in this model. The purpose of the figure is to compare those dimensions with the distribution of land and ocean along the equator. The correspondence is sufficiently regular to justify more detailed measurement. Google Earth is used here as a practical tool for making the initial geographical comparisons.

8.2. Measurements Along the Equator

To evaluate the proposed land-ocean pattern, the relevant endpoints must be defined and the geological and geophysical setting of each boundary considered. The measurements shown here use the equatorial line as a first-order geographical reference. The apparent regularity is therefore an observation to be tested in detail, including the departures from exact multiples of 30°.

The following figures show measurements made on a Google Earth base map along the equator. The yellow measurement line is used to connect the relevant reference points and to compare their longitudinal separation.

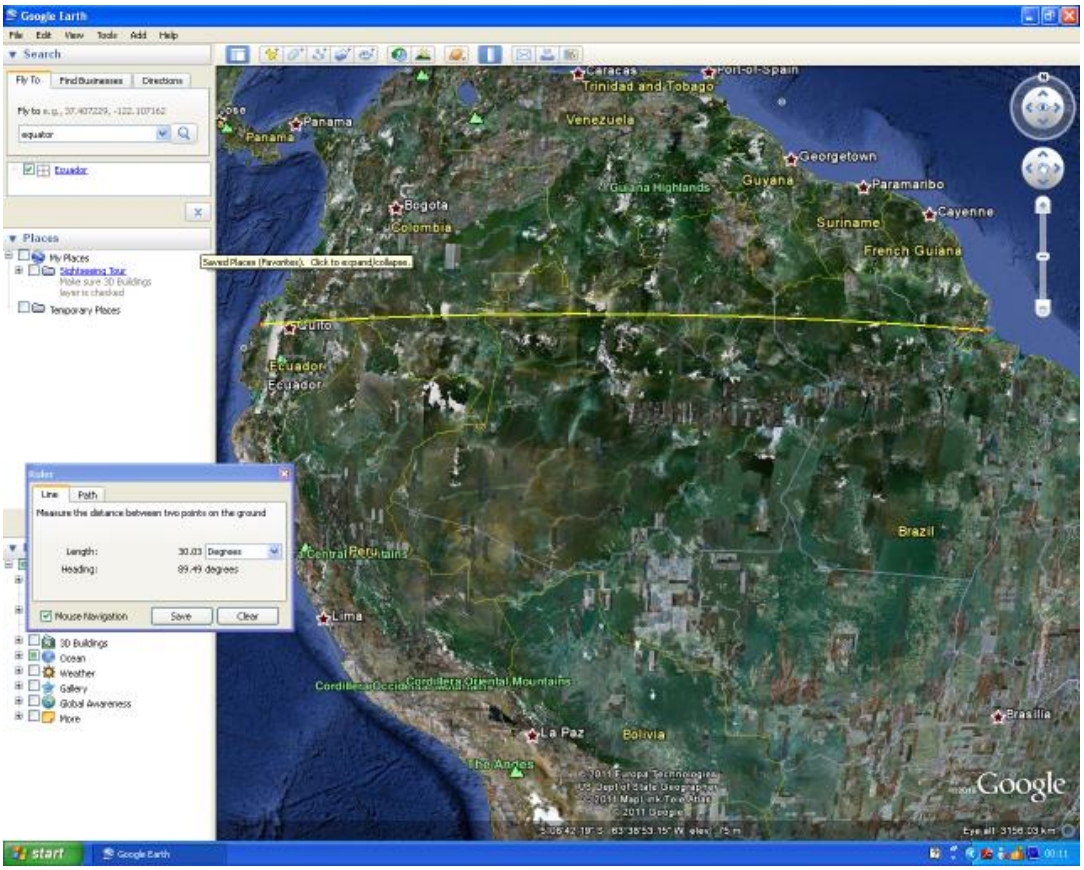

Figure 45: Equatorial span of South America, approximately 30° in the measurement shown.

In the measurement shown, South America spans approximately 30° along the equator. A single 30° interval could of course be coincidental; the significance of the observation depends on whether comparable multiples recur in the adjoining sectors.

The next comparison is therefore the distance between South America and Africa across the Atlantic Ocean.

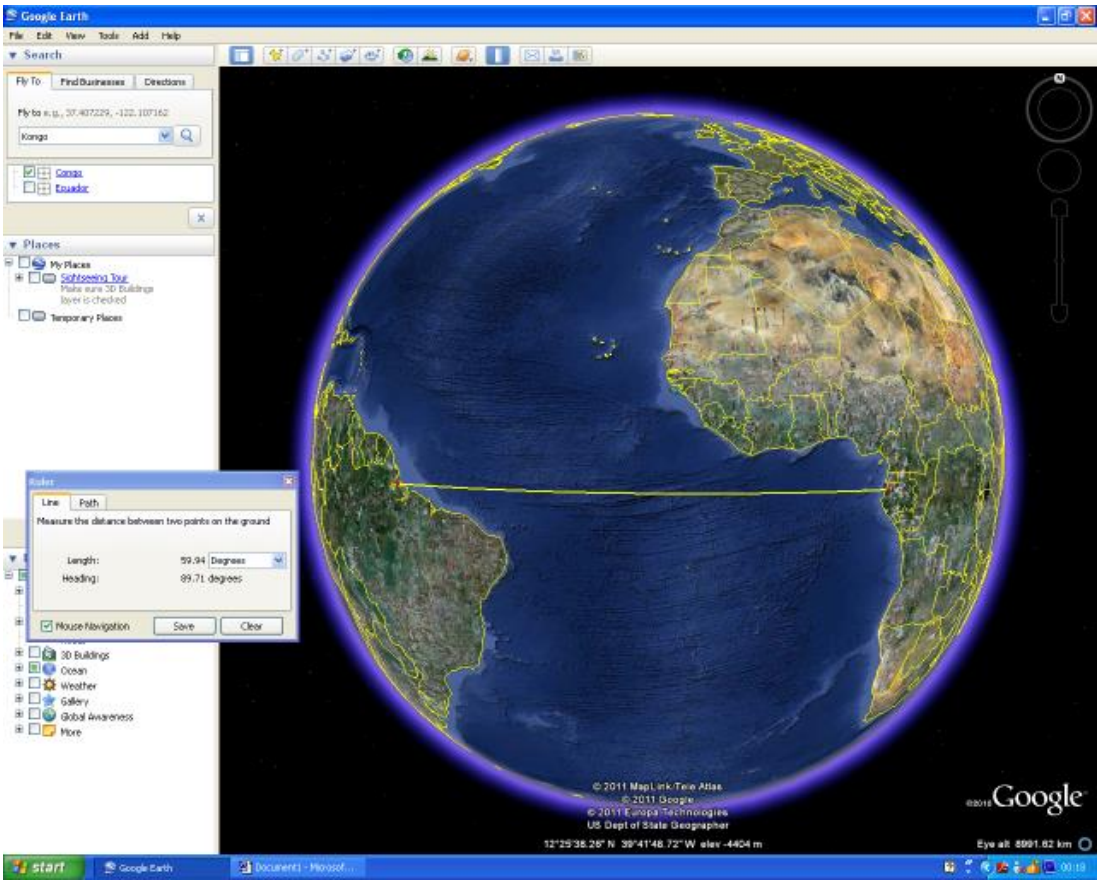

Figure 46: Equatorial width of the Atlantic Ocean between South America and Africa, approximately 60°.

The equatorial distance between South America and Africa is approximately 60°. Within the proposed model, this corresponds to two adjacent 30° lower-mantle cells. The Mid-Atlantic Ridge lies within this sector and changes trend near the equator, providing an additional tectonic feature that can be compared with the geometrical division. The use of Google Earth here is simply to make the geographical distances explicit and reproducible.

If the large lower-mantle cells each span approximately 30° along the equator, repeated intervals and multiples of that value are more informative than any single match. From the western coast of Africa to the eastern part of the Great Rift Valley, the equatorial separation is also close to 30°, as shown in the following figure.

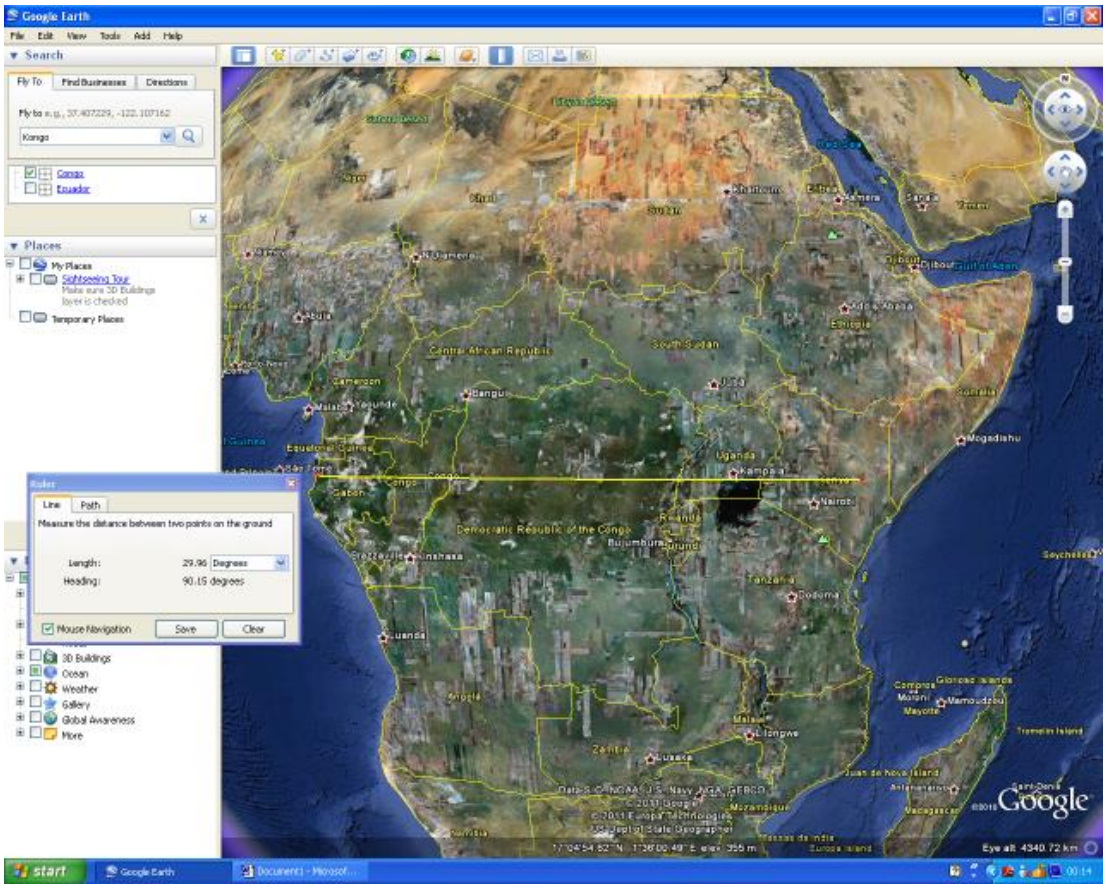

Figure 47: Equatorial span from western Africa to the Great Rift Valley, approximately 30°.

From the same Great Rift Valley reference point to the coast of Indonesia, the equatorial span is approximately 60°, as shown here.

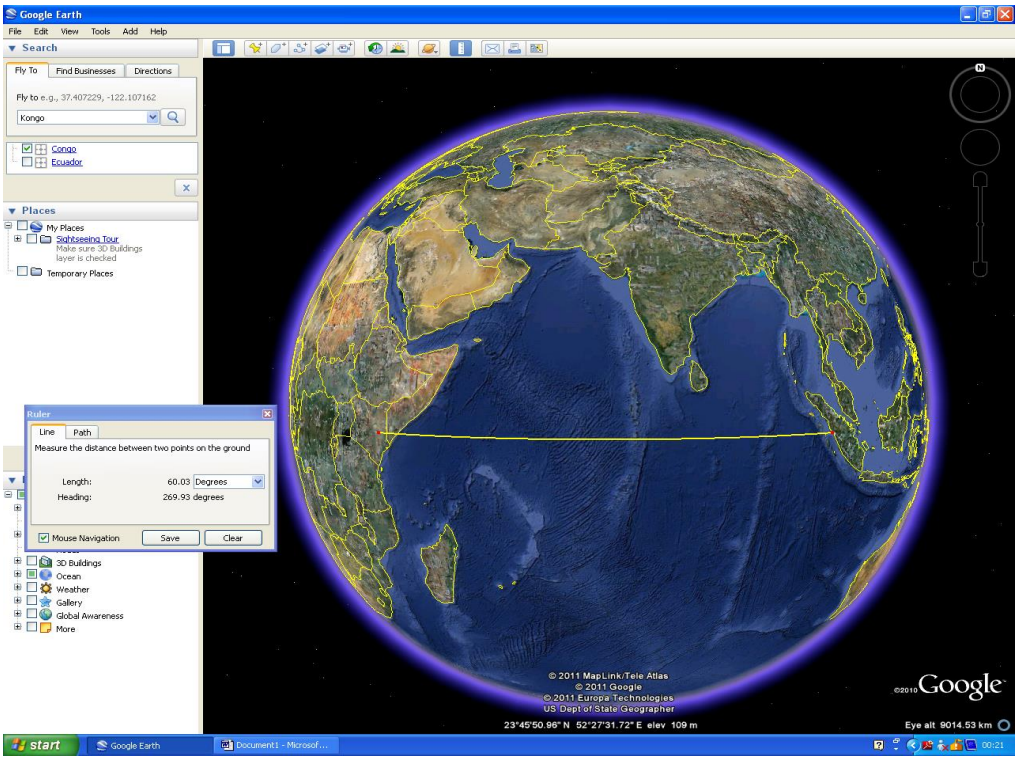

Figure 48: Equatorial span from the Great Rift Valley to Indonesia, approximately 60°.

The final measurement in this sequence shows that the equatorial width of Indonesia is approximately 30°.

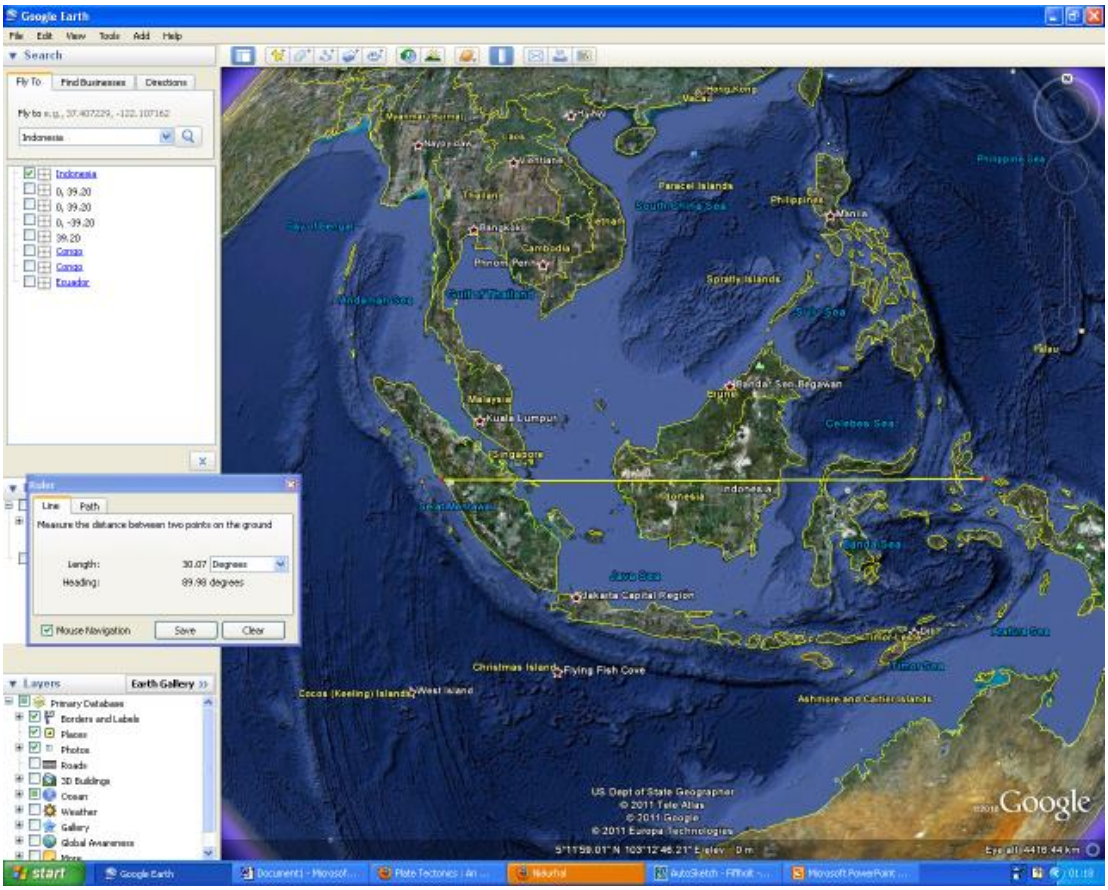

Figure 49: Equatorial width of Indonesia, approximately 30° in the measurement shown.

Taken together, these measurements produce a sequence of approximately 30°, 60°, 30°, 60° and 30°. In the model proposed here, the Atlantic and Indian Ocean sectors therefore correspond to two large convection cells each, while the intervening land or tectonic sectors correspond to one cell each. The remaining Pacific sector spans about 150°, equivalent geometrically to five such 30° intervals. This is a model-based interpretation of the observed distances and should be evaluated together with the additional tectonic comparisons below.

The sequence is summarized in the following three-dimensional schematic.

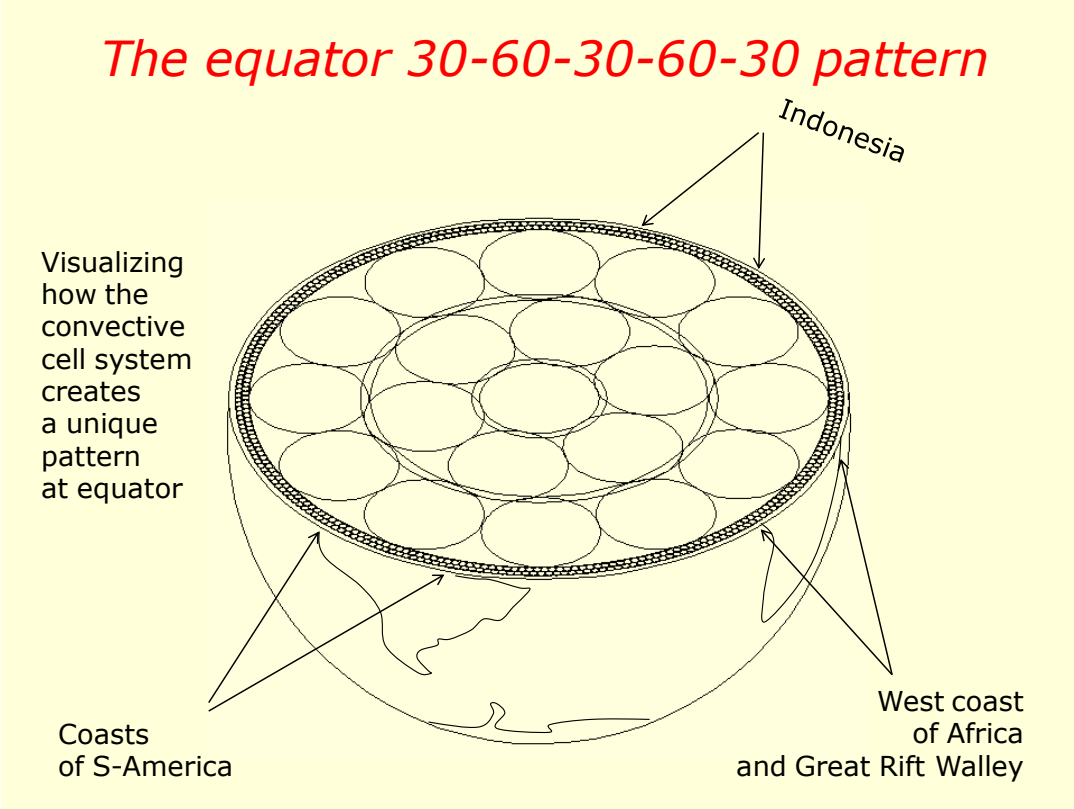

Figure 50: Schematic summary of the 30°-60° land-ocean pattern along the equator.

8.3. Ocean Ridges Along the Equator

A second comparison involves the positions of the major ocean-ridge systems where they meet or approach the equator. Their distribution is less geometrically simple than the land-ocean sequence, but it provides an independent set of tectonic features against which the proposed 30° framework can be compared.

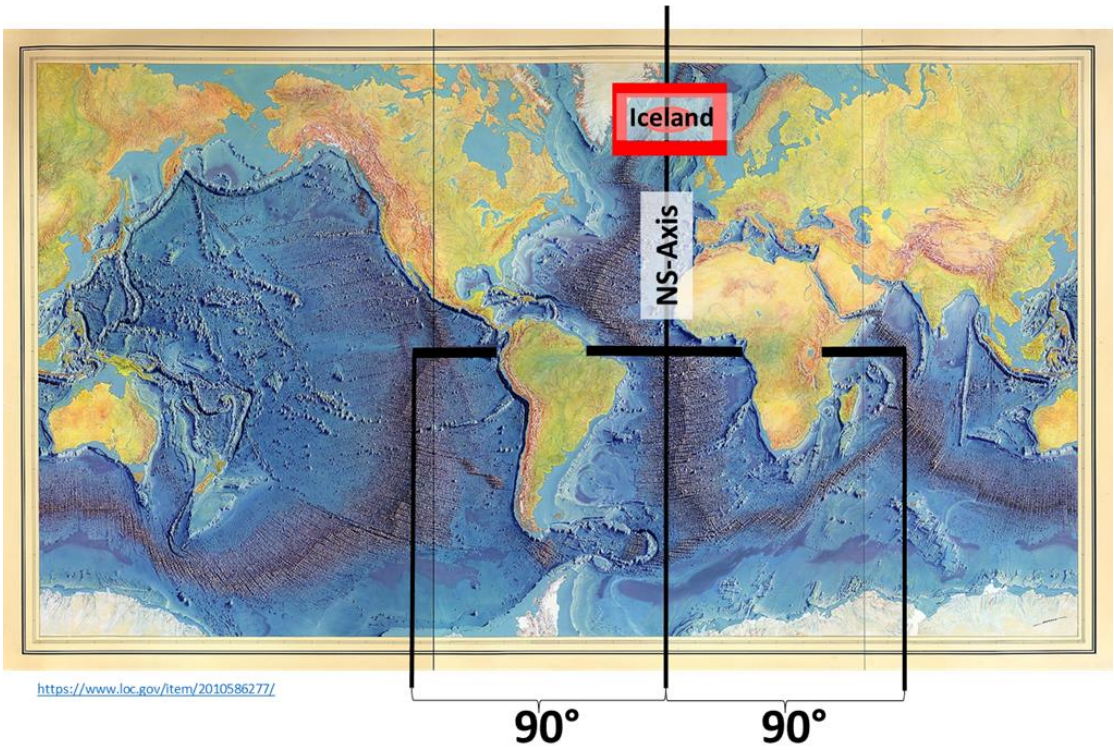

Figure 51: Equatorial cross-section showing the distribution of the main Pacific, Atlantic and Indian Ocean ridge systems.

In the cross-section, the Indian Ocean and Pacific ridge systems appear above converging branches of the large lower-mantle circulation proposed in this model. In the uppermost asthenospheric layer, however, the model places divergent flow immediately beneath the ridges, directed away from the ridge axes to the east and west. The distinction between the large lower-mantle cells and the smaller upper-layer cells is therefore important when interpreting the figure.

The ridge pattern does not display the same regular 30°-60°-30°-60°-30° sequence as the land-ocean measurements. Nevertheless, several ridge positions show a notable correspondence with the proposed 30° framework. One apparent irregularity concerns the Pacific ridge system, which does not form a simple 90° relationship with the central Atlantic reference. In the present interpretation, this departure is considered in

relation to the geometry of the Cocos-Nazca spreading system and the adjacent Pacific Plate triple-junction region.

Accordingly, a sequence of approximately 30° divisions can be traced through several major equatorial reference points: the eastern boundary of the Pacific Plate, the west and east coasts of South America, the central Atlantic, the west coast of Africa, the Great Rift Valley, the central Indian Ocean, and the west and east sides of Indonesia. These points define eight successive intervals, accounting for about 240° of the equatorial circumference. The remaining approximately 120° lies within the Pacific sector, where the pattern is less directly expressed by comparable equatorial boundaries.

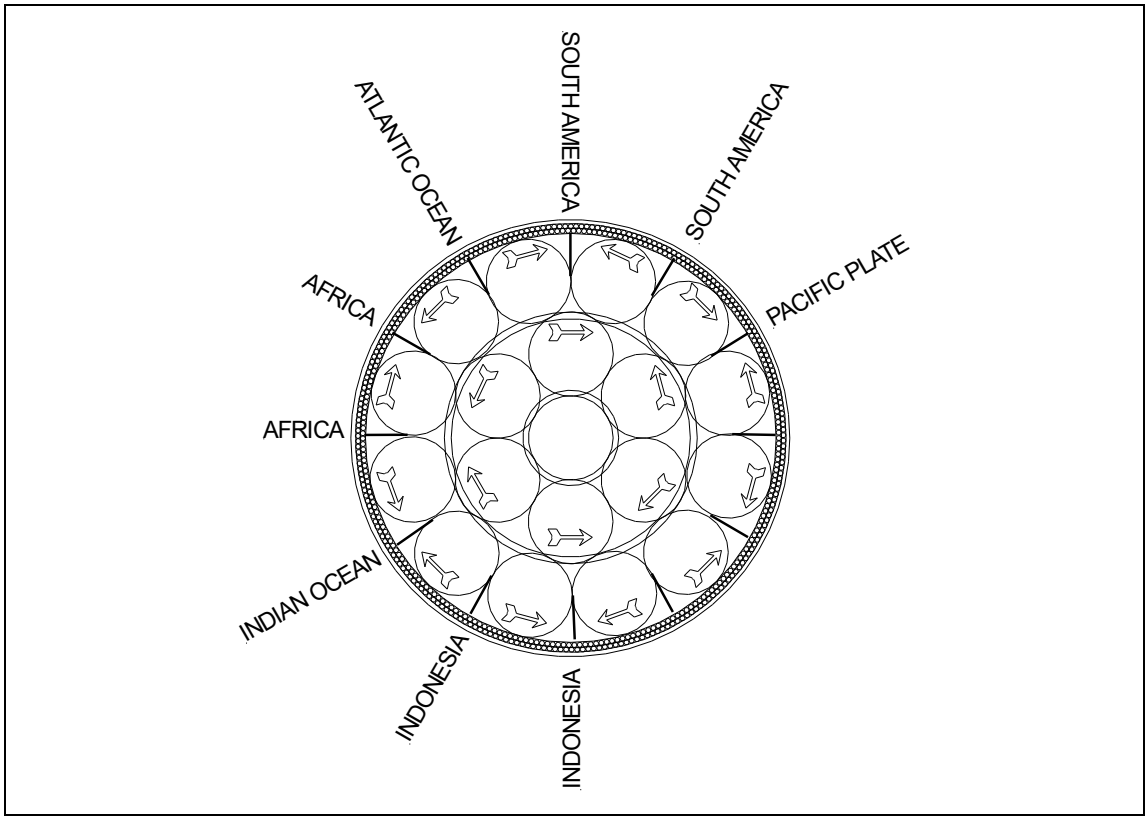

Figure 52: Comparison between the proposed convection-cell divisions and major tectonic features along the equator.

This comparison accounts for most of the major equatorial reference points used in the model. Three expected division lines do not show equally obvious markers directly at the equator; these are associated in the global construction with the sectors extending from Japan, the Bering Strait and Hawaii, respectively. Their significance is considered further when the full world map is developed in the next chapter.

These surface comparisons provide a second line of analysis, distinct from the physical and geometrical derivation in Part I. The purpose here is to ask whether mapped geological and geographical features are consistent with a model whose basic dimensions were derived independently from geophysical measurements. Agreement strengthens the case for further investigation, while discrepancies provide equally important tests of the model.

Several of the reference longitudes happen to lie close to round-number values, including approximately 50°W, 20°W, 10°E, 40°E, 70°E, 100°E and 130°E. Departures from the idealized 30° spacing should therefore be quantified individually rather than overlooked. Their size and geological context provide a way to test the proposed systematic interpretation rather than assume it in advance.

8.4. Why Might the Equatorial Pattern Have Been Overlooked?

I have not found this particular equatorial pattern explicitly described in the literature consulted for this work. Several practical reasons may help explain why such a relationship is easy to overlook on a conventional world map.

Reason no. 1: The African interval is not a simple coast-to-coast measurement. Its western reference lies near the Gabon coast, while the eastern reference is associated with the Great Rift Valley system, where the Somali Plate is separating from the main African Plate. The comparison is therefore tectonic as well as geographical. In the proposed pattern, the approximately 60° interval from the Great Rift Valley to Indonesia provides the adjoining measurement against which this African segment can be assessed.

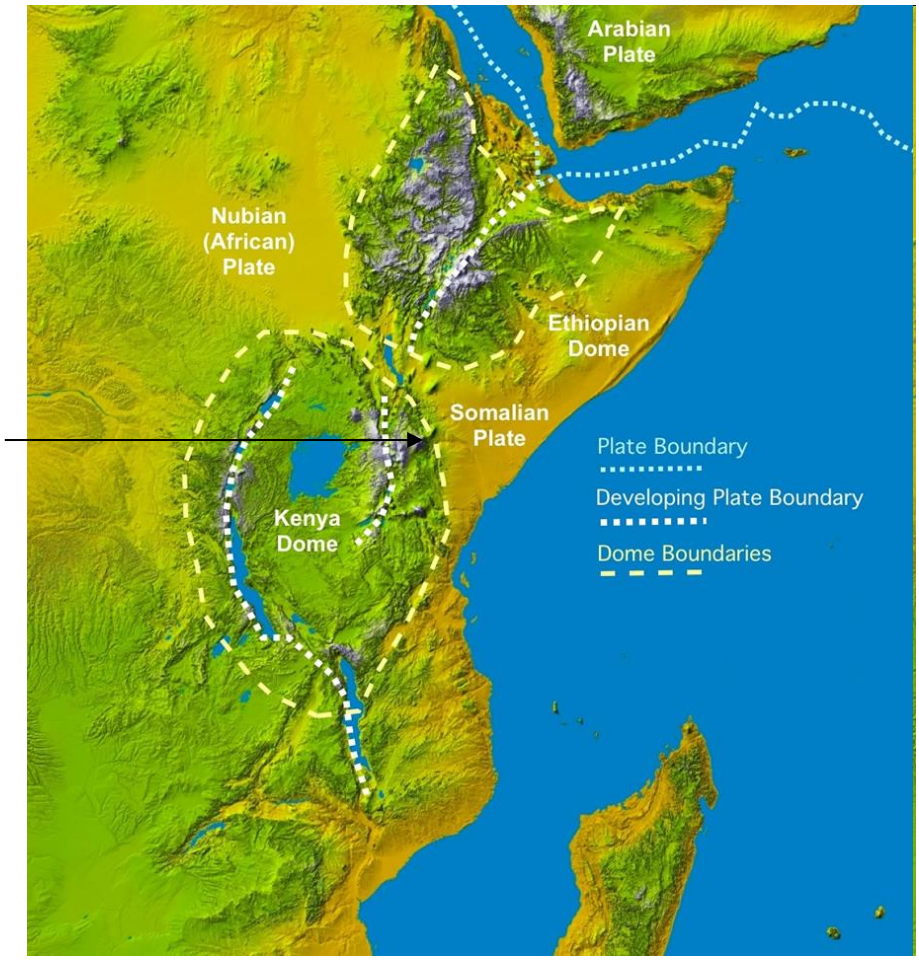

Figure 53: Proposed intersection point of large convection cells beneath Africa.

Reason no. 2: Plate motion is continuous, so the present-day pattern is only a snapshot. The geometry would have been different in the past and will continue to change in the future. Any interpretation of a regular present-day arrangement must therefore be reconciled with tectonic drift rather than treated as permanently fixed. This also suggests that palaeogeographic reconstructions could provide an important future test of the model.

Reason no. 3: Indonesia is an archipelago rather than a single visually continuous continent. As a result, the sequence of three approximately 30° land or tectonic sectors separated by two approximately 60° oceanic sectors is not immediately obvious on a standard geographical map. The geological and geographical boundaries do not coincide in a simple visual way.

Reason no. 4: The coastlines of both South America and Indonesia are oblique to the equator, trending broadly northeast-southwest or northwest-southeast. Moving only a small distance north or south therefore produces a substantially different

pattern. The relationship described here is tied specifically to the narrow equatorial reference line, where the Coriolis parameter changes sign.

Reason no. 5: The ocean-ridge geometry is itself complex. The Mid-Atlantic Ridge changes trend near the equator, the Indian Ocean ridge system is branched, and the eastern boundary of the Pacific Plate turns south of the equator. These features make it difficult to recognize the proposed relationship between ridge positions and the land-ocean pattern at a single glance.

Reason no. 6: The equator is not normally singled out as a primary tectonic boundary. Within the present model, however, the vanishing of the Coriolis parameter at the equator provides a specific physical reason to examine that line separately and to test whether an unusually regular surface pattern occurs there.

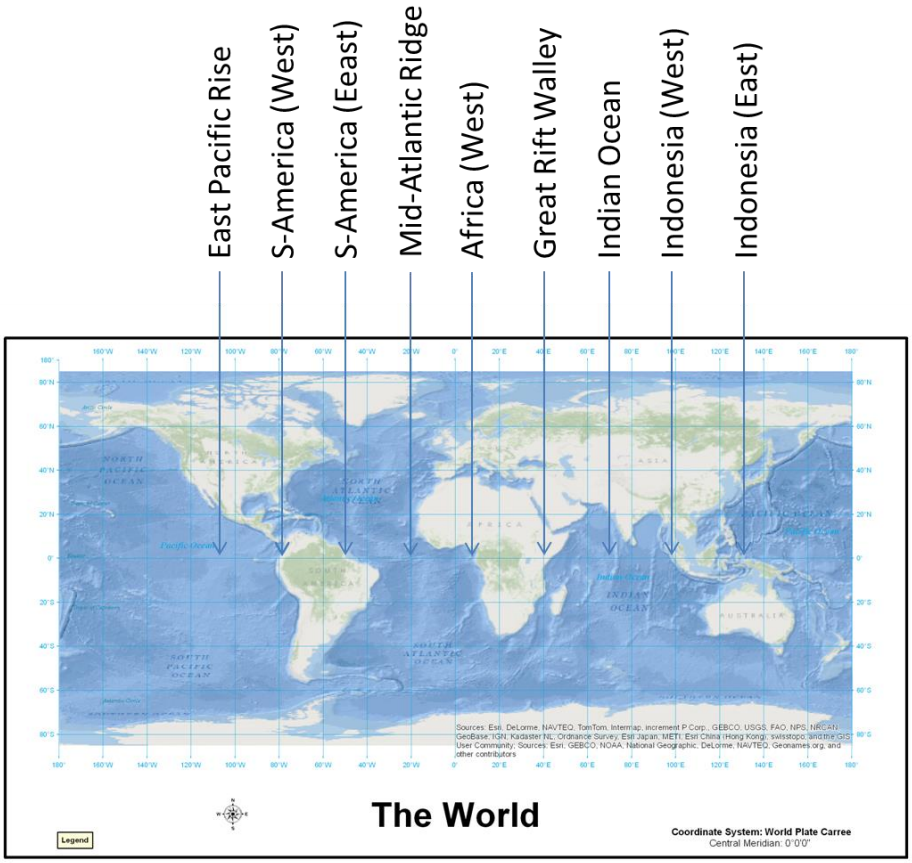

The obvious "30° stepstones" along equator

Figure 54: World-map summary of the proposed 30° divisions along the equator.

Figure 55 summarizes the proposed 30° divisions along the equator. The pattern

should be treated as a present-day geometrical observation rather than as a timeless configuration. Because tectonic plates continue to move, past and future arrangements must differ. A fuller evaluation of the model will therefore require connecting the present pattern with the long-term evolution of plate positions and tectonic boundaries.

Chapter 9 - The World Map

Having established both an internal geometrical framework and an equatorial surface comparison, the next step is to extend the proposed convection-cell system to a global map.

9.1. Preconditions for Tracing the System North and South

Within the model developed here, twelve large convection cells, each spanning approximately 30° along the equator, are proposed to underlie the regular equatorial divisions discussed in Chapter 8. If this interpretation is correct, the same geometry should also have consequences away from the equator. The positions of continents, their tectonic history, the distribution of major volcanic regions and other large-scale features can therefore be compared with the predicted global pattern. The examples in this chapter are presented at several scales in order to examine whether the same framework remains useful from the global to the regional level.

The preceding chapters considered the geophysical observations and physical premises used to construct the convection-cell model. The present chapter projects that model onto the Earth's surface. At the global scale, the pattern is compared with major volcanic regions and with broad aspects of plate motion. At the regional scale, Iceland provides a particularly detailed example because the hemispheric and polar parts of the proposed system intersect there. At the local scale, the finer grid of upper-mantle convection cells can be compared with individual volcanic and geothermal areas. These successive scales provide different ways of testing the same geometrical framework.

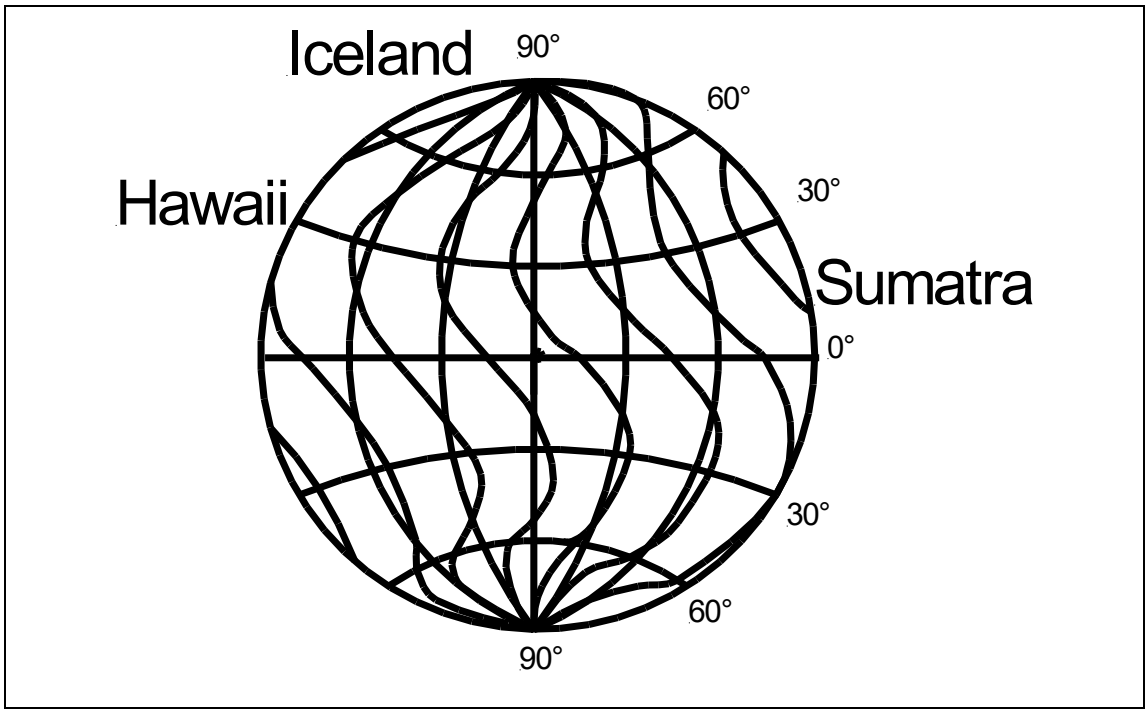

Figure 55: Transition from the internal geophysical model to comparisons with surface features.

9.2. Global View

Iceland and Hawaii are among the most prominent volcanic regions commonly discussed in relation to mantle upwelling. In the model presented here, their relative positions provide one constraint on the horizontal dimensions of the proposed convection rolls. They are separated by four large lower-mantle cells in the geometrical construction. This relationship was one of several observations used when developing the horizontal scale of the system. In the final construction, each hemispheric cell forms a circle on an idealized longitude-latitude grid, centred near 32° latitude and extending to approximately 67° in one direction and about 3° across the equator in the other. The generalized global arrangement is shown below.

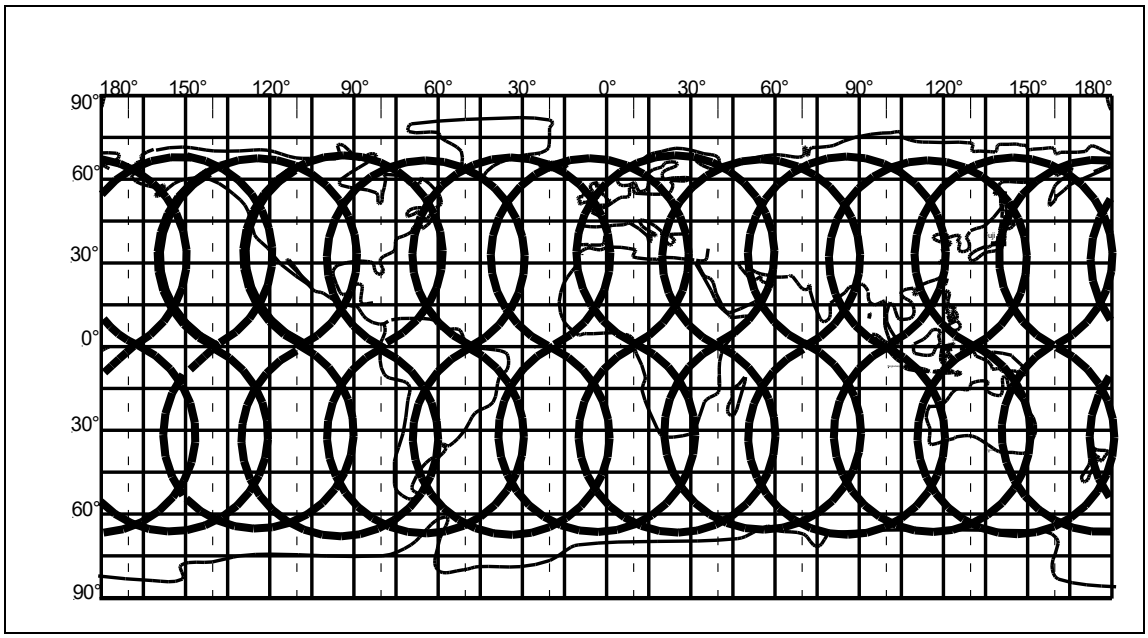

Figure 56: Global map showing the twelve principal division lines of the proposed system.

Figure 57 shows the generalized horizontal pattern projected onto a world map. At this scale, only the principal lines can be displayed clearly. When the model is enlarged over a smaller region such as Iceland, the predicted geometry can be compared with mapped features at a much finer scale. A complete representation of every line in the system would be too dense to show effectively on a single A4 page.

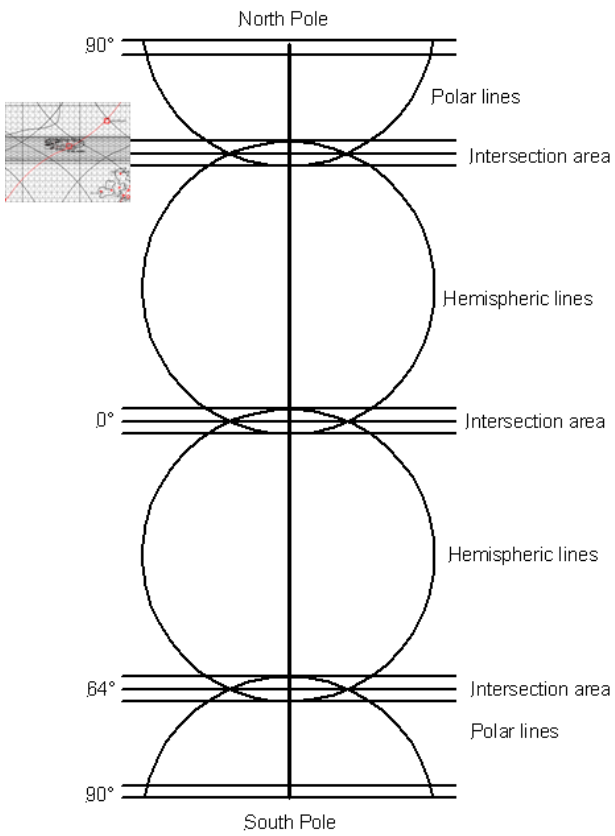

Figure 57: Iceland shown in relation to the horizontal convection-cell model.

Iceland occupies a particularly useful position for examining the proposed geometry. It lies on the Mid-Atlantic Ridge and, in the interpretation used here, above a major mantle-upwelling region. The model also requires separate consideration of the polar portions of the convection cells, extending approximately from 60.7° to 90° north and south, and the hemispheric portions, extending from the equator to about 67.3° in each hemisphere. On the idealized map used here, the northern hemispheric arc is represented as part of a circle centred near 32°N. Its radius therefore extends approximately from 32°N to 67.3°N and to about 3.3°S. The polar section is constructed with the same curvature, and the corresponding geometry is mirrored in the Southern Hemisphere.

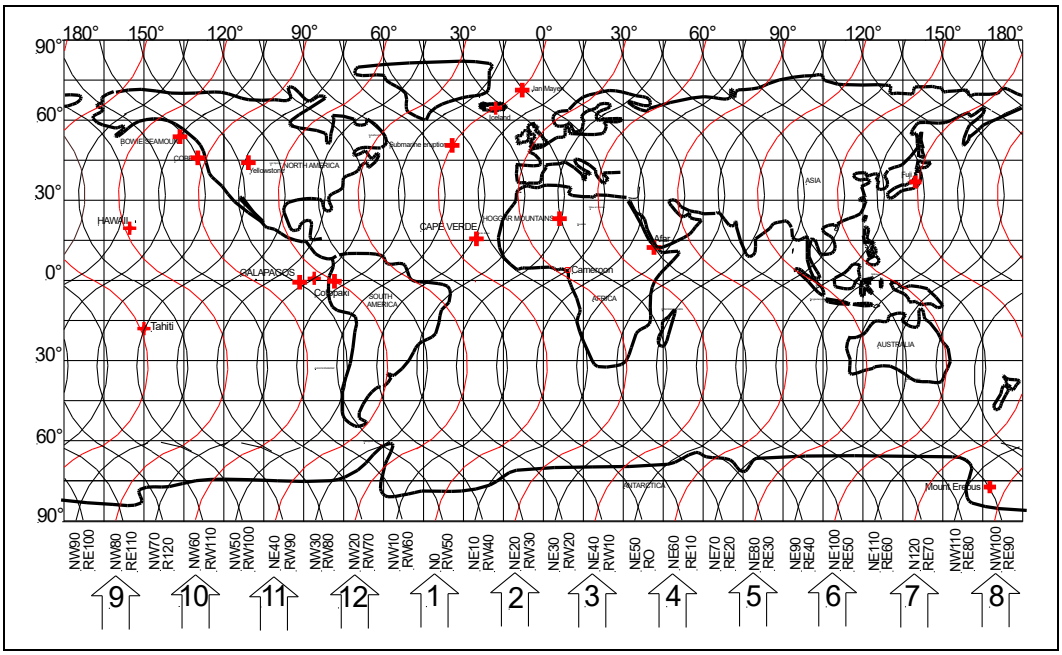

Figure 58: Global convection-cell framework with selected volcanic regions shown for comparison.

The world map shows 24 S-shaped principal lines and 24 corresponding mirror-shaped lines as a simplified representation of the system. In the more detailed construction, a total of 240 S-shaped lines is used. The convection cells are numbered, and the global map shows both cell boundaries and selected central lines. This is an idealized regular framework; meaningful comparison with any particular geological region requires additional local information and should not rely on the global sketch alone. A portion of the more detailed construction is shown below

Figure 59: North Atlantic section of the more detailed convection-cell model.

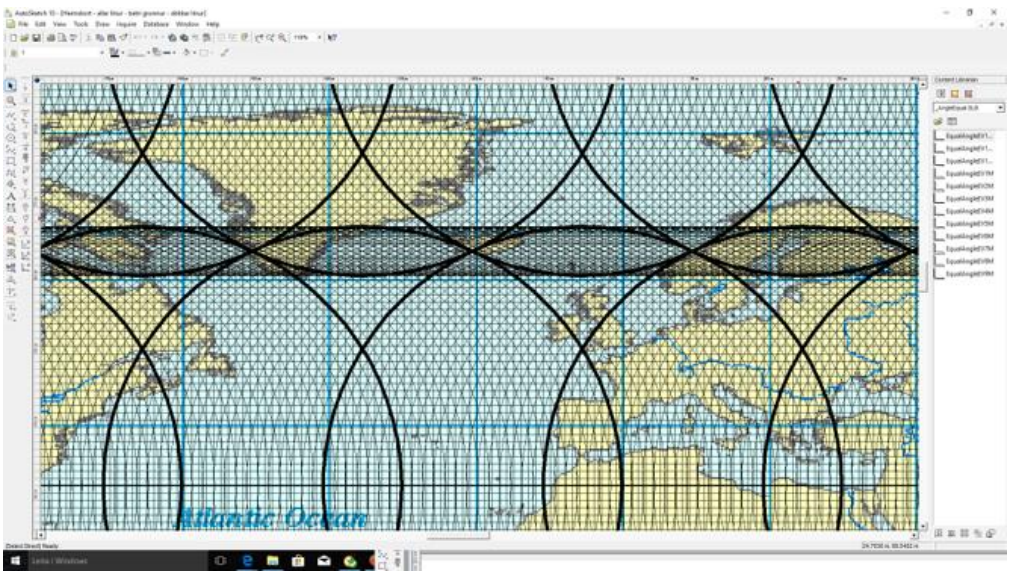

9.3. Connection Between Iceland and Hawaii

Irvine (1989) noted that Iceland and Hawaii subtend an angle of almost exactly 90° at the Earth's centre and suggested that this relationship might reflect a regular feature of the mantle. The Icelandic geologist Kristján Sæmundsson drew my attention to this article in 2010 as an example of an attempt to identify large-scale organization within the Earth's interior. In the convection-cell model developed here, the approximately 90° separation is interpreted as the combined result of two geometrical relationships: an interval of 120° along the 64th parallel between an Icelandic convection cell and one associated with Hawaii, followed by an approximately 45° longitudinal component along the corresponding arc. Irvine (1989) expressed the significance of the relationship as follows:

> In view, of the prominence of Hawaii and Iceland as global hot spots, this 90° relationship seems more than coincidence, and the proposition explored here is that it is a direct reflection of the Earth's convection structure.

Irvine considered the relative positions of Iceland and Hawaii in the context of a comparatively fixed mantle framework. The same general question is pursued here, although the present model attempts to derive the geometry of that framework in considerably greater detail.

In the model, the positions of continents and volcanic regions can be examined in relation to the convection-cell grid at global, regional and local scales. Iceland and Hawaii are used as two primary reference regions because both are associated with major melting anomalies and mantle upwelling. A third reference upwelling in the same geometrical construction is placed in the Indonesian region.

These three regions - Iceland, Hawaii and Indonesia - provide geographical reference points for estimating the horizontal dimensions of the proposed convection-cell system. Combined with the geophysical constraints developed in the preceding chapters, they allow the three-dimensional convection-roll geometry to be constructed with progressively greater precision.

The world map contains the principal convection-cell divisions at 30° intervals along the equatorial reference framework. The following comparison enlarges the regions around Hawaii and Iceland.

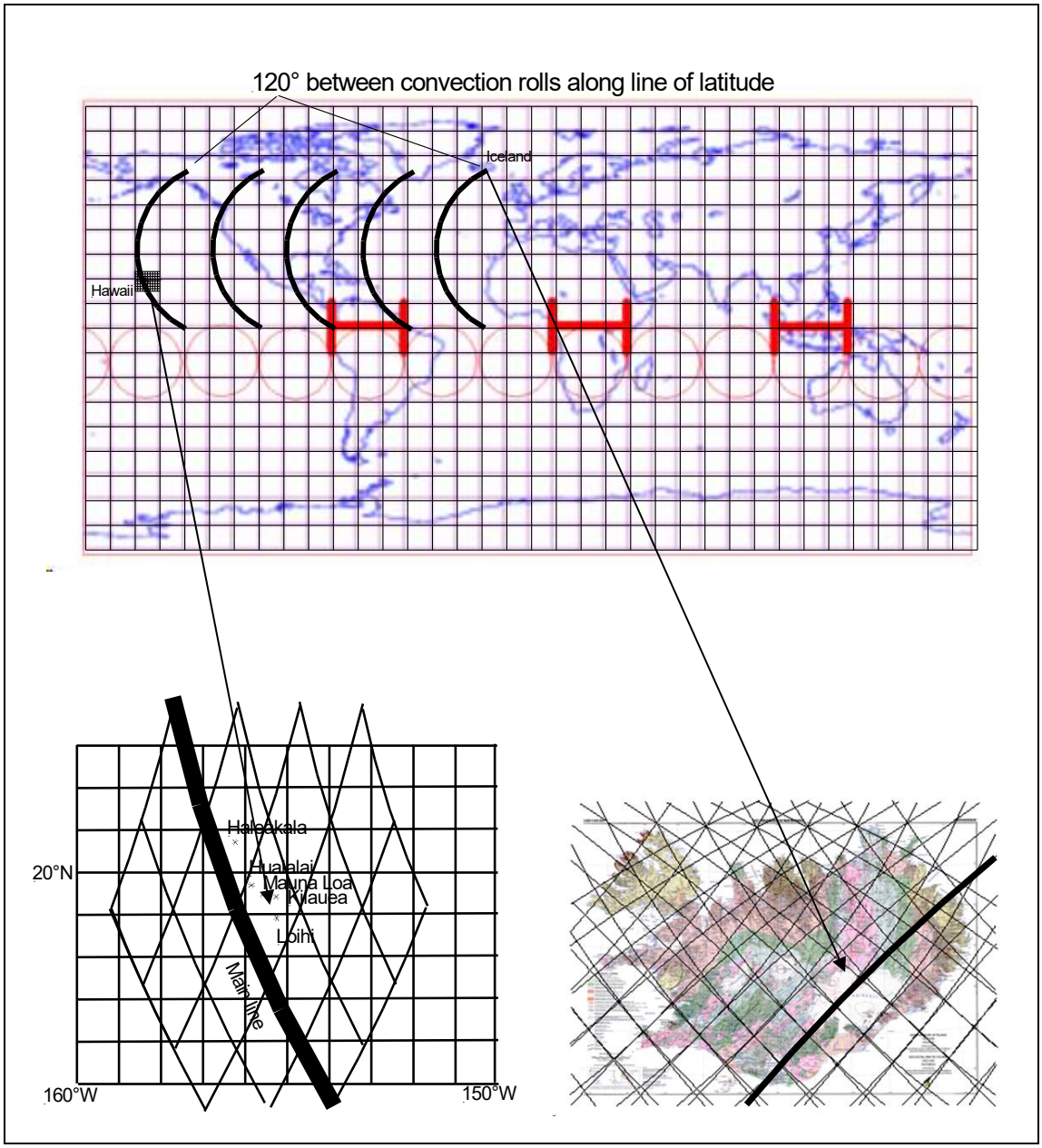

Figure 60: Hawaii and Iceland shown in relation to convection-cell lines separated by 120° in the proposed framework.

The dots in the Hawaii inset mark currently active volcanoes. In this comparison, their distribution follows approximately the same general trend as the principal line of the proposed convection system. In Iceland, the corresponding calculated line passes through or close to Katla, Grímsvötn and Kverkfjöll, approaches the Bárðarbunga caldera, and crosses western Vatnajökull, an area commonly associated with the Icelandic melting anomaly. The purpose of the comparison is to test the predicted orientation against mapped volcanic features rather

than to assume a direct one-to-one causal relationship.

Both calculated lines, for Hawaii and Iceland, are derived from Equation 1 on page 54:

$$(x^2 - C_n) + (y^2 - 32) = 35.34$$

where Cn = -123.2 for Hawaii and Cn = -3.2 for Iceland.
Here, x represents longitude and y represents latitude on the rectangular map grid used for the calculation.

This comparison provides another test of the internal consistency of the model. The parameters were derived from the geometrical and physical premises described in the preceding chapters; the calculated lines can therefore be compared independently with the observed orientations of the volcanic regions.

A further point concerns the relative fixity of hot spots. Hot-spot positions are now recognized as less rigidly fixed than was once assumed (Foulger 2010). Within the convection-cell model, however, the relevant comparison is not that Iceland and Hawaii remain fixed as individual points, but that both melting anomalies occur along strong lines of the proposed convection framework. The recent southward migration interpreted for Hawaiian volcanism is therefore considered here in relation to movement along one of those convection-cell boundaries.

A corresponding 120° interval along the relevant latitudinal framework is also found between Iceland and Indonesia. That relationship is noted here but would require a separate detailed analysis.

9.4. The North Atlantic

The 64th parallel occupies a special position in the proposed system, although unlike the equator the Coriolis parameter is not zero there. Its significance in the model arises because two parts of the convection-cell system meet within this latitude range. It is therefore useful to ask whether geometrical relationships comparable with the equatorial pattern can also be recognized in the North Atlantic. One such relationship is the approximately 30° longitudinal separation between the Icelandic volcanic zone, represented here by Hekla, and the coast of Norway near 64°N. On the global scale, the Bering Strait is also positioned near a boundary between two of the large lower-mantle cells. Figure 62 summarizes the North Atlantic comparison.

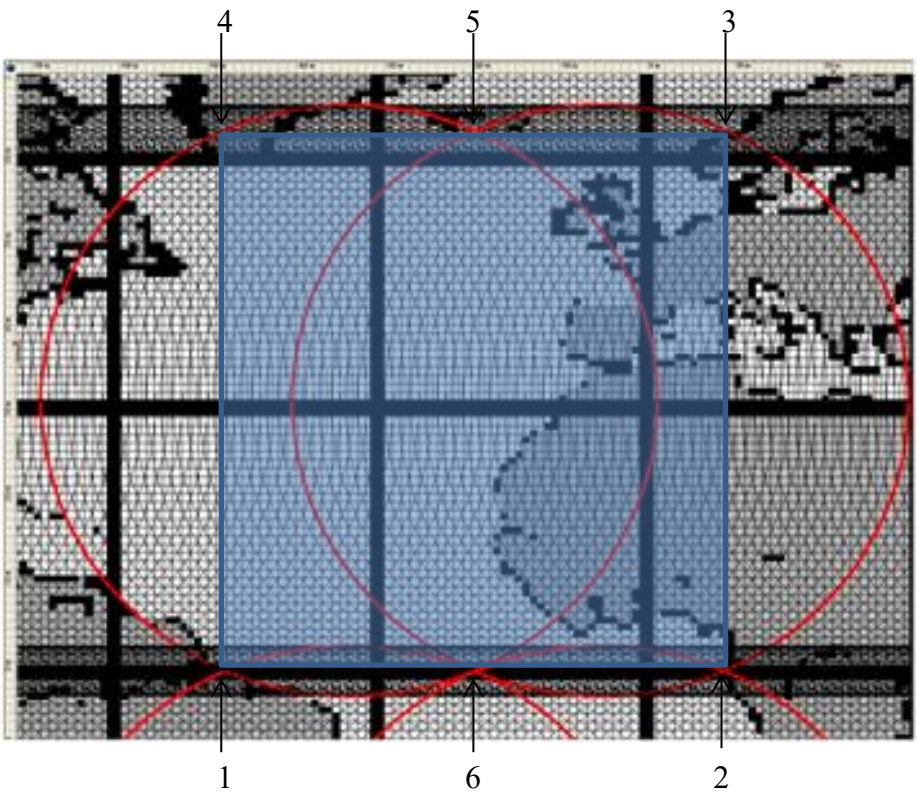

Figure 61: Schematic North Atlantic pattern used for comparison with the equatorial framework.

From South America (1) to Africa (2): approximately 60°. The coast of Norway at 64°N (3) lies near the same longitude as the African reference point (2). From Norway (3) to the western Greenland reference (4): approximately 60°. Hekla (5) and the equatorial crossing of the Mid-Atlantic Ridge (6) lie near the same longitude.

A first-order examination of the 64th parallel therefore reveals several relationships comparable with those described along the equator. The approximately

30° separation between the Hekla volcanic system and the Norwegian coast is especially relevant when compared with the 30° and 60° intervals used in the equatorial construction.

A further reference relationship is that Hekla lies close to the longitude assigned here to the centre of the Atlantic Ocean at the equator.

Taken together, these points define a simple North Atlantic framework involving Hekla, the Norwegian coast near 64°N, the equatorial central-Atlantic reference, and the equatorial coasts of South America and Africa.

Greenland introduces an important complication. In the idealized construction, the Greenland and Norwegian reference points near 64°N and the South American and African reference points at the equator form an approximately rectangular arrangement. The present eastern coastline of Greenland does not fit that geometry directly, while the western reference used here lies near the boundary between the ice-covered interior and the mountainous coastal region. For the present discussion, the Hekla-Norway-Africa-central Atlantic-South America pattern is used as the principal comparison. The position of the northwestern point remains more difficult to define because Greenland's present topography and ice cover complicate the choice of an equivalent boundary.

One unusual biological observation is the occurrence of Crymostygius thingvallensis (Kristjansson og Svavarsson 2002), a freshwater amphipod found in Þingvellir, Iceland. Its survival through glacial periods raises questions about the long-term continuity of suitable groundwater habitats in the rift system. In the present geometrical model, Þingvellir lies close to the longitude assigned to the equatorial centre of the Atlantic, while the 64th parallel is treated as a northern mathematical counterpart to the equatorial transition. The biological observation is therefore mentioned here as a potentially interesting, but necessarily speculative, line of comparison rather than as proof of the convection-cell system.

9.5. Kamchatka and Iceland Compared

Kamchatka has a pronounced linear topographic structure and is also one of the world's major volcanic regions. Its tectonic setting differs fundamentally from that of Iceland, making it useful as an independent comparison. The question examined here is whether the same geometrical formula used in the model predicts the dominant orientation of the peninsula, including the mountain chain and the boundary between the mountainous and lower-lying regions.

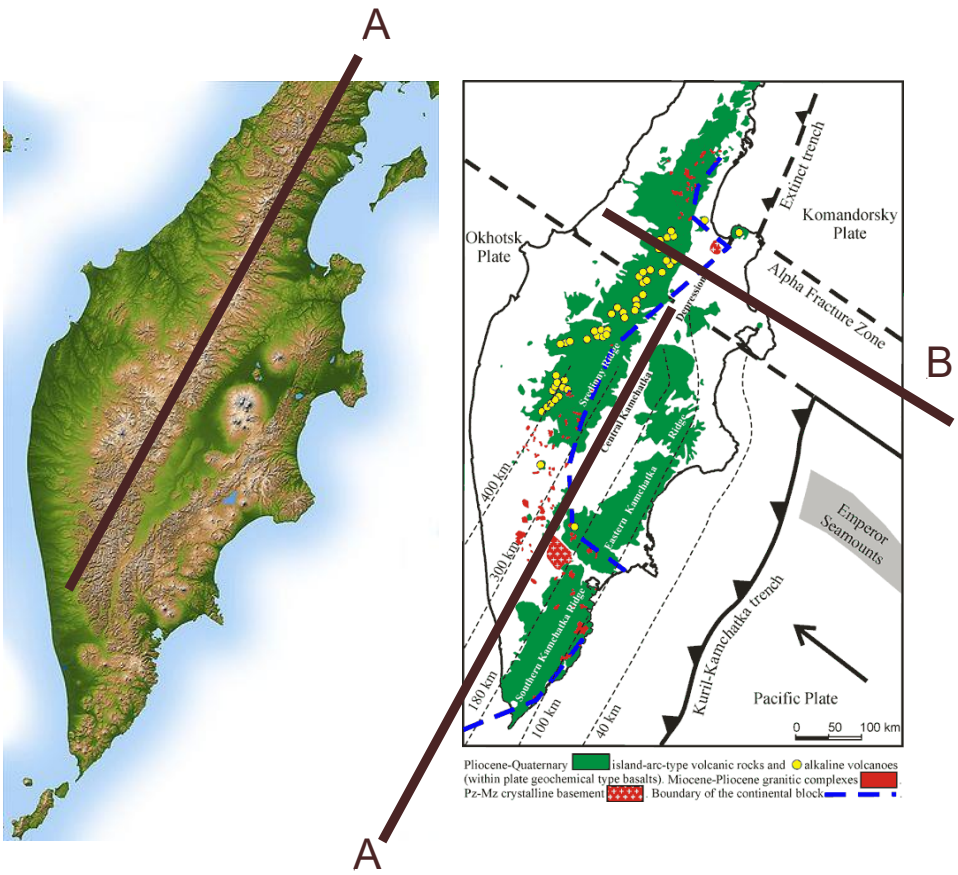

Figure 62: Comparison between the calculated convection-cell direction and the dominant topographic trend of Kamchatka.

The calculation illustrated in Figure 62: Comparison between the calculated convection-cell direction and the dominant topographic trend of Kamchatka. uses $\varphi = 57°$ for the hemispheric convection cells. The resulting direction is N28.6°E, shown as line A in each drawing, and closely follows the dominant trend of the peninsula. The adjacent Alpha Fracture Zone is approximately perpendicular to the Kuril-Kamchatka Trench and to the principal tectonic and topographic trend. Line B, oriented N58.2°W, represents the approximately half-angle relationship considered elsewhere in this

work. This secondary angle is included because similar relationships recur in several of the regional comparisons.

This secondary relationship is discussed further in connection with the SISZ (see 10.5. The South Iceland Seismic Zone (SISZ)) and in the comparison between the Reykjanes and Snæfellsnes peninsulas.

South Iceland:

A second comparison can be made with a calculated orientation in South Iceland.

The inserted line is calculated from formula (7) for polar lines at latitude 64.1°, using the centre of Lake Langisjór as the reference point. In the comparison shown, the surrounding hyaloclastite mountain ridges follow approximately the predicted polar-cell orientation of N42.5°E.

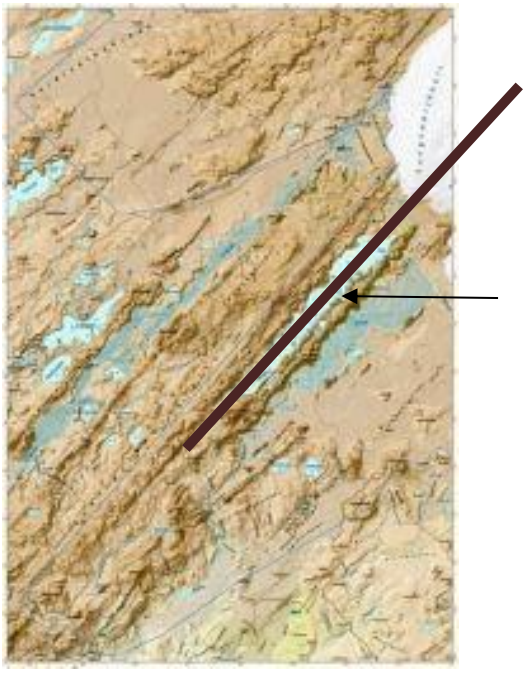

Figure 63: Comparison of the calculated trend from Equation 6 with the EVZ in Iceland and the Kamchatka example.

Langisjór follows the same broad structural trend as the surrounding Eastern Volcanic Zone (EVZ), which is compared elsewhere in this work with the proposed convection-cell system. The value of this example is therefore not that Langisjór is treated as an isolated feature, but that the same set of geometrical relationships can be compared with both Iceland and Kamchatka, and in principle with any other region for which the relevant latitude and structural trend are known.

At these latitudes, the calculated trends of the polar and hemispheric cells are sufficiently similar that distinguishing their possible surface expressions may be

difficult. Petrological information can therefore provide an additional constraint when evaluating which layer or flow component might be relevant in a particular area. The surface expression of the proposed system is necessarily more complex than the idealized geometry of individual convection rolls. Beneath Iceland, the four upper layers form a grid whose intersections and polygons must be considered as parts of a single system rather than as independent lines.

Moving farther north, the hemispheric formula used for Kamchatka can also be applied to the North Iceland Seismic Zone, including the Tjörnes Fracture Zone.

As discussed previously, the orientation of the proposed convection rolls can be calculated as a function of latitude. In the model, the associated Munroe lines are assigned the same orientation and are interpreted as having a surface expression in tectonic and topographic structures. The Tjörnes Fracture Zone off northern Iceland provides one example. Earthquake epicentres define a broad linear zone that can be compared with the calculated trend. Applying formula (6) at latitude 66°10' gives:

We get α = N61°12’W.

The same hemispheric formula can therefore be compared with both the Tjörnes Fracture Zone north of Iceland and the dominant trend of Kamchatka. At Tjörnes, the comparison involves not only the mapped structural orientation but also the distribution of earthquake epicentres. The similarity is presented here as a test of the predicted direction rather than as evidence from a single line alone.

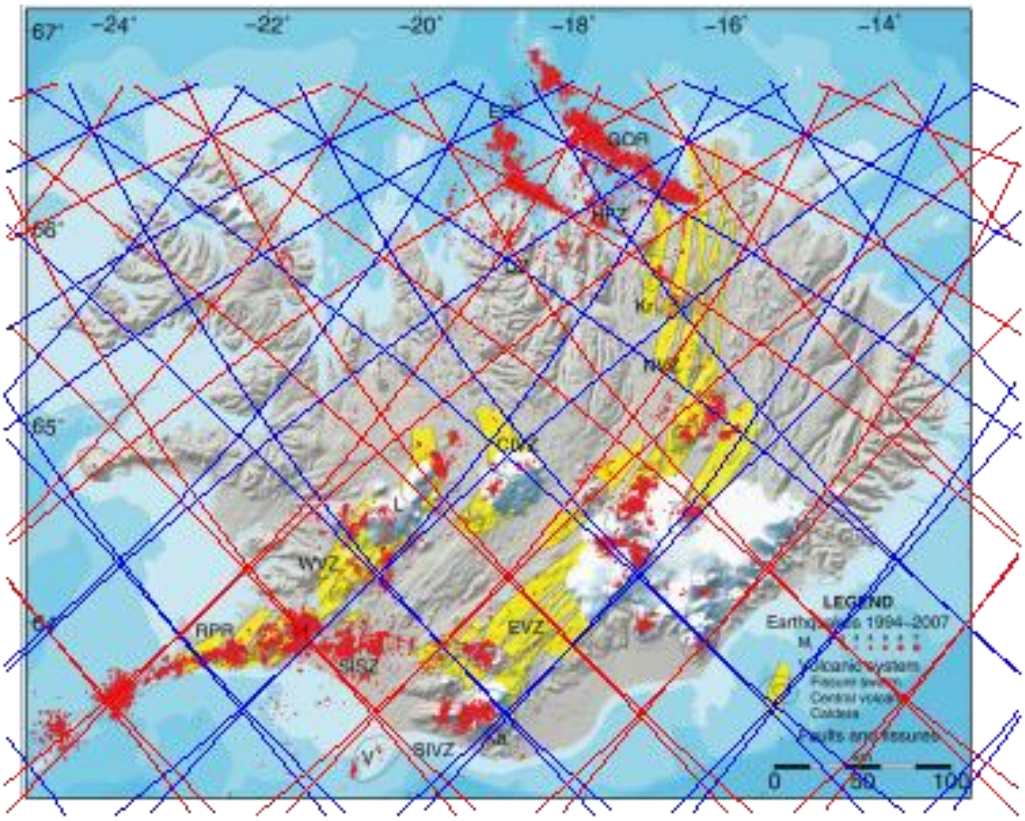

Figure 64: Simplified comparison between the calculated direction and the Tjörnes Fracture Zone.

The calculated line is approximately parallel to the Tjörnes Fracture Zone in the comparison shown. A geometrical match by itself is not sufficient to establish a direct connection with the convection-cell model; the local tectonic setting must also be considered. The Tjörnes region is structurally complex and is therefore discussed again in later sections of the book.

9.6. Trenches

As discussed from page 31 onward, the 410 and 670 km discontinuities are incorporated into the convection-cell system proposed here. Subduction zones provide an important additional test because earthquake hypocentres trace descending slabs to depths approaching the mantle transition zone. As an illustrative example, the original analysis used the Havre Trough region near 180°E and approximately 20-30°S, selected as a representative trench setting for comparison with the model.

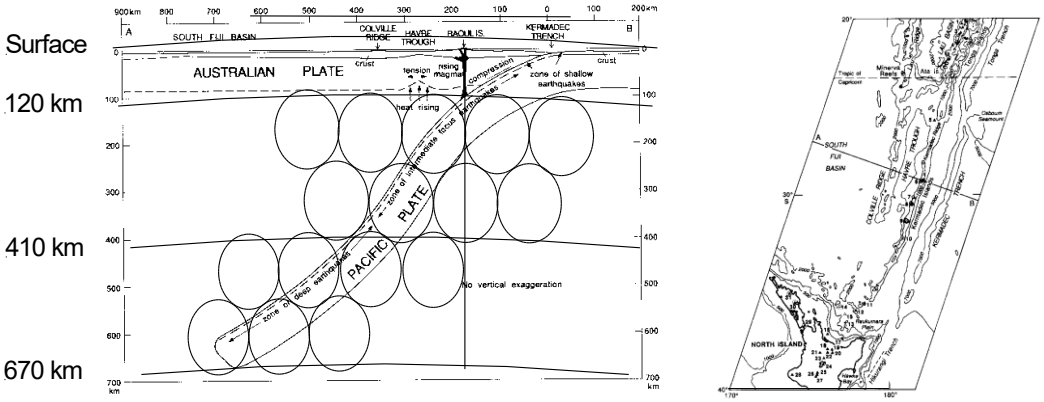

Figure 65: Schematic example of the Pacific Plate underthrusting the Australian Plate in relation to the proposed convection-cell framework.

This relationship provides a basis for further testing of the model at subduction zones. In the interpretation proposed here, a descending pair of convection cells accommodates the subducting plate, while an adjacent ascending component to the east contributes to extension. The plate is then represented as curving concavely through one convection cell of layer 2 (elsewhere referred to as the OIB layer) and becoming convex after passing through the 410 km discontinuity. At approximately 30°S, the model places a boundary between two large lower-mantle cells beneath the region, with upward flow dividing toward the east and west. The westward component in the 410-670 km interval is therefore proposed as a possible influence on the geometry of the deeper part of the slab.

9.7. The Arctic

Like the geographical grid of latitude and longitude, the proposed convection-cell system reaches a geometrical limit at the poles. The east-west circumference available to the cells decreases continuously toward 90°, where it converges to a single point. The question is therefore not whether the basic geometrical rules cease to apply, but how the circulation represented by those rules can remain continuous as the available horizontal width approaches zero.

One way to examine this problem is to follow an idealized particle through the model. Within the hemispheric part of the system, a particle can be represented as moving along the MORB layer from the equatorial region northward toward the transition zone between approximately 61° and 67°N. There it is transferred, in the proposed geometry, to an OIB line and continues along the complementary part of the circular path back toward the equator. The sign of the Coriolis deflection changes between hemispheres, while the complete trajectory is represented as a continuous circulation within the rotating Earth.

The polar system can be considered in a similar way. A particle following the MORB layer toward the North Pole must, in the model, be able to transfer to a corresponding OIB path for the return flow. Because the longitudinal spacing of the convection rolls becomes progressively smaller toward the pole, the model provides many closely spaced potential intersection or transfer points. This is the simplest geometrical interpretation of how continuous horizontal circulation might be maintained in the polar region.

The mathematical construction becomes unusual close to the pole. The polar-cell equations used here place the theoretical centre of the horizontal circulation at 96°N (and, by symmetry, at 96°S), beyond the geographical pole. Mathematics and physical geography can be reconciled in the model only by allowing the idealized trajectory to pass through the polar point and continue on the opposite meridian. In that representation, the particle crosses the pole and then moves southward, reaching the corresponding 84th parallel on the opposite side of the globe and forming the next geometrical relationship near 78°N.

The polar circulation does not therefore need to terminate at the pole in the model. The larger convection cells beneath the upper layers must also be considered. The proposed geometry allows flow associated with the North Polar region to connect southward with the deeper cells, while an opposite arrangement is envisaged near the

South Pole. In this interpretation, the polar regions provide transfer zones between different parts and depths of the overall convection system rather than endpoints of circulation.

Chapter 10 - Iceland

I am naturally more familiar with the geology of Iceland than with that of other parts of the world. Iceland contains numerous volcanic systems, and geothermal activity occurs across much of the country. The general geological setting is described extensively in textbooks, so there is no need to repeat the basic geology here. Instead, this chapter compares Icelandic tectonic, volcanic and geothermal features with the framework predicted by the convection-roll model. Within that framework, a striking degree of correspondence appears. Iceland is undergoing active extension, and roughly a quarter of its area lies within volcanic zones, which are distributed mainly from southwest to northeast. The influence of deeper processes should therefore be most readily detectable in these actively deforming regions. The 64th parallel is of particular interest because several volcanic and tectonic features occur near positions that are critical within the proposed convection-cell system.

10.1. The hemispheric and polar lines over Iceland

As described earlier, four convection-cell layers are proposed beneath Iceland between 120 and 410 km depth. Two are associated with rolls extending northward from the equator to about 67.3°N, producing the pattern shown below.

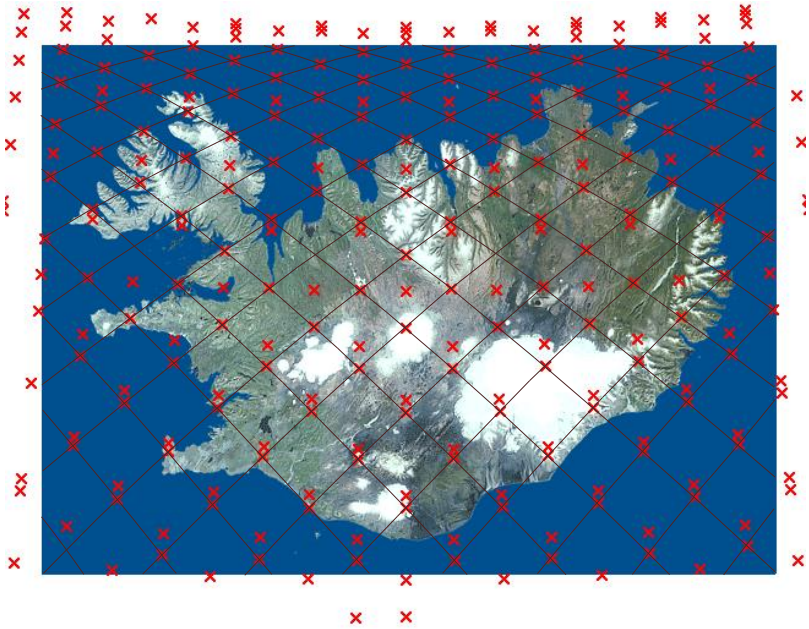

Figure 66: The hemispheric convection-cell pattern over Iceland.

In the same way, convection rolls extending southward from the North Pole to approximately 60.7°N produce a second set of projected lines across Iceland.

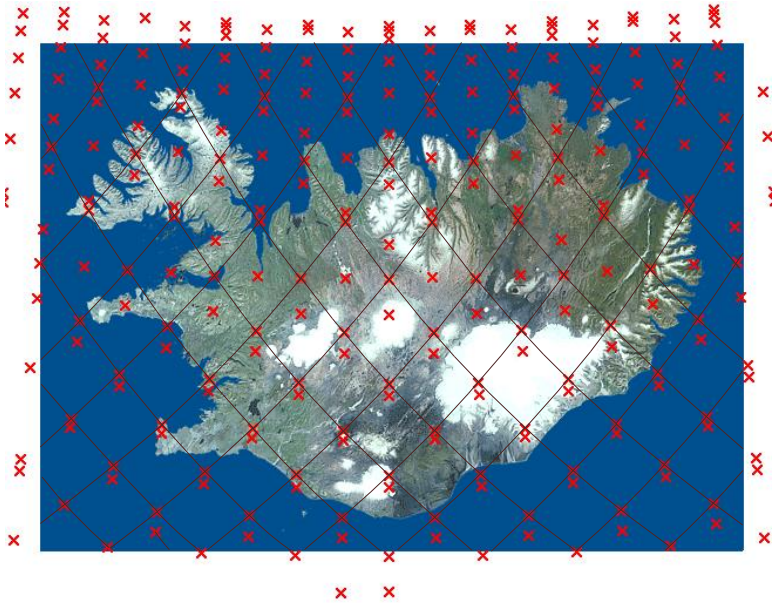

Figure 67: The polar convection-cell pattern over Iceland.

These maps are quite accurate as compared to the model.

Together, the four sets of rolls produce the combined pattern shown below:

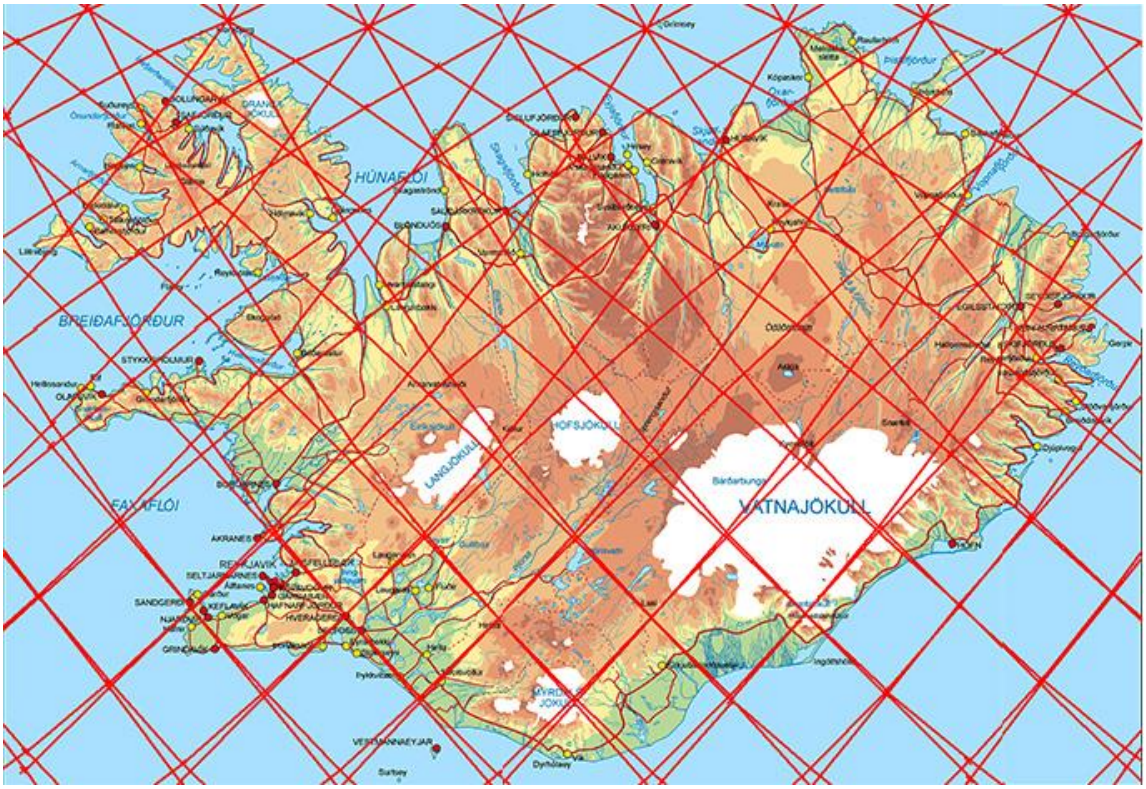

Figure 68: The combined Icelandic grid of convection cells.

The same construction can, in principle, be extended globally. Its geometry is derived from the geophysical layering of the Earth and from the physical assumptions concerning the behaviour of convection cells developed in Part I. Iceland provides a particularly detailed area in which to compare the resulting grid with observed geological features.

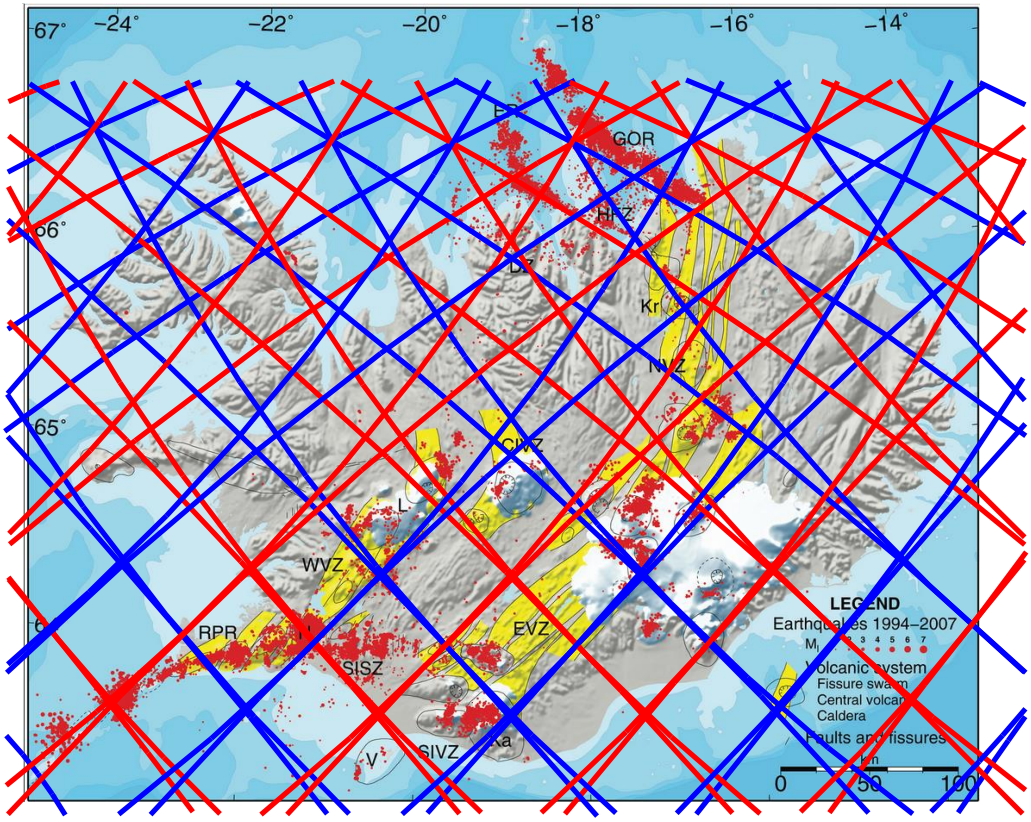

Figure 69: Upwelling lines marked with red lines and downwelling lines blue.

10.2. A pattern in the distribution of the most active sites

Iceland is well known for its volcanoes and geothermal fields, but a smaller number of sites stand out as especially prominent or active. The map below provides an initial comparison between several of these volcanic and geothermal sites and the proposed convection-cell grid.

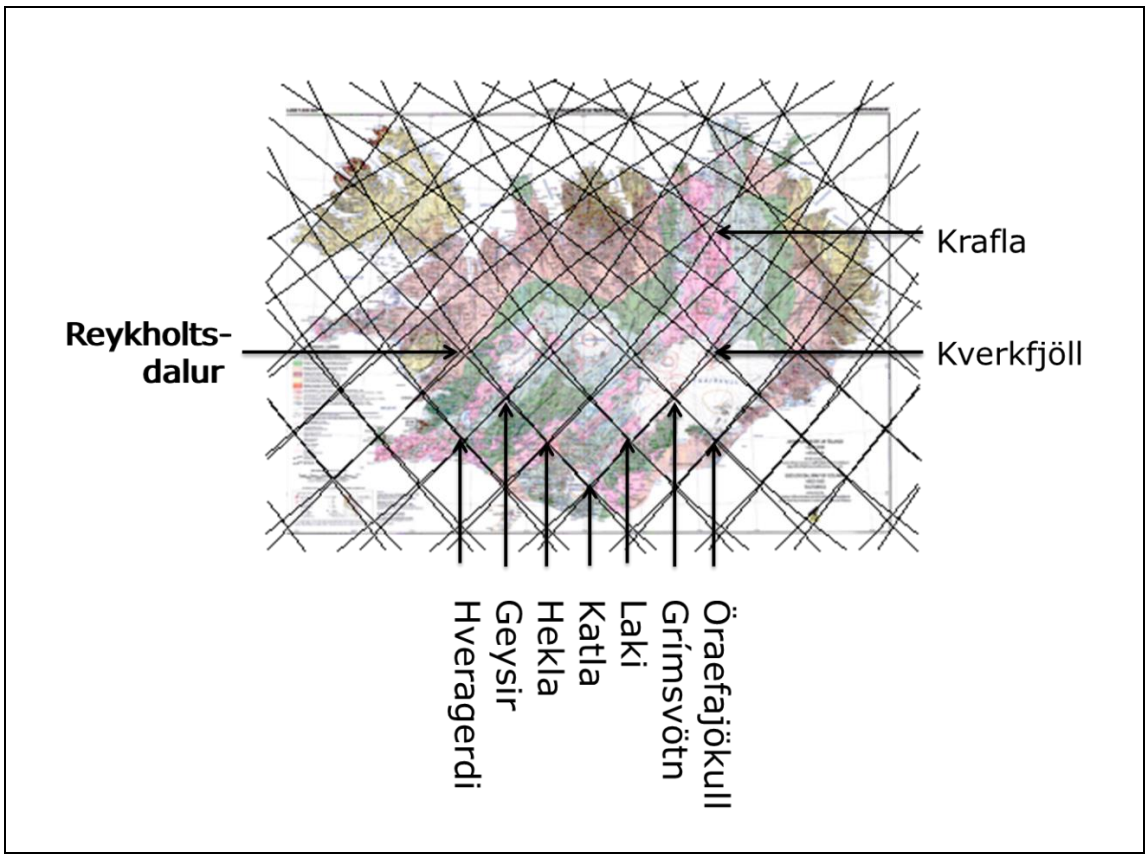

Figure 70: Prominent volcanic and geothermal sites compared with calculated intersection points.[1]

Within the framework proposed here, the concentration of major active areas near particular lines and intersections is interpreted as evidence that the grid may be related to Iceland's geological structure.

This first comparison is only an overview. Volcanic centres, seismic zones and both high- and low-temperature geothermal areas can be examined in considerably greater detail against the same convection-cell framework.

[1] Map base from Náttúrufræðistofnun.

A comparable pattern can also be identified in northern Iceland within the closely spaced network of polygons.

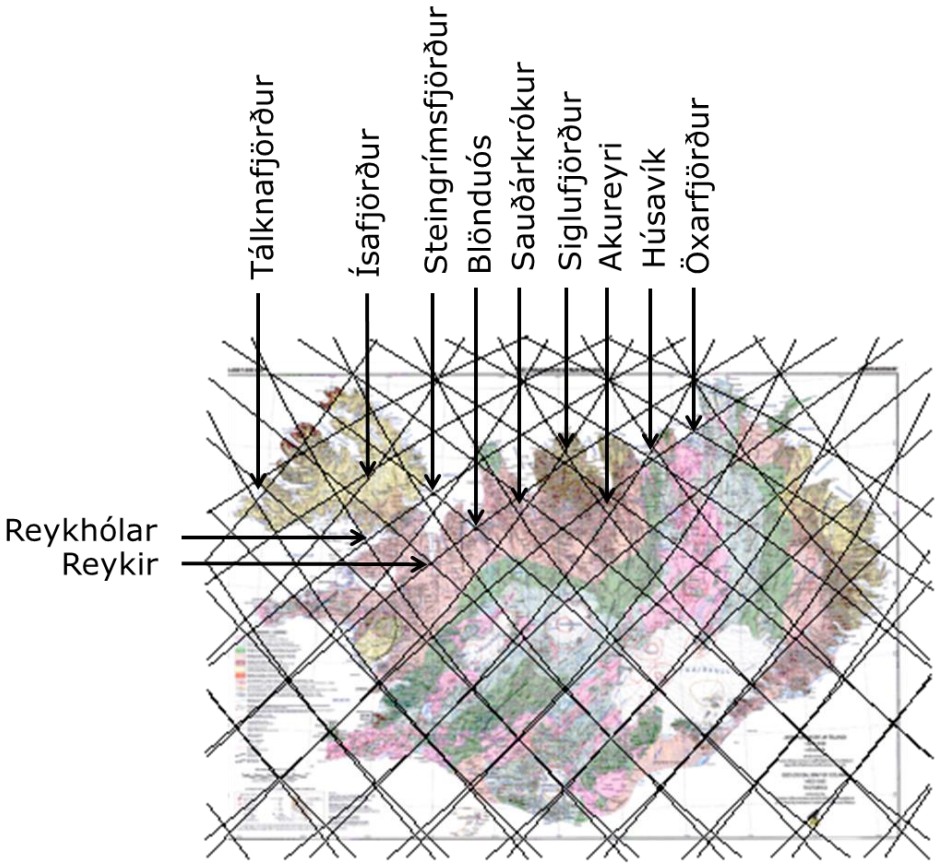

Readers familiar with Icelandic geology will recognize that many of the principal active areas are represented. In the next section, a map showing geothermal sites is used to examine more closely the relationship between geothermal and volcanic activity and the proposed convection-cell system.

10.3. High-temperature geothermal areas

The grid can be compared with maps containing many different types of geological information. One particularly useful comparison concerns geothermal activity. Iceland's high-temperature geothermal areas are associated with the volcanic zones, where magmatic heat is transferred into the upper crust. The volcanic zones themselves form a continuous regional pattern. If the grid generated by the proposed convection rolls is relevant to that pattern, the locations of the high-temperature areas should show some relationship to the calculated lines. On the map below, many of these areas occur on or near such lines.

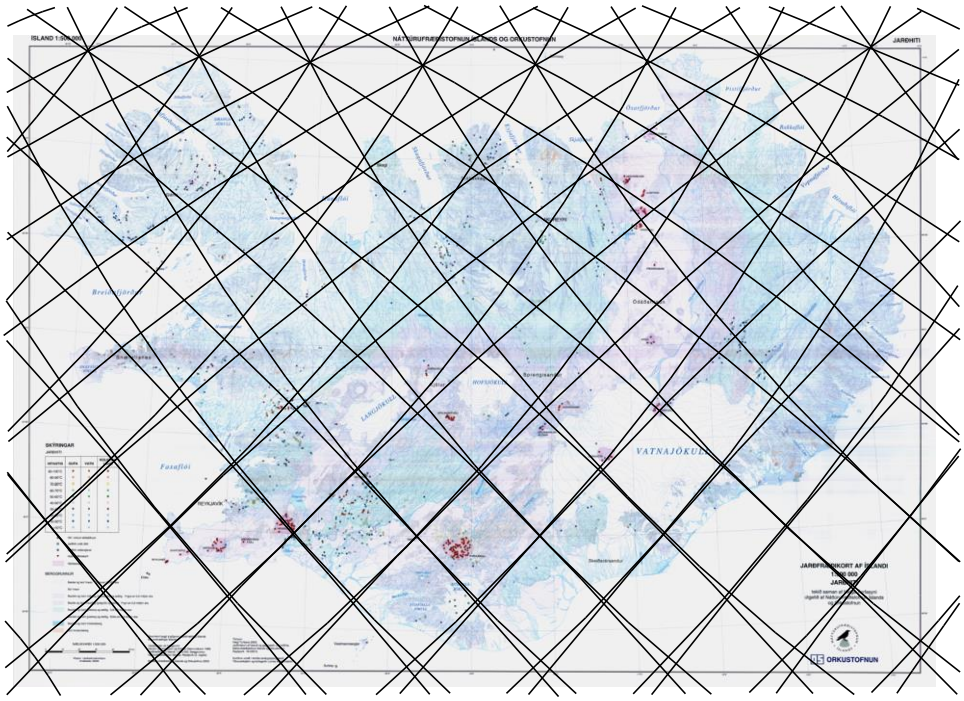

Figure 71: Geothermal activity compared with the convection-cell grid.

On the Orkustofnun geothermal map (Jarðfræðikort af Íslandi 1:500.000 – jarðhiti), the spatial relationship can be examined in greater detail. The high-temperature areas show a noticeable correspondence with the calculated lines. Within the model, this is consistent with the proposition that magma and heat may be transferred upward along structures associated with the Munroe-line system. The mapped lines represent the projected boundaries of convection rolls at depths exceeding 100 km; they are drawn over a topographic map for comparison and should not be interpreted as literal surface traces of those deep boundaries.

High-temperature geothermal systems are sufficiently large that they may extend some distance from the line with which they are associated in the model. Hellisheiði, approximately 30 km east of Reykjavík, provides a clear example. Other geothermal areas are not crossed directly by a calculated line. This need not, within the proposed framework, constitute a contradiction: magma can migrate laterally within the crust, particularly within actively extending volcanic zones. Torfajökull, the largest high-temperature geothermal area in Iceland, is not crossed by one of the principal lines but lies northeast of a Munroe line that the model identifies as a possible pathway for deeper magmatic input. Subsequent petrological and rheological processes within the crust could then distribute heat and magma through a much broader area.

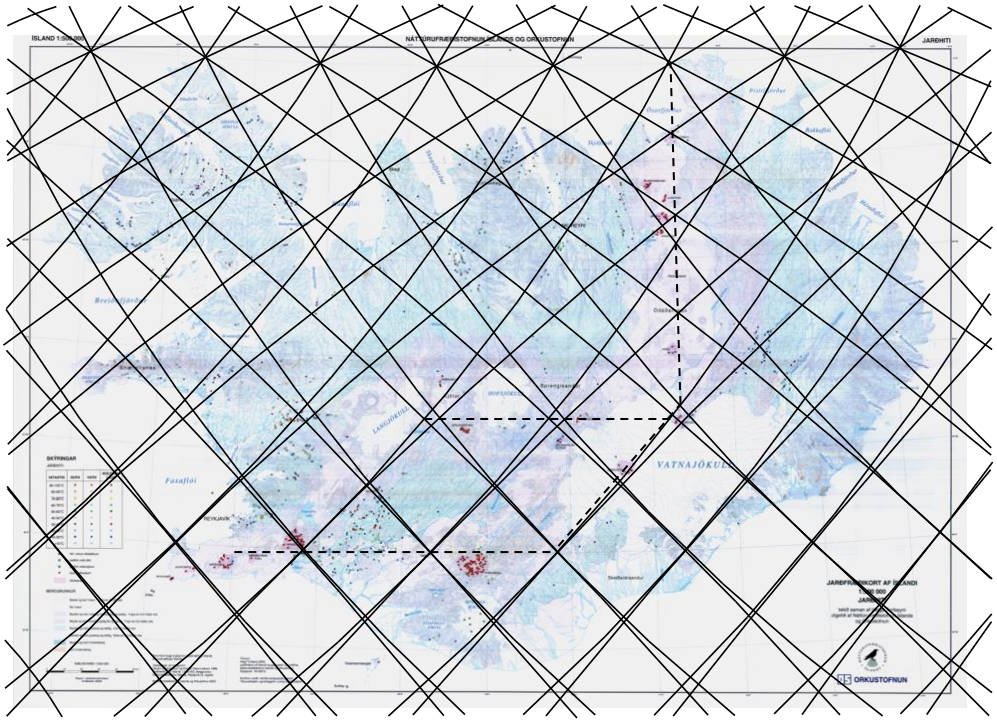

The dotted lines shown on the map pass through or near most of the high-temperature areas. This relationship can later be compared with the position of the boundary between the North American and Eurasian plates discussed in Chapter 11.

10.4. Low-temperature geothermal areas

Low-temperature geothermal areas also show a relationship to the grid, although of a different kind. The convection-roll lines divide the map into areas referred to here as grid polygons, many of which are approximately diamond-shaped. The polygon boundaries appear to separate regions with different concentrations of low-temperature geothermal activity. Within the model, this is interpreted in terms of differences in stress and fracturing between adjacent polygons. If Munroe lines separate the ductile bases of neighbouring grid areas, tectonic extension may produce distinct fracture conditions within each polygon. Some polygons would consequently be more favourable than others for the circulation of low-temperature geothermal water, while individual springs could occur at many positions within a favourable polygon.

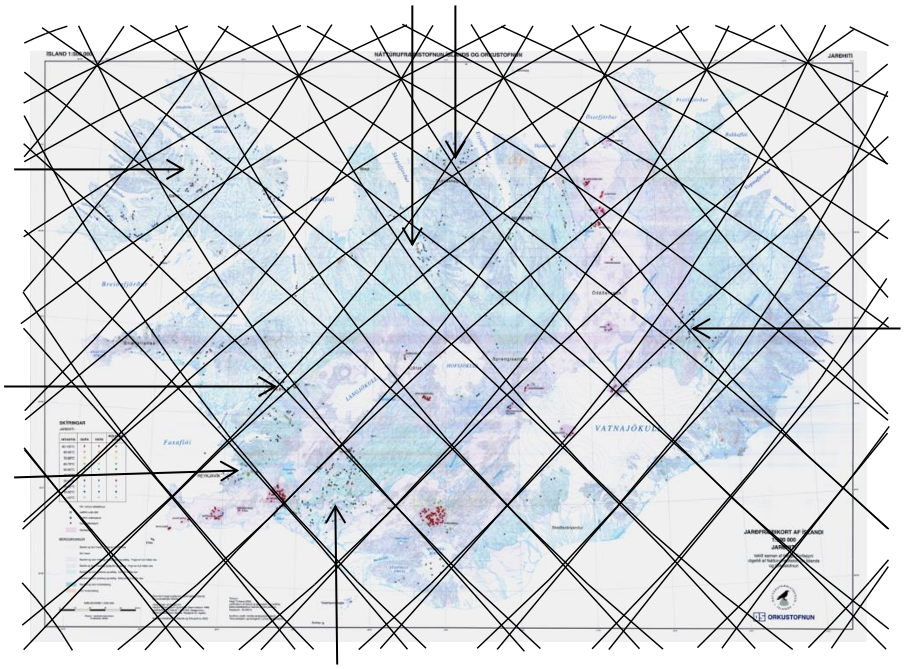

Figure 72: Most low-temperature geothermal areas in Iceland occur within distinct grid polygons.

10.5. The South Iceland Seismic Zone (SISZ)

As a student, I worked with Professor Páll Einarsson on mapping earthquake faults in the South Iceland Seismic Zone. I was particularly impressed by the observation that the deeper fault system appeared to be predominantly north–south oriented (Einarsson 2001). The symmetric convection-cell model provides a possible geometrical explanation for this orientation. The following figure shows how the principal seismic zone, which has produced several major earthquake sequences in Iceland, relates to one of the polygons in the proposed grid.

Many features of Iceland can be compared with the convection-cell pattern, but the SISZ provides a particularly useful case. The region has been interpreted as a distinct tectonic block, although the precise boundaries used in published models differ (Sigmundsson og Einarsson, Jarðskjálftabeltið á Suðurlandi, jarðskorpuhreyfingar 1986-1992 ákvarðaðar með GPS-landmælingum. 1996). In the grid proposed here, the SISZ corresponds closely to a single polygon, as illustrated below.

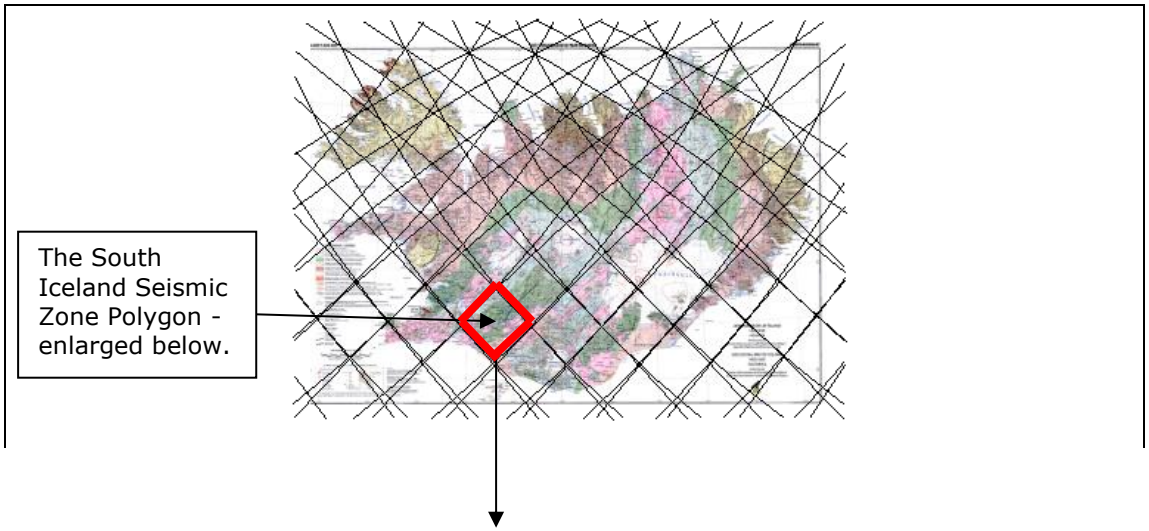

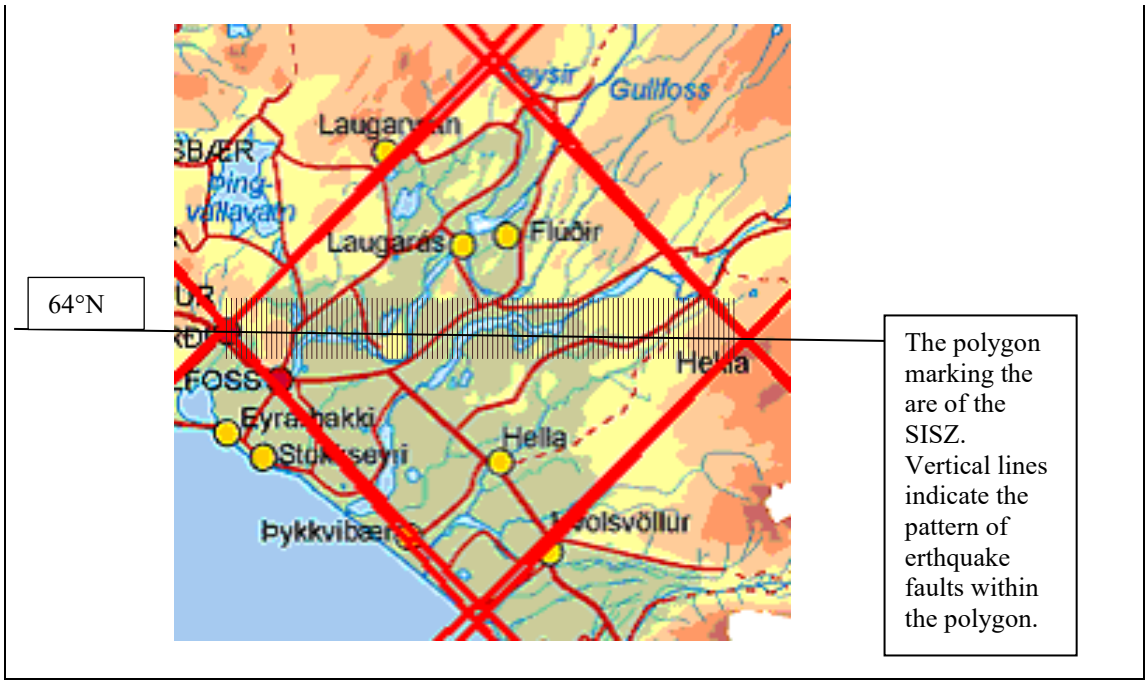

Figure 73: The South Iceland Seismic Zone in relation to the proposed grid polygon.

Within the interpretation proposed here, the geometry is consistent with the idea that the principal, deeper north–south faults are related to failure within ductile material subjected to oblique confining stresses, which can be considered using Mohr's circle (Plujim og Marshak 1997). The size and shape of the seismic zone can be mapped from surface observations. During my own mapping of the region, I found that north–south-oriented faults occurred at intervals of approximately 715 m near the 64th parallel between Hekla and Hveragerði. For tectonic extension to generate this systematic internal faulting, the margins of the deforming region must also accommodate differential motion. In the present model, the Munroe lines are proposed as boundaries separating the ductile parts of adjacent polygons.

Roth (2004), p. 1314, defines the area of strong seismic events as extending approximately from 21.2°W, 63.9°N to 19.7°W, 63.9°N. These positions lie close to the western and eastern corners of the grid polygon framing the Southern Lowlands. Taken together, the north–south fault orientation, the Mohr-circle interpretation and the observed east–west extent of the seismic zone are consistent, within this model, with stress acting within a diamond-shaped framework whose lateral corners occur near these coordinates.

This correspondence can be regarded as qualitative evidence supporting the proposed underlying geometry. It complements the quantitative relationships discussed earlier between the Earth's internal layering, the convection-cell dimensions

and the equatorial distribution pattern, but it does not by itself constitute proof of the model.

10.6. Explanation of fracture orientations within the SISZ

Because the Southern Lowlands are among the parts of Iceland with which I am most familiar, it is useful to examine in more detail how the earthquake fractures may have formed and why their deeper structures tend to be north–south oriented. In the model developed here, the ductile material beneath the SISZ is treated as a diamond-shaped block separated from neighbouring grid polygons by Munroe lines. The four sides of this polygon are oriented approximately 45° from north, as derived from the equations presented earlier.

It is important to distinguish the brittle upper part of the lithosphere from the much thicker ductile material below it. In the SISZ, the uppermost approximately 10–20 km are treated here as brittle. Surface fractures therefore need not reproduce the geometry of the deeper structures exactly. They commonly strike northeast–southwest and form en-échelon or side-stepping segments above the deeper fault system.

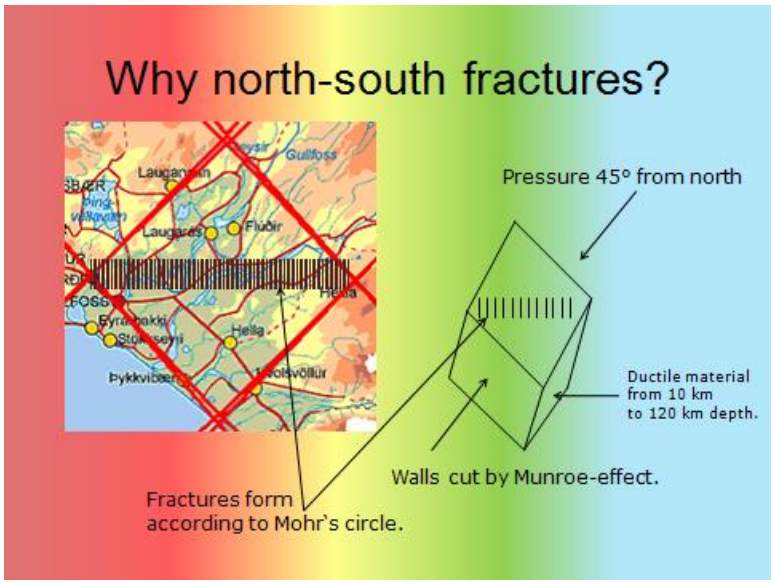

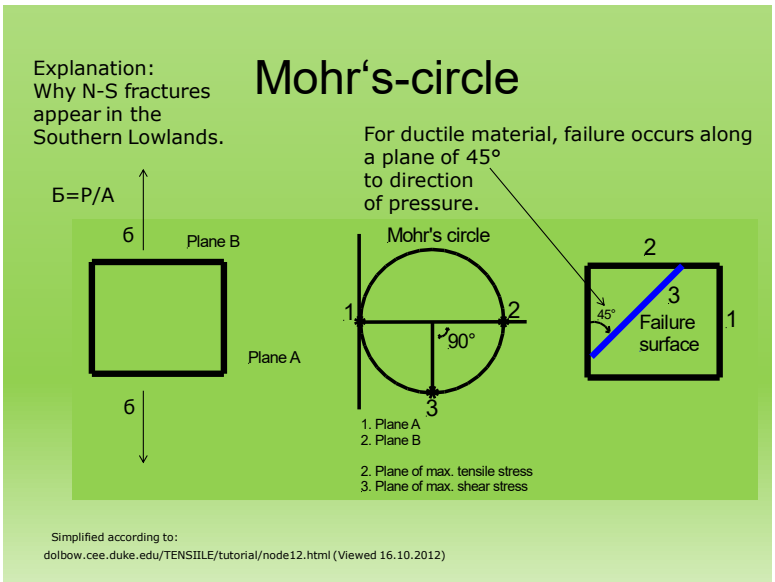

By tracing these surface fracture arrays over distances of several kilometres, the underlying north–south orientation can be inferred.

Under the simplified stress conditions assumed in the model, ductile material subjected to compression or shear should develop preferred failure orientations related to the principal stress directions. In the SISZ, the resulting geometry is interpreted as being consistent with the observed fault system. I further propose that this relationship can be used to estimate the central line between the polar and hemispheric parts of the convection-cell system. Roth (2004) places the relevant seismic belt near 63.9°N; for the geometrical construction used here, the 64th parallel is retained as the central reference, with an estimated precision of approximately 64.0 ± 0.1°.

Again, the distinction between the brittle upper crust and the deeper ductile part of the plate is essential. The idealized 'bookshelf' arrangement proposed by the model applies primarily to the ductile environment. At the surface it can only be expressed indirectly, so the observed fault pattern appears more irregular and individual fractures commonly strike somewhat northeast–southwest rather than exactly north–south.

10.7. Seismic areas in general

After examining the SISZ, the same framework can be compared with Iceland's other principal earthquake region, the Tjörnes Fracture Zone off the north coast.

The Tjörnes Fracture Zone has a more complex structure, consisting of several major strands. Its geometry is clearly expressed on cumulative maps of earthquake epicentres.

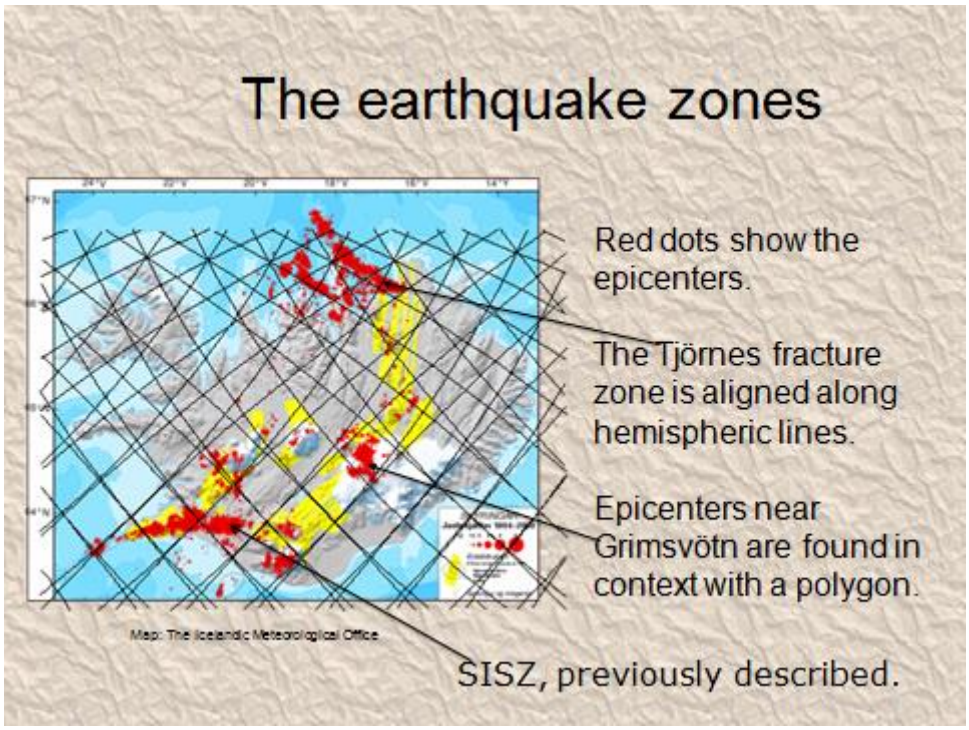

Seismic Activity in Iceland 1994-2000[1].

In the interpretation presented here, the distribution of epicentres in the Tjörnes Fracture Zone follows the hemispheric lines particularly closely, and earthquakes tend to cluster within certain grid areas. This is consistent with the proposition that Munroe lines beneath the brittle crust separate individual polygons, allowing differential stress to accumulate in the overlying brittle layer. Tectonic extension is therefore expressed through a complex earthquake pattern while still showing a possible relationship to the underlying polygonal framework.

[1] http://www2.vedur.is/media/jar/myndasafn/frodleikur/medium/jardskjalftakort-GG_94-00_is.gif (viewed 10.11.2012)

10.9. The volcanic zones

One of the clearest proposed surface expressions of the global convection-cell system in Iceland is the geometry of the volcanic zones. Their positions and orientations can be compared directly with the combined grid of division lines between the underlying convection cells. In southern Iceland, the Western Volcanic Zone (WVZ) and Eastern Volcanic Zone (EVZ) are separated by a region that, within the model, corresponds to adjacent polygons subjected to different stress conditions. As described earlier, individual polygons may be preferentially extended or compressed. The east–west tectonic extension across Iceland is therefore interpreted as opening a connected sequence of polygons that together form the principal volcanic zones.

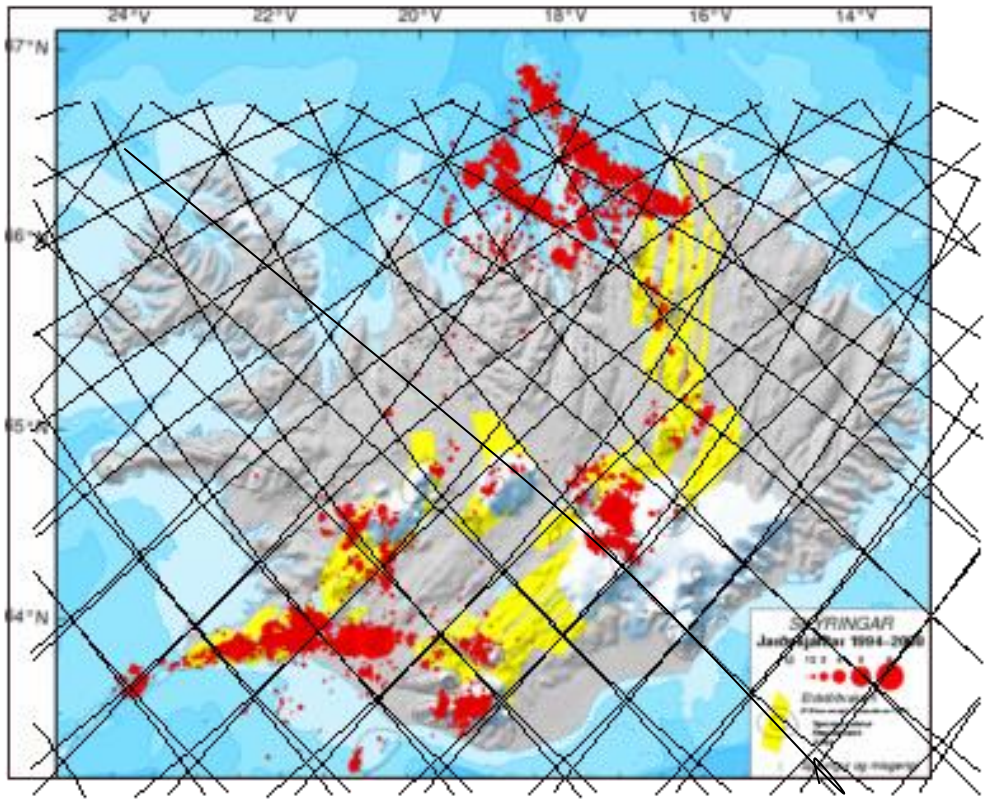

The volcanic systems shown in yellow also display a close visual relationship to the proposed convection-cell pattern.

The relationship is most immediately apparent for the WVZ and EVZ. The Northern Volcanic Zone follows a north–south axis that is also incorporated into the

model. The Snæfellsnes and Öræfajökull volcanic systems are not shown on this particular map. Snæfellsnes, in particular, is not explained simply by inspection of the polygon boundaries; its relationship to the model requires the secondary geometrical considerations discussed above.

Within the proposed framework, the episodic relocation of Icelandic volcanic zones over multimillion-year timescales is interpreted as a consequence of changing stress between neighbouring polygons. Extension within the WVZ would increase compression or reduce opening in adjacent polygons. Because the tectonic displacement is asymmetric, the model proposes that, over time, extension can shift to a polygon farther east, while the intervening polygon remains relatively compressed. This provides a geometrical hypothesis for the stepwise development of new volcanic zones.

10.10. The 64th latitude

The 64th parallel is of special importance in the model because it lies near the centre of the horizontal intersection zone of the convection-cell system. Four volcanic zones occur in relation to this latitude: Reykjanes, the Western Volcanic Zone, the Eastern Volcanic Zone and the Öræfajökull Volcanic Zone. The map below highlights several locations along or near the parallel. Outside the volcanic zones, the principal additional feature is the South Iceland Seismic Zone, discussed separately above.

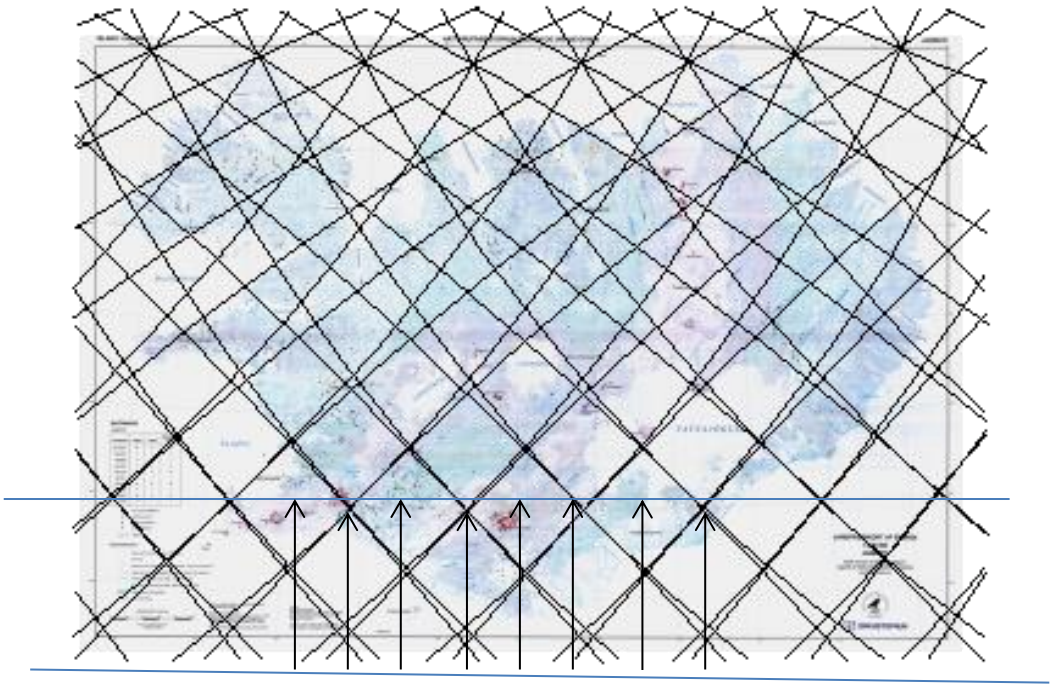

Figure 74: The 64th parallel as the central line of the proposed transition zone.

At approximately 64°N, the horizontal circles used in the model become tangent to one another, so the polygonal pattern differs from that at neighbouring latitudes. Each tangential point can therefore be examined separately. Hekla and Öræfajökull are particularly notable because both volcanic centres lie close to sets of tangential points. Within the model, this geometry allows the effects associated with the four upper-mantle and asthenospheric convection layers to coincide beneath the same surface region.

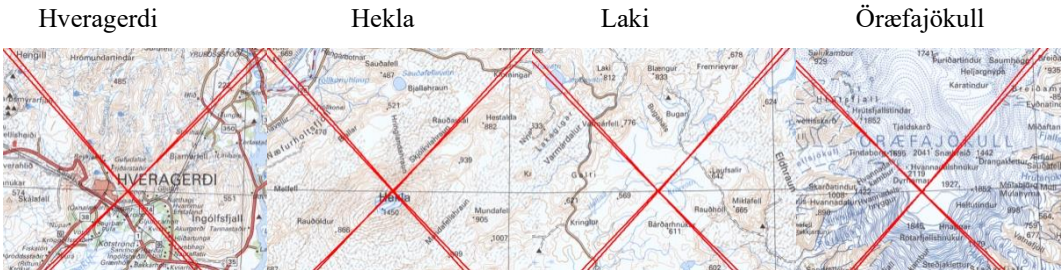

Tangential points along the 64th parallel, with volcanic and geothermal sites occurring near several of them.

Öræfajökull also lies on a north–south axis containing volcanic and geothermal sites, as discussed in the next section. The same axis is related in the model to the geometry of the Northern Volcanic Zone, discussed in Section 10.11. The longitude axis of Öræfajökull – Kverkfjöll – Theistareykir. Hekla lies on another north–south axis and is also used as the symmetry axis for the comparison between Snæfellsjökull and Snæfell discussed in Section 10.12. The mirrored location and morphology of the two Snæfell volcanoes.

Additional geometrical comparisons are made along the 64th parallel. The longitudinal span from the Hekla system to the Norwegian coast is approximately 30°, while the span from Hekla to the Bering Strait is approximately 150°. These relationships are considered because the spherical geometry developed earlier (see p. 51) predicts particular significance for this latitude. In the same framework, the Eurasian landmass spans approximately 180° along the parallel.

10.11. The longitude axis of Öræfajökull – Kverkfjöll – Theistareykir

The correspondence between the calculated lines and the two principal volcanic zones of southern Iceland, the WVZ and EVZ, is relatively straightforward within the model. The smaller Öræfajökull Volcanic Zone (ÖVZ) also lies near an intersection point on the 64th parallel. The Northern Volcanic Zone (NVZ), however, is not bounded directly by grid lines on both sides, and the margins of individual volcanic systems may lie within the interiors of polygons. This provides a useful test of whether the model can account for a less obvious geometrical relationship rather than only the clearest examples.

The plate boundary across Iceland is wide and structurally complex, and different segments need not express the underlying geometry in the same way. In this case, the model emphasizes symmetry about a single north–south longitude axis that passes through the endpoints of a sequence of polygons. The relationship between this axis and the Northern Volcanic Zone provides another proposed correspondence between the calculated grid and observed geology.

Central north–south axis

The central axis, oriented N-S through the North Iceland Volcanic Zone and Öræfajökull on the longitude 16°39′40′′W.

fajökull at longitude

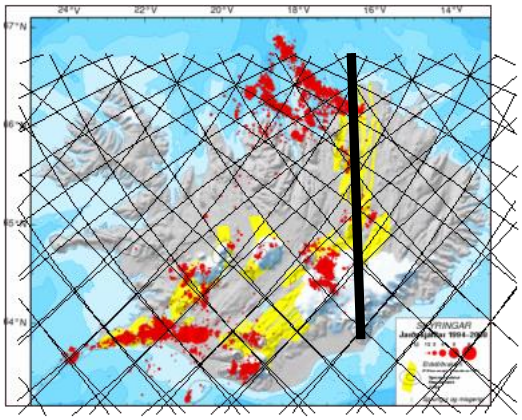

Figure 75: The north–south axis from Öræfajökull to Theistareykir in relation to the polygon arrangement.

This feature can also be compared with the earlier map of volcanic and geothermal sites relative to the small polygons and with the map of tectonic-motion directions. Together, these comparisons illustrate the proposed significance of this north–south axis.

10.12. The mirrored location and morphology of the two Snæfell volcanoes

Two Icelandic mountains share the name Snæfell: Snæfellsjökull in western Iceland and Snæfell in eastern Iceland. In the model, their positions and broader geological settings form an approximate mirror relationship across the central framework of Iceland.

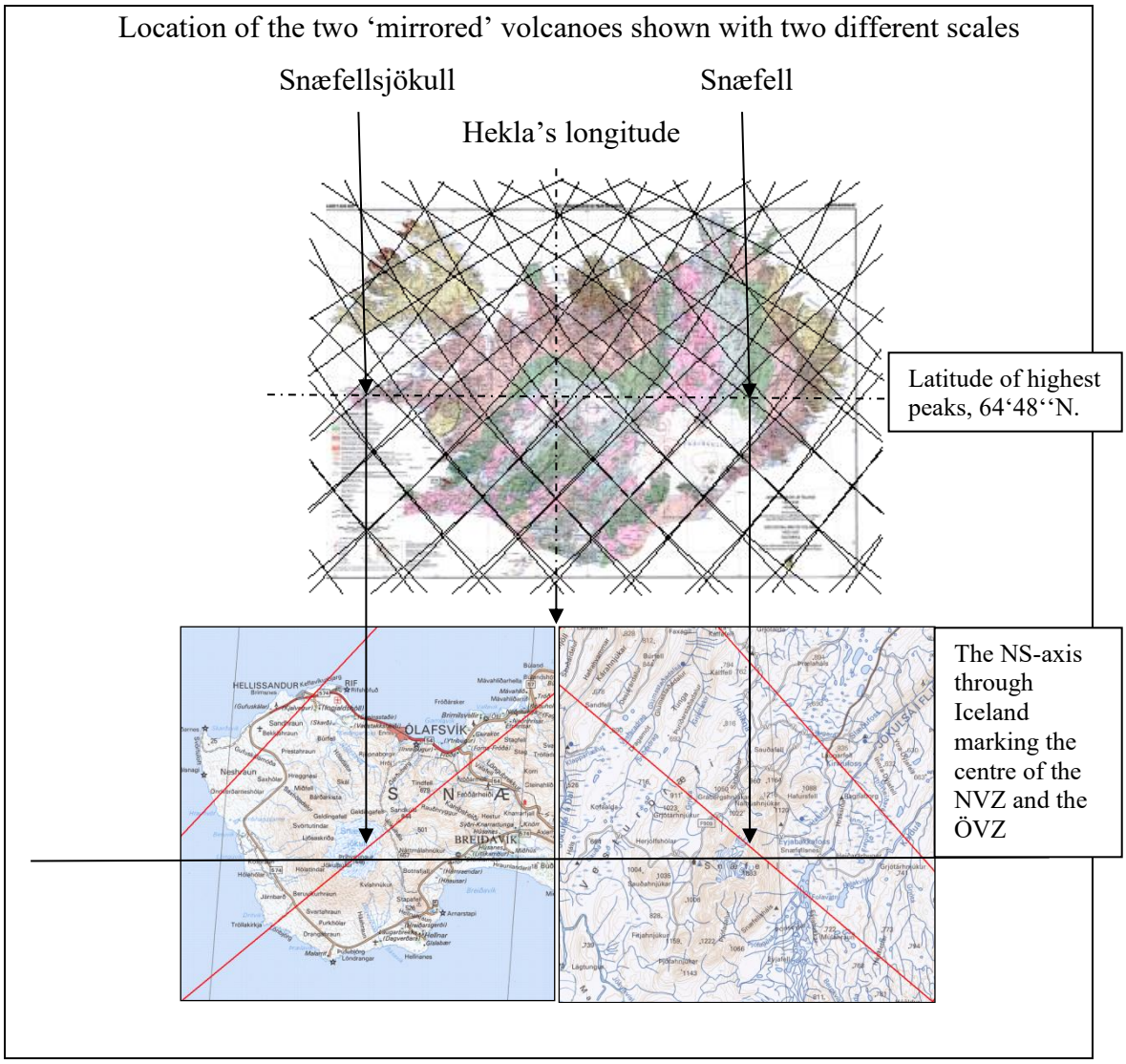

Figure 76: Detailed maps of Snæfellsjökull and Snæfell shown side by side.

The vertical dotted lines on the upper map illustrate the proposed mirror relationship of the two volcanoes about the longitude of Hekla. A simple visual analogy is to place the wrists together and compare the two open palms as mirror forms. The highest points of the two mountains lie at approximately the same latitude. Geologically, the volcanoes occupy the western and eastern extremes of comparatively recent volcanic activity in Iceland. The symmetry becomes especially

relevant when the tectonic-motion pattern is considered later in the book.

Within the larger geometrical framework, Hekla is also compared with the central structure of the Atlantic at the equator. This motivates the search for regional symmetry about Hekla within Iceland. The relationship between Snæfellsjökull and Snæfell is presented here as an additional line of evidence to be evaluated alongside the other geometrical correspondences in the model.

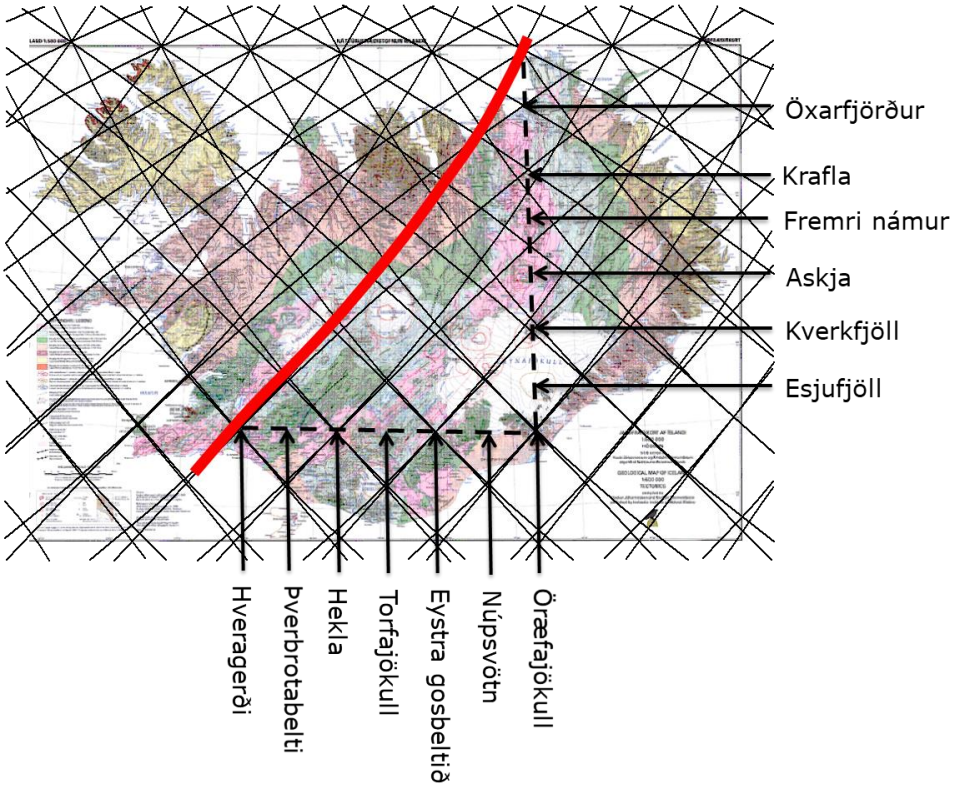

The east–west and north–south axes.

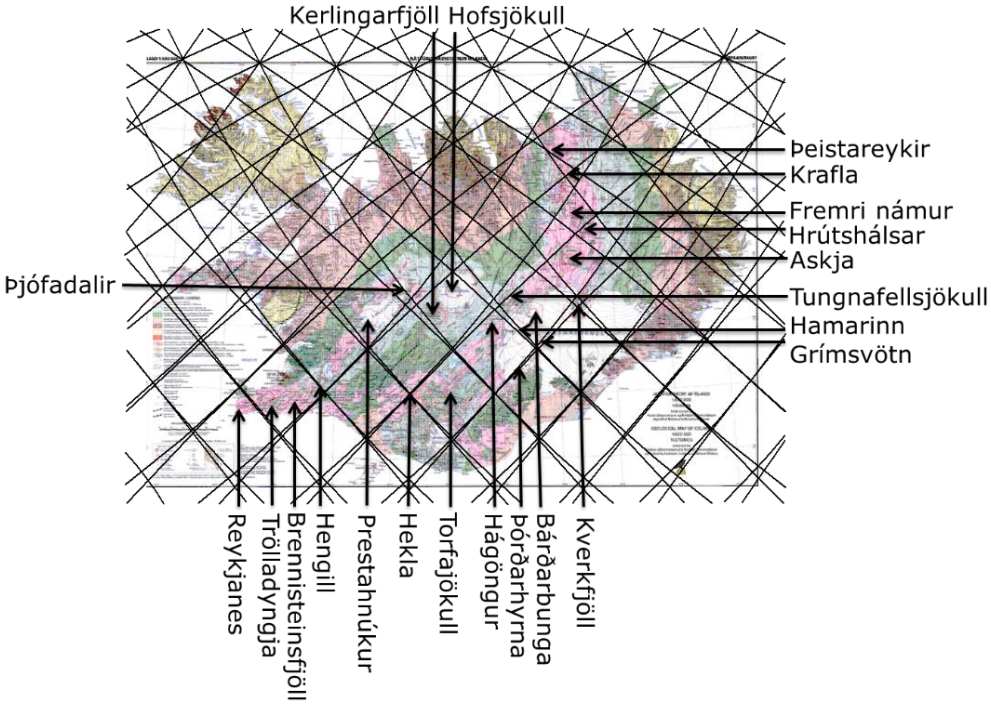

Volcanic systems within the divergent rift zones.

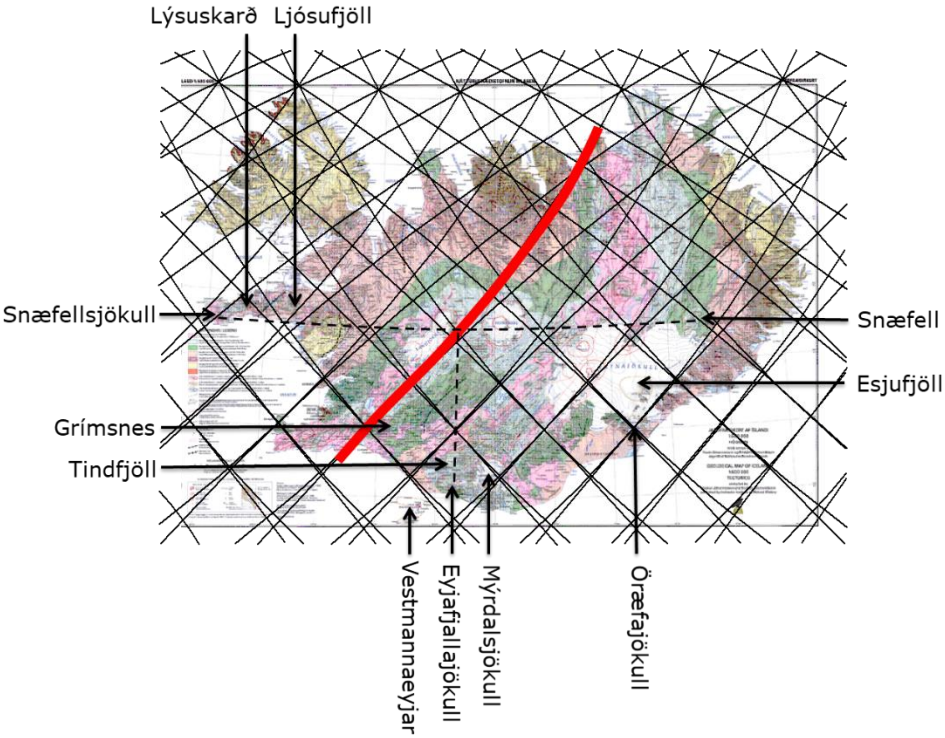

Volcanic systems outside the divergent rift zones.

A further north–south axis can be drawn from Eyjafjallajökull through the central Þjófadalir point and continued approximately the same distance northward to

Drangey in Skagafjörður. Drangey has been interpreted here in relation to an older volcanic zone that became active at roughly the same stage as the modern Snæfellsnes volcanic zone. Although that volcanic zone later became inactive, its position is compared with the three other volcanic areas outside the principal rift zones. Within the geometrical framework developed here, the alignment is notable.

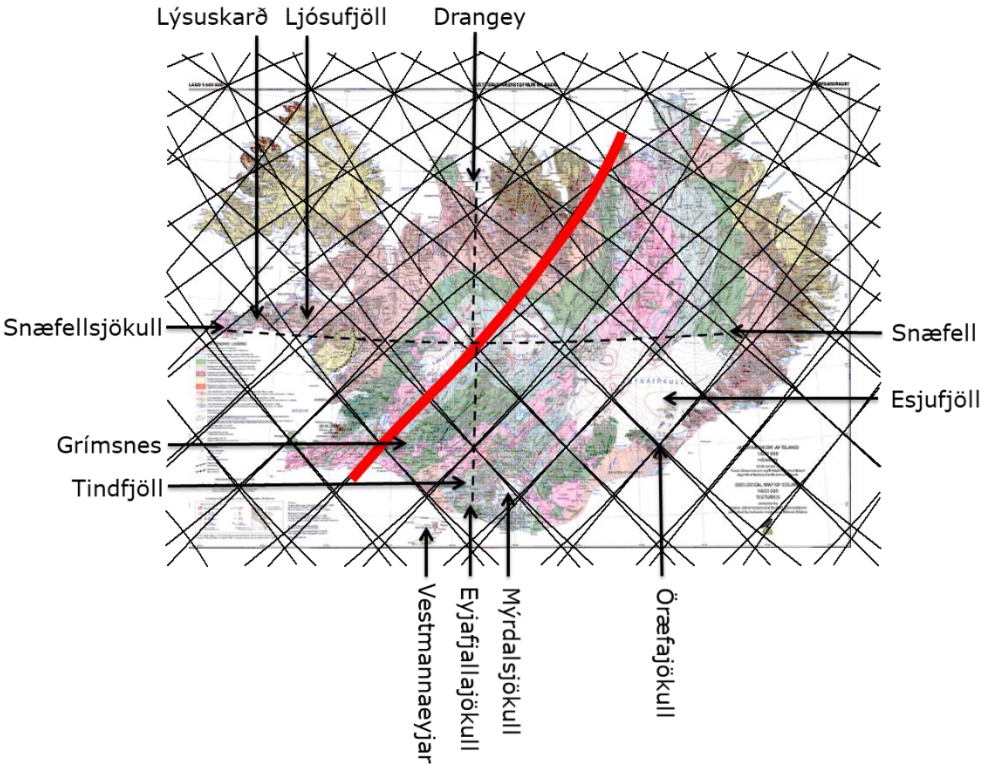

Relationship of the former Drangey volcanic zone to the pattern of volcanic systems outside the principal rift zones.

Volcanism on the Snæfellsnes Peninsula has long required explanation because it lies well away from the main continuation of the Mid-Atlantic Ridge through Iceland. Whereas the principal rift-related volcanic zones in Iceland generally trend northeast, structures on Snæfellsnes trend northwest (Jóhannesson 1982). Within the model proposed here, Snæfellsnes is considered as a geometrical counterpart to structures in eastern Iceland. This interpretation also leads to potentially practical applications, as considered in the next section.

10.13. An example of a fault in Iceland

Iceland has made extensive use of geothermal energy, but accessible hot water is not equally abundant in every region. On the Snæfellsnes Peninsula, geological and drilling investigations identified a fault capable of supplying geothermal water to Stykkishólmur. The structure has been mapped and used as an example of geothermal exploration based on a series of boreholes and measurements of the temperature gradient.

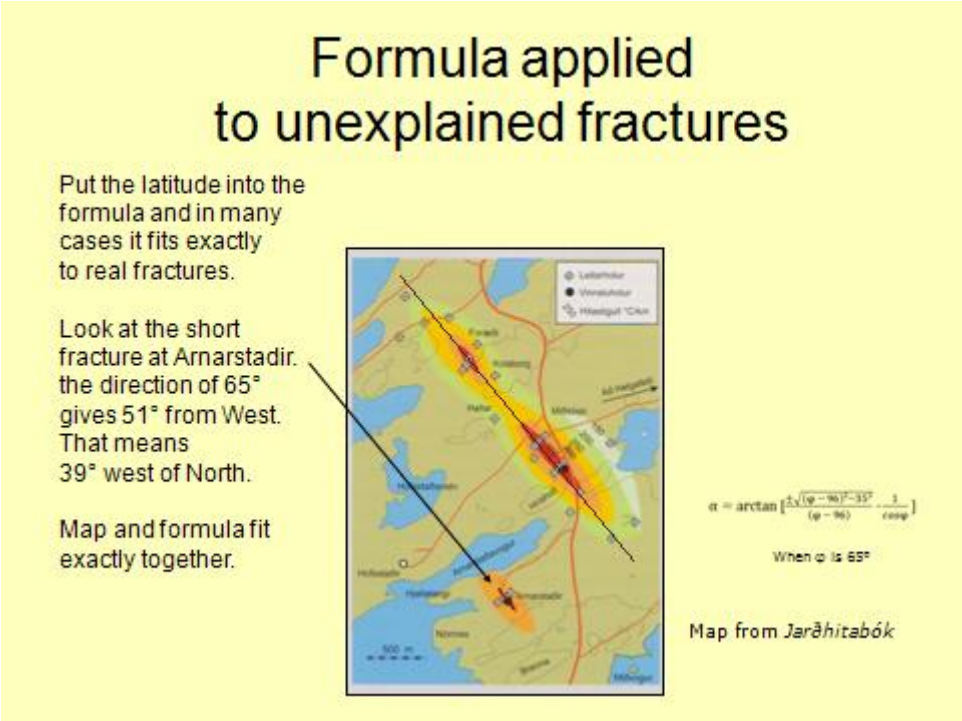

Figure 77: Calculated direction compared with an important geothermal fault.

The orientation of this fault can be compared directly with the direction predicted by the convection-roll model. A larger collection of independently mapped faults could therefore provide a quantitative test of whether the calculated directions occur more frequently than expected by chance.

The possibility of calculating preferred fault directions is one of the potentially practical implications of the model. I have also applied the same framework when identifying a geothermal prospect in the Skógarströnd area, not far from this site.

10.14. Bedrock boundaries

Comparison with a tectonic map of Iceland, on which bedrock units of different ages are shown in different colours, reveals several additional geometrical relationships. In particular, boundaries of Upper and Middle Miocene bedrock in the Westfjords can be compared with the projected convection-cell lines, and similar correspondences appear elsewhere. No single mechanism is proposed here to account for every such boundary. Rather, the comparison is included because long-term tectonic deformation and erosion may both reflect, directly or indirectly, the regional structural framework.

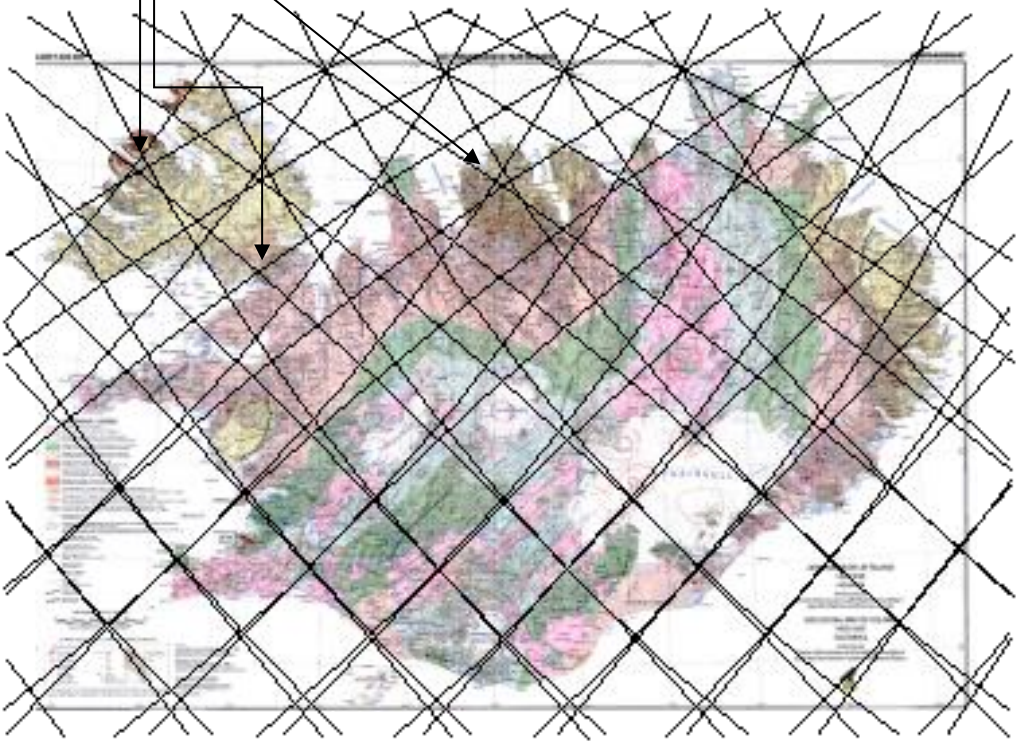

Geological Map of Iceland – Tectonics
(Published by Icelandic Institute of Natural History)

Erosion has modified the original outlines of these older rock units, exposing them in patterns controlled by structure as well as topography. Compared with the larger tectonic and volcanic relationships discussed above, this correspondence is less distinct and may be coincidental. It is nevertheless included as an observation worth testing against the broader model.

10.15. The Holuhraun eruption

The 2014 Holuhraun eruption and the associated dyke intrusion were monitored in exceptional detail. The underground dyke propagated for approximately 45 km (Sigmundsson, Segmented lateral dyde growth in a rifting event at Bárðarbunga volcanic system, Iceland 2014), a distance comparable to the scale of the relevant grid polygon. In the model, both the path of the intrusion and its changes in direction are compared with the surrounding Munroe-line framework. The superimposed lines in the figure represent calculated directions.

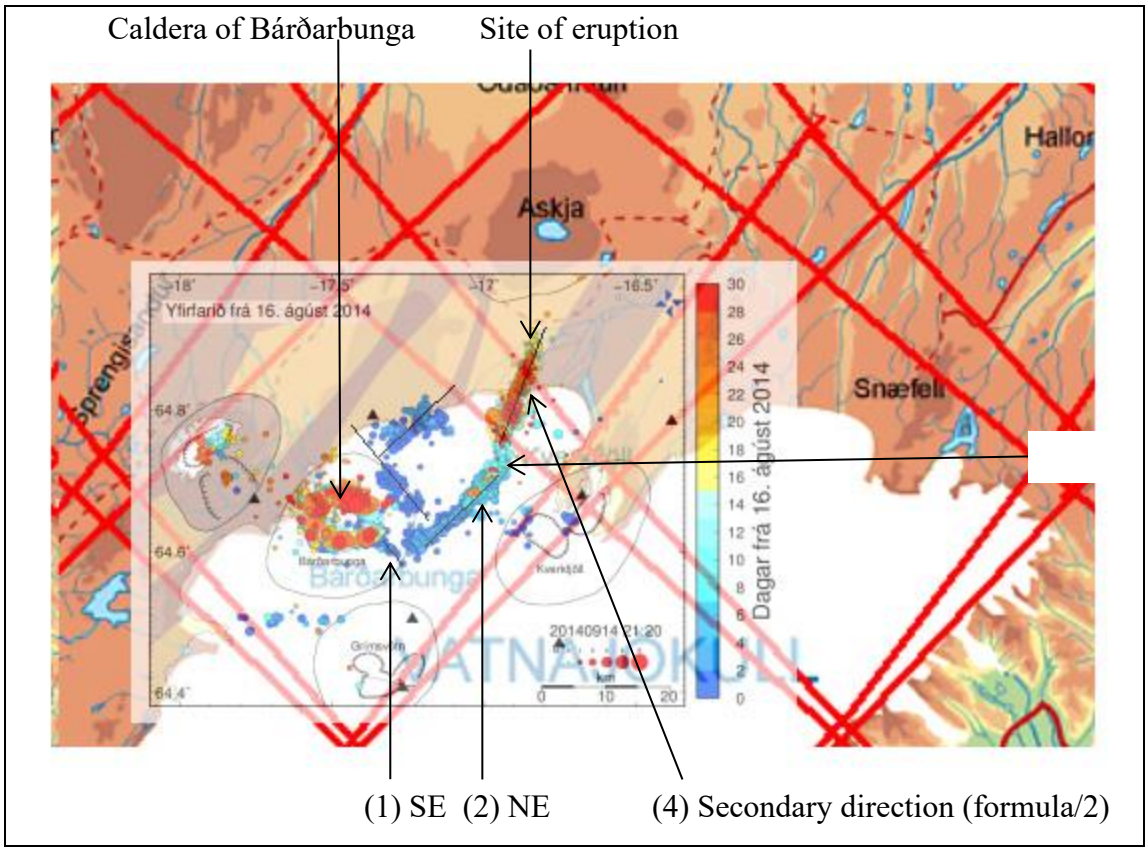

Figure 78: Earthquake map from the Icelandic Meteorological Office, with calculated directions superimposed.[1]

The map does not resolve every short segment of the dyke path, but its large-scale geometry can be compared with the calculated polygon boundaries. Focusing too closely on individual small deviations could obscure the broader directional changes that are being tested here.

[1] Preliminary analysed data by the SIL seismic monitoring group of the Icelandic Meterorological Office. Date of delivery from the data bank: 14. September 2014.

The proposed propagation path can be divided into four main segments, indicated in the figure:

1. During the first kilometres, the dyke propagated southeast, approximately parallel to the relevant sides of the polygon.
2. It then turned and developed a long northeast-trending segment approximately parallel to the hemispheric boundary of the polygon, continuing until it approached the polygon's east–west axis.
3. The dyke subsequently turned left into a segment trending almost due north. In the model, this segment approached the Munroe-line boundary along the northeastern side of the polygon.
4. Between the hemispheric and polar Munroe lines on the northeastern side, the dyke propagated along a comparatively straight path, extending a few kilometres beyond the outer polar line before the eruption began.

Earthquake activity then propagated in pulses from the vicinity of the intersection between the polar line and the dyke towards the eventual eruption site.[1]

Additional magma input from an unidentified source was reported from roughly a week after the dyke began to form (Sigmundsson, Segmented lateral dyde growth in a rifting event at Bárðarbunga volcanic system, Iceland 2014). Within the interpretation proposed here, the timing is compared with the stage at which the dyke crossed the Munroe lines. The eruption also produced unusually large quantities of SO2, which is considered here as a possible indication of additional or deeper magmatic input. The model therefore proposes a testable possibility: after travelling roughly 40 km, the dyke may have intersected hotter magma supplied from below. If two distinct magmatic contributions were involved, corresponding petrological or geochemical signatures should in principle be detectable.

The most immediate comparison between the model and the measured data is the sequence of directions defined by the earthquake locations. The superimposed lines represent directions calculated from the proposed deep convection framework.

[1] Observed by looking at a video (*Bárðarbunga 16/08 – 23/09 2014*) processed by the Icelandic Met Office; Preliminary analysed data by the SIL seismic monitoring group of the Icelandic Meterological Office (17.12.2014).

Northwest–southeast orientations appear in two parts of the path in relation to the polar set of lines. The intrusion first propagated southeast from the Bárðarbunga caldera and then turned northeast, broadly following the hemispheric direction towards the next Munroe line extending from the Kverkfjöll region. After crossing that line, the dyke changed direction again towards a secondary, half-angle trend before continuing across another polygon boundary.

The final stage is the onset of the eruption itself. In the model, the eruption began in Holuhraun close to a Munroe-line boundary, suggesting a possible relationship between the propagating dyke and that polygon margin. This is presented as a hypothesis about where additional magma or heat might enter the intrusion system, rather than as a demonstrated mechanism.

A comparable geometry is proposed for the 1783 Laki eruption. The dyke system is related to Grímsvötn, while the Laki fissures lie close to a calculated polygon boundary. Near 64°N two sets of lines occur close together because of the intersection geometry described earlier. As at Holuhraun, the eruption site is therefore compared with a polygon boundary. If this relationship is systematic, future dyke-propagation events could provide a direct test of whether eruptions preferentially begin when an intrusion approaches or crosses such a calculated line.

The Eldgjá fissure system, associated here with the Katla volcanic system and the eruption of 934, can be compared with the same polygonal framework.

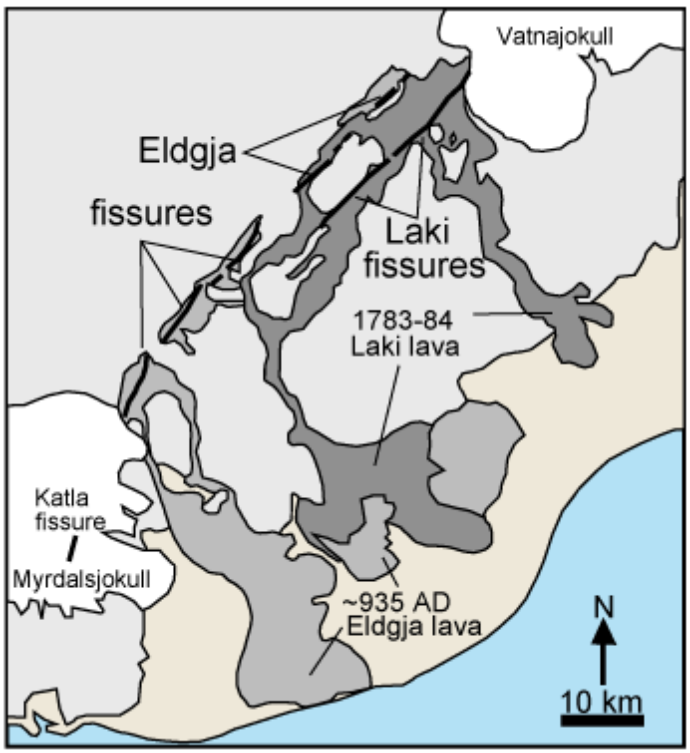

Figure 79: Locations of the Laki and Eldgjá fissure systems relative to the proposed grid.

Chapter 11 - Tectonic drift

Since the 1960s, advances in our understanding of tectonic plate motion have contributed greatly to geoscience. The present work does not propose a new description of ridges or trenches; rather, it compares the convection-roll system developed here with established observations of tectonic drift.

11.1. Tectonic drift of Iceland

An apparent correlation can be seen between the polar convection lines and the measured tectonic drift of Iceland. Eastern Iceland moves toward the northeast, whereas western Iceland moves toward the northwest (Guðmundur Þór Valsson 2007). At comparable latitudes, the drift vectors on the eastern and western sides show a marked symmetry relative to north. At approximately 66°N, for example, the directions are about 33° east and west of north. The velocity is about 2.2 cm/yr in the western part and approximately 1.7 cm/yr in the eastern part. These measurements differ from the simpler traditional picture of Iceland opening approximately east-west at about 1 cm/yr on each side.

One striking feature of the measurements is the near-mirroring of drift directions in western and eastern Iceland. Symmetry across the Reykjanes Ridge was already familiar from magnetic anomalies on the ocean floor and is commonly associated with seafloor spreading. The mirrored northward components of the measured drift vectors are less intuitive. Within the framework proposed here, however, this symmetry can be examined in relation to the geometry of the convection-cell system.

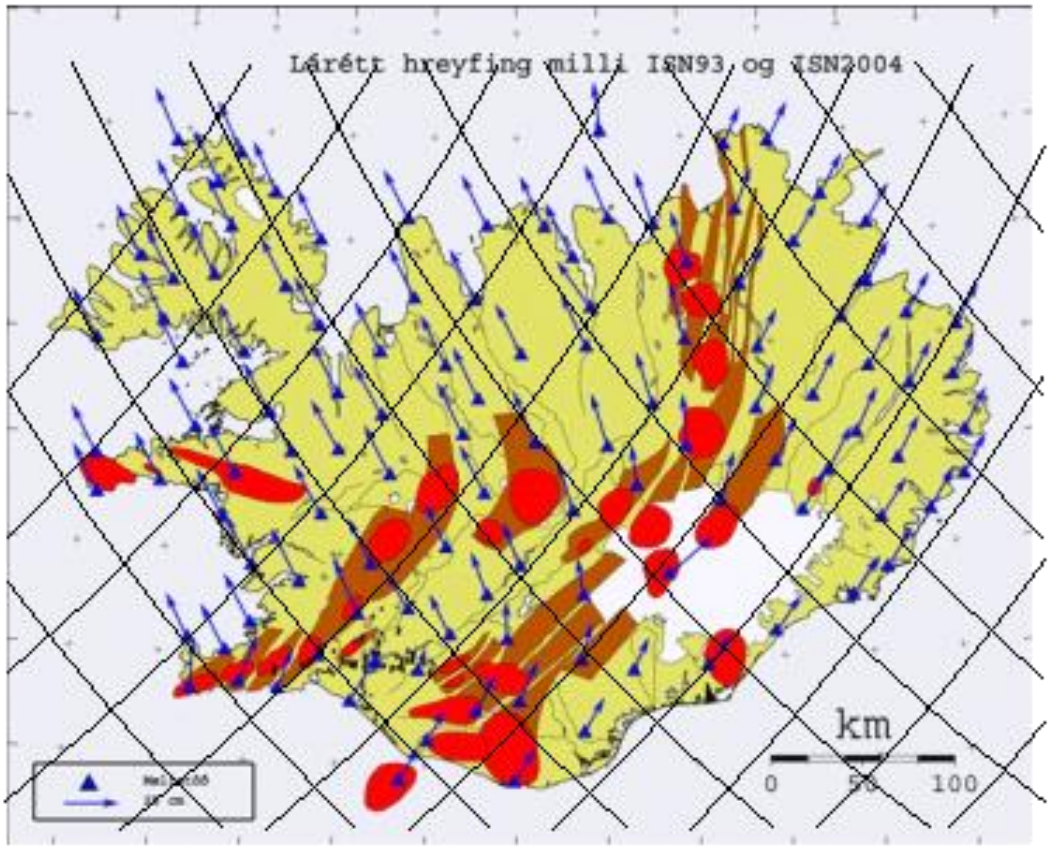

Figure 80: The tectonic drift vectors with lines superimposed.

Outside the main volcanic zones, the drift vectors tend to align approximately parallel to the grid lines of the proposed convection-cell system. The two inserted arrows highlight vectors at the same latitude. Their deviations from north are nearly symmetrical: one is directed east of north and the other west of north.

A broad correspondence is therefore apparent between the proposed grid and the direct geodetic measurements. This provides an opportunity to examine whether the convection-cell framework can help explain the geometry of tectonic drift in greater detail.

11.2. The division line between the American and European plates through Iceland

With this framework in mind, the plate boundary through Iceland can be examined in greater detail. The theoretical boundary between the North American and Eurasian plates is represented schematically below:

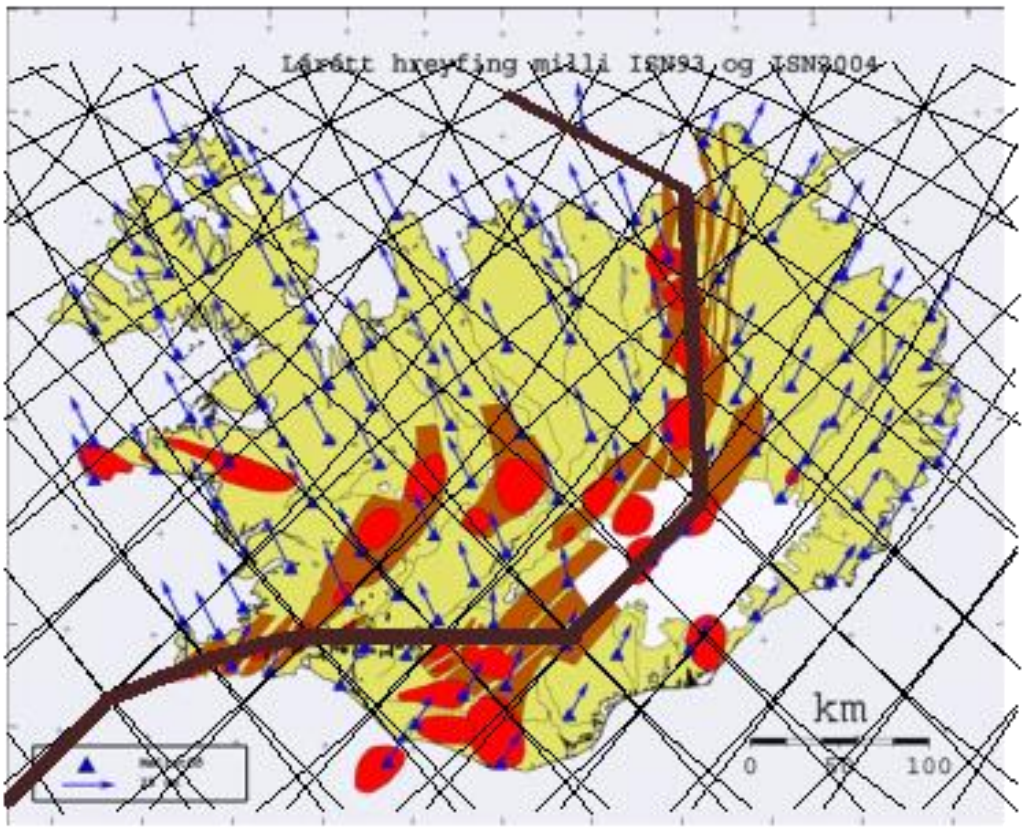

Figure 81: Theoretical boundary between N-American and Eurasian Tectonic Plates

In the proposed interpretation, this boundary follows the grid and can be described in seven principal sections:

1) The Reykjanes Ridge follows a grid line to the corner of a polygon.
2) Two polygons lie between the main part of the Reykjanes Ridge and the SISZ polygon. Near the southwestern corner of Iceland, the plate boundary appears to shift from the Reykjanes Ridge toward the Eastern Volcanic Zone rather than following a single continuous line. The Reykjanes polygon differs from the nearby SISZ polygon in that it contains a series of volcanic systems. In the model, this allows the boundary to bend southwestward toward the Atlantic

before it again aligns with the convection-cell pattern along the Reykjanes Ridge.

3) The SISZ polygon and the adjacent EVZ polygon share an approximately east-west axis through their centres. The seismic and volcanic faults and fissures collectively accommodate the same general boundary, with its eastern end close to the Laki fissure system.
4) From Laki, one section of the boundary continues through two polygons, via the Grímsvötn area, to Kverkfjöll.
5) From Kverkfjöll, the boundary extends northward toward Öxarfjörður.
6) The northern end is more complex and involves the Tjörnes Seismic Zone, also referred to here as the North Iceland Seismic Zone.
7) The North Iceland Seismic Zone accommodates the transition from the Northern Volcanic Zone (NVZ) to the Kolbeinsey Ridge. The Kolbeinsey Ridge can be traced farther south toward the mouth of Eyjafjörður, as shown below:

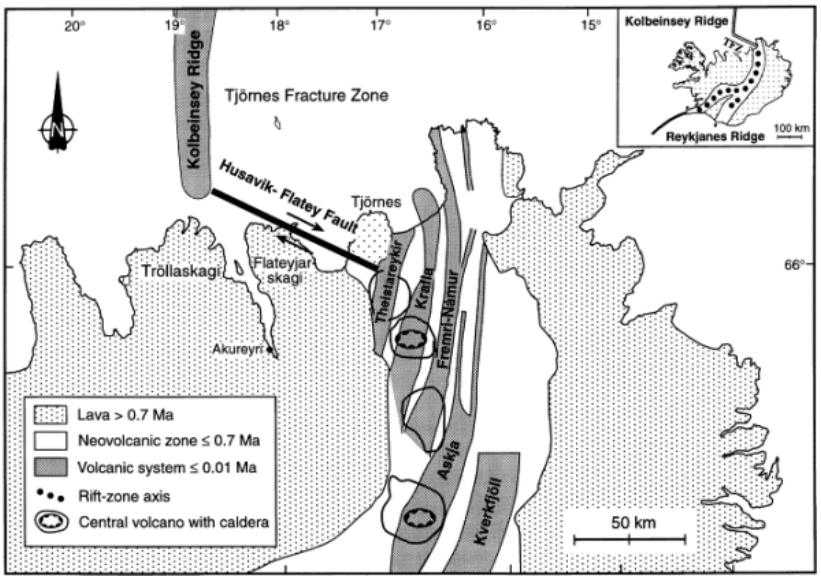

http://www.earth-of-fire.com/page-8786992.html

The Kolbeinsey Ridge extends southward toward the shores of the Tröllaskagi peninsula. Similarly, the NVZ extends northward toward the northernmost part of Iceland. Describing the boundary between the North American and Eurasian plates as a single line is therefore an oversimplification. The following drawing provides a more complete representation, although it too necessarily simplifies the actual conditions.

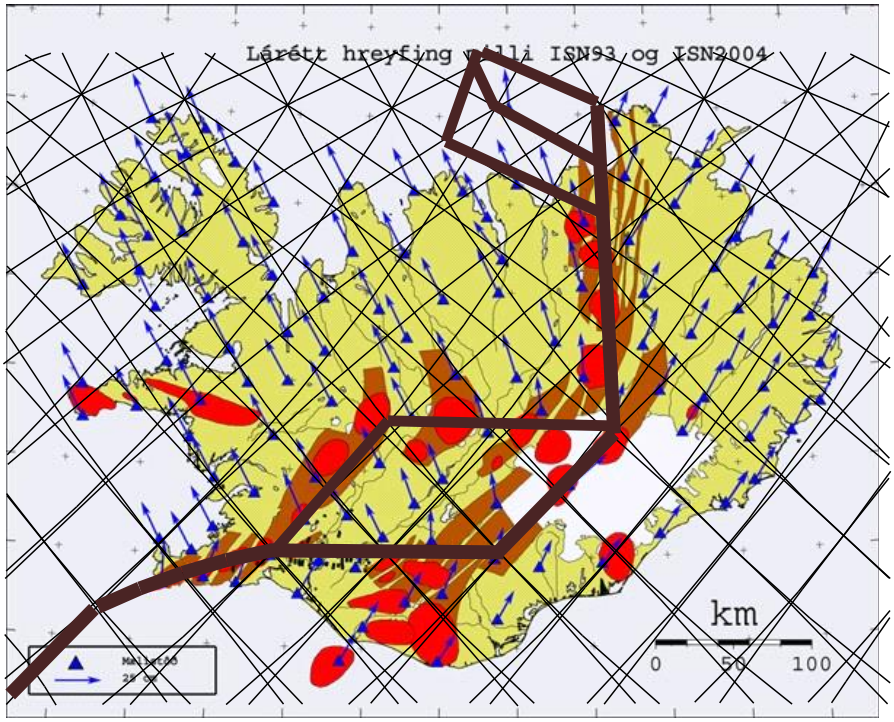

Figure 82: Division lines

According to the model, the orientation of the smaller convection rolls requires an upwelling line beneath Reykjanes. At first this may appear counterintuitive, because the upwelling associated with the large cells does not coincide with shallow upwelling at the 64°N parallel. Instead, shallow upwelling occurs along two lines of smaller cells on either side of the deeper division line. These divergent lines of the uppermost cells are particularly important because they lie directly beneath the tectonic plate.

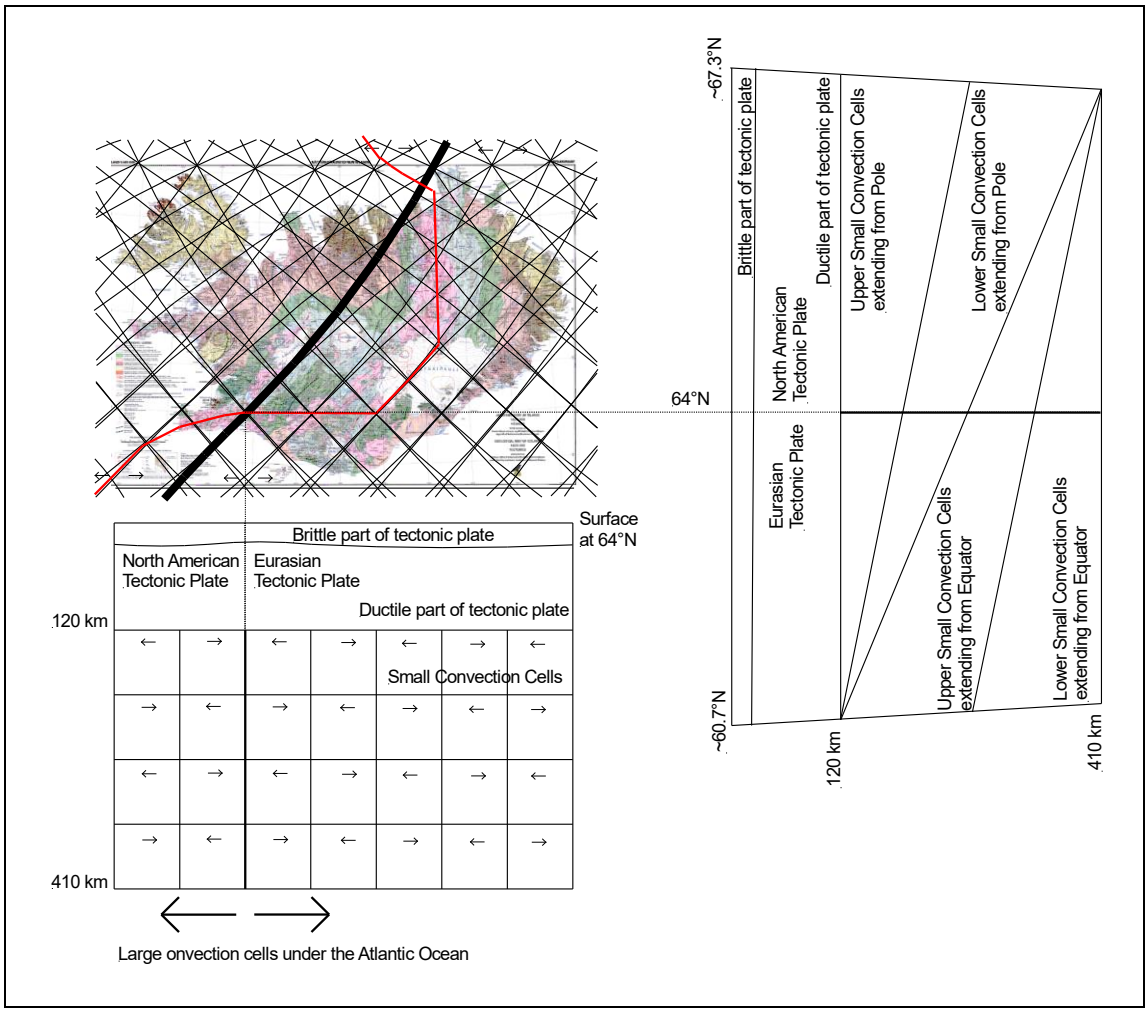

Figure 83: Comparing the convection cells of 64°N and the division line between the tectonic plates.

The geometry described above, in which the upper convection cells approach a balanced arrangement near 64°N, provides a basis within the model for interpreting the shift from the Reykjanes Ridge toward Hekla and the eastern side of the Eastern Volcanic Zone (EVZ).

1. The cells extending northward from the equator become relatively lower than the polar cells, and when their thicknesses become comparable near 64°N, the polar cells become dominant in the proposed model. Because the crust beneath Iceland is thicker than the oceanic crust beneath the Reykjanes Ridge, a narrow rift valley does not develop in the same way; instead, a broader zone across western Vatnajökull forms part of the rift system.
2. Because the vertical component of convection is important at these latitudes, the usual tendency to develop a ridge above an upwelling line west of the main lower-mantle division line is reversed in the model. The divergent line can be

traced toward Hekla, whereas the surface expression of the plate boundary follows the eastern edge of the EVZ.

3. North of the transition zone, under conditions interpreted here as more typical of the polar system, the tendency for a ridge to lie west of the principal lower-mantle division line becomes dominant again.
4. Where the main lines of northern and southern flow intersect, convection currents aligned NW-SE affect the net balance between upward and downward motion. In the model, the polar currents have a net downward component, favouring stronger upwelling along the inner line. Within the Icelandic transition zone, however, the net upward component of the uppermost cells becomes positive. This provides the proposed explanation for the shift from the Kolbeinsey Ridge across the main lower-mantle division line toward Theistareykir, Krafla and, farther south, Hekla.

11.3. Why does the drift direction follow the lines?

The tectonic drift of Iceland broadly follows certain lines of the grid defined by the proposed mantle convection system. It is therefore tempting to relate the measured motion to horizontal flow along these lines. The convection rolls themselves must also be considered, because in this model they provide part of the mechanical influence acting on the plate. This raises an important question: adjacent rolls rotate in opposite directions, so why should their horizontal effects on the plate above not largely cancel one another? Several factors need to be considered. Beneath the smaller upper-mantle rolls lie the much larger convection cells, which in the model contribute to large-scale plate motion. In addition, horizontal circulation must accompany the predominantly vertical circulation represented in a simple cross-section. This horizontal component can be regarded as an additional or 'excess' flow that may influence the combined effect of neighbouring rolls.

A further element of the model is the proposed system of Munroe lines. These lines are interpreted as zones that segment the ductile part of the tectonic plates and, in some places, may also influence the brittle part. Such segmentation could make local adjustment easier as the plate moves through changing conditions. In this interpretation, the Munroe-line system may help explain why measured drift directions in Iceland tend to follow grid lines rather than simply being perpendicular to individual convection rolls. Repeated adjustment along polygon boundaries could also reduce the amount of stress that would otherwise accumulate within a moving plate.

This leads to a broader question: does tectonic drift elsewhere in the world also follow the convection-cell grid? The answer proposed here is not that every surface structure should follow a grid line directly. The SISZ example discussed earlier shows that secondary structures may arise from the interaction between plate tectonics and the underlying convection geometry. At the surface, geological patterns are necessarily more varied than within the mantle and asthenosphere. The advantage, however, is that surface motion and structure can be measured directly. The task is therefore to compare the predicted geometry of the underlying system with the geological and tectonic conditions in each region. The model is intended as a framework for making those comparisons more systematic.

11.4. Tectonic drift of the whole world

During a visit to the National Land Survey of Iceland (Landmælingar Íslands), I asked about the measured northward motion of Iceland. I was told that the magnitude of the northward component had initially been unexpected, but that no error had been identified in either the measurements or the processing of the data. My own earlier picture had focused mainly on Iceland widening by about 2 cm per year and on the possibility of westward motion relative to the hot spot presumed to lie beneath Vatnajökull.

In this context, the broader pattern of tectonic drift derived from GPS measurements around the world becomes relevant. The northward component measured in Iceland can then be considered as part of a much larger pattern of plate motion.

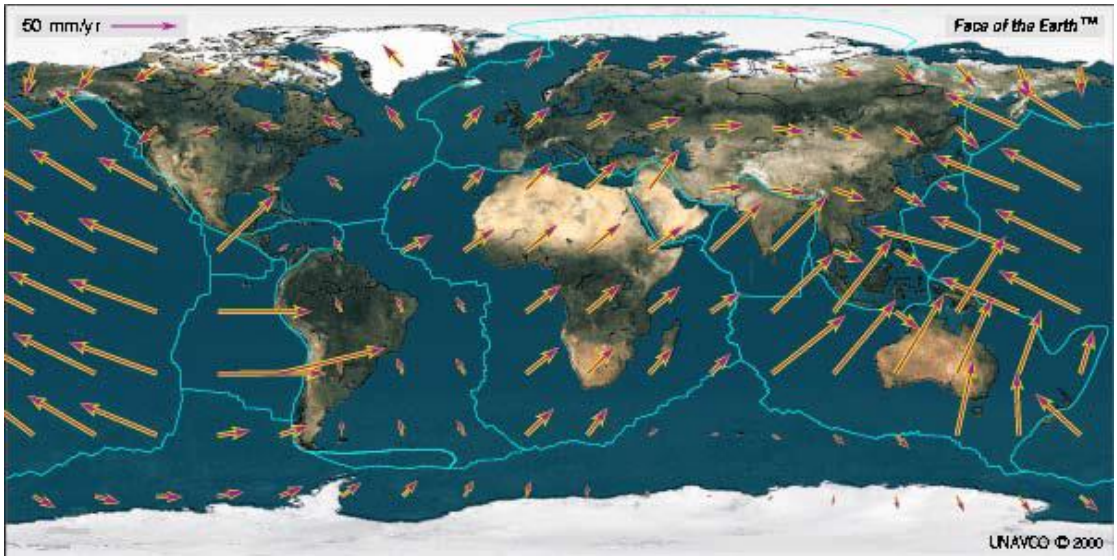

Figure 84: The drift of the tectonic plates (from the Internet).

When the tectonic drift measured in Iceland is compared with the global plate-motion pattern, one feature of particular interest is the opposite sense of rotation of the Eurasian and North American plates. In this simplified representation, the smaller North American plate follows a shorter radius. Iceland lies on the Mid-Atlantic Ridge and therefore provides a particularly useful location for comparing local drift vectors with this larger-scale pattern. The simplified map below illustrates why the measured directions in Iceland may correspond with the alignment of the proposed convection-cell system.

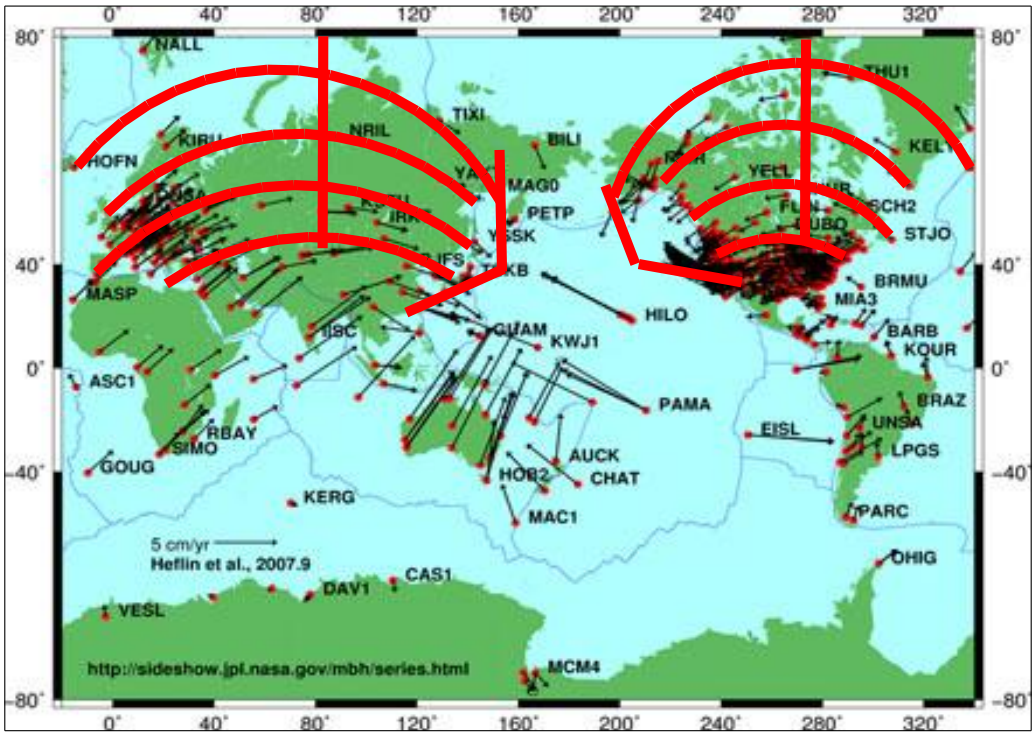

Figure 85: How the Eurasian and North American plates rotate in opposite directions (http://www.geologyin.com/2015/03/driving-forces-of-plate-motion.html)

The arrows emphasize the continuation of the Icelandic drift vectors and the broadly symmetrical, opposite-sense rotation of the North American and Eurasian plates.

11.5. Grid of reference

The GPS measurements show a substantial northward component of tectonic drift in Iceland, meaning that the measured positions move toward higher latitudes within the adopted terrestrial reference frame. The east-west component is likewise measured within a global reference system. This is more complex than the traditional picture of Iceland simply 'widening'. Establishing a stable geographical reference grid has been a central problem in geodesy for centuries, particularly for longitude. Latitude, by contrast, is directly related to the equator and the rotation axis. This distinction is important when the northward and east-west components of Icelandic plate motion are considered separately.

11.6. The tectonic drift of Iceland reversed

To explore how the older parts of Iceland may have moved apart, the measured drift vectors can be reversed in a simple kinematic reconstruction and extrapolated over roughly the last 10 million years. The schematic arrows on the map below indicate the approximate directions from which the two principal areas of oldest exposed bedrock would have moved under that assumption.

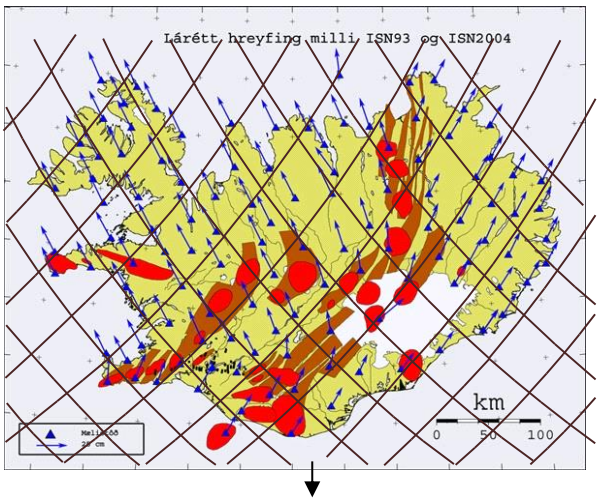

Base map with the polar convection-cell grid

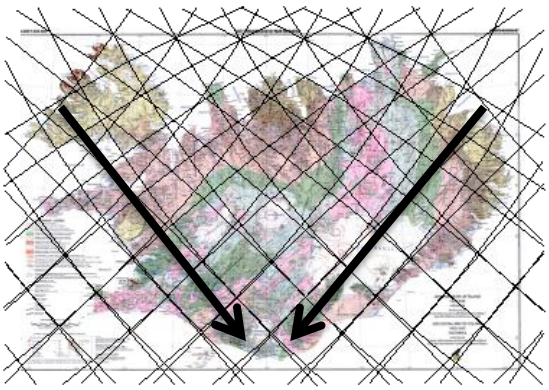

Direction of drift (velocity ignored)

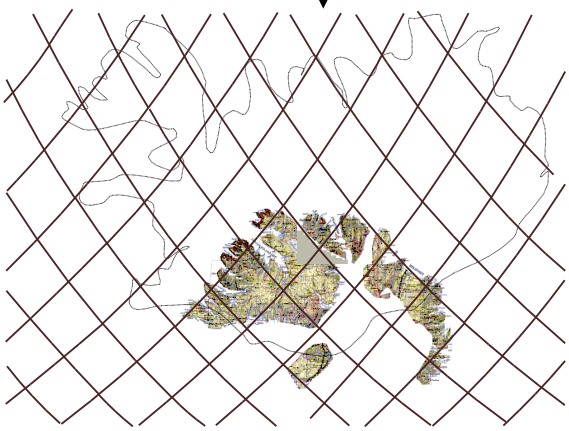

Reconstruction of the oldest bedrock. Approximate position of the oldest bedrock about 10 million years ago, based on present-day tectonic drift directions and velocities

Using this simplified reversal, the older bedrock areas can be brought together to produce a schematic reconstruction of Iceland about 10 million years ago. The reconstruction is necessarily approximate. Additional land would have existed around the areas shown, particularly to the north, where crust that once formed part of the region is now beneath the ocean. The result differs from a reconstruction in which the various parts are brought together only by reversing east-west spreading.

11.7. The continental microplate extending from Jan Mayen to Öræfajökull

Evidence has been interpreted to suggest that magma at Öræfajökull contains material derived partly from continental crust. The crust beneath eastern Iceland is reported to be up to 32 km thick[1] (Torsvik 2015). In the proposed convection geometry, a convection line can be traced from Öræfajökull toward Jan Mayen.

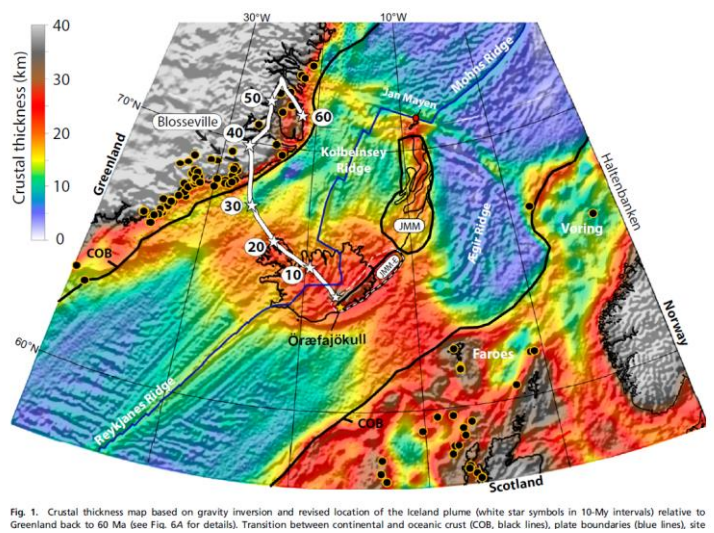

Fig. 1. Crustal thickness map based on gravity inversion and revised location of the Iceland plume (white star symbols in 10-My intervals) relative to Greenland back to 60 Ma (see Fig. 6A for details). Transition between continental and oceanic crust (COB, black lines), plate boundaries (blue lines), site

Figure 86: Resemblance between polar cells and continental microplate between Iceland and Jan Mayen.

In the proposed model, the microplate broadly follows one of the polar lines of the convection-cell system. The reconstructed path of the hot spot also shows a degree of correspondence, particularly when the effects of tectonic drift are taken into account. The presence of zircon in Öræfajökull lava does not by itself demonstrate that continental crust extends continuously beneath the volcano. Within the model proposed here, an alternative possibility is that southward mantle flow along the convection path extending from Jan Mayen could transport material derived from continental crust in that region.

[1] Forskning.no/2015/03/sunket-kontinent

Chapter 12 - Back to the beginning with the 'Ocean Basins'

Harry Hess (1962) wrote about the ocean basins in a paper that described mantle convection in terms that provide an important point of comparison with the system analysed here. He referred to his ideas as 'geopoetry'; in Iceland, where poetry has long held a prominent place, we learn to say, 'Half my fatherland is the ocean.' Iceland's geology is also closely connected with ocean-basin processes and differs in important respects from typical continental settings. For that reason, Iceland provides an unusual opportunity to examine how the proposed mantle-convection system may be expressed at the surface.

12.1. Pinpointing the regional and local systems

The dimensions of the proposed system have been derived from carefully selected reference points based on scientific measurements. The resulting grid represents the boundaries of convection rolls within the Earth, with each calculated line extending continuously from the North Pole to the South Pole.

A map on which degrees of latitude and longitude are plotted at a fixed scale is particularly useful for tracing the calculated lines. Hot springs can provide reference points for their orientation, but other surface features associated with zones of crustal weakness, including faults and some major topographic boundaries, can also be compared with the grid. As discussed earlier, the equator provides a useful large-scale reference because the principal sectors identified in this analysis span approximately 60° across the Atlantic, 30° across Africa, 60° across the Indian Ocean, 30° across the Indonesian region, and 150° across the Pacific. This regularity is presented here as one of several correspondences with the proposed convection-cell system. The Icelandic volcanic system provides another comparison: it lies directly north of the central Atlantic reference point at the equator, and the mathematical formulation developed earlier connects the two positions along the same longitudinal framework, from the equator to 64°N. The corresponding equatorial coastal points can therefore be examined as potentially significant reference locations within the model.

On the world map, the continental coastlines at these equatorial reference points can be compared with the calculated junctions between mantle convection

cells. The construction may appear complex, but the individual relationships form a single framework. Apart from a limited number of geological reference points used to position the grid, the global convection-cell pattern is generated from the mathematical rules developed in the preceding chapters. Several locations in Iceland can be used to constrain its position locally, after which the same geometry can be extended globally. Although Iceland is geographically an island above sea level, much of its geological setting is closely associated with processes characteristic of the ocean floor.

12.2. Zooming in on Iceland and then zooming out

The system forms a regular and symmetrical pattern. Over Iceland, the calculated network becomes dense and produces numerous polygons. Their areas vary considerably, from more than 2,000 km2 to only a few square kilometres. At the tangent points along the 64th parallel, the polygons approach point-like dimensions in the idealized geometry. In the model, areas associated with the smallest polygons are often interpreted as locations of enhanced geological activity.

A basic description of Icelandic geology emphasizes the continuation of the Mid-Atlantic Ridge rift system through Iceland from southwest to northeast. However, the distribution of volcanoes and geothermal areas does not follow a single ridge-parallel pattern. Several well-known sites lie within, or close to, small polygons in the grid that the present model associates with the alignment of convection cells below. The preceding chapters have shown how the analysis proceeds step by step from the measured layering of the Earth to a detailed representation of this proposed convection grid in Iceland.

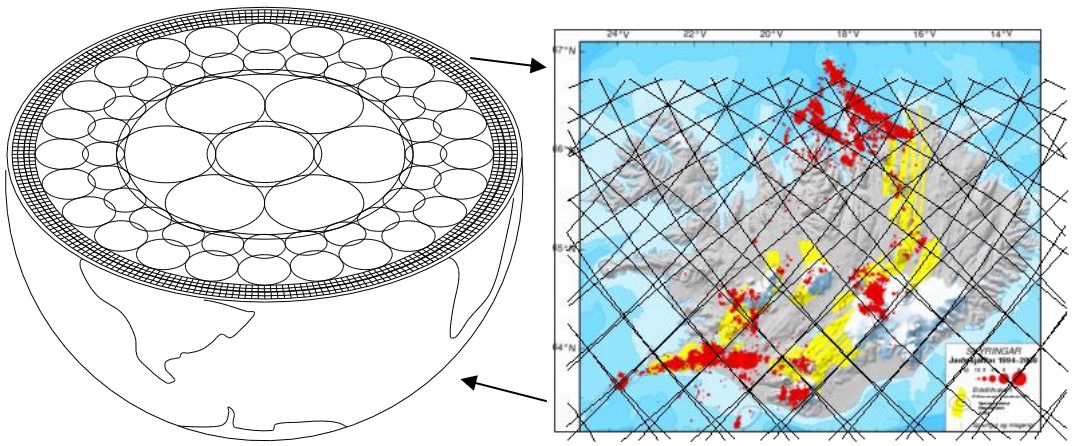

Figure 87: Examining Iceland helps increasing accuracy of global model.

The Icelandic grid can be extended globally. As noted earlier, the convection-cell grid can be examined at progressively finer scales in Iceland. At this scale, the proposed relationship between surface geology and the Earth's interior becomes particularly clear within the framework developed here. The procedure can then be reversed: the Icelandic pattern can be used as a local reference from which the global system is reconstructed. This reverse step is not essential to the derivation, but using both induction and deduction helps to clarify the internal consistency of the model.

12.3. Ocean ridges around Iceland

The Reykjanes Ridge provides an example of a large geological feature that can be compared with a single line of the proposed convection-cell grid over a distance of roughly a thousand kilometres. Extending the ridge trend beyond the ridge itself begins to reveal the broader geometry developed in this study. If the same grid also corresponds with independent geological features in Iceland, the Reykjanes Ridge becomes one of the clearest large-scale tests of the proposed convection-cell framework.

The Reykjanes Ridge is particularly useful for further comparison because the magnetic pattern recorded in rocks on either side of the ridge provides information about its development, while the associated V-shaped ridges provide an additional record of changes in volcanic activity along the ridge.

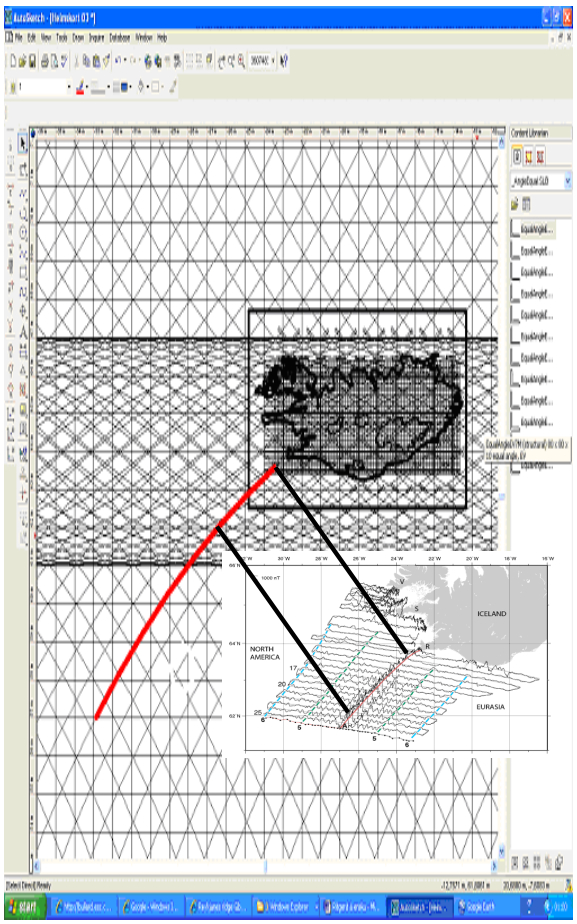

The inserted map is provided for comparison and shows the mapped position of the Reykjanes Ridge. (Source: http://www.mantleplumes.org/Disclosure.html, (viewed 02/06/2012)).

Note: The two straight reference lines are parallel and of equal length. The same geometrical relationship continues along the red line.

Comparison of the Reykjanes Ridge with the orientation of the convection-cell system

12.5. Taking more examples.

The Reykjanes Ridge proper begins near the southern corner of a polygon whose centre is aligned with the 64th parallel. This provides another opportunity to emphasize the importance of that latitude in the model. From one geometrical point of view, the 64th parallel plays a role comparable to that of the equator: it forms the central line of the proposed intersection zone between the polar convection cells of the upper mantle and asthenosphere and the corresponding hemispheric cells.

The model is developed in detail for Iceland and the surrounding ocean, but the same latitudes also cross continental regions with thicker crust and very different volcanic conditions. This provides a useful test: if the calculated grid has broader significance, some correspondence might also be expected in continental topography and tectonic structure. In the examples considered here, the orientations of selected rivers, fjords and coastlines are compared with the calculated grid lines. The simplified map below is provided as a reference for that comparison.

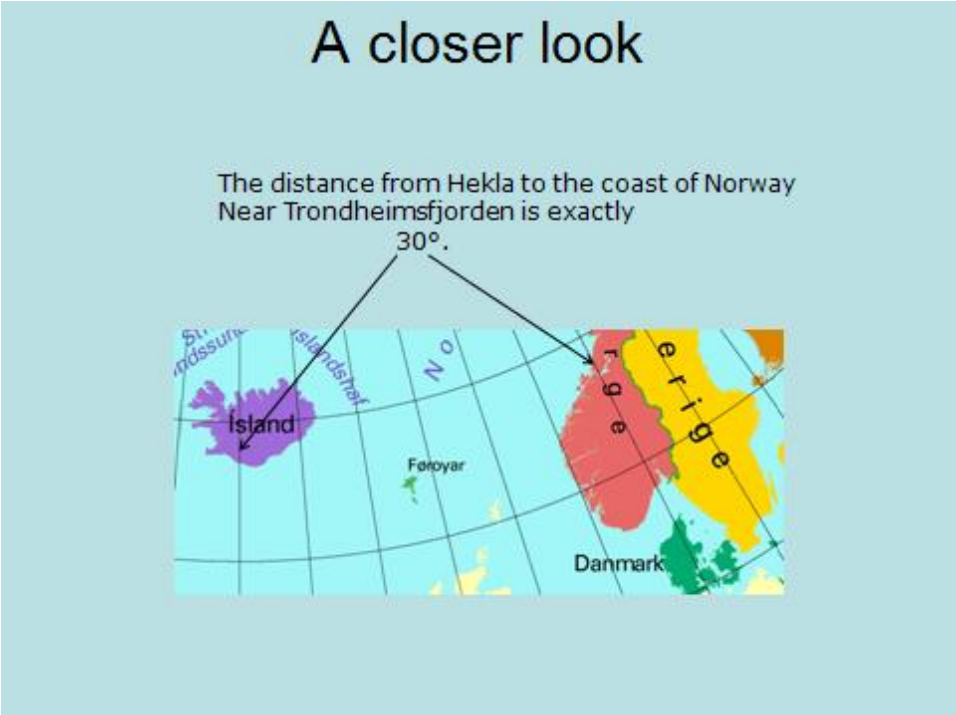

Iceland and Norway: a geometrical comparison.

In the comparison presented here, the orientation near Hekla and at the corresponding Norwegian locality is approximately N60°E. Because the calculated Munroe lines have an orientation of about N44°E, the N60°E trend is treated as a secondary

direction within the model. Hekla's fault orientation also differs from the approximately N45°E trend of the Icelandic volcanic system as a whole. The similar N60°E orientation identified in the Norwegian landscape is therefore presented here as a potentially relevant directional correspondence, rather than as evidence that the two areas share the same local tectonic process.

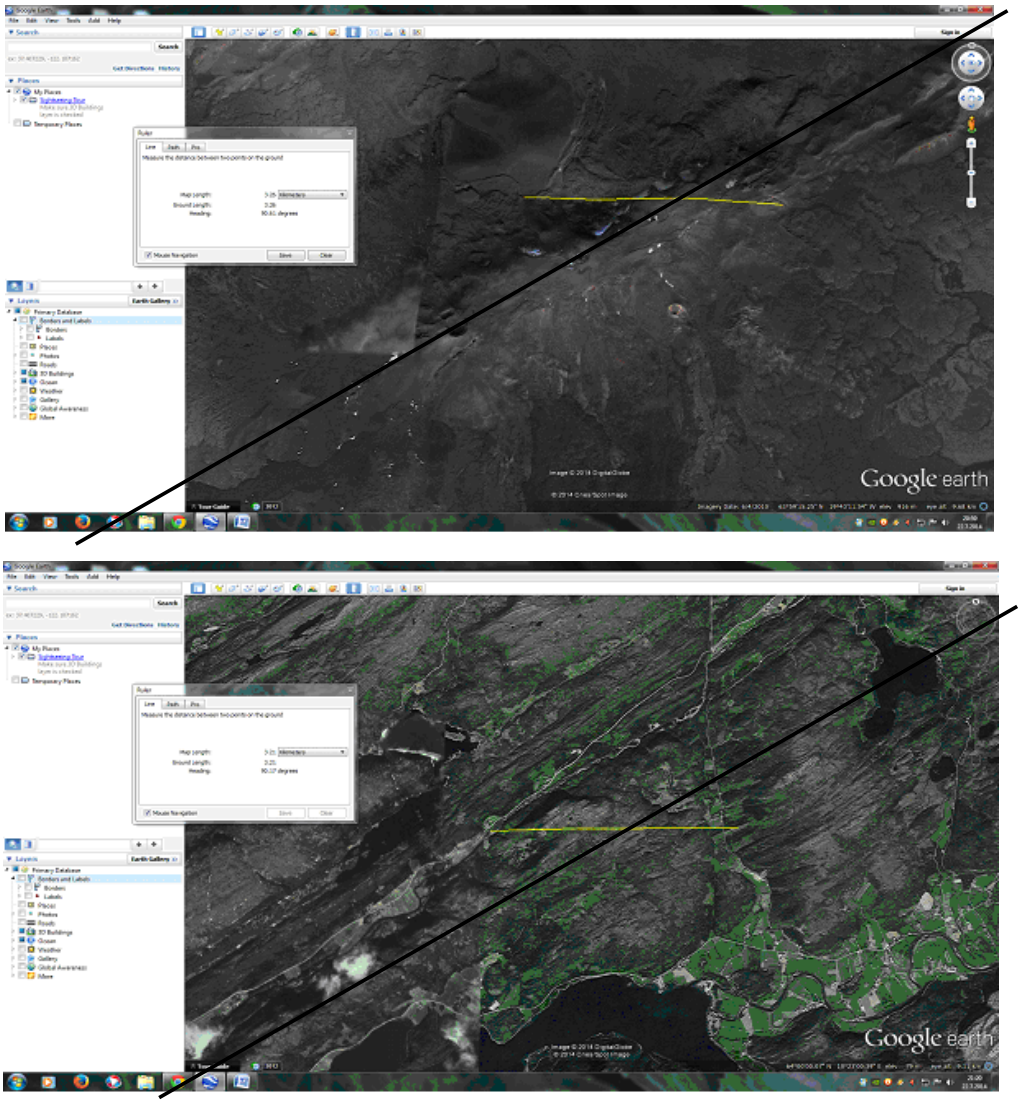

Figure 88: Comparison of tectonic orientations near Hekla and Trondheim, 30° apart.

The comparison places the two localities on the same latitude and 30° apart within the proposed grid.

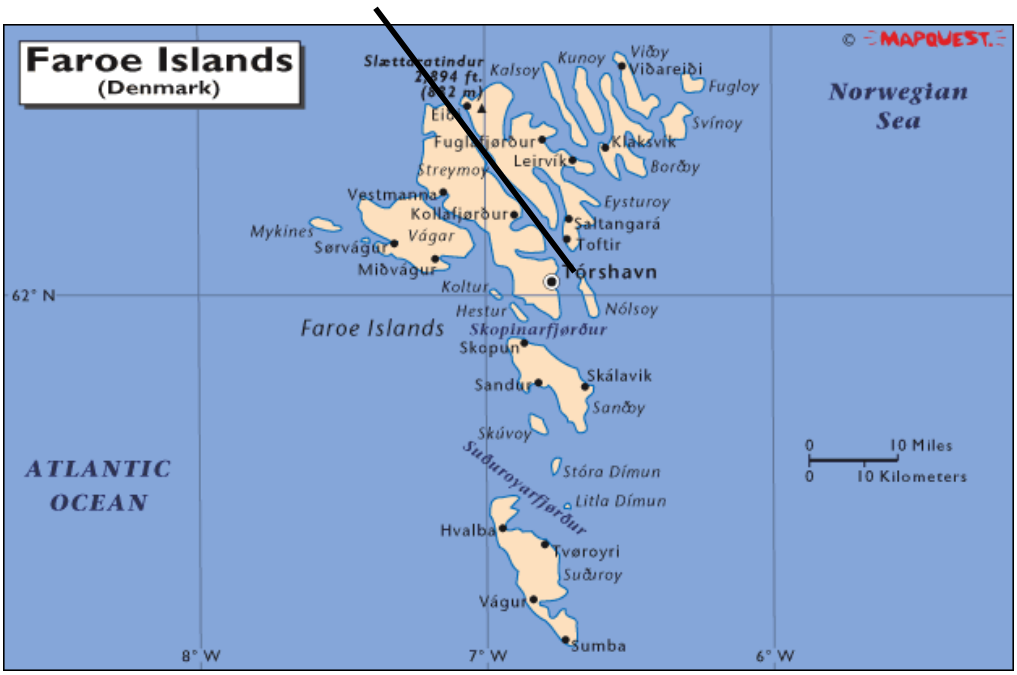

http://go.hrw.com/atlas/norm_map/faroeis.gif

On the simplified map of the Faroe Islands, a line drawn at N37°W, as calculated for the direction of a hemispheric convection cell at the 62nd parallel, provides a close match to the dominant trend through the islands. The Westray Fault Zone and Brynhild Fault Zone are presented here as additional tectonic features with a comparable orientation, providing another test of the calculated direction against mapped geology.[1]

1 http://jgs.lyellcollection.org/content/168/1/27/F1.large.jpg

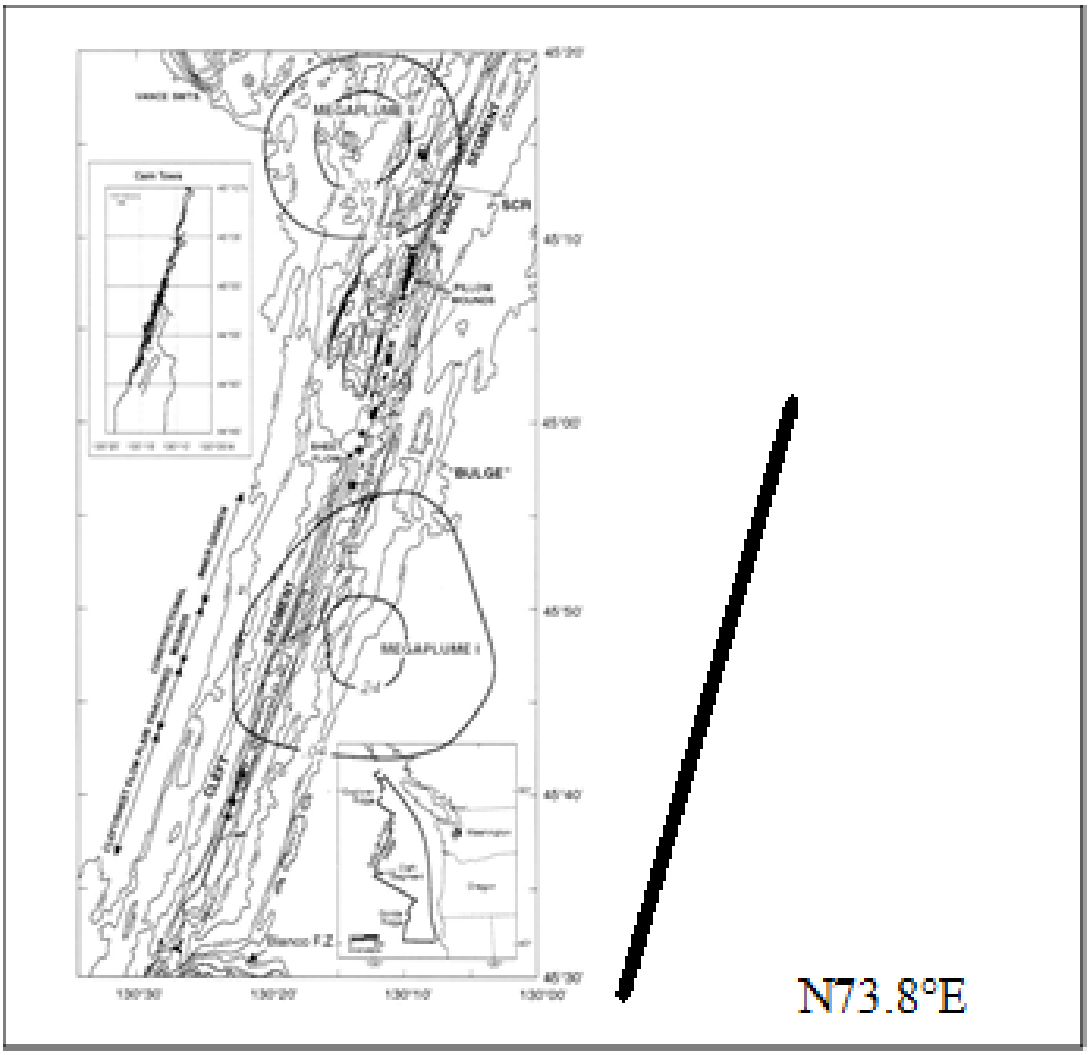

Figure 89: Juan de Fuca with calculated direction[1]

As a further example, the formula gives a direction of N16°E at 45°N. This direction can be compared with the mapped orientation of the Juan de Fuca region. Similar comparisons can be made at many other locations, providing a broad set of observations against which the proposed convection-cell geometry can be evaluated. This has now been examined further.

[1] http://www.pmel.noaa.gov/pubs/outstand/embl1429/figures.shtml

Chapter 13 – The Ring of Fire and the two other Tectonic Rings

13.1. Antarctica as a Geometrical Reference

The analysis of the Ring of Fire has raised the possibility that its overall form is considerably more regular than is generally apparent, and that its geometry may be controlled by large-scale mantle circulation together with the configuration of adjacent parts of the Earth. This naturally directs attention toward Antarctica, which is itself arranged in a remarkably systematic way around the South Pole.

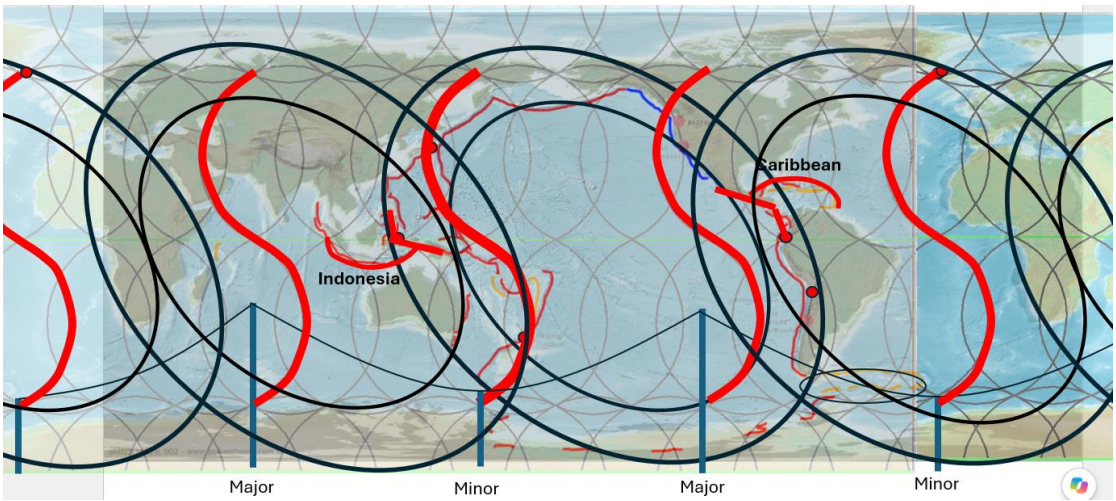

Figure 90: The Ring of Fire, along with Rings of both Indian Ocean and Atlantic Ocean.

Most important lower mantle divisons marked with thick red lines.

The division of Antarctica into East and West Antarctica is well established, and the geological boundary between the two passes relatively close to the geographic South Pole. When the entire Antarctic Plate is considered, rather than only the continental landmass, its overall form is elongated and can be approximated by an ellipse. Significantly, the minor axis of this ellipse follows the principal division between East and West Antarctica.

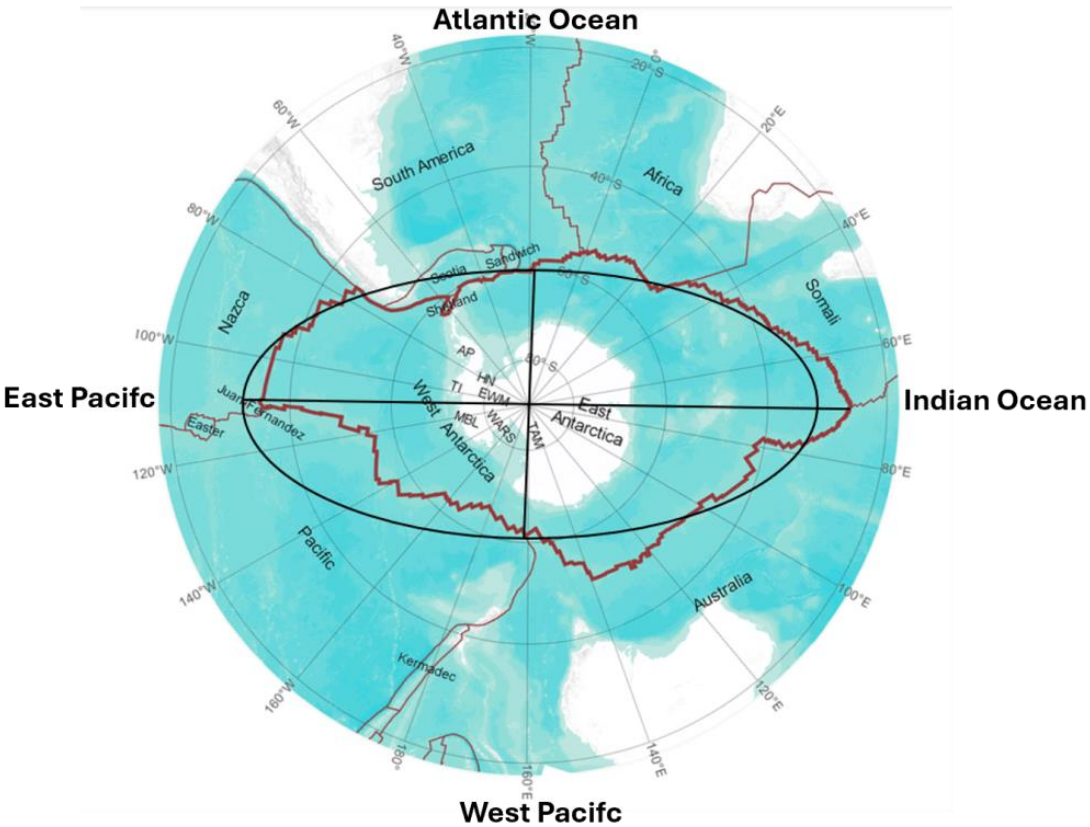

Figure 91: Antarcit Tectonic Plate and its elliptical form.

The World's Oceans in Relation to the Elliptical Geometry of the Antarctic Plate.

The endpoints of the major axis correspond approximately to the major oceanic-ridge junctions on opposite sides of Antarctica: toward the Indian Ocean ridge system on one side and the East Pacific Rise system on the other.

The Mantle Convection Roll Model also corresponds closely with the orientations of the major and minor axes in the western and eastern Pacific sectors surrounding Antarctica. The relevant boundaries intersect these axes near 64°S. A considerable degree of geometrical agreement therefore emerges between the Ring of Fire, the proposed mantle-convection-roll system, and the principal axes of the Antarctic Plate in the southern Pacific region. This relationship is illustrated on the accompanying map.

13.2. Extending the Geometry Beyond the Pacific

To examine whether this correspondence represents a broader global pattern, the Atlantic and Indian Ocean regions must also be considered. The inner boundary of the

Ring of Fire spans here theoretically 120° from east to west where it crosses the equatorial region. This suggests a simple research hypothesis: if the Pacific system occupies approximately one third of the Earth's circumference, comparable tectonic rings might occupy the other two 120° sectors.

The first test of this idea can deliberately be kept as simple as possible. A mathematical ellipse is constructed to span 120° at the equator, with its centre positioned 6° south of the equator and with a major-to-minor axis ratio of 1.5. A second, outer ellipse is then constructed around it, spanning 150°, while retaining the same centre. The 150° span corresponds to measureable distance between concrete points along the equator. This provides a straightforward geometry that can be compared directly with mapped tectonic structures. In the Atlantic case, the centre of the proposed elliptical system is placed at approximately **6°S, 29.5°W**. The important point is that these parameters are established before detailed geological adjustment. The question is therefore not whether an ellipse can be fitted retrospectively to selected tectonic features, but how well a deliberately simple geometrical construction corresponds to the actual tectonic pattern.

13.3. Correspondence with Major Tectonic Structures

When this geometry is plotted on a global map, the agreement with several major tectonic structures appears unexpectedly strong. One of the clearest examples is the **Kermadec–Tonga system**, which fits naturally into the proposed Indian Ocean Ring. This is particularly significant because Kermadec–Tonga is conventionally regarded as part of the wider Pacific Ring of Fire. In the present model, however, it lies within the sector where the Pacific and Indian Ocean tectonic systems overlap.

A similar relationship appears between the Pacific and Atlantic systems. The Caribbean region and Indonesia occupy broadly corresponding positions at the intersections between the major rings: the Caribbean at the junction between the Pacific and Atlantic systems, and Indonesia at the junction between the Pacific and Indian Ocean systems. Both therefore occupy geometrically comparable positions relative to the proposed mantle-convection-roll framework and to major divisions in the lower mantle. This correspondence is important because the two regions are among the most tectonically complex areas on Earth. Rather than lying randomly

within the global pattern, each appears close to a junction between two of the proposed large-scale tectonic systems.

A further complex relationship occurs between South America and Antarctica. The Scotia–Drake Passage–South Sandwich region contains a particularly complicated combination of spreading, transform motion and subduction, yet this system also appears to display symmetry relative to intersection points derived from the mantle-convection-roll geometry.

13.4. Overlapping Tectonic Rings

The derivation of these tectonic rings is in several respects more difficult than the derivation of the mantle-convection-roll system itself. The latter concerns an idealized organization within the mantle, whereas the tectonic rings are expressed through lithospheric plates that have evolved, fragmented, rotated and interacted over geological time. The regions where the proposed rings overlap therefore constitute a separate field of investigation.

Nevertheless, it is significant that such a simple initial construction produces such extensive correspondence with mapped tectonic structures. The geometry was not derived independently for each region. Instead, the same basic parameters are repeated around the Earth and then compared with the geology. Considerable work is still required before the system can be defined precisely. Among the factors that must be examined are the geometry of the Earth's geoid, the use of latitude and longitude on a curved rather than planar surface, and the apparent southward displacement of the tectonic-ring system, which in the present construction places the centres approximately 6° south of the equator.

The distinction between mathematical geometry on a map projection and geometry on the actual surface of the Earth is particularly important. Future calculations should therefore define the ellipses geodetically rather than treating longitude and latitude simply as Cartesian coordinates.

13.5. The Red Sea as a Particularly Strong Correspondence

Apart from Kermadec–Tonga, the **Red Sea** appears to provide one of the clearest correspondences with the tectonic geometry derived from the Ring of Fire. The outer

boundary of the proposed Atlantic Ring runs approximately along the central axis of the Red Sea. This is especially interesting because the Red Sea is not merely a geographical depression but an active divergent plate boundary containing an axial spreading system and developing oceanic crust. Its position therefore provides a potentially important test of the model.

The Red Sea relationship also appears to repeat a geometrical pattern observed on the opposite side of the system, along western North America. From the San Andreas region southward through Mexico and the Gulf of California, active plate-boundary structures and spreading centres follow a broadly comparable orientation along the outer margins of the large-scale tectonic ellipses. The corresponding boundary lines are separated by approximately 105°, consisting of 90° between the parallel outer edges of the two elliptical systems plus the intervening 15°-wide tectonically active zone.

The comparison is not intended to imply that these regions have identical tectonic histories. Rather, they appear to occupy corresponding positions and orientations within the larger geometrical framework.

13.6. Repeated Ridge Orientations at 90° Intervals

This relationship recalls an earlier observation concerning the **Reykjanes Ridge** and the **Juan de Fuca Ridge**. These ridge systems occur approximately 90° apart within the proposed global geometry, yet follow corresponding structural directions. Such repetitions become increasingly important when several independent tectonic features are considered together. A single alignment can readily be coincidental. A repeated combination of alignments, orientations, intersection points and distances is more informative and can be tested quantitatively.

The mantle-convection-roll system also provides a direct geometrical continuation from the minor axis of Antarctica toward the Reykjanes Ridge and Iceland. Thus, Iceland does not appear in this framework merely because it lies on the Mid-Atlantic Ridge. Its position can also be related to one of the principal Antarctic axes and to the wider system of global tectonic divisions.

The resulting pattern is therefore not based on one isolated correspondence. Several different relationships appear simultaneously: The axes of the Antarctic Plate, the

geometry of the Ring of Fire, the proposed Atlantic and Indian Ocean Rings, major spreading ridges, major subduction systems, complex plate-boundary junctions, and the mantle-convection-roll divisions all show repeated geometrical relationships.

Previous analysis has also shown that the world's principal geyser regions can be placed within the same geometrical framework. Iceland, Yellowstone, Kamchatka, New Zealand, Chile and East Africa each occupy positions that can be related to major axes, ring boundaries, intersections or tectonic divisions within the proposed system. This does not by itself establish a common physical cause. It does, however, considerably increase the number of independent geological observations against which the geometry can be tested.

13.6. A Working Global Hypothesis

The purpose of the present construction is therefore not to claim that the three tectonic rings have already been demonstrated as physical mantle structures. At this stage they are best regarded as a **geometrical research hypothesis derived from the observed form of the Ring of Fire**.

The procedure is intentionally simple: First, identify the regularities already present in the Ring of Fire; then construct equivalent geometrical forms at 120° intervals around the Earth; and finally compare those forms with independently mapped tectonic structures.

The surprising result is that the comparison does not produce random relationships. Instead, major structures repeatedly appear close to predicted axes, boundaries, overlaps and intersection zones. If further quantitative analysis confirms these relationships, the three-ring geometry may provide an additional way of examining how the lithosphere is organized above large-scale mantle circulation. The central question is therefore no longer simply why the Pacific Ring of Fire has its familiar form. A broader question arises:

Is the Ring of Fire one visible part of a larger, globally organized tectonic system extending through the Pacific, Atlantic and Indian Ocean regions and geometrically linked to Antarctica and the underlying mantle circulation?

he African Plate is characterized by several unusually long boundary segments with predominantly N–S or E–W orientations. To the north it is bounded by the Mediterranean region, to the west by the Mid-Atlantic Ridge system, to the east by the East African–Red Sea tectonic system, and to the south by the Antarctic Plate. Within the geometrical framework considered here, these boundaries can be analysed as a sequence of segments related either to the mantle-convection-roll division system, to the elliptical boundaries of the tectonic rings, or to transitions between the two.

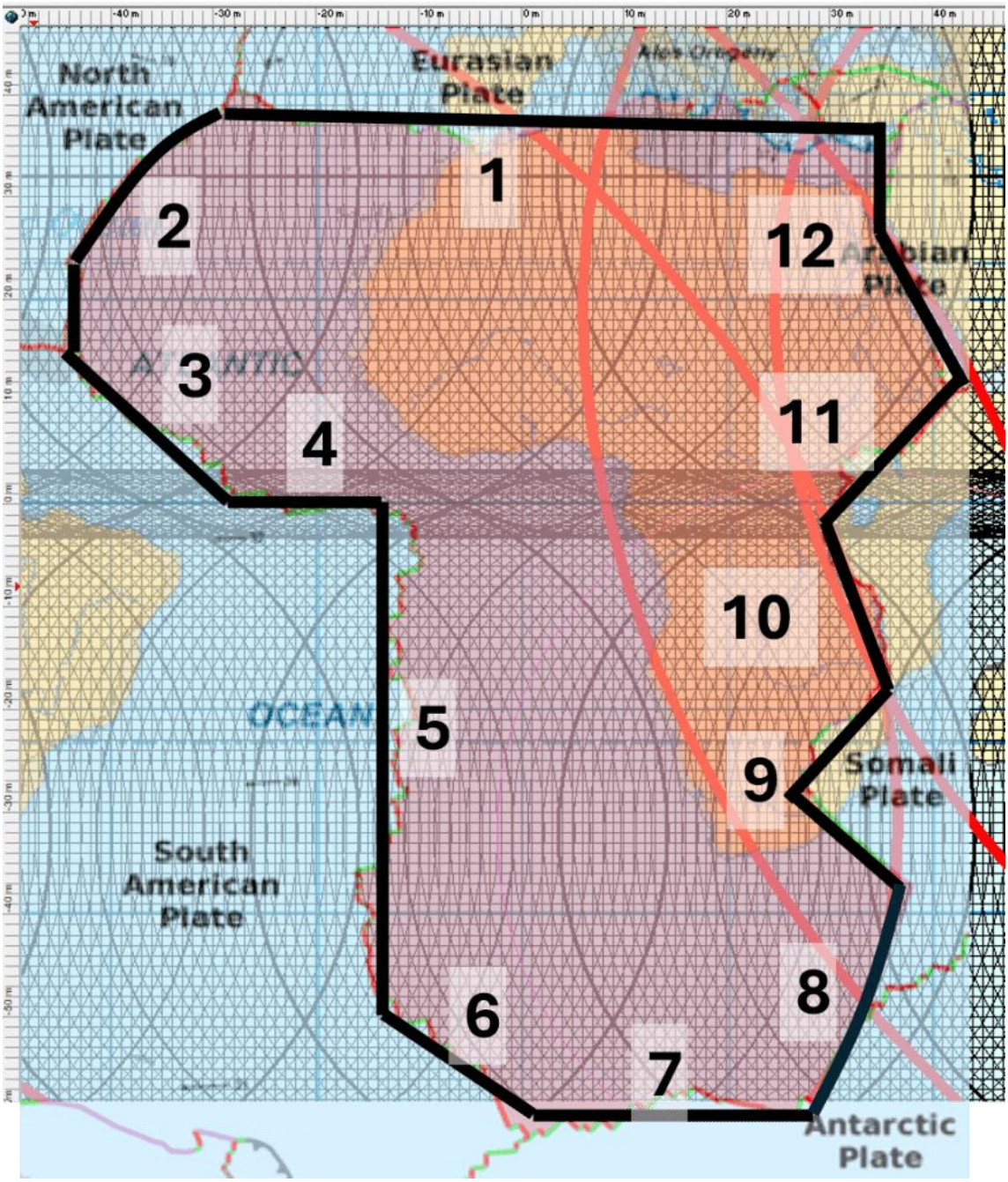

Figure 92: The African Tectonic Plate, marked by mid-ocean ridges and tectonic rings.

1. The Mediterranean plate-boundary system has a pronounced E–W orientation, and this general direction continues westward through the Gibraltar region into the Atlantic, along the boundary between Africa and Eurasia. The endpoints of this broad E–W system are not regarded here as arbitrary. Its eastern end is located close to a major lower-mantle convection-roll division north of the northern end of the Red Sea, while the western end approaches an important N–S axis in the Atlantic. The Mediterranean system can therefore be viewed, in this model, as an E–W connection between two larger N–S structural elements.

2. The boundary then connects with the next major N–S structural axis farther west. Part of this section has a pronounced N–S component before reaching the plate-boundary system extending from the Caribbean region into the central Atlantic. The longitudinal separation between the principal structural lines is approximately **15°**. This 15° spacing is important within the convection-roll model because it represents a secondary subdivision of the larger lower-mantle geometry.

3. The next section trends toward the **southeast**, approximately parallel to the calculated direction of the convection-roll system. Again, the longitudinal displacement is about **15°**, but in this case the shift is from west to east. The bend occurs approximately on the same longitude as the transition between Sections 1 and 2, producing a repeated geometrical relationship between the major N–S axes and the oblique plate-boundary segments.

4. At the equator, the boundary turns into an almost directly E–W segment. This part extends for approximately 15° of longitude. Its position directly along the equatorial reference line makes it particularly significant in the convection-roll framework, in which the equator provides the simplest geometrical expression of the major and subsidiary mantle divisions.

5. A particularly long section of the African Plate boundary then trends approximately N–S. This segment follows a calculated central line within the convection-roll system, located midway between two principal lower-mantle division lines. It is therefore not

associated directly with one of the major lower-mantle boundaries, but with the geometrically defined centre of the interval between them.

6. The boundary then turns toward the southeast, continuing to the region where the South American, Antarctic and African plates meet. Within the convection-roll model, this junction is also located close to an intersection of major lower-mantle division lines. The plate triple junction and the calculated mantle intersection therefore occupy approximately the same structural region.

7. From this intersection, the plate boundary again assumes an approximately E–W orientation. It extends from the lower-mantle convection-roll intersection toward the inner elliptical boundary of the Atlantic tectonic ring. This section therefore forms a direct geometrical link between the convection-roll framework and the younger elliptical tectonic system.

8. The boundary then turns toward the NNE and follows the inner ellipse of the Atlantic tectonic ring for a considerable distance. Here the elliptical geometry becomes the dominant structural relationship. This is an important contrast with the preceding sections, where the plate boundary was more closely associated with the convection-roll divisions.

9. Farther north, the boundary bends into the African continent before turning back toward the inner Atlantic ellipse. It returns to the region where the inner Atlantic ellipse and the inner ellipse of the Indian Ocean tectonic ring approach one another and become closely associated. This is the same broad geometrical interaction zone discussed in connection with the East African Rift and Lake Malawi.

10. Along this section, the boundary of the African Plate coincides with the boundary of the Somali Plate. The plate boundary occupies the narrow region associated with the two inner tectonic ellipses. This section is therefore especially important because the same geometry can be analysed from either side: as the eastern boundary of the African Plate or as the western boundary of the Somali Plate.

11. Farther north, the plate boundary leaves the inner Atlantic-ring boundary and crosses toward the outer Atlantic ellipse. Its orientation corresponds approximately to the direction of the underlying convection-roll system. The segment terminates at the Afar Triple Junction. This provides another clear example of a plate boundary

transferring between two elements of the model: inner tectonic ellipse, convection roll alignment, outer tectonic ellipse.

12. From Afar, the boundary continues northward along the Red Sea. In the present geometrical interpretation, the Red Sea follows the outer ellipse of the Atlantic tectonic ring. Near its northern end, the boundary develops a more pronounced N–S orientation, marking another transition between the elliptical tectonic geometry and the principal directional structure of the convection-roll system.

The African Plate provides a particularly useful continental-scale example because its boundary includes several fundamentally different types of tectonic environment: mid-ocean spreading ridges, continental rifts, convergent margins and complex transition zones. Despite these differences, the boundary can be divided into a sequence of relatively simple geometrical segments. Some are predominantly N–S or E–W, some follow calculated convection-roll divisions or intermediate lines, and others follow the inner or outer ellipses of the Atlantic and Indian Ocean tectonic rings.

A recurring feature is the approximately 15° longitudinal spacing between several major structural elements. The boundary repeatedly shifts from one such element to another before continuing along a new N–S, E–W or oblique direction.The African Plate is therefore not interpreted here as following one single geometrical structure. Rather, its outline appears to result from the interaction of an older mantle-convection framework with the younger elliptical tectonic-ring system.

The African Plate provides a particularly clear continental-scale example of how plate boundaries may alternate between mantle-convection divisions, equatorial and meridional structural axes, and the elliptical boundaries of the Atlantic and Indian Ocean tectonic rings.

Proof?

The purpose of this final section is not to claim that the model has been proved in an absolute sense, but to summarize the converging lines of evidence presented in this book. The proposed system is simple in its basic geometry, yet complex in its implications because it brings together geophysical measurements, physical principles, and geological and topographic observations. The model should therefore be judged by whether these independent relationships are internally consistent, quantitatively reproducible, and open to falsification.

The principal steps used to derive the dimensions and geometry of the proposed convection system can be summarized as follows:

VERTICAL GEOMETRY

1) Convection rolls with a characteristic diameter comparable to that of the inner core are fitted to the principal internal layers of the Earth.
2) Two layers of smaller convection rolls are proposed between depths of approximately 120 and 410 km.

HORIZONTAL GEOMETRY – LATITUDINAL

3) The diameter of the horizontal circulation extending from the equatorial region is derived.
4) Corresponding polar systems are derived.
5) Intersection zones around the 64° parallels are analyzed.

HORIZONTAL GEOMETRY – LONGITUDINAL

6) The longitudinal positions of the horizontal circulation systems are constrained by comparison with geographical and geological features.

The most important test is whether the geometry derived from the internal model can be recognized independently at the surface. Several examples have been examined in this work. The volcanic zones of Iceland and the Reykjanes Ridge can be compared with the predicted directions of the system. The alternating distribution of major land and ocean sectors along the equator provides a second test in the region where the Coriolis parameter is zero. Within Iceland, the positions of volcanic centres, including Hekla and Öræfajökull, provide further opportunities for comparison. Taken

together, these examples allow the proposed internal geometry to be tested against observations at several different scales.

Within the framework developed here, several physical concepts are brought together: Rayleigh–Bénard-type convection, the Coriolis effect, radiative heat transfer, and the proposed application of the Munroe effect. Irvine (1989) also emphasized the importance of the extremely long timescales involved in mantle dynamics. In the interpretation adopted here, these long timescales favour a comparatively stable convective organization. Work on the South Iceland Seismic Zone undertaken with Páll Einarsson provided an additional example of how stress, ductile behaviour, and fracture orientation can be considered together. Mohr-circle relationships provide a geometrical framework for relating the direction of principal stress to fault and fracture orientations. In the present model, these surface stress relationships are then compared with the directions attributed to the underlying convection system and its proposed Munroe lines.

GPS-derived plate-motion vectors provide one of the strongest independent tests considered in this work, because measured directions can be compared directly with directions predicted by the model. The geometrical correspondence between convection cells of approximately comparable height and width and the measured internal layering of the Earth provides the starting hypothesis, but it is not sufficient by itself to establish the model. The subsequent construction of a three-dimensional convection system, its comparison with tectonic motion, and the proposed roles of radiative heat transfer and Munroe lines provide additional, partly independent tests of the same framework.

This leads to the question posed by the title of this section: can the model be proved? In science, a model of this kind is better evaluated by asking whether its assumptions are explicit, whether its predictions can be reproduced, and whether observations can falsify it. The central geometrical proposition—that the principal convection cells have approximately comparable height and breadth and that their characteristic dimensions correspond to the Earth's internal layering—can be tested directly. The subsequent calculations and surface comparisons can then be tested independently. Errors may remain in the logic, measurements, calculations, maps, or interpretations presented here, and individual parts of the model may require revision. A useful scientific criticism should therefore identify a specific assumption, calculation, prediction, or comparison and show where it fails. The strength of the model, if it survives such tests, lies in the convergence of several different lines of evidence rather

than in any single observation.

This work necessarily builds on the observations and ideas of many other researchers. One book that encouraged me to complete and publish this study was Gillian R. Foulger's Plates vs Plumes: A Geological Controversy. The conventional plume hypothesis is commonly represented by hot, buoyant mantle material rising from considerable depth and contributing to uplift, melting, geothermal activity, and volcanism. Foulger critically examines whether deep mantle plumes are required to explain such observations and argues for alternative interpretations of many so-called hotspots or melting anomalies.

Against this background, Foulger writes (Foulger 2010):

> Since that moment I have worked to see for myself whether such a hypothesis can stand – that Iceland does not owe its volcanism to a deep mantle plume but to processes rooted at shallow depth. And if such a hypothesis can stand for Iceland, can it also stand for other places traditionally assumed to be underlain by plumes.

The model developed here takes this question in a particular direction. Processes expressed at relatively shallow levels are interpreted as being organized by dynamics below approximately 120 km depth. The proposed heat-transfer sequence combines radiative transfer toward the deep interior, convective return of heat and material, and outward radiation from the convection cells. Within this framework, the Munroe effect is proposed as a mechanism by which focused pathways of melt may extend upward into the tectonic plates, supplying heat and material to crustal processes that ultimately contribute to geothermal and volcanic activity.

Appendix 1: Basic Model Compared with the World Map

To make the construction of the maps easier to follow, this appendix presents the basic geometry step by step. It illustrates what is meant by hemispheric and polar convection rolls and how their calculated paths are transferred to a geographical map. The examples initially focus on the two proposed convection-roll layers between approximately 120 and 410 km depth.

The sequence of diagrams introduces the principal features one at a time and then combines them into the complete map.

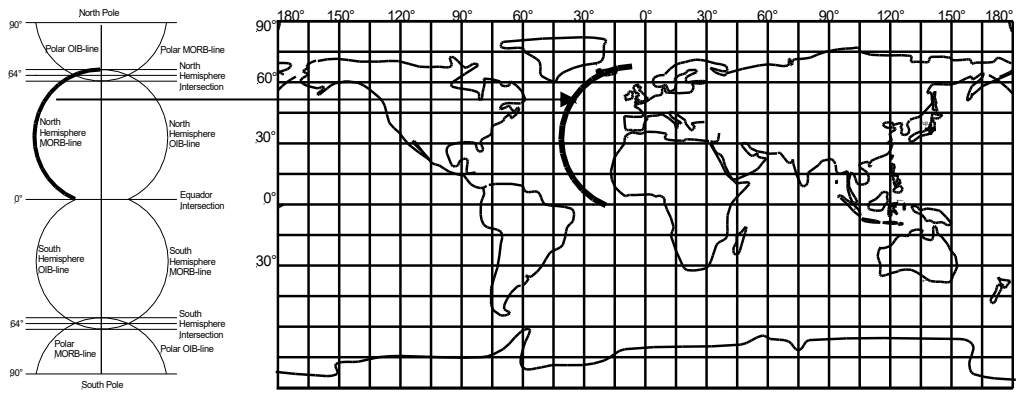

Explanation 01: A “MORB line” extending from the equator to 67.34°N.
The MORB and OIB lines represent convection rolls within two different proposed layers between approximately 120 and 410 km below the Earth’s surface.

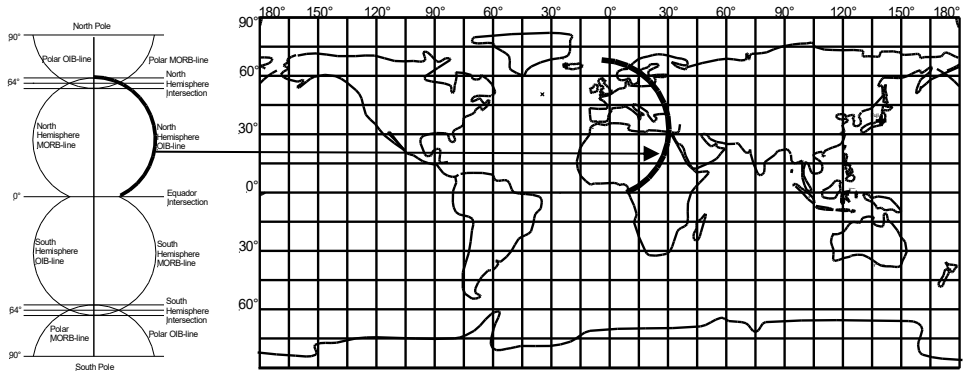

Explanation 02: An “OIB line” extending from 67.34°N to the equator.

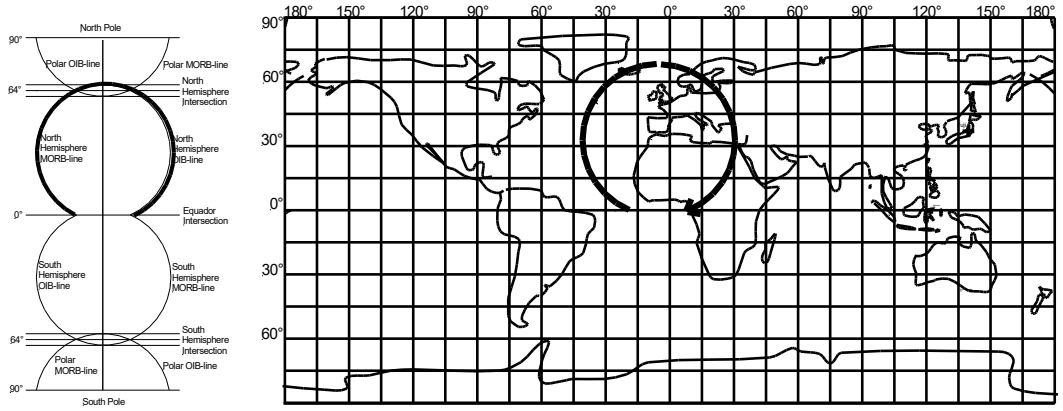

Explanation 03: The two semicircular paths shown in Explanations 01 and 02 are joined end to end at approximately 67.3°N. In the model, the convection rolls in the two layers between 120 and 410 km thereby form one complete circulation path. The arrowhead indicates the proposed direction of horizontal particle motion.

A particle following this path is therefore assumed to be carried within the upper layer from the equator to approximately 67.3°N and then within the lower layer back toward the equator.

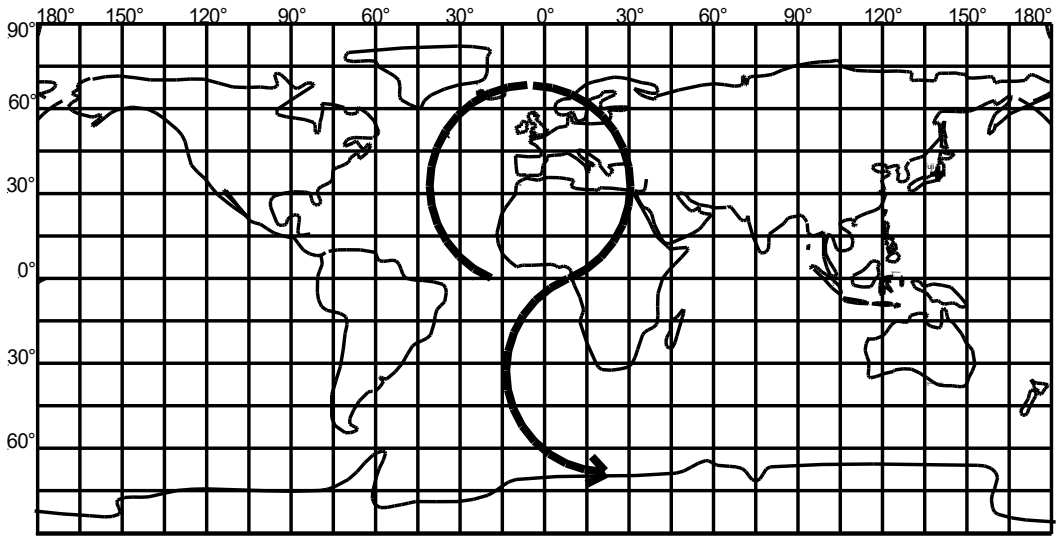

Explanation 04: The modeled path continues across the equator and curves into the Southern Hemisphere. The particle is then carried within the OIB layer toward approximately 67.3°S. The arrowhead indicates the proposed horizontal-flow direction. From there, the circulation returns toward the equator within the MORB layer.

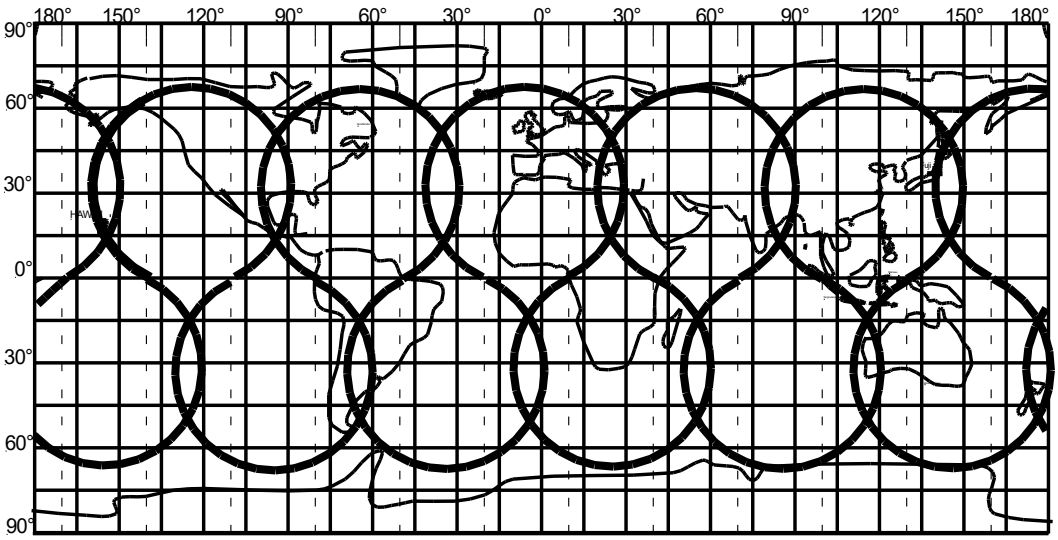

Explanation 05: The complete modeled path of a horizontally moving particle is traced around the globe. On a conventional map the path appears to oscillate north and south, whereas within the rotating reference frame its geometry is interpreted through the Coriolis effect. The dotted lines mark the longitudes at which the illustrated convection roll crosses the equator. Adding parallel circulation paths at 1.5° longitudinal intervals produces the full hemispheric system.

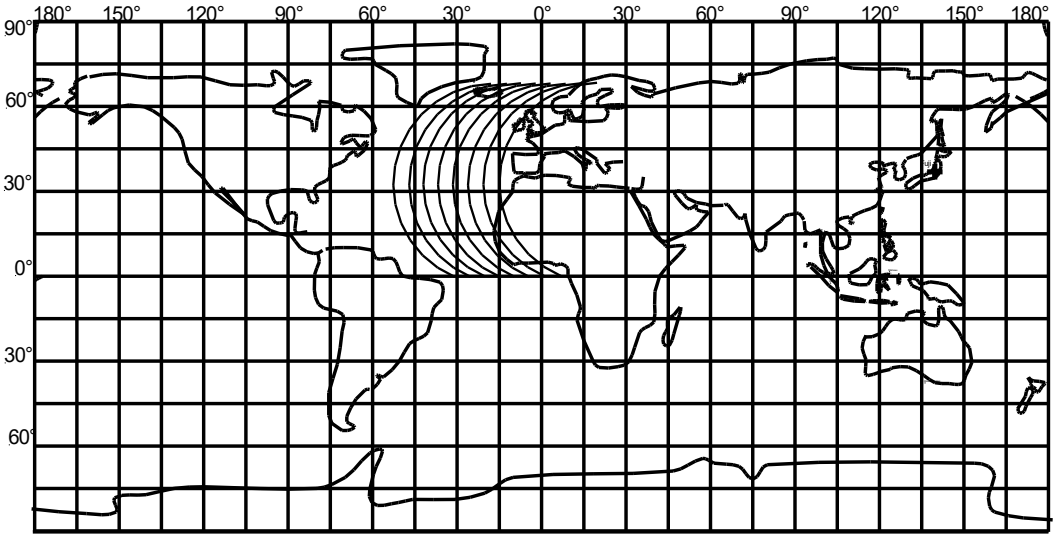

Explanation 06: A set of parallel curved lines represents adjacent MORB-layer convection rolls. Their widths are not shown to scale. The geometry is the same as in Explanation 01.

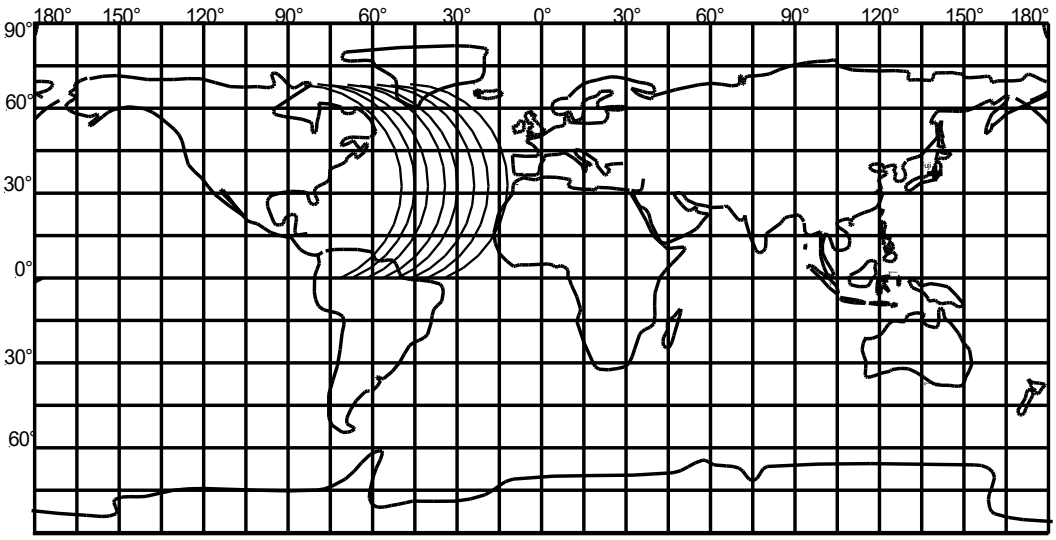

Explanation 07: A set of parallel convection rolls represents the proposed southward horizontal circulation within the OIB layer, which in this model lies directly below the MORB layer.

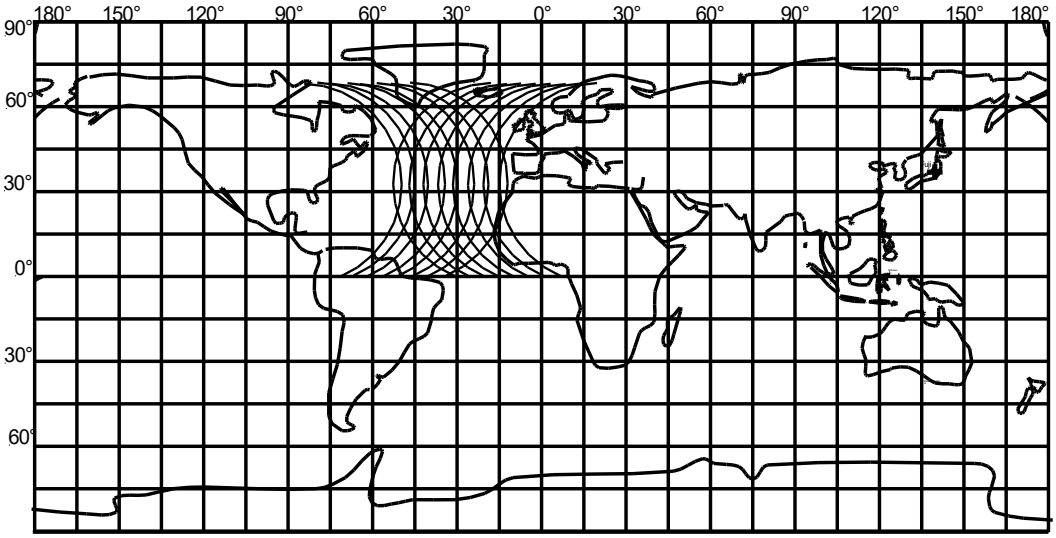

Explanation 08: The geometries shown in Explanations 06 and 07 are combined. When the lines representing convection rolls in the upper and lower layers are plotted together, they form the pattern shown here. The drawing is schematic and the roll widths are not to scale. The resulting diamond-shaped polygons are particularly important for later comparisons.

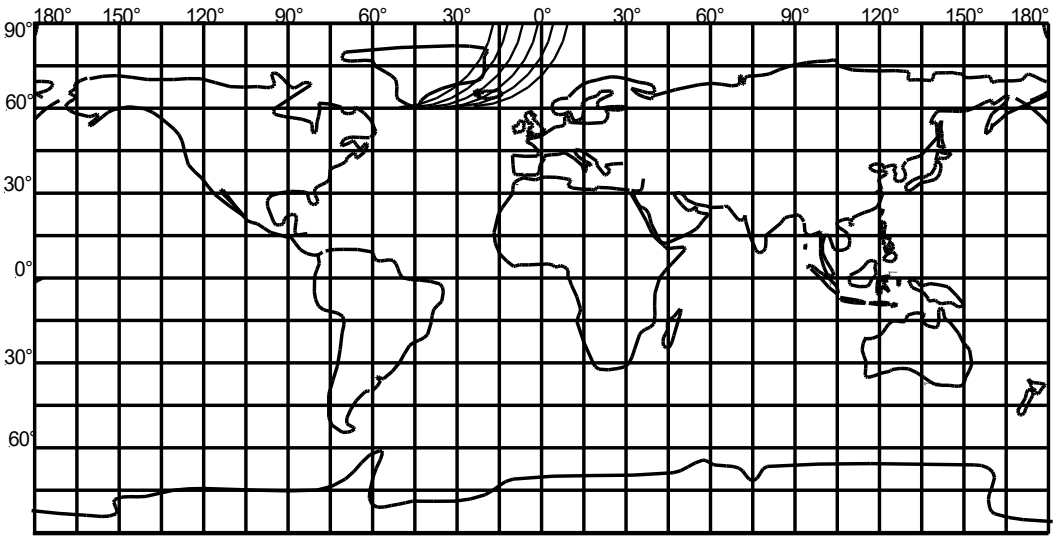

Explanation 09: Several lines representing the polar convection-roll system are added to the world map. As with the hemispheric system, a second proposed layer lies below the one illustrated here. The polar lines are treated separately. Building the map step by step makes it easier to follow the geometry of the individual convection paths before considering the complete system.

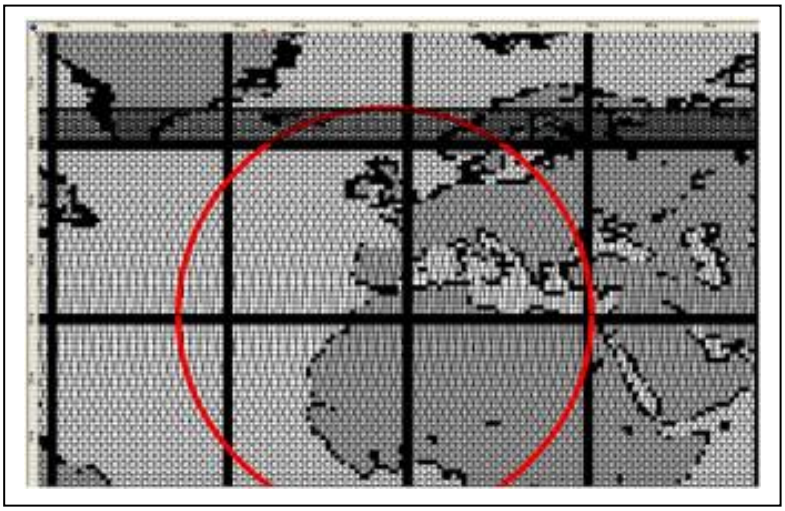

Explanation 10: The completed schematic map contains circulation paths spaced at 1.5° intervals. One complete path, consisting of two semicircular components, is highlighted for clarity.

The convection system of Earth‘s mantle

and how heat is conveyed to the surface

Steingrimur Thorbjarnarson and Thorbjorn Armann Fridriksson

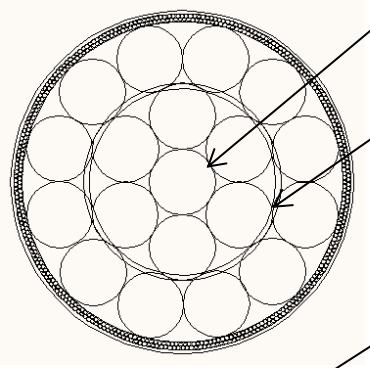

The basic model of convection along the plane of equator

The preconditions

The layers of the Earth shown drawn to scale. Circles of the same diameter as the inner **core** fit into the diagram. The match is due to physics, whereas the mantle, under balanced conditions, should form convection cells equally high and wide.

The Gutenberg layer

The Gutenberg layer is here considered to be an intersection between the core and the mantle.

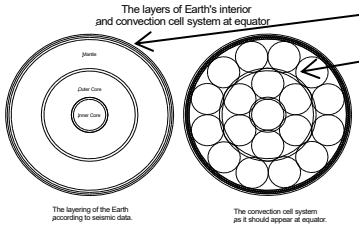

Measurements and physics

The layers of Earth drawn according to scale. The circles are drawn to represent Bénard type of convection.

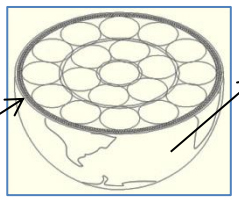

3D aspect

This simple match of basic measurements and physical law can be explored further to the North and South to develop a **3D model**.

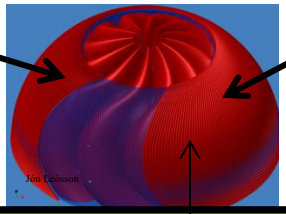

3D drawing of the system according to the difference of angular velocity from one infinte step of latitude to the other, resulting in a curvature with diameter of the order of Earth‘s radius.

Vertical heat flow:

- Radiation towards core
- Convection from core
- Munroe effect through crust

These three types of flow are shown here:

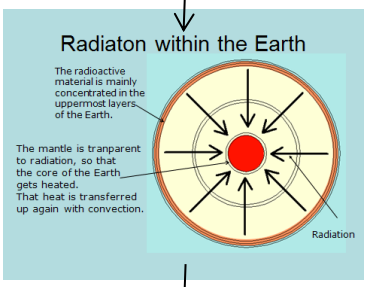

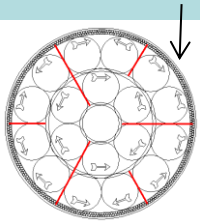

Convection from core towards crust.

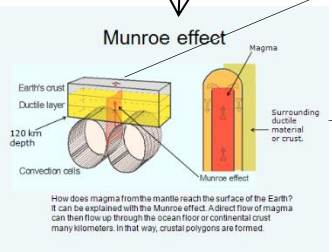

Convection rolls under crust create Munroe effect.

Horizontal paths:

Found for 240 parallel rolls covering the Earth underneath the crust. One of those paths is shown here.

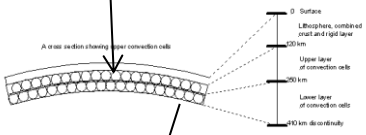

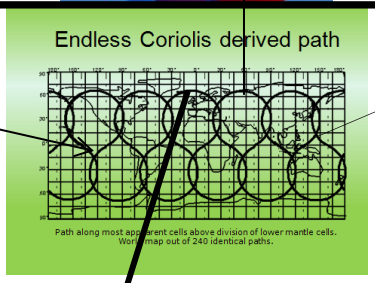

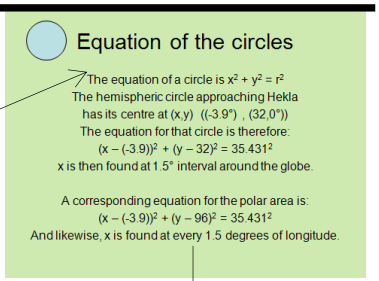

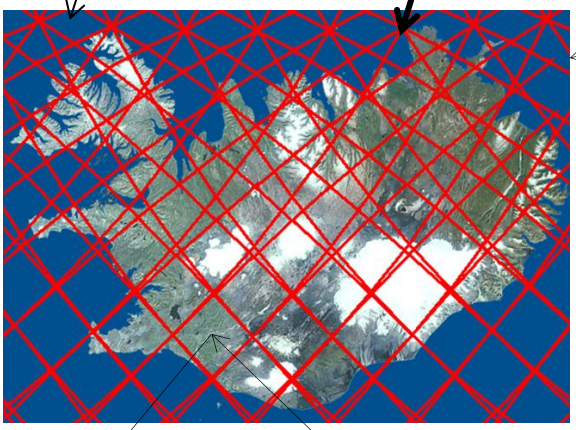

The grid resulting from 4 layers of convection rolls under Iceland

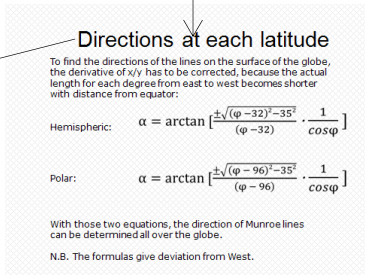

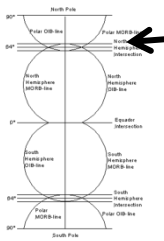

Iceland is located within an intersection zone of the polar and hemispheric parts of the total convection cell system. From the basic system drawn here, the grid under Iceland is derived. This grid can be referred to explaining the basics of the geology of Iceland.

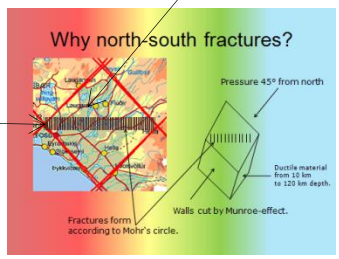

The South Iceland Seismic Zone can be explained by referring to the grid formed by the layers of convection rolls.

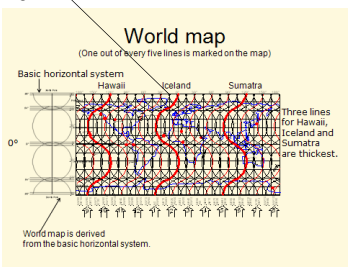

The grid is absolutely regular and possible to zoom in to analyse all kinds of tectonic features and geological phenomena and explain them thoroughly.

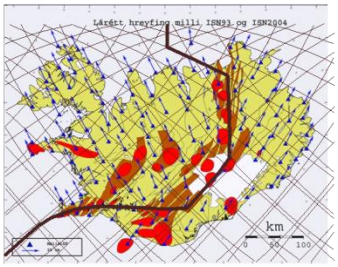

Tectonic drift in Iceland does match with convection rolls pattern.

The Convection System of Earth's Mantle and the Transfer of Heat to the Surface

Abstract

A method is presented for calculating the predicted directions of tectonic features at different latitudes from a geometrical model of mantle convection. The approach combines the proposed convection-roll geometry with the Coriolis effect, thereby moving from measured dimensions to quantitative directional predictions. Two principal assumptions provide the starting point. First, convection rolls under the near-balanced conditions considered in the model are approximated as having comparable vertical and horizontal dimensions. Second, these characteristic dimensions are compared with the measured thicknesses of the Earth's internal layers. The horizontal component of the circulation is then extended over the curved surface of the Earth and modified as a function of latitude. This construction produces testable directional predictions; the volcanic zones of Iceland provide one example.

The calculated paths can be mapped separately for each proposed convection layer. Superimposing the different layers produces a global grid extending from the South Pole to the North Pole. The grid can then be examined regionally, with Iceland providing a particularly detailed test area because of its high level of tectonic, volcanic, and geothermal activity. In the model, adjacent convection rolls are represented by lines following their calculated horizontal trajectories. These lines are interpreted as marking the central zones associated with convective upwelling or downwelling and can therefore be compared with observed geological structures at the surface.

The study was developed over almost two decades and brings together several physical processes that are not usually considered within a single geological model. The proposed heat-transfer framework follows energy through the Earth's interior and compares the resulting convection geometry with surface observations. The radiation component of the model was examined with Þorbjörn Ármann Friðriksson. Within this interpretation, radiative transfer is considered in relation to the thermal state of the core, while the Munroe effect is proposed as a mechanism for focusing melt pathways upward through the tectonic plates.

The principal value of the framework is that it produces quantitative spatial and directional predictions that can be compared with volcanoes, geothermal areas, earthquake zones, plate-motion vectors, and topographic or bathymetric structures. If these relationships withstand independent testing, the approach may provide a more quantitative basis for examining how deep-Earth heat transfer is expressed at the surface. The model is therefore presented as a unified and testable framework rather than as a replacement for the observational foundations of modern geoscience.

Þorbjörn Ármann Friðriksson
Steingrímur Þorbjarnarson
Oddabraut 13
Þorlákshöfn

Works Cited

Allen, C. W. 1983. *Astrophysical Quantities.* UK: The Athlone Press.

Condon, E. U., and Oddshaw Hugh. 1967. *Handbook of Physics.* USA: McGraw - Hill Book Company.

Cristopherson, Robert W. 1992. *Geosystems. An Introduction to Physical Geography.* USA, 616 pp.: Macmillan Publishing commpany.

Davies, Geoffrey F. 1999. *Dynamic Earth. Plates, Plumesw and Mantle Convection.* United Kingdom, 457 pp.: Camebridge University Press.

Einarsson, Páll. 2001. „Suðurlandsskjálftar 2000: Orsakir og atburðarás.“ *Goðasteinn* 195-217.

Foulger, Gillian R. 2010. *Plates vs Plumes - A Geological Controversy.* Oxford: John Wiley & sons.

Francis, Peter. 2000. *Vocanoes - A Planetary Perspective.* USA, 443 pp.: Clarendon Press.

Grand, H. E. Le. 1988. *Drifting Continents and Shifting Theories.* Great Britain, 313 pp.: Cambridge Univeristy Press.

Guðmundur Þór Valsson. 2007. *ISNET 2004 - Niðurstöður úr endurmælingum Grunnstöðvanets Íslands.* Mælingasvið, Reykjavík: Landmælingar Íslands.

Hess, Harry. 1962. „History of Ocean Basins.“ *Petrologic studies: a volume in honor of A. F. Buddington* Geological Society of America: 599-620.

Jones, Stephen M., Nicky White, og John MacLennan. 2002. „V-shaped ridges aroound Iceland: Implications for spatial and temporal patterns of mantle convection.“ *G3 - an Electric Journnal oof the Earth Sciences* 3, Number 10: 1059. doi:10.1029/2002C000361.

Kristjansson, Bjarni Kr., og Jörundur Svavarsson. 2002. „Helladýr úr forneskju.“ Í *Þingvallavatn - Undraheimur í mótun*, eftir Pétur M. Jónasson og Páll Hersteinsson, 303. Reykjavík: Mál og Menning.

Manneville, Paul. 2010. *Instabilities, Chaos and Turbulence.* 2nd. London, 439 pp.: Imperiala College Press.

McBirney, Alexander R. 1993. *Igneous Petrology.* England, 508 pp.: Jones and Bartlett Publishers.

Munroe, Charles E. 1943. „Munroe-effect.“ *Science.*

Paldor, Nathan, and D. Peter Killworth. 1988. "Inertial Trajectories on a Rotating Earth." *Journal of the Atmospheric Sciences* 4013-4019.

Plujim, Ben van der, og Stephen Marshak. 1997. *Earth Structure: An Introduction to Structural Geology and Tectonics.* USA: WCB/McGraw-Hill.

Ritsema, J., H. J. van Heijst, and J. H. Woodhouse. 1999. "Complex shear wave velocity structure imagined below Africa and Iceland." *Science, 286* 1925-1928.

Sigloch, K., Mihalynuk, M. 2013. „Intra-oceanic subduction shaped the assembly of Cordilleran North America.“ *Nature* 496: 50-56. doi:10.1038/nature12019.

Sigmundsson, Freysteinn. 2014. „Segmented lateral dyde growth in a rifting event at Bárðarbunga volcanic system, Iceland.“ *Nature* 5-10.

Sigmundsson, Freysteinn, og Páll Einarsson. 1996. „Jarðskjálftabeltið á Suðurlandi, jarðskorpuhreyfingar 1986-1992 ákvarðaðar með GPS-landmælingum.“ *Náttúrufræðingurinn* 37-46.

Torsvik, et al. Trond H. 2015. „Continental crust beneath southeast Iceland.“ *Earth, Atmospheric and Planetary Sciences* 1-10.

Valsson, Guðmundur Þór. 2008. *ISN2004.* Reykjavik: Gutenberg.

Walzer, Uwe. 1971. „Convection Currents in the Earth's Mantle and the Spherical Harmonic Development of the Topography of the Earth.“ 87: 73-92.

Þorbjarnarson, Steingrímur. 2000. *Hnettirnir.* Reykjavík: Steindórsprent-Gutenberg hf.

Additional Sources Consulted During Preparation

Árnason, Knútur, and Magnússon, Ingvar Thor. 2001. Niðurstöður viðnámsmælinga í Kröflu. (Resistivity measurements in the Krafla geothermal field, NE Iceland.) Landsvirkjun, Iceland, 72 pp.

DECKER et al. 1987. Volcanism in Hawaii. U.S. Government Printing Office, Washington.

Einarsson, Páll. 2001. Suðurlandsskálftar 2000: Orsakir og atburðarás. Goðasteinn 2001, pp. 195–217.

FREEDMAN, ROGER A. and KAUFMANN, WILLIAM J. 2001. Universe. W.H. Freeman and Company, USA.

HRÓARSSON, BJÖRN and JÓNSSON, SIGURDUR SVEINN. 1992. Geysers and Hot Springs in Iceland. Mál og Menning, Iceland, 158 pp.

Irvine, T. Neil. 1989. A Global Convection Framework: Concepts of Symmetry, Stratification, and System in the Earth's Dynamic Structure. Geophysical Laboratory, Carnegie Institution of Washington, Washington, D.C. 20008.

JÓHANNESSON, HAUKUR. 1982. Yfirlit um jarðfræði Snæfellsness. Árbók F.Í. 151-174.

PLUIJM, BEN VAN DER AND MARSHAK, STEPHEN. 1997. Earth Structure: An Introduction to Structural Geology and Tectonics. WCB/McGraw-Hill, USA, 493 pp.

ROTH, FRANK. 2004. STRESS CHANGES MODELLED FOR THE SEQUENCE OF STRONG EARTHQUAKES IN THE SOUTH ICELAND SEISMIC ZONE SINCE 1706. PURE AND APPLIED GEOPHYSICS (PAGEOPH), 161(7), PP. 1305–1329. BIRKHAUSER VERLAG, SWITZERLAND.

Rothery, David A. encyclopedia.com (website), accessed 04/09/2011.

SIGMUNDSSON, FREYSTEINN and EINARSSON, PÁLL. 1996. Jarðskjálftabeltið á Suðurlandi, jarðskorpuhreyfingar 1986-1992 ákvarðaðar með GPS-landmælingum. Náttúrufræðingurinn 66 (1), pp. 37-46 1996.

STANLEY, STEVEN M. 1999. Earth System History. W.H. Freeman and Company, 615 pp.

TORFASON, HELGI. 2003. Jarðhitakort af Íslandi og gagnasafn um jarðhita. Náttúrufræðistofnun Íslands og Orkustofnun, Reykjavík. NÍ-03016.